School of Pharmacy

Investigating Magnetic Fields for Pharmaceutical Processing

By

Victoria Louise Bratty, MPharm, MRes

Thesis submitted to the University of Nottingham for the degree of Doctor of Philosophy

August 2020

Abstract

Many pharmaceutical compounds have poor aqueous solubilities that can result in difficulties in formulation, and ineffective therapeutic treatments. Pharmaceutical compounds can exist in different states (i.e. amorphous or crystalline), as well as existing in different polymorphic forms, which can dramatically affect physicochemical properties. However, a technique called containerless processing has shown promise in the control of crystallisation and crystal form. Using high strength magnetic fields (> 16 T) that are strong enough to freely levitate pharmaceutical solutions we investigated the potential of magnetic levitation for containerless processing.

Initial experiments included the characterisation of starting materials and production of reference materials, to be used as a comparison to samples in later chapters. Initial levitation studies involved the levitation of paracetamol solutions (water/ ethanol) using our helium-cooled, closed-cycle superconducting magnet. We showed that it was possible to crystallise pharmaceutical materials whilst levitated. Form I paracetamol was predominantly formed, whilst form II was occasionally also formed showing that there could be an influence of the process on the crystal form produced. In further levitation studies we used clotrimazole, which had already been shown to form amorphous gels when levitated by acoustic levitation. Our study was therefore a comparison of acoustic and diamagnetic levitation methods. Interestingly droplets were found to produce an amorphous gel, crystalline shell, or a combination of both. Optimisation of the experimental set up with mirrors allowed filming of the droplet from the side, which allowed investigation into the crystallisation/ amorphisation processes involved. Final experiments include more detailed investigations into the influence of the magnetic field. Paracetamol, clotrimazole and propranolol were crystallised from solution under magnetic fields of 1 T. Low strength magnetic fields

did not have any effect on the crystallisation of paracetamol or clotrimazole. However, propranolol crystallised under low strength magnetic fields produced form III propranolol which is not usually formed from solution, usually from a melt. It is therefore demonstrated that diamagnetic levitation offers a unique ability to investigate crystallisation/ amorphisation of different pharmaceutical drugs in solution.

Acknowledgements

I would firstly like to thank my supervisors, Professor Stephanie Allen, Dr Richard Hill and Dr Jonathan Burley for their advice and support throughout my PhD. I would also like to extend my thanks to the technical staff at the School of Physics and Astronomy for their help with the construction of the Perspex box to fit on top of the magnet, the bore inserts and cuvette holders used in this thesis.

I would also like to thank the members of B200 (the mag lev lab) Oliver, Liam and Kyle for their stimulating conversations and advice with the magnet set up. For their humour, sanity (sometimes!) and company in the pharmacy labs Georgina, Tamara, Emanuela and Amanda.

Last but by no means least I would like to thank my family, my grandparents Tom and Sarah, Billy and Audrey, my parents Raymond and Louise, my siblings Rachael (Peg), Andrew and Laura and of course my boyfriend Adam for their support and encouragement.

Contents

List of figures

List of tables

Abbreviations

API	Active pharmaceutical ingredient
ATR	Attenuated total reflectance
DSC	Differential scanning calorimetry
FT-IR	Fourier transform infrared
HPMC	hydroxypropylmethylcellulose
IR	Infrared
Mag Lev.	Magnetic levitation
PDMS	Poly(dimethylsiloxane)
PMMA	Poly(methyl methacrylate)
UV	Ultra violet

1 Introduction

1.1 An overview of containerless processing

Research into containerless (or non-contact) processing has gathered momentum in the last few years and containerless techniques have been used to study the vitrification (Tangeman et al. 2001), supercooling (Weber et al. 2009) and nucleation (Takahashi et al. 2006) of a wide range of materials. Due to the removal of container walls liquids can be supercooled and supersaturated under high purity conditions. The removal of vessel walls also allows for better quality crystals to be grown; by removing heterogeneous nucleation (often caused by vessel walls) crystals can grow with less mismatched facets and thus be of enhanced quality. The technique of acoustic levitation has shown promise in this regard as it has also been able to create amorphous versions of pharmaceutical compounds that were previously difficult to amorphise (Benmore and Weber 2011).

Many new drugs in the pharmaceutical pipeline have poor solubility which can cause problems for pharmaceutical companies; it is essential that when the patient takes the active pharmaceutical ingredient (API) it is properly absorbed and utilised before being excreted. Poor solubility can affect the efficacy of the medicines, and drugs that do not dissolve completely have the potential to cause irritation in the gastrointestinal tract. Poorly soluble drugs may require a larger dose of the drug compound being formulated which can be expensive to formulate especially if a large amount may be excreted by the patient. Low solubility drugs may be particularly problematic during pre - clinical trials, as large quantities (up to 100 times the usual dose) may be given to assess the compound's toxicity (Weber et al. 2017).

One solution to a poorly soluble pharmaceutical compound is to create the amorphous form of the compound. Amorphous pharmaceutical compounds have better bioavailability, solubility and enhanced dissolution compared to their crystalline versions (Benmore and Weber 2011). Techniques used to create amorphous compounds including freeze and spray drying, milling, hot melt extrusion and melt quenching in containers (Weber et al. 2012). However, not all compounds can be processed by these means, for example melt quenching is only suitable if the compound is thermally stable at temperatures slightly above its melting point (Weber et al. 2017). Therefore there is interest in containerless methods for pharmaceutical processing.

In addition to providing a route to amorphous materials containerless processing can also provide better quality protein crystals. High quality protein crystals of sufficient size are required for x – ray diffraction analysis for complete protein structure analysis. Containerless crystallisation research has been stimulated by the results of Littke and John, who performed a microgravity experiment in the US Space Shuttle (Littke and John 1984). Littke and John crystallized two proteins: beta galactosidase and lysozyme in microgravity. Their results show that, in comparison to the crystals grown on earth, they were of increased size and quality. Littke and John's results suggested that the microgravity environment could be favourable for macromolecular crystallization (DeLucas et al. 2002). Beneficial effects of microgravity on macromolecular crystallisation include more synchronised nucleation and growth, less heterogeneous nucleation on solid surfaces, fewer crystals with larger volume, and well-shaped crystals with fully developed faces (Lorber 2002).

Large superconducting magnets can levitate diamagnetic objects creating a microgravity environment. Diamagnetic objects are

materials that are repelled by the magnetic field due to induced magnetic fields caused within the material (for a more detailed explanation see section 1.3- 1.3.3). Using diamagnetic levitation enhanced by the magneto-Archimedes effect Maki et al. (2004) crystallized lysozyme in a floating and containerless state. Using magnetic fields of 3.8 T and a crystallising agent of gadolinium chloride they were able to produce optically flawless crystals. As the lysozyme crystals are diamagnetic and the gadolinium solution paramagnetic the upward magnetic buoyancy could be enhanced.

1.2 Types of containerless techniques

This section contains an overview of the main containerless techniques used in materials processing. Examples of containerless techniques include acoustic, magnetic, and aerodynamic levitation (Brandt 1989) which are summarised in Table 1-1 and Table 1-2.

Type of containerless manufacture	**Description**
Acoustic	Uses high intensity sound waves to levitate sample(s) (Santesson et al. 2003)
Aerodynamic	A fluid jet is used to levitate the sample (Hennet et al. 2011)
Gels	Crystals grown without touching the container walls can be considered containerless (Cao et al. 2013)
Magnetic	Using a high strength magnetic field diamagnetic material can be levitated (Maki et al. 2004)
Micropipette	Small volumes of crystallisation solution pipetted into oil/ immiscible solvent (Kinoshita et al. 2016)
Oils	Crystallisation fluid can be suspended in oil (Cao et al. 2013)

Table 1-1 Different types of containerless manufacture.

Acoustic levitation	Magnetic levitation	Aerodynamic levitation
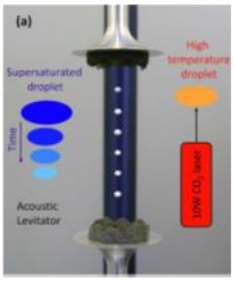 a)	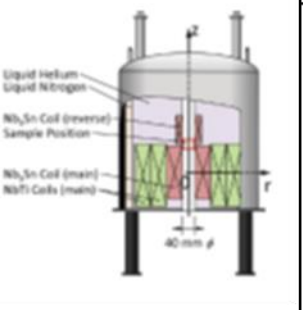 b)	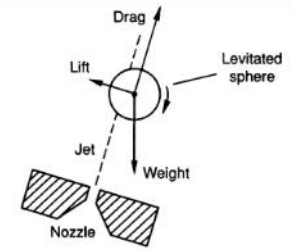 c)
Gels	Oils	Micropipette
 d)	 d)	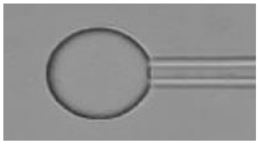 e)

Table 1-2 Table comparing the different types of containerless processing (a) Image taken from Benmore and Weber (2011) (b) Image taken from Nakamura et al. (2012) (c) Image taken from Brandt (1989) (d) Image taken from Cao et al. (2013) (e) Image taken from Rickard et al. (2010).

1.2.1 Acoustic levitation

Acoustic levitation uses the pressure produced by sound waves to levitate small objects. Acoustic levitation relies on the ability to create standing waves, which occurs when two waves of the same frequency interfere when travelling in the opposite direction. Therefore an acoustic levitator usually consists of a transducer and a reflector, with the reflector positioned a few multiples of the wavelength above the transducer. The transducer emits an ultrasonic wave which is then reflected back on itself in exactly the opposite direction. The destructive points of interference along the wave are called nodes, here there is very little wave movement and hence low pressure. Below the nodes are points of maximum displacement called antinodes where the pressure is highest. Objects tend to move from high pressure to low pressure so any sample placed in the standing wave will move to the closest node. Therefore, the low pressure nodes are an ideal place for samples to rest in a standing wave (Figure 1-1).

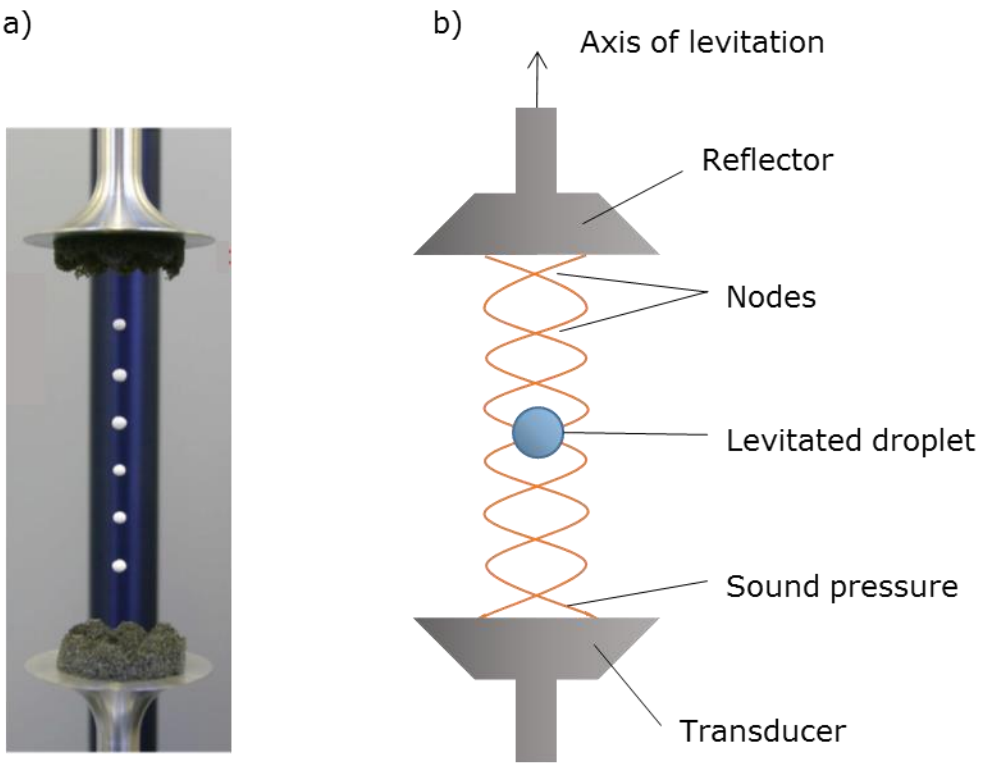

Figure 1-1 (a) A photograph of an acoustic levitator levitating several samples (white spheres). Image taken from Benmore and Weber (2011) (b) A diagram of an acoustic levitator showing a standing wave with a droplet being levitated in the node of the wave. Image adapted from Leiterer et al.(2008).

Cao et al. (2012) developed an ultrasonic levitation system which allowed crystals to be grown in the containerless state. Crystals grown include NaCl, NH_4Cl, proteinase K and lysozyme. Results show that both inorganic and protein crystals can be successfully grown. Data demonstrated that crystals had a higher growth rate, were larger in size, were better shaped, and had fewer twins and shards in comparison to the controls.

Santesson et al. (2003) was able to produce high quality large molecular weight protein crystals via acoustic levitation whilst Chung and Trinh (1998) used a combined ultrasonic electrostatic levitator as a method for growing protein crystals.

By coupling acoustic levitation with a portable Raman spectrometer Puskar et al. (2007) levitated 5 μL suspensions of red blood cells. Using their experimental set up they were able to study heme dynamics as well as the detection of hemozoin in malaria infected cells. The authors suggest that their set up has potential to be taken to remote environments for in situ diagnosis of malaria.

Disadvantages of acoustic levitation are that acoustic levitators can only levitate samples with diameters less than half the wavelength. Typically levitated samples have volumes of 5 nL to 5 μL (with corresponding diameters of 0.2 – 2 mm) (Leiterer et al. 2008). Another disadvantage is that acoustic levitation is open to contamination, (Benmore and Weber 2011) admit that no steps were taken to minimise dust which could cause unwanted crystallisation.

1.2.2 Aerodynamic levitation

Aerodynamic levitation uses a fluid jet (or gas jet) to levitate spherical specimens. The fluid jet is aimed at an off axis specimen causing asymmetry on one side (where flow is faster) which produces a centring force stabilising the specimen. The friction caused by the fluid at the surface of the off axis specimen causes rapid rotation resulting in an additional centring force. In the vertical direction levitation is stabilised by the divergence of the jet decreasing drag with increasing height (Brandt 1989).

Using an aerodynamic levitation system Oran and Berge (1982) were able to heat, cool, melt and solidify small spherical spheres in a containerless way. Small beads of alkali borosilicate glass and lead (up to 4 mm in diameter) were levitated by air or argon gas and heated using an elliptical radiant heater.

By combining wide-angle x-ray scattering and small-angle x-ray scattering with aerodynamic levitation Greaves et al. (2008) were able to study in situ phase transitions of liquid material in a containerless fashion. Yttria-alumina was levitated by a vertical steam of argon and heated by a laser whilst being analysed by x-ray scattering in situ.

Hennet et al. (2011) also combined aerodynamic levitation with laser heating, x – ray and neutron diffraction allowing the structural analysis of high temperature liquids including alloys, ceramics, glass, oxides and metals.

The disadvantages of aerodynamic levitation are that vibrational instabilities prevent levitation of liquids (Brandt 1989). Cao et al. (2012) reiterate this by stating that aerodynamic levitation involves a complex system and that levitated droplets display poor stability.

1.2.3 Crystallisation from gels

Crystallisation from gels can be considered containerless as the crystals grow in a viscous gel without any contact with the container walls (Table 1-2).

Gels can be considered to mimic microgravity because they reduce crystal sedimentation and convection. (Biertümpfel et al. 2002). By reducing convection gels allow more homogenous molecular transport during crystal growth. (García-Ruiz et al. 2001) As crystals cannot move or sediment they are able to remain suspended and grow in three dimensions within in the mother liquor (Lorber and Giegé 1996; García-Ruiz et al. 2001; Sauter et al. 2002). Such a stable environment has shown to stop twinning in alcohol dehydrogenase crystals (Sica et al. 1994).

The crystalline quality of hen egg white lysozyme (HEWL) crystals grown in silica and agarose gels have been compared to crystals grown from solution (Vidal et al. 1999). Crystals were analysed by x - ray diffraction and x – ray topography and crystals were of lower mosaicity and had more homogenous lattices compared to crystals grown in solution. Crystals grown from agarose gel were better than crystals from solution, however crystals grown from silica gel were of the best quality.

Lorber et al. (1999) also compared crystals grown from solutions and gels. Three proteins; thaumatin, turkey egg white (TEW) lysozyme and bacterial aspartyl-tRNA synthetase (AspRS) were crystallised as well as a tomato bushy stunt virus (TNSV). For the turkey egg white lysozyme and thaumatin better quality crystals can be obtained more reproducibly when crystallised from gel. X – ray topographs support the fact that gel improves the crystalline quality.

Cao et al. (2013) use agarose gel to crystallise several protein crystals including hen egg white lysozyme and proteinase K. Morphological comparison with control crystals showed improvement in crystal size and shape when using silica gels. The crystals were analysed by x – ray diffraction analysis and the samples crystallised from the agarose gel had better diffraction properties than the control crystals which were in contact with the vessel walls.

The disadvantages of crystallisation from gel include a small sample size and Cao et al. (2013) reported that crystallisation in agarose gel was more difficult than in silicone oil. Care must also be taken during solution preparation to avoid the formation of bubbles and denaturing the protein due to the transient high temperature of the agarose gel solutions.

1.2.4 Crystallisation from oils

Oils can be used for containerless crystallisation of protein crystals, the crystallisation solution is injected into a vessel of high density oil; for example silicone oil. The crystallisation droplet maintains a spherical, or elliptical shape within the oil (Table 1-2).

Using low and high density silicone fluids Lorber and Giegé (1996) were able to levitate droplets of protein in an aqueous crystallisation fluid between the two interfaces. Six proteins and one virus were crystallised using the floating droplet technique including thaumatin, hen and turkey egg white lysozyme and horse serum albumin. Once conditions were optimised large perfect single crystals could be grown. Crystals would nucleate at the interface between the crystallisation droplet and the silicone oil, with crystals growing inwards into the droplet. The crystals showed no preference to growing on the top or bottom silicone layer, whilst crystals that grew on the top interface would often cause the droplet to rotate round due to the weight of the crystal. After 30 to 50 days crystals were counted for both the control and levitating drops and for tetragonal thaumatin, hexagonal turkey egg white lysozyme and tetragonal hen egg white lysozyme nucleation is significantly and reproducibly reduced in the floating droplets.

A containerless environment for protein crystallisation was created by Chayen (1996) by using two layers of silicone oil, one of higher density compared to water and common precipitating agents and one of lower density. The crystallisation solution is then pipetted into the low density silicone oil and the crystallisation droplet re-positions itself between the two layers. Results agree with Lorber and Giegé (1996) that the floating droplets have significantly reduced nucleation compared to control samples grown on a container surface.

Cao et al. (2013) use silicone oil to crystallise several protein crystals including protein crystals including hen egg white lysozyme and proteinase K. Crystals grown from silica gel showed improvement in crystal size and shape when compared to the control crystals. However, agarose crystals had better morphology than the crystals grown in silicone oil, although crystallisation in agarose gel was more difficult than in silicone oil. X –ray diffraction analysis confirmed that the crystals demonstrated better diffraction properties than the control crystals.

The crystallisation of salt microcrystals was studied by Quilaqueo and Aguilera (2016) using saline droplets in a hot oil phase. The saline solution would be added to a beaker of hot oil using a syringe and rapid evaporation of the water would encourage the formation of salt microcrystals. The effects of droplet volume, brine concentration, and oil temperature were studied. Crystal size decreased by increasing the volume, solution concentration and temperature of the oil. The microcrystals had a dissolution rate twice that of the original crystals. The authors suggest it would be beneficial in the food industry, for example adding to surface salted snacks to reduce or optimise salt intake while maintaining saltiness perception.

A disadvantage of containerless crystallisation in oils is that the crystallisation medium has to be carefully selected as some organic molecules (for example, ethanol, phenol, and dioxane) are soluble in oils (Chayen 1996). When preparing samples for the floating drop method Lorber and Giegé (1996) caution that when mixing concentrated protein and precipitant solutions supersaturation may be reached at their interfaces which can cause denaturation of part of the macromolecule. The authors also note that dust particles favourably stick to the crystallisation droplet within the silicone oil causing unwanted heterogeneous nucleation by generating surface imperfections.

1.2.5 Micropipette crystallisation

The micropipette technique involves pipetting small volumes of an aqueous supersaturated solution into a second immiscible solvent.

Using sodium chloride solutions Utoft et al. (2018) studied microcrystallisation, solvent dissolution and crystal morphology of microdroplets. As demonstrated by Bitterfield et al. (2016) when an aqueous sodium chloride microdroplet is introduced into an immiscible medium for example a long chain alcohol, the water dissolves out into the solvent, increasing the concentration of sodium chloride in the droplet. When there is no external nucleation site the solubilised sodium chloride will undergo homogenous nucleation. Utoft et al. (2018) describe the affect that changing the bathing medium from octanol to decane made on the sodium chloride microdroplets. In the decane system loss of water was slower, with a concomitant slower increase in sodium chloride concentration, resulting in a lesser tendency to nucleate and slower crystal growth compared to the octanol system. In the decane system slower nucleation resulted in single cubic crystals whilst fast dissolution and nucleation in the octanol system formed dendritic crystals.

Protein dehydration was investigated by Rickard et al. (2010) using a micropipette technique. A protein microdroplet was introduced into a dehydration medium which removed water from the lysozyme microdroplet. The removal of water resulted in a spherical, single phase glassy protein bead. The amount of water remaining in the glassy bead could be calculated by knowing the initial lysozyme concentration of the microdroplet and by measuring the change in diameter of the microdroplet. The micropipette technique offers an alternative to lyophilisation, during which ice can damage the protein secondary structures. When decanol is used as the dehydration medium water can be removed within minutes at room temperature.

Aniket et al. (2014) also used a micropipette to create solid amorphous microspheres; a process they named microglassification. Microdroplets of serum bovine albumin solution were introduced into decanol or pentanol which removed the water from the microdroplet creating a glassy bead.

Disadvantages of the micropipette technique for containerless crystallisation include the small volumes used and the careful choice of solvent required.

1.2.6 Magnetic (diamagnetic) levitation

Using large superconducting magnets diamagnetic materials can be levitated. Diamagnetic materials are ones that induce their own magnetic field antiparallel to an externally applied magnetic field causing repulsion. Many objects are diamagnetic and examples include; water, alcohol, organic chemicals, frogs and flies. In the superconducting magnet the repulsion force is enough to counterbalance the force of gravity levitating the object (for a detailed explanation see section 1.3 - 1.3.3).

Advantages over other containerless techniques include the ability to levitate larger volumes of solution (the Cryogenic magnet used at the University of Nottingham can levitate up to approximately 20 mL). No extra considerations need to be taken for the crystallisation medium, unlike crystallisation in oils where some solvents are soluble in oil. Using a bore insert the temperature of the magnet bore can be controlled and varied as required. An extra advantage is that a Perspex box set up can potentially reduce unwanted nucleation from dust in the lab unlike the acoustic levitation set up.

1.3 Introduction to magnetism

The most well-known magnetic material is iron, with nickel and cobalt sharing similar magnetic properties. Iron, nickel and cobalt are attracted to magnets and this common type of magnetism is known as ferromagnetism. However, all ordinary substances are also very weekly magnetic - although a thousand to a million times less than ferromagnetic materials. This weak magnetism can be divided into two types; materials that are attracted to magnetic fields (paramagnetic) and those that are repelled (diamagnetism) (Feynman et al. 2010)

1.3.1 Magnetic moments

All materials consist of atoms. The nucleus of atoms are made up of one or more atomic particles (protons and neutrons), creating a positively charged centre. This positive centre is orbited by one or more negatively charged electrons. These electrons spin as they orbit the nucleus producing a magnetic field. The strength of the magnetic field is called the magnetic moment and the direction of the electron spin and orbit determine the magnetic field direction (Knight 2008).

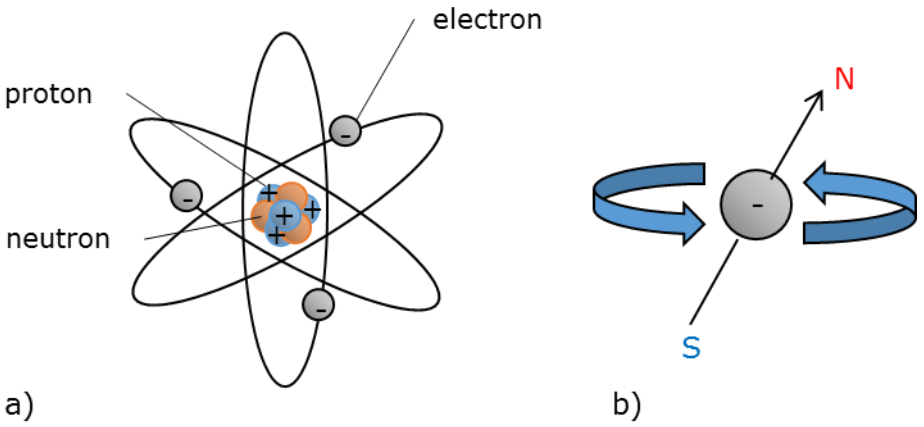

Figure 1-2 (a) A diagram of electrons orbiting the atomic nucleus (b) A diagram depicting the magnetic moment of an electron spinning anticlockwise.

1.3.2 Types of magnetic materials

Ferromagnetic materials are commonly thought of as being "magnetic". Examples of this include fridge magnets or horse shoe magnets which are commonly made from iron. Ferromagnetic materials include iron, cobalt, nickel and manganese; the prefix *ferro* meaning iron like. In iron and other ferromagnetic materials the spins interact with each other in such a way that the magnetic moments all tend to line up in the same direction creating a macroscopic magnetic dipole. The material has north and south magnetic poles, creates its own magnetic field, and when placed in an external magnetic field aligns parallel to the applied magnetic field (Figure 1-3). When removed from the external magnetic field ferromagnetic materials can retain some residual magnetisation, meaning that they can be permanently magnetised (Knight 2008).

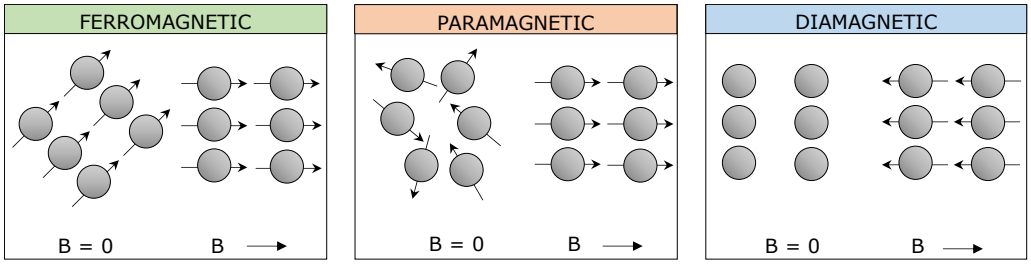

Figure 1-3 Schematic representation of magnetic materials at rest and in a magnetic field (B). Adapted from Iacovacci et al. (2016).

In paramagnetic materials the atoms have a permanent magnetic moment which means that the electron spins and orbits create a net circulating current that is not zero. An example of a paramagnetic substance is oxygen whose unpaired electrons give rise to incomplete cancellation of the electron's spin magnetic moments. These unpaired electrons give rise to a net magnetic moment, even in the absence of an external magnetic field. Unlike ferromagnetic material the magnetic moments do not align and are randomly orientated in the absence of a magnetic field. However, when an external magnetic field is applied (B) the moments try to line up with the external magnetic field, and the induced magnetism can even enhance the magnetic field (Figure 1-3) (Feynman et al. 2010; Iacovacci et al. 2016).

Diamagnetic materials have no permanent magnetic moments because the magnetic moments within each atom balance out, meaning there is zero net moment; the electron spins and orbits exactly cancel out so that each atom has no average magnetic moment. Water is an example of a diamagnetic substance. When oxygen bonds to two hydrogens, all the electrons are paired up meaning their spins and orbits cancel out. When an external magnetic field is applied little currents are created inside the atom through induction. These little currents are in such a direction to oppose the magnetic field i.e. the magnetic moments align in the opposite

direction to the magnetic field. Diamagnetic materials do not retain magnetisation after the external magnetic field is removed (Figure 1-3) (Feynman et al. 2010; Iacovacci et al. 2016).

1.3.3 Magnetic levitation

Diamagnetic materials such as water, organic chemicals, diamonds and even whole organisms (for example frogs and mice) can be levitated by strong magnetic (10 T) fields, which are now quite standard to generate (Geim 1998).

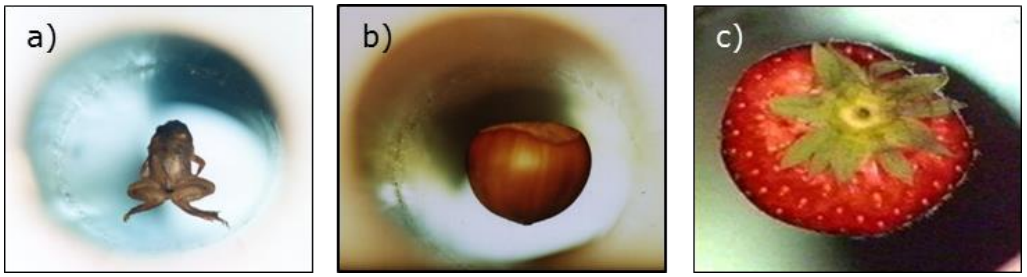

Figure 1-4 Examples of objects levitated by diamagnetism. (a) A frog, (b) A chestnut and (c) A strawberry. Images taken from Radboud University, high field magnet laboratory website, http://www.ru.nl/hfml/research/levitation/diamagnetic/ [Accessed on 07/08/2020]. Images of the frog and hazelnut also available from Geim (1998).

Diamagnetic materials create their own magnetic field that is antiparallel to an externally applied magnetic field, causing repulsion. However, if this magnetic force can counterbalance the force of gravity then the object can be levitated. Diamagnetism is felt at the molecular level, with both gravity and magnetism having an effect on molecules. Therefore, magnetic levitation has been considered by some to be an equivalent condition to microgravity in space. It has been proposed that similar experiments could thus be carried out

within magnets as those performed on the space shuttle (Tagami et al. 1999).

1.3.3.1 Forces on diamagnetically levitated objects

As explained in section 1.3.3 diamagnetic materials can be levitated by strong magnetic fields, produced for example by large superconducting magnets. Water droplets can be levitated by placing them in the field of a large superconducting magnet, where they create their own magnetic field antiparallel to the field of the superconducting magnet. When the upwards repulsive force is strong enough it can balance out the force of gravity allowing the droplet to levitate within the bore of the magnet. Figure 1-5 (b) depicts the forces on a droplet of water levitating within the magnet bore. Field lines (B) are indicated by the black arrows. The droplet is also stabilised laterally by the magnetic field which is stronger by the walls of the magnet (lines are closer together) so the droplet is pushed in towards the centre of the bore.

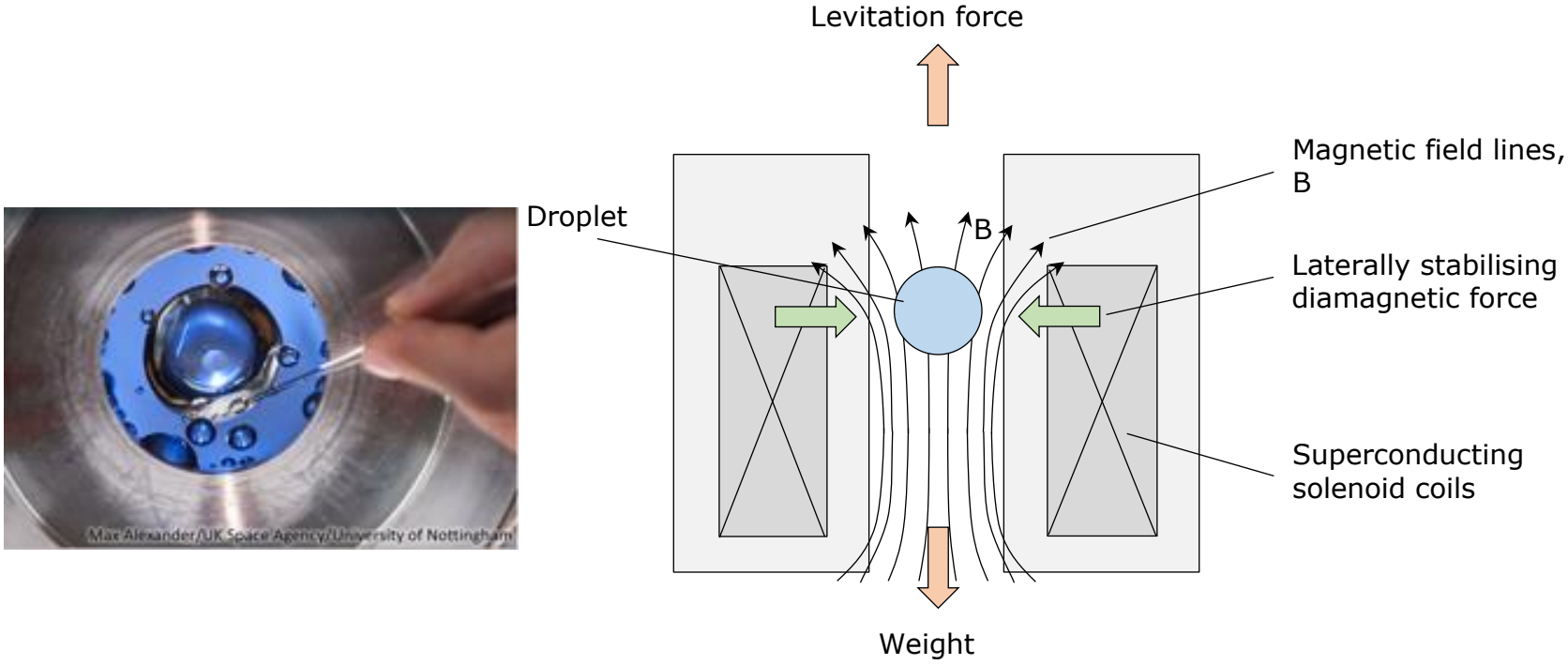

Figure 1-5 (a) Bird's eye view of a droplet being levitated in the bore of the magnet (b) Cross section of a superconducting magnet levitating a droplet of water. The schematic depicts forces on the droplet of water in a homogenous magnetic field. Image (a) taken from the University of Nottingham, levitation in the lab blog. https://blogs.nottingham.ac.uk/physics/2017/09/27/levitation-in-the-lab/ [Accessed 07/08/2020]

1.4 Introduction to nucleation and crystal growth

In crystallisation the critical phenomena are the formation of new crystals (nucleation) and crystal growth. Nucleation and crystal growth determine the size of the crystal and size distribution. The driving force for crystallisation and crystal growth is the level of supersaturation in the solution (Doran 2013).

1.4.1 Solubility and supersaturation

The solubility of a substance is the maximum concentration of the solute in a particular solvent that can be dissolved under set conditions of pressure and temperature whilst remaining thermodynamically stable. A saturated solution is one that contains this maximum concentration. A supersaturated solution is one that contains more dissolved solute than the saturated concentration. In general it is quite easy to create such solutions, however supersaturated solutions are thermodynamically unstable. Sometimes supersaturated solutions can be metastable which means that they are able to resist small disturbances but become less stable when perturbed (Doran 2013).

Typical results for solute concentration as a function of temperature are displayed in Figure 1-6.

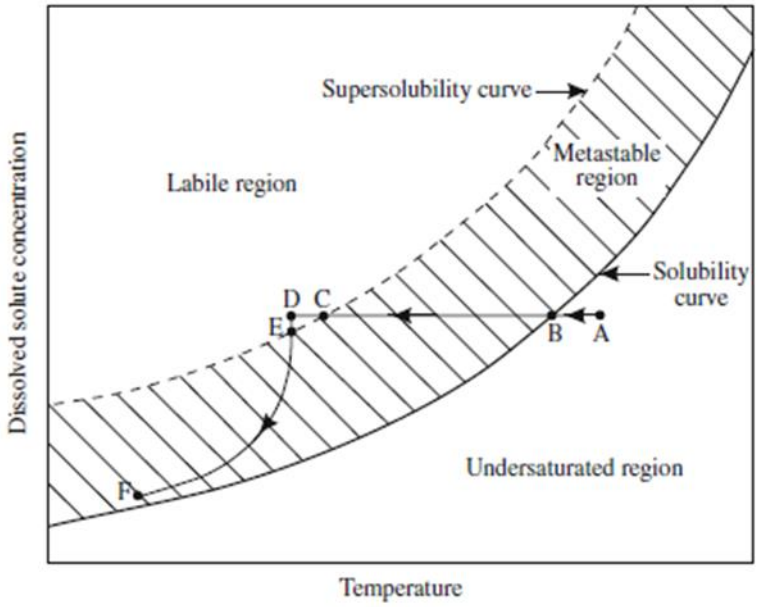

Figure 1-6 A solubility diagram displaying solubility and supersolubility curves as a function of temperature. Points A to F indicate a hypothetical pathway for batch crystallisation without the need of seed crystals. Image taken from Doran (2013).

Thermodynamic equilibrium between the liquid and solid phases is represented by the solubility curve (Figure 1-6). Below the solubility curve is the undersaturated region where crystallisation is impossible. Above the solubility curve is the shaded area of the metastable zone, where crystal nucleation is unlikely but any crystals already present will start to grow. The dashed line is the supersolubility curve which represents concentrations and temperatures that will make spontaneous crystallisation likely. The area above the supersolubility curve is the labile or unstable area of supersaturation where spontaneous crystallisation is likely to occur.

1.4.2 Nucleation

Nucleation is the formation of a crystal from a liquid or amorphous phase. Nucleation can be classed as primary or secondary (Figure

1-7). When nucleation occurs in a solution that was previously crystal free it is classified as primary nucleation. When the solution moves into the labile region of a supersaturation curve, this is when primary nucleation occurs (Figure 1-6). In these conditions the solute molecules join together, initially forming clusters which then become ordered and take up the structural geometry of the crystalline form.

Primary nucleation can be classified as homogenous or heterogeneous. Homogenous nucleation occurs spontaneously in a clean solution with no impurities. However, heterogeneous nucleation is induced by particles such as dust or on vessel walls (Myerson 2002; Karthika et al. 2016; Yazdanpanah and Nagy 2020)

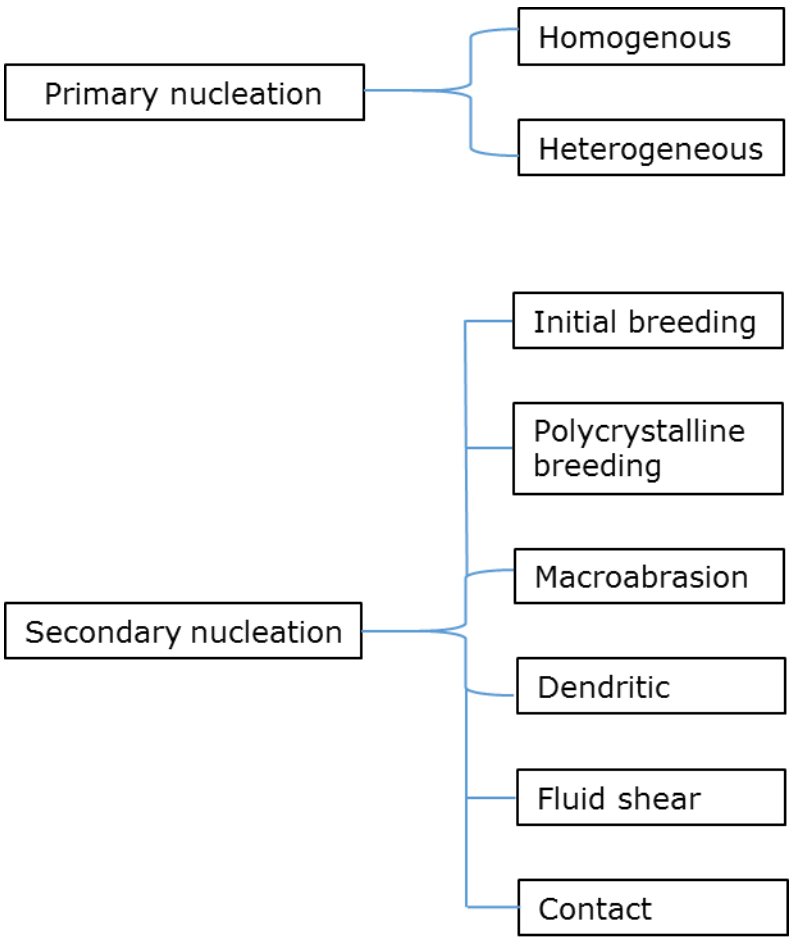

Figure 1-7 Mechanisms of nucleation. Image adapted from Myerson (2002).

The creation of new crystals by crystals already in the suspension is called secondary nucleation. Secondary nucleation is thought to be caused by several factors such as collisions between crystals or between crystals and the vessel walls, dislodgement of very small crystals from the surface of larger crystals and crystal attrition or breakage (Doran 2013).

1.4.3 Crystal growth

Crystal growth is described by the addition of more solute molecules to the nucleation site or crystal lattice to produce larger crystals (Aulton 2002; Myerson 2002). When a crystal is in a supersaturated environment the flux of growth units (e.g. molecules, atoms, or ions) to the surface is greater than that leaving, therefore resulting in crystal growth. The ability of the crystal to capture growth units as they arrive depends on the strength and number of interactions they can form between the surface and the growth unit. In Figure 1-8 the inner crystal contains molecules bound to four of its neighbours, however on the surface, less intermolecular interactions are available. On surface one, two intermolecular interactions are available whilst on surface two only one intermolecular interaction is possible. Therefore, when molecules attach to surface one it gains twice as much energy compared to surface two meaning surface one will grow twice as fast as surface two.

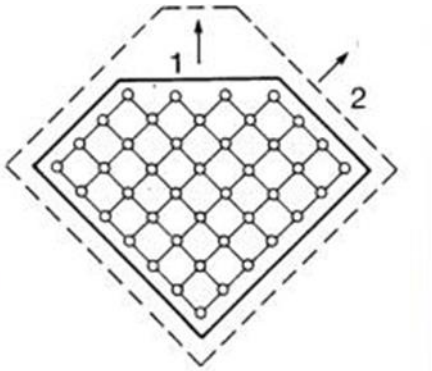

Figure 1-8 A diagram of a two dimensional crystal, the dotted line indicates crystal growth after a period of time. Surface 1 grows faster than surface 2. Image taken from Davey and Garside (2000).

In three dimensions it is possible for a growth unit to form a maximum of three bonds with the crystal surface (Figure 1-9). Hartman and Perdok (Woensdregt 1993) introduced a classification system for the different surfaces/ faces based on how many bonds are possible with the growth unit. A face where just one surface bond is possible is classified as a flat face (F face), a face where two surface bonds are possible is called a step face (S face) and a surface where three faces are possible is called a kink face (K face).

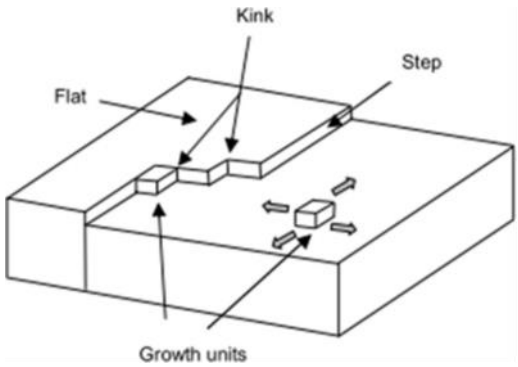

Figure 1-9 A diagram of a three dimensional crystal showing kink, step and flat sites. Image taken from El – Zhry El-Yafi and El-Zein (2014).

Assuming that the linear growth rate, v, of a face is proportional to the total binding energy of a growth unit joining that surface, it would be expected that $v_K > v_S > v_F$. As indicated in Figure 1-8 the final shape of the crystal is defined by the slowest growing flat face.

1.4.4 Crystalline or amorphous

Compounds in the solid state can be either amorphous, crystalline or a mixture of both. In crystalline solids the molecules are stacked in a defined order, which repeats throughout the particle. A material in the amorphous state is solid; however, the molecules are not in a repeating ordered fashion.

1.4.5 Polymorphism

1.4.5.1 What is polymorphism?

Many of the pharmaceutical drugs we use today exist in one or more crystalline forms. Examples include carbamazepine (Rustichelli et al. 2000), sulfamerazine (Sun and Grant 2001), venlafaxine (Roy et al. 2005), axitinib (Campeta et al. 2010). The property of being able to exist in different forms is known as polymorphism, with each crystalline form called a polymorph. Olanzapine which is used to treat schizophrenia and related psychoses crystallises in 25+ forms (Reutzel-Edens et al. 2003) form II and IV polymorphs are displayed in Figure 1-10. The packing arrangements of the two polymorphs are completely different, in form II dimers are stacked in parallel whilst in form IV they are arranged in a herringbone arrangement.

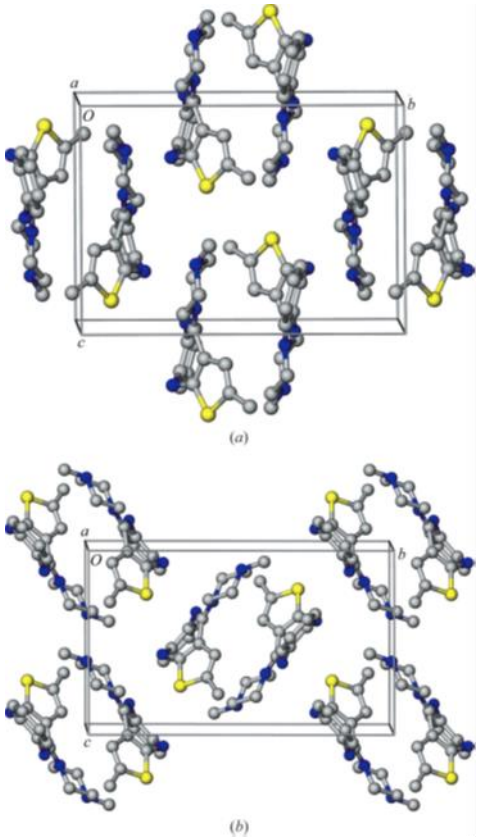

Figure 1-10 (a) the parallel stacking of olanzapine dimers in olanzapine form II (b) the herringbone arrangement of dimers in form IV. Image taken from Thakuria and Nangia (2011).

By changing the manufacturing conditions it is possible to produce different polymorphs. Methods used to obtain polymorphs include; crystallisation from single or mixed solvents (Morissette et al. 2004), crystallisation from the melt (Sun et al. 2008), seeding (Beckmann et al. 1998), laser induced crystallisation (Zaccaro 2001) or crystallisation from a supercritical fluid (Bettini et al. 2001).

A colourful example of physical properties changing with different polymorphs is the polymorphism of ROY (red, orange, yellow or 5-methyl-2-[(2-nitrophenyl)amino]-3-thiophenecarbonitrile). ROY was initially synthesised as an antipsychotic and has 10 different polymorphic forms. The different polymorphs vary in colour and

melting points (Brog et al. 2013). Examples of different ROY polymorphs are displayed in Figure 1-11

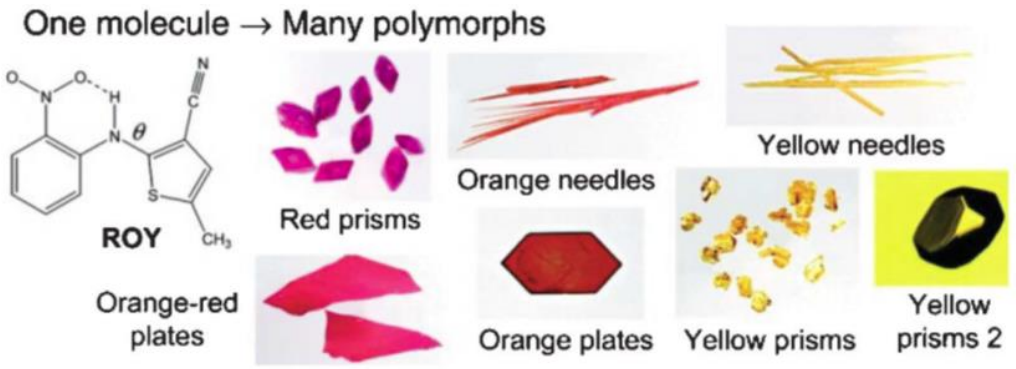

Figure 1-11 Different crystal forms of ROY (5-methyl-2-[(2-nitrophenyl)amino]-3-thiophenecarbonitrile. Image taken from Yu (2010).

1.4.5.2 Why is polymorphism important?

Polymorphism is important to the pharmaceutical industry because changing the polymorphic form of a compound can change its physicochemical properties. Properties that can be altered with changing the polymorphic forms include thermodynamic properties such as melting temperatures and solubility or mechanical properties such as hardness, flow and blending, compactability and tabletting. Other properties that can be altered include chemical, kinetic, surface and packing properties, which are summarised in Table 1-3 (Lee et al. 2011; Lee 2014).

Chemical	Kinetic	Mechanical	Packing/ physical	Surface	Thermodynamic
• Photochemical reactivity • Chemical reactivity	• Rate of dissolution • Stability • Rate of crystal growth • Solid state reaction kinetics	• Tabletting • Harndess • Powder flow • Compactability • Tensile strength	• Colour • Particle morphology • Density (molecular volume) • Hygroscopicity • Refractive index • Conductivity	• Surface area • Surface free energy • Interfacial tensions	• Melting and sublimation temperature • Vapour pressure • Enthalpy and entropy • Heat capacity • Chemical potential, free energy and solubility

Table 1-3 Properties that can be altered by choosing different polymorphic forms. Adapted from Lee et al. (2011) and Lee (2014).

Polymorphism can affect the mechanical properties of the pharmaceutical compound which can have an impact on manufacturing. Examples of polymorphs affected by altered mechanical properties include paracetamol (Di Martino et al. 1996; Joiris et al. 1998; Nichols and Frampton 1998; Beyer et al. 2001), metoprolol tartrate (Ragnarsson and Sjogren 1984; Singhal and Curatolo 2004), carbamazepine (Otsuka et al. 1999; Roberts et al. 2000), phenobarbitone and phenylbutazone. A common effect of polymorphism on pharmaceutical compounds is the alteration in powder flow between the polymorphs. Crystals with needle like morphology will have poor flow compared to crystals with cubic morphology (Singhal and Curatolo 2004). Carbamazepine is an example where polymorphism changes crystals morphology, which is displayed in Figure 1-12.

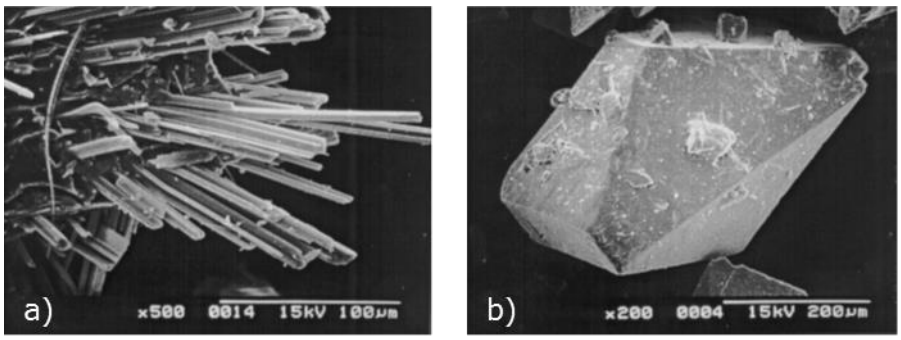

Figure 1-12 (a) Scanning electron micrograph of α - carbamazepine (b) Scanning electron micrograph of β - carbamazepine. Images adapted from Roberts et al. (2000).

Different polymorphs of the same pharmaceutical compound can have different solubilities due to their crystalline structures and free energy required to dissolve. Therefore polymorphs of the same compound can have a range of different solubilities. Differences in solubility between polymorphs can affect the bioavailability of the

solid dosage form especially if bioavailability is limited by dissolution (Bauer et al. 2001).

Unwanted polymorphism can have a dramatic effect on commercial pharmaceuticals, one example is that of Ritonavir ([5S-(5R*,8R*,10R*,11R*)]-10-Hydroxy-2-methyl-5-(1-methylethyl)-1-[2-(1-methylethyl)-4-thiazolyl]-3,6-dioxo-8,11-bis(phenylmethyl)-2,4,7,12-tetraazatridecan-13-oic acid, 5-thiazolylmethyl ester) which is an antiviral compound formulated for the treatment of AIDS (Acquired Immunodeficiency Syndrome). Ritonavir was not bioavailable from the solid form so was formulated as an oral liquid and semi-solid capsules, both of which contained ritonavir in ethanol/ water based solutions and marketed in 1996. During formulation development only one crystal form was discovered and capsules were produced with no stability problems. However, in 1998 several batches failed dissolution testing, and when analysed by x – ray powder diffraction a new polymorph was discovered which had vastly reduced solubility compared to the original polymorph. The sudden appearance of this less soluble polymorph caused the formulations to be unmanufacturable and it had to be reformulated (Bauer et al. 2001).

1.5 Crystallisation in droplets

Small impurity free droplets can be used for crystallisation studies on homogenous nucleation (Goh et al. 2010; Murray et al. 2010). Protein crystallisation is frequently studied using this approach with advantages such as ease of theoretical prediction and crystal stability (Chayen et al. 1992; Galkin and Vekilov 2000). Microfluidic systems have also been used for protein crystallisation (Song et al. 2006) and other homogenous nucleation experiments (Leng and Salmon 2009).

Kuil et al (2002) studied the crystallisation of protein crystals in nanolitre droplets. As no nanowell plates were available commercially the authors used PDMS (poly(dimethylsiloxane)) elastomer to create nanowells. PDMS was chosen as it is optically isotropic and transparent in the visible part of the spectrum, meaning crystals could be viewed with a microscope and CCD camera. Using a piezo-electric dispensing method droplets (10 -250 pL) of hen egg white lysozyme solution were dispensed on to the elastomer mould. To prevent quick evaporation of the lysozyme droplets paraffin oil was placed on top along with a glass microscope cover slide. Lysozyme crystals formed within 20 hours, with one crystal per nanowell. In comparison, crystallisation of lysozyme in larger vessels produced larger volumes of crystals over one to two days. Preliminary comparisons between nanowell and the µL droplet processes were that nucleation events in the nanowells appear to be lower than in the µL droplets. In nanowells it was proposed that it is easier to grow a single crystal and that reduced nucleation (number of nuclei per droplet) allows the testing of highly supersaturated solutions. As nanowells reduce nucleation, it opens up the possibilities of growing single crystals from samples that would usually produce intergrown clusters or showers of crystallites. In the authors experience the crystals grown in the nanowells had less growth defects than crystals grown from the same solution in a larger volume, although crystals grown from more proteins need to be analysed as they commented that this data was anecdotal.

Using patterned self-assembled monolayers (SAMs), Stephens et al. (2011) studied the crystallisation of calcium carbonate ($CaCO_3$) in picolitre sized droplets. The experimental set up allowed the study of crystallisation in a volume and reservoir limited environment, unlike other crystallisation templating systems such as porous polymers or membrane pores which offer confinement but are still open to the bulk solution. It was found that limiting the reaction volume had

significant results on the crystallisation of $CaCO_3$; crystallisation of calcium carbonate was retarded due to the small volume of the droplet compared to bulk solution. Secondly, crystallisation terminated early due to the finite conditions, which in the study revealed intermediate forms of calcium carbonate. As crystallisation was slower in the droplet than in bulk solution the mechanism of crystallisation could be observed, which progressed via amorphous calcium carbonate. The authors suggested that the droplet arrays provided a method for studying nucleation and crystal growth, which usually occur rapidly in bulk solution, without the need for sophisticated equipment such as X-ray scattering techniques or cryogenic transmission electron microscopy.

Crystallisation of calcium carbonate polymorphs could also be controlled by using droplet based microfluidics (Yashina et al. 2012). The authors compared calcium carbonate crystallisation methods by using a segmented-flow microfluidic reactor, a continuous flow microfluidic reactor and crystallisation in bulk solution. Previously, calcium carbonate microfluidic experiments involved continuous flow mixing at a T junction (Yin et al. 2009). These microfluidic experiments predominantly formed the calcite polymorph. The residence time distributions reduced control over the reaction times, which lead to a wide size distribution of the crystals and limited control of the polymorph being formed. The segmented flow regime used by the authors allowed picolitre droplets to be encapsulated by oil meaning that they did not interact with the channel walls, and moved at a constant linear velocity which reduced residence time distributions. By using the segmented flow method the authors were able to selectively produce different polymorphs. Concentration of reagents of 4 mM and 8 mM produced calcite and vaterite respectively, while 10 mM produced a mixture of vaterite and calcite. The droplets also had a narrower size distribution compared to the other methods investigated i.e. continuous flow microfluidics and

crystallisation from bulk solution. In the continuous flow microfluidics and bulk solution experiments a mixture of vaterite and calcite crystals were formed in all solution concentrations.

Using microfluidics, Teshima et al (2013) developed a method for crystallising a metastable crystal in microdroplets. The amino acid, L-glutamic acid, has two polymorphs, a metastable α form and a stable β form. The α form is usually obtained prior to the β form under rapid cooling, while the β form is obtained prior to the α form under slow cooling. However, as the α form is thermodynamically metastable it is impossible to obtain it alone. The authors used a microdroplet system where crystallisation takes place in an aqueous droplet surrounded by fluorinated fluid (immiscible carrier). Crystallisation of the L-glutamic acid took two hours and Raman spectroscopy confirmed all the samples had formed the metastable α polymorph. After the initial studies on L-glutamic acid, pharmaceutical compounds paclobutrazol, indomethacin and an amino acid L-phenylalanine were also crystallised in the microdroplet system. The crystals formed in these experiments were also confirmed to be the metastable form, by FT-IR spectroscopy for L-phenylalanine, Raman spectroscopy for indomethacin and microscopy for paclobutrazol. Long term stability of the crystals was monitored by FT-IR or Raman spectroscopy. The results indicated no spectral changes for at least three months for L-phenylalanine, and at least five months for paclobutrazol and indomethacin.

Microfluidic protein crystallisation can also be controlled using spontaneous emulsification (Fukuyama et al. 2015). The advantage of using microdroplets for crystallisation is the control of nucleation numbers, however, with a small volume, nucleation also takes a relatively long time. Therefore, in order to improve microdroplet crystallisation for high throughput screening the degree of supersaturation was enhanced by removing water from the protein

solution. The authors reported a simple method to control the rate of water transport which was based on nanodroplet formation by spontaneous emulsification. A microfluidic device made from PDMS with 100 microwells was used. Aqueous microdroplets containing the protein were introduced into the microwells and exposed to a flow of dodecane (organic phase) containing Span 80 which isolated each microdroplet. Nanodroplets were formed at the interface of the microdroplet, which allowed water to be transported from the microdroplet to the nanodroplets. As a result, the concentration of the protein and precipitant in the microdroplet increases and a protein crystal forms. Increasing concentrations of Span 80 were used and the number of crystals in a droplet counted using a CCD (charge-coupled device) camera. As expected, increasing the concentration of Span 80 increased the nucleation frequency. The authors concluded that the rate of water transport from the microdroplets could be controlled by Span 80, which in turn could control the number of crystals formed within the microdroplets. It was proposed that the method could increase the flexibility of a protein crystallisation screening system.

Buanz et al. (2019) studied the crystallisation of D-mannitol in ink jet printed droplets, compared to spray dried droplets. D-mannitol has three known polymorphs; the stable β form (orthorhombic), and the metastable α (orthorhombic) and δ forms (monoclinic). The crystals formed were very small which made analysis by powder X-ray diffraction (PXRD) difficult, therefore the authors used Raman microscopy instead to identify the polymorphic forms. Ink jet printed droplets were found to produce the metastable α and δ polymorphs. Increasing the droplet size predominantly produced the metastable α polymorph. However, the smallest droplets (100 pL) produced the stable β polymorph. In the spray dried samples, the β polymorph was predominant, however, when Eudragit (a polymer) was added the metastable forms were produced. Spray drying with Eudragit

favoured the metastable α polymorph supporting the author's hypothesis that it is a surface induced polymorph. The authors proposed that the crystallisation of D-mannitol polymorphs depends on the presence or absence of surface to favour either the metastable or stable polymorphs.

1.6 Protein crystallisation in magnetic fields

Creating a single large high quality crystal for analysing the three dimensional structure of protein molecules for X-ray diffraction has proven difficult. Challenges to producing a high quality crystal include the initiation of nucleation and reducing the number of nuclei. Research has grown in the use of magnetic fields to influence the nucleation and growth of protein crystals. Sazaki et al. (1997) used a super conducing magnet (Hasebes et al. 1996) to research the effects of a magnetic field on the nucleation and growth of protein crystals. Crystallisation of horse spleen ferritin and hen egg white lysozyme was carried out under a uniform magnetic field of 10 T whilst control crystals were grown under 0 T. The results indicated that the magnetic field reduced the quantity of nuclei, oriented the crystals as well as altering the habit of the protein crystals.

Hen egg white lysozyme was grown in magnetic fields in the range of 0 – 10 T using a superconducting magnet (Yanagiya et al. 1999). The authors report that the degree of orientation depends on the container geometry and the crystal growth rate, in addition to the magnetic field strength.

Using a superconducting magnet with a magnetic field strength of 8 T or 10 T crystallisation experiments were carried out on two proteins; human estrogenic 17b-hydroxysteroid dehydrogenase (17b-HSD1) and snake muscle fructose-1,6-bisphosphatase (Fru-1,6-Pase).

Researchers report improved quality of crystals for both proteins. (Lin et al. 2000).

Sato et al. (2000) crystallised HEWL (hen egg white lysozyme) in high strength magnetic fields. A supersaturated solution was placed in the bore of the magnet and crystals were grown under a homogeneous and static magnetic field of 10 Tesla for 11 days. Their results indicated the magnetic field improved the quality of the orthorhombic crystals, the resolution of the X-ray diffraction increased and so did the dimensions of the unit cell.

Yin et al. (2003) crystallised hen egg white lysozyme in a magnetic field using a 10 T superconducting magnet. Results agreed with previously reported experiments in that the crystals aligned to the direction of the magnetic field. Yin et al. also report that the magnetic field causes differences in the growth rates of faces, which therefore leads to differences in the crystal morphology.

Numoto et al. (2013) used a superconducting magnet to produce steep gradient magnetic fields to crystallise light harvesting complex 2 (LH 2) from a photosynthetic bacterium, *Thermochromatium tepidum*. The light harvesting complex 2 produced rod shaped crystals in the magnetic field and oriented parallel to the magnetic field direction. X-ray diffraction indicated that the crystals had improved R value and mosaicity.

Yin (2015) reviewed recent literature and reports protein crystals that had enhanced crystal quality due to magnetic fields. As well as hen egg white lysozyme examples include; monomeric sarcosine oxidase (Hirose et al. 2007), bovine adenosine deaminase, (Kinoshita et al. 2003) and bacterial UMP kinases (Tu et al. 2007).

1.7 Diamagnetic levitation for protein crystallisation

Since Geim and co-workers (Berry and Geim 1997; Geim 1998) famously levitated a frog there has been increased interest in diamagnetic levitation.

Yin et al. (2008) levitated and crystallized hen egg white lysozyme (HEWL) in a super conducting magnet. The supersaturated solution was levitated in the bore of the magnet at 22 $^{\circ}$C and the crystallisation was captured on a CCD camera installed above the magnet. The researchers found that the crystal would slowly rotate (about 2 degrees per hour), however, the crystals inside the droplet would stay still relative to each other indicating that there was no obvious internal flow. They also discovered that most of the crystals were in the lower half of the droplet. The difference in density and magnetic susceptibility between the solution and crystals meant the crystals didn't cluster together at the bottom, however they were not completely freely suspended either. They reported that levitation may have positive effects on crystal quality and it is well known to be effective for decreasing heterogeneous nucleation. The authors concluded that it was reasonable to expect a positive effect on the levitated crystal quality and that verification was underway in their group.

Wada et al. (2012) used a 16 T super conducting magnet to crystallise protein solutions under quasi - microgravity. The samples were placed in a crystallisation cell in the microgravity zone of the magnet bore and photographs taken every week of the crystal precipitates. The authors summarise that a microgravity environment retards convection and substantially slows the crystallisation of proteins. Preliminary X-ray diffraction analysis suggests crystal quality improvement of protein crystals grown in quasi-microgravity within the magnet bore.

With the increase in interest in high strength magnetic field work Okada et al. (2013) developed a protein crystal formation system within a superconducting magnet. Using magnetic fields strong enough to compensate gravity samples were crystallised in the magnet bore within crystallisation cells. The crystallisation cells were temperature controlled between 4 and 20 $^{\circ}$C and the system had observational equipment to allow in situ monitoring of the protein solutions. The experimental set up was able to exert high magnetic forces on the proteins and also reduce convection in the solutions. By carrying out numerical simulation analysis the authors showed that the magnetic force does suppress convection.

1.8 Processing of materials using magnetic levitation

Using a hybrid magnet consisting of a superconducting magnet and water cooled magnet Tagami et al. (1999) levitated and solidified water. Images were captured by a micro-CCD camera inside the magnet bore and include; the droplet before solidification, the initial solidification creating an ice shell, the appearance of inner water at the top of the ice shell and the appearance of bubbles of dissolved air. The researchers report their method could be applied to crystal growth from levitating solutions in a magnetic field.

Motokawa et al. (2001) crystallised ammonium chloride (NH_4Cl) and melted glass using magnetic levitation. Using a hybrid magnet NH_4Cl solution was levitated at 18.1 T and 20 T. It is reported that crystallisation in the levitating droplet reduces the number of crystals grown which implies a decrease in heterogeneous nucleation which usually occurs due to container walls. During the 18.1 T experiment crystallisation grows along the surface of the droplet due to the sedimentation of the nucleus at the bottom of the droplet. This is

attributed to the liquid gas interface suggesting that mass transport at the interface is larger than the bulk solution. A second observation is that the magnetic susceptibility of NH_4Cl is smaller than that of water meaning the crystal sediments in the droplet. However, in the 20 T experiment the magnetic force acting on the NH_4Cl crystal is upwards and the crystal grows on top of the droplet. This is reportedly the first example of sedimentation of a crystal at the top of a solution.

Magneto – Archimedes levitation can be used to create large polymer spheres (Yamato et al. 2002). The usual method for creating polymer spheres is by suspension and emulsion polymerisation. However, difficulties arise in producing larger droplets as increasing the size relies on a stable suspension of monomer and a resulting high sphericity which becomes difficult to attain as the droplet size increases. Spheres produced by suspension and emulsion polymerisation are usually in the μm range, however using magneto - Archimedes levitation spheres in the range of 7-9 mm were created. Magneto – Archimedes levitation involves using a paramagnetic gas or liquid instead of air, allowing more moderate strength magnetic fields to be used due to the magnetic buoyancy given by the paramagnetic gas/ liquid in addition to the magnetic repelling force directly acting on the levitating particle. The monomer used in this study was benzyl methacrylate (which is diamagnetic) and the aqueous solution (suspending liquid) used was manganese chloride (which is paramagnetic) to create large polymer spheres.

Strong magnetic fields can be used in conjunction with vertical vibrations to separate binary granular mixtures. Catherall et al. (2005) were able to separate out millet seeds and small insulating beads (both with a diameter of 2 mm) using a loud speaker to vibrate the seeds and beads vertically whilst in a strong magnetic field. Both the millet seeds and small insulating beads are weakly diamagnetic. When the beads and seeds are vibrated for 300 seconds with zero

magnetic field separation is poor. When the beads and seeds are vibrated in the upper part of the magnet bore separation is complete with the millet seed above the beads which is explained by effective gravity where the component with the lower effective gravity lies above the component with the higher effective gravity. A third experiment sees the beads and seeds being vibrated in the lower part of the magnet bore, separation is complete but this time the millet seed is lying below the beads. The component with the lower effective gravity once again lies on top of the lower section.

Biological specimens can be levitated and moved by magnetic traps by taking advantage of the natural diamagnetism of virtually all biological specimens. Using a superconducting solenoid Coleman et al. (2007) levitated yeast cells using a magnetic field strength of 4.1 to 8.5 T. Results indicate that gravity effects gene expression, whilst the magnetic field changed the yeast growth rate, which can also be linked with changes in the cell cycle and gene expression.

Using magnetic levitation Mirica et al. (2009) set up a system to measure the densities of solids and water immiscible organic liquids < 1 mL. The method used two permanent magnets positioned with like poles facing each other, between them a container with a paramagnetic solution of manganese chloride dissolved in water. The sample was then placed into the container and the density calculated depending on the position of the sample in the device relative to the bottom magnet. As gravitational and magnetic forces determine the vertical position of the sample, knowing this position allows the density to be calculated. Very small samples sizes can be analysed by this method making it well suited for calculating the density of resource limited samples. Mirica et al. (2010) also used the same experimental set up to analyse water and food samples. The magnetic levitation device was used to estimate the salinity of water and to compare the contents of fat in cheese, milk and peanut butter.

Diamagnetic levitation can be used to levitate droplets of water and Hill and Eaves (2010) investigated the vibrations of a levitated droplet by measuring the frequencies of small amplitude shape oscillations. The levitating droplet levitated in a magnetogravitational potential trap and as such the restoring forces of the trap acted on the droplet surface, in addition to the surface tension increasing the frequency of the oscillations.

Liquid bacterial cultures can be levitated using diamagnetism and Dijkstra et al. (2011) investigated the effect of levitation on liquid bacterial cultures. *Escherichia coli* (Gram-negative) and *Staphylococcus epidermidis* (Gram-positive) were levitated by a 17 T superconducting magnet. The samples were levitated in a nutrient liquid broth and the bore of the magnet was kept at 37 °C by forced air flow. A reduction in sedimentation of the cells is observed and an increase in the population growth rate. Microarray gene analysis indicated that the increased growth rate is due to enhanced oxygen availability. Researchers propose that the paramagnetic force on dissolved oxygen can cause convection around the liquid culture enhancing the oxygen availability to the cells.

Previous studies on the common fruit fly *Drosophila melanogaster* during Earth's orbit have shown that it walks more quickly and frequently during microgravity compared to its travels on Earth. However, the fruit flies were subject to physical and environmental changes during launch making it difficult to expose the control flies to the same changes. To address this Hill et al. (2012) studied the motions of *D. melanogaster* in a pseudo-weightless environment, pseudo-hypergravity environment and a normal environment using a strong magnetic field produced by a superconducting solenoid. Compared to the 1g* (* indicates the presence of a strong magnetic field) experiment the fruit flies had a greater mean speed in the 0g* experiment, and smaller mean speed in the 2g* experiment. The

distanced (mean-squared) travelled by the fruit flies grew more quickly with time in the 0g* experiment than in the 1g* experiment and slower in 2g* experiment. Comparing the weightlessness produced by diamagnetism to the weightlessness produced by an orbiting spacecraft the researchers identify the cause of the fruit flies behaviour as altered effective gravity.

The effects of a diamagnetic levitation on the common fruit fly *Drosophila melanogaster* were investigated by Herranz et al. (2012). Using a superconducting magnet, fruit flies were levitated for up to 22 consecutive days. A delay in the fruit flies development was seen from embryo to adult fly. Imagoes that developed from larvae under hypergravity and levitation conditions had changes in gene expression when analysed by microarray. Significant changes were observed in the expression of temperature-, immune-, and stress-response genes. Exposure to a strong magnetic field produced similar effects to the genes expression independent of the hypergravity/ levitation conditions.

Magnetic levitation can be used to separate out mixtures of different crystal polymorphs. Using two fixed magnets with like poles facing each other and a paramagnetic solution between them Atkinson et al. (2013) were able to separate polymorphs of four different compounds, *trans*-cinnamic acid, sulfathiazole, carbamazepine and 5-methyl-2-[(2-nitrophenyl)amino]-3-thiophenecarbonitrile (ROY). The benefits of using magnetic levitation to separate polymorphs is that different packing arrangements of molecules in the crystals can often result in different densities for the different polymorphs allowing easy separation and the method is non-destructive.

Magnetic levitation is not just beneficial for crystallisation experiments as Tseng et al. (2014) used magnetic levitation to make a three dimensional co-culture model of the aortic valve. The aortic

valve co-cultures consisted of valvular interstitial cells and endothelial cells which were assembled using magnetic levitation and cultured for three days. The model created will serve as a basis to future experiments to help understand biology of the valve.

Diamagnetic levitation can be used to study the formation of tektites; glassy stones which form from molten rock ejected from asteroid impacts Tektites often have a dumb-bell shape due to their rotation mid-flight before solidification. Using a superconducting magnet Baldwin et al. (2015) levitated liquid wax and spun the droplets using air from two air nozzles placed in the magnet bore. Comparison of the tektite dimensions with numerical models shows good agreement.

Using a MagLev (magnetic levitation) device Matheys et al. (2016) were able to separate out crystals from cocrystals. The MagLev device consisted of two magnets with like poles facing each other and an aqueous paramagnetic solution between the magnets, for example manganese chloride. Cocrystals of carbamazepine and salicylic acid and conformer crystals of salicylic acid were separated by the MagLev device. In a second experiment they separated cocrystals of carbamazepine and camphoric acid and coformer crystals of camphoric acid. Results indicate that diamagnetic levitation is efficient in separating pure coformer crystals from the cocrystals.

Diamagnetic levitation can be used to investigate the stability and shape of free electrically charged and spinning liquid droplets Liao and Hill (2017). Using a superconducting magnet droplets of water/ tertbutanol and ethanol were levitated and charged by using a thin grounded wire. In addition to Taylor cone-jet fission and binary fission it is observed that an unusual mode occurs which appears to be a hybrid of the two.

1.9 Processing of materials using high and low magnetic fields

Torbet et al. (1981) were able to orient fibrin fibres within gels by polymerising in strong magnetic fields of up to 18 T. Comparing scanning micrographs of the polymerised fibres formed in the strong magnetic field and the control (no magnetic field) it is was demonstrated that the fibrin gels orientated parallel to the magnetic field.

Multi-walled carbon nanotubes can be aligned by strong magnetic fields (Kimura et al. 2002). Using magnetic fields of 10 T Kimura *et al*. were able to align the carbon nanotubes in a monomer solution of unsaturated polyester resin, and then polymerise the monomer matrix. Using analytical techniques such as electrical conductivity, elastic modulus measurements, and transmission electrical microscopy (TEM) they confirmed that the multi-walled carbon nanotubes were aligned parallel to the magnetic field in the matrix.

With the help of magnetic nanoparticles carbon nanotubes can also be aligned by low magnetic fields (0.2 T). Correa-Duarte et al. (2005) deposited layers of magnetite/ maghemite nanoparticles on carbon nanotubes using polymer wrapping and layer by layer assembly. When in a zero field, the magnetic moments of the nanoparticles pointed in random directions meaning there was no overall net magnetisation. However, when the magnetic field was applied, the magnetic moments of the nanoparticles aligned and the carbon nanotubes reoriented and formed chains of nanotubes.

Strong magnetic fields can also be used to align aromatic peptide tubes. Hill et al. (2007) investigated the alignment of FF tubes in a strong magnetic field. FF is a diphenylalanine motif of the Alzheimer's disease β-amyloid polypeptide. The FF tubes were suspended in a

HFIP-water solution (1, 1, 1, 3, 3, 3,-hexafluoro-2-propanol – water solution) and a substrate coated with a droplet of solution left to dry whilst held in a 12 T magnetic field. The peptide tube coated orifices where then analysed by AFM (atomic force microscopy). In the 0 T images there was no overall alignment and the same was observed with the 3 T sample. However the 7 T and 12 T images indicated that the tubes align with their long axis parallel to the magnetic field.

Supramolecular chirality can be selected using gravitational, rotational and orienting forces during self-assembly (Micali et al. 2012). Most biological molecules only exist in one enantiomer as left or right handed forms and it was shown that this can be selected by using magnetic forces. Using J-aggregates of achiral tris-(4-sulfonatophenyl)phenylporphyrin ($TPPS_3$) and magnetic field strengths of up to 25 T the authors investigated selective chirality. Samples of aggregating $TPPS_3$ solution were placed in vials in a magnet bore, and rotated clockwise or anticlockwise at a fixed frequency, temperature and field strength. Once the experiment was complete the samples were left to stand for three days. Magnetic and rotational forces generated an external chiral influence which caused the $TPPS_3$ to self-assemble. Over time the small nano-assemblies (short helices) grew into larger chiral structures. Depending on the symmetry of angular momentum (either clockwise or anticlockwise rotation) and the effective gravity the system grew into left or right handed aggregates.

High strength magnetic fields have been used to orient polymer stabilised liquid crystals (PSLC). Polymer stabilised liquid crystals consist of a polymer mesh and a continuous liquid crystal phase. The purpose of the polymer mesh to assist in the alignment of the liquid crystalline bulk by acting as an anchor. The macroscopic order in polymer stabilised liquid crystals depends on two effects; the order parameter and the domain order parameter. The domain order

parameter is induced by external stimuli for example electric fields, magnetic fields and substrates, and the order parameter is given by the temperature. Fernandez et al. (2015) studied thick polymer stabilised liquid crystals that were unsuitable for substrate interactions, and used magnetic fields for the alignment instead. Using 4-octyl-4'-cyanobiphenyl based crystal polymer liquid crystals they showed how the magnetic field and temperature can influence the overall order parameter. Samples polymerised in magnetic fields in excess of 5 T and at room temperature were optimal for macroscopic alignment.

Using magnetic fields it has been shown that it is possible to direct peptide assembly in liquid crystal templates. The advantages of using magnetic fields are that it is a non-contact method that applies to all shapes and sizes, whilst the liquid crystal template also provide high magnetic susceptibilities. van der Asdonk et al (2016) used a magnetic field to align peptide amphiphiles in a lyotropic chromonic liquid crystal template. The peptide amphiphiles self-assembled in the aqueous liquid crystal template and as time elapsed they bundled into micron – millimetre sized structures. The magnetically responsive lyotropic chromonic liquid crystal template was found to reduce the magnetic field required for alignment by 10 fold. The authors proposed that this magnetic field reduction for alignment opens up the possibility to create more complex structures at higher magnetic fields. The method may have the potential to make complex structures of functional soft matter.

Stopin et al. (2016) created an anisotropic organogel, formed using magnetic fields to align polymeric organogels. Applying a magnetic field during the gelification of poly(3-hydroxybutyric acid-*co*-3-hydroxyvaleric) acid in toluene an anisotropic organogel was created. The authors proposed there are two alignment steps in the process; in the liquid phase and during gelification. Using low magnetic fields

of 2 T the fibres in the material could be aligned giving the organogel the property of birefringence. The organogel was also found to be anisotropic, changing from transparent to opaque upon rotation of a polarizer.

1.10 Containerless processing of pharmaceuticals

Containerless methods have allowed research into non equilibrium forms that cannot be made by other means, which often have novel structures. These methods also can be used to investigate high temperature melts and glasses (Price 2010; Weber et al. 2012). Recent developments also include acoustic levitation experiments on supercooled liquids made from pharmaceutical and organic substances. Acoustic levitation experiments can also be used to research low temperature supersaturated solutions (Weber et al. 2012).

Active pharmaceutical ingredients with poor solubility can lead to reduced efficacy of medication. However, bioavailability and solubility can be increased by vitrification (Willart and Descamps 2008; Kawakami 2009). In 2011, Benmore and Weber (2011) used acoustic levitation to develop a method for synthesizing pharmaceuticals in the amorphous form. The proof of concept method was demonstrated for several drugs with different glass forming abilities. The developed method was used to investigate the ability of the acoustic approach to produce amorphous forms of different drugs; the two main variations on the method were explored including laser heating and solvent evaporation. Ibuprofen, dibucaine, clotrimazole, ketoprofen, were dissolved in ethanol and probucol in acetone, and the solutions introduced into the acoustic levitator by a 1 mL syringe. A high energy X-ray diffraction beamline was used to analyse the structure of the starting materials, the samples produced from the levitator and

monitor the evaporation progress. As high energy X-rays are very sensitive to glass formation they could accurately determine the amount of amorphous material to within approximately 0.2% compared to a few percent using a laboratory X-ray source. Benmore and Weber observed that as the levitated liquids evaporated a supersaturated solution formed, which lead to the formation of a viscous amorphous gel. To preserve the amorphous form the gels were quenched in a small volume of liquid nitrogen. The cold solid sample(s) were then recovered, re-levitated and whilst re-warming to room temperature in situ X-ray measurements taken. Ibuprofen, clotrimazole, clofoctol and ketoprofen remained amorphous despite the cryogenic temperatures, indicating that they could be stored at low temperature. The dibucaine and probucol shattered upon immersion in liquid nitrogen and dibucaine fragments were found to be crystalline.

The second method applied by Benmore and Weber (2011) involved the levitation of solid crystalline pharmaceutical compounds which were heated by a CO_2 laser beam whilst levitating. The melted levitating droplets were then repositioned out of the laser beam where they cooled and formed glassy or partially glassy solids. For a non-levitated comparison the same pharmaceutical compounds were heated by a laser in a copper hearth; under these conditions all the samples formed polycrystalline forms. Miconazole nitrate, carbamazepine and cinnarizine when levitated and heated were found to be fully vitrified, whereas the non-levitating samples left to cool in containers formed the crystalline form.

In summary, the levitated melt quenched carbamazipine and cinnazirine remained completely amorphous for a minimum of four months. However, clofoctol crystallised out within a few weeks and dibucaine a few minutes. The authors propose that their levitation technique offered a new route to processing amorphous materials.

Weber et al. (2012) published an article that briefly reviewed the advances made in acoustic levitation and presented more details on their levitation experiments. They demonstrate that acoustic containerless methods can produce amorphous ibuprofen and carbamazepine; these are both low molecular weight drugs which are typically hard to vitrify and usually form unstable glasses. Work was therefore in progress to investigate the stability of the amorphous materials made and to investigate the addition of stabilizers to composition.

Rehder et al. (2013) were able to acoustically levitate particles and monitor the real time solid state phase transformations by using NIR (near infrared) and Raman spectroscopy. Prior to levitation they created amorphous ibuprofen by quench cooling (heating the material until molten and then quickly cooling it by pouring into liquid nitrogen). The authors then levitated a single amorphous glassy state ibuprofen particle in an acoustic levitator. At ambient temperature the particle transformed from the glassy state to a rubbery state and then recrystallized within a few minutes. NIR and Raman spectroscopy tubes were placed near to the levitating droplet to obtain spectroscopic data. The authors showed that acoustic levitation in combination with Raman spectroscopy, NIR and MCR (multivariate curve resolution) are valuable for monitoring solid state phase transformations. Raman spectroscopy was beneficial as it gave an insight to recrystallization on the molecular level, whereas NIRs could give an estimation of recrystallization kinetics. MCR data analysis was a useful tool in the analysis of the results; despite the small sample size and poor signal to noise ratio.

Using acoustic levitation Leiter et al. (2008) followed the crystallisation of vitamin c and aspirin as it crystallised from a levitating saturated solution. By using in situ X-ray diffraction the authors were able to monitor the crystallisation of the droplets.

In conclusion, several different groups have looked at diamagnetic levitation for improving protein crystal quality/ growth, which are promising. However, little research has been carried out on the crystallisation and amorphisation of pharmaceuticals using diamagnetic levitation. Benmore and Weber (2011) have recently carried out research on the amorphisation of pharmaceuticals using acoustic levitation. However, acoustic levitation has limitations such as the size of sample that can be levitated. Therefore, in this thesis we intended to explore the fundamentals of crystallisation by using diamagnetic levitation as a way to control the environment. Diamagnetic levitation has the potential to levitate much larger droplets than acoustic levitation which can only levitate droplets/ samples with diameters no more than half the size of its wavelength (typically 5 mL to 5 µL). Unlike crystallisation in droplets within a microfluidic device, there is no need for a surfactant or oil to emulsify the droplet as it floats freely when levitated by diamagnetism. Using the magnet set up at the University of Nottingham different parameters such as the air flow and temperature within the magnet bore can also be controlled. The crystallisation process can also be monitored with cameras and mirrors in-situ giving a unique insight to the crystallisation process in diamagnetic levitation. We intended to also explore containerless crystallisation of pharmaceutical compounds using diamagnetic levitation.

Research into the effects of high and low magnetic fields on different materials has been undertaken by several different groups For example, peptide nanotubes can be aligned by high strength magnetic fields (Hill et al. 2007) and more recently magnetic fields have been used to crystallise a different polymorph of coronene; a polycyclic aromatic hydrocarbon (Potticary et al. 2016). Little research has explored the effect of high/ low strength magnetic fields on the polymorph formation of different pharmaceuticals, so in the

later part of this thesis (chapter 6) magnetic fields for polymorph selection is explored.

1.11 Aims

The aims of this thesis were to investigate the use of diamagnetic levitation as a containerless crystallisation technique to study the fundamentals of crystallisation. We aimed to explore the crystallisation, amorphisation and polymorphism of pharmaceutical compounds. We also intended to explore changing the physical properties of the droplet, for example the pharmaceutical compound used, the concentration of the drug, the volume of the droplet and the solvent used. As well as physical conditions we aimed to change the environmental conditions, for example the strength of the magnetic field, temperature of the magnet bore along with the nitrogen/ air flow used. A secondary aim was to investigate the potential of high and low magnetic fields for the formation of pharmaceutical polymorphs which involves crystallisation at a fixed point in the centre of the bore i.e. not levitating.

The work herein discusses the experimental methods performed in this thesis. The experimental configurations of the magnet system at the University of Nottingham and analytical techniques/ methods are described in more detail. Chapter 3 focuses on creating reference materials and spectra for each pharmaceutical compound. For example, producing amorphous versions and different polymorphic forms of the pharmaceutical compounds to be studied. Once the amorphous/ polymorphic forms had been produced they were analysed using different analytical techniques. The analytical techniques employed include DSC, FT-IR (ATR) and handheld Raman. Chapter 4 is a proof of concept chapter where the levitation of paracetamol solutions is explored. A secondary aim was investigating

diamagnetic levitation for polymorphic control i.e. was it possible to selectively create form II paracetamol in the magnet? In chapter 5 we explored the use of diamagnetic levitation for the amorphisation of clotrimazole These initial experiments were compared to the acoustic levitation work carried out by Benmore and Weber (2011). Chapter 6 explores low strength magnetic fields for polymorph selection. Pharmaceutical compounds paracetamol, clotrimazole, propranolol and the polyaromatic hydrocarbon coronene are crystallised in the magnet bore under low strength magnetic fields. In chapter 7 the results are discussed and future work suggested.

2 Instrumental methods

2.1 Experimental configurations

2.1.1 The magnet system at the University of Nottingham

Within the Mag Lev lab at the University of Nottingham there are two superconducting magnets. The first magnet, the Cryogenic (Cryogenic Ltd, London), has been used for most experiments performed within this thesis. The cryogenic magnet is an 18.5 T (185,000 Gauss) superconducting solenoid magnet. The magnet has a vertical 58 mm diameter bore that is kept at room temperature due to insulation from the liquid helium coolant at 4K (-269.15 °C). Figure 2-1 shows the laboratory with the Cryogenic Ltd superconducting magnet in the centre.

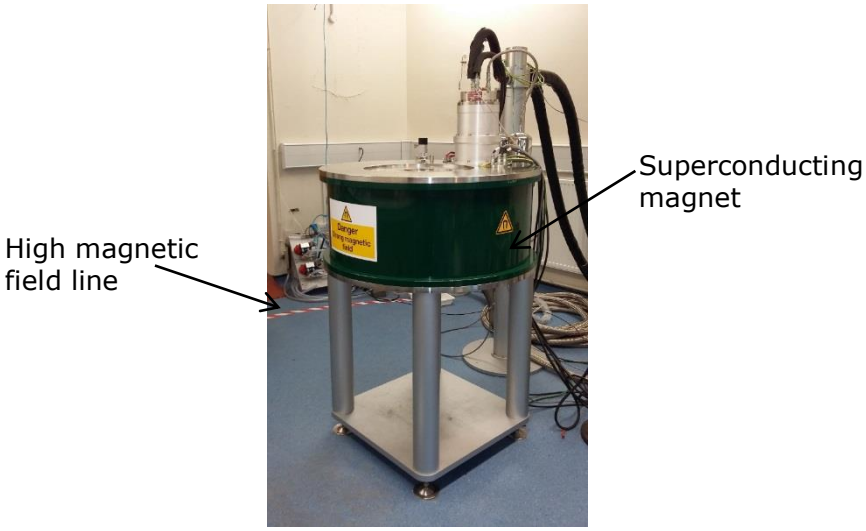

Figure 2-1 The Cryogenic Ltd superconducting magnet based in the Mag Lev lab at the University of Nottingham. The red and white tape on the floor denotes the 30 Gauss field line, and no magnetic objects are permitted within this circumference.

The second magnet within the Mag Lev lab is the Oxford magnet (Oxford Instruments, Abingdon, UK), which like the Cryogenic

magnet is a superconducting solenoid magnet. The solenoids are cooled by liquid helium and are contained in a thermally insulated vessel. The Oxford magnet can support a field of 17 T (170,000 Gauss).

2.1.2 The bore insert for the Cryogenic magnet

As explained in section 2.1.1 the Cryogenic magnet has a vertical bore where the levitation experiments are performed. To control the temperature of the bore, a bore insert was designed and made by the technicians working within the School of Physics at the University of Nottingham. The bore insert was connected to a thermostatically controlled (GR150; Grant Instruments (Cambridge) Ltd., Royston, UK) 20 L water bath (R4 series refrigerated circulating bath, Grant Instruments, (Cambridge) Ltd, Royston, UK) using foam lagged polypropylene tubing which connected to the bottom of the bore insert (Figure 2-2). Connecting the bore insert to a water bath with an external pump allowed water to flow around the bore insert and back into the water bath allowing the temperature of the bore insert to be maintained.

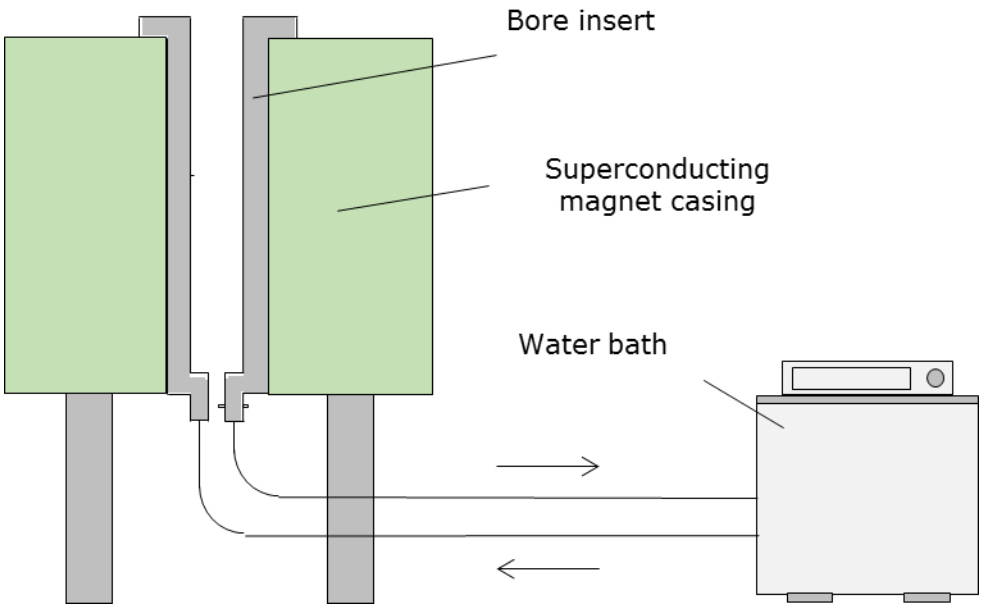

Figure 2-2 A schematic of the bore insert set up within the magnet bore. The bore insert was connected to a water bath using foam lagged polypropylene tubing which allowed the temperature of the bore insert to be set at the required temperature.

2.1.3 Collection devices and sample holders

In chapter 4 paracetamol solutions were levitated and over time as evaporation occurred paracetamol crystals formed. Once the crystals were too heavy for the magnetic field to levitate they would fall out of the solution. To collect the crystals a collection device consisting of a plastic petri dish (35 mm diameter), and a non-magnetic pole was created. The petri dish was modified by cutting a large circle hole in the lid, leaving just the rim, allowing filter paper to be held in place when in the centre of the bore. A small amount of sticky tape would sometimes be required to hold the plastic rim in place as it had a tendency to levitate when in position. For aqueous samples the petri dish was filled with silica gel (self-indicating, BHD, Poole, England) and covered with a layer of filter paper (Schleicher & Schuell, Whatman, UK). For ethanolic samples tissue paper was used instead of the silica gel. The petri dish, contents and lid were placed into the

petri dish holder and inserted into the bore insert before performing a levitation experiment (Figure 2-3 a).

In chapter 6 low field experiments are undertaken, which involved placing the pharmaceutical solutions in a cuvette within the magnet bore whilst evaporation and crystallisation occur. A cuvette holder was designed by cutting a small square with rounded edges in a non-magnetic metal plate which was then attached to a non-magnetic pole (Figure 2-3 b).

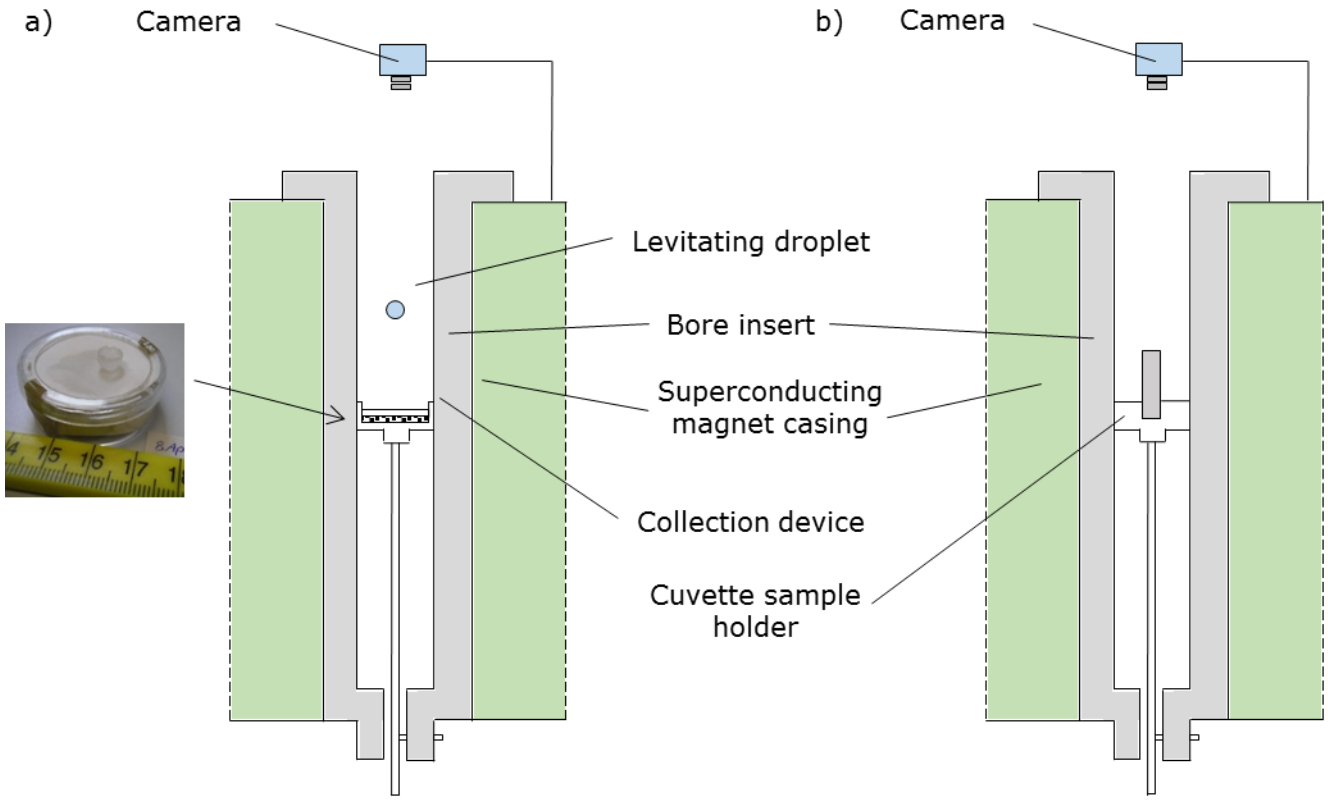

Figure 2-3 (a) A diagram of the petri dish sample collector within the magnet bore insert (b) A diagram of the cuvette holder within the magnet bore insert.

2.1.4 Apparatus to observe levitating droplets

In chapters 4 and 5 levitating droplets are filmed from above (bird's eye view). A Fire-i digital camera (Unibrain S.A., Athens, Greece) was mounted on a clamp stand above the magnet bore to allow imaging from above of the levitating droplet. The camera was modified to allow it to be used in close range of the magnetic field, by removing non-essential ferromagnetic parts, such as screws, and replacing them with brass equivalents. The firewire cables were also stripped of non-essential magnetic parts.

To image the droplet from the side (chapter 5) a 25 mm^2 mirror (Melles-Griot, Carlsbad, California) was attached to a 45° nylon wedge. The nylon wedge was attached to an aluminium ruler (Wickes, Northampton, UK) and was lowered down into the bore of the magnet, being held in position (just below the levitation point of the droplet) by a clamp stand (Figure 2-4).

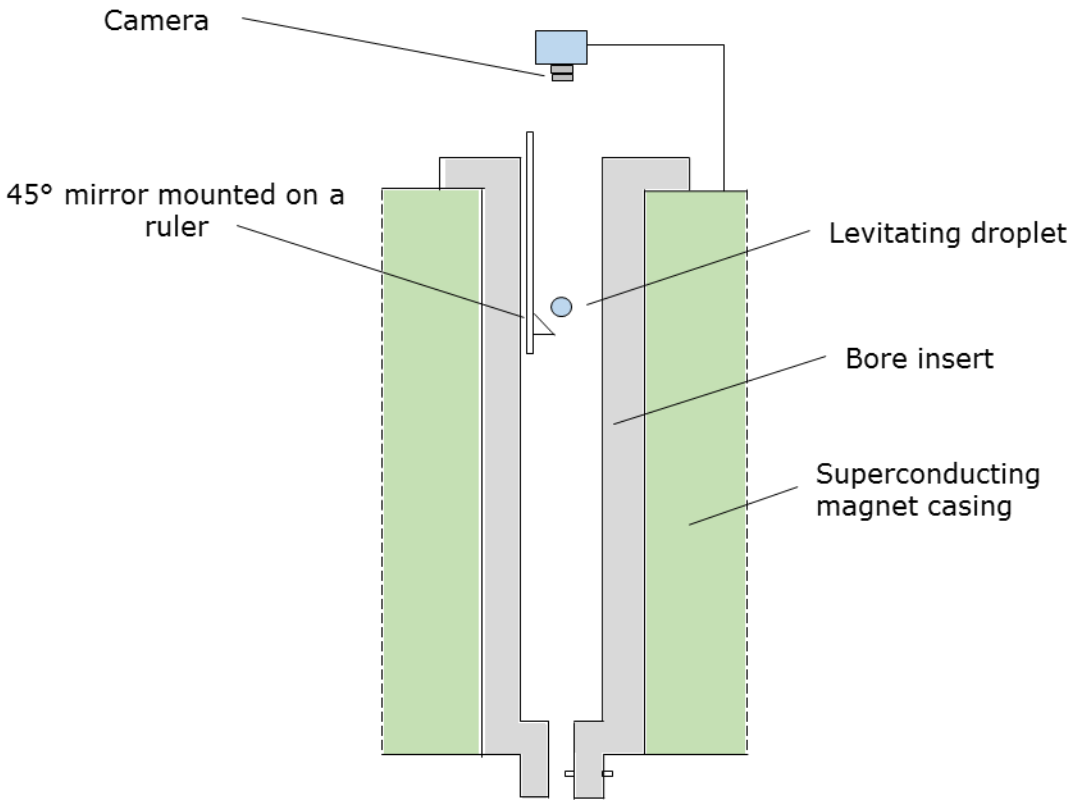

Figure 2-4 A diagram of equipment used to film the levitating droplets from the side (using a 45° mirror carefully positioned under the levitating droplet).

2.1.5 Air/ nitrogen flow in the magnet bore

Initially air or nitrogen was blown in an upward direction into the magnet bore. The set up consisted of attaching the air/ nitrogen line, controlled by an airflow meter gage (Cole-Palmer, St. Neots, UK) to the bottom of the petri dish sample holder's non-magnetic pole. The non-magnetic pole was hollow and had holes drilled into it to allow airflow to reach the droplet. This set up has been named set up 1 and is displayed in Figure 2-5.

Set up 1

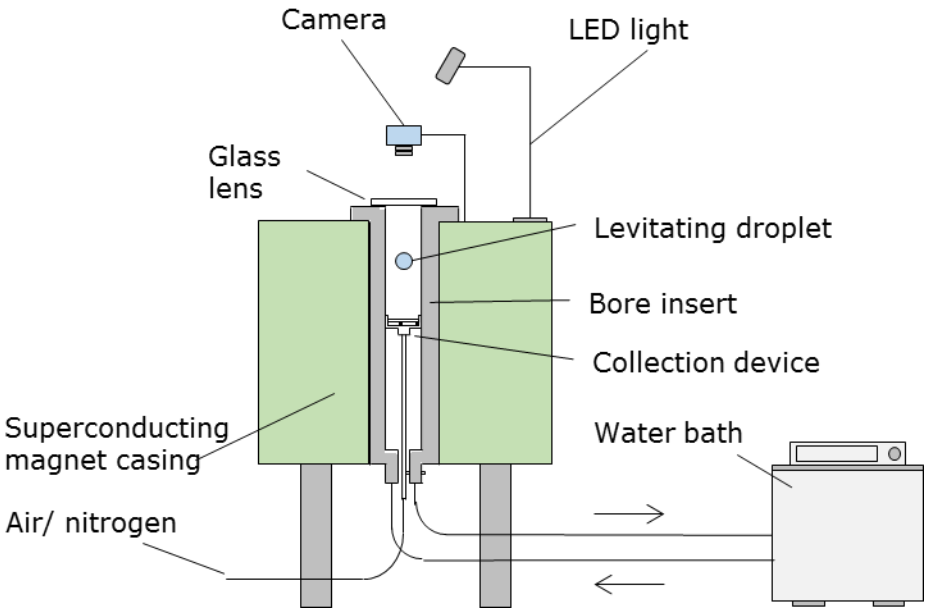

Figure 2-5 Schematic diagram of set up 1 with the air/ nitrogen line attached to the bottom of the petri dish sample holder pole, which is hollow to allow the air to flow around the droplet.

For later experiments where keeping the droplets free from dust, which could cause unwanted nucleation was a priority a Perspex box was designed to sit on top of the magnet covering the magnet bore. The Perspex box had an inlet to allow compressed air or nitrogen to be blown into the box keeping it at a positive pressure. This set up has been named set up 2 (Figure 2-6).

Set up 2

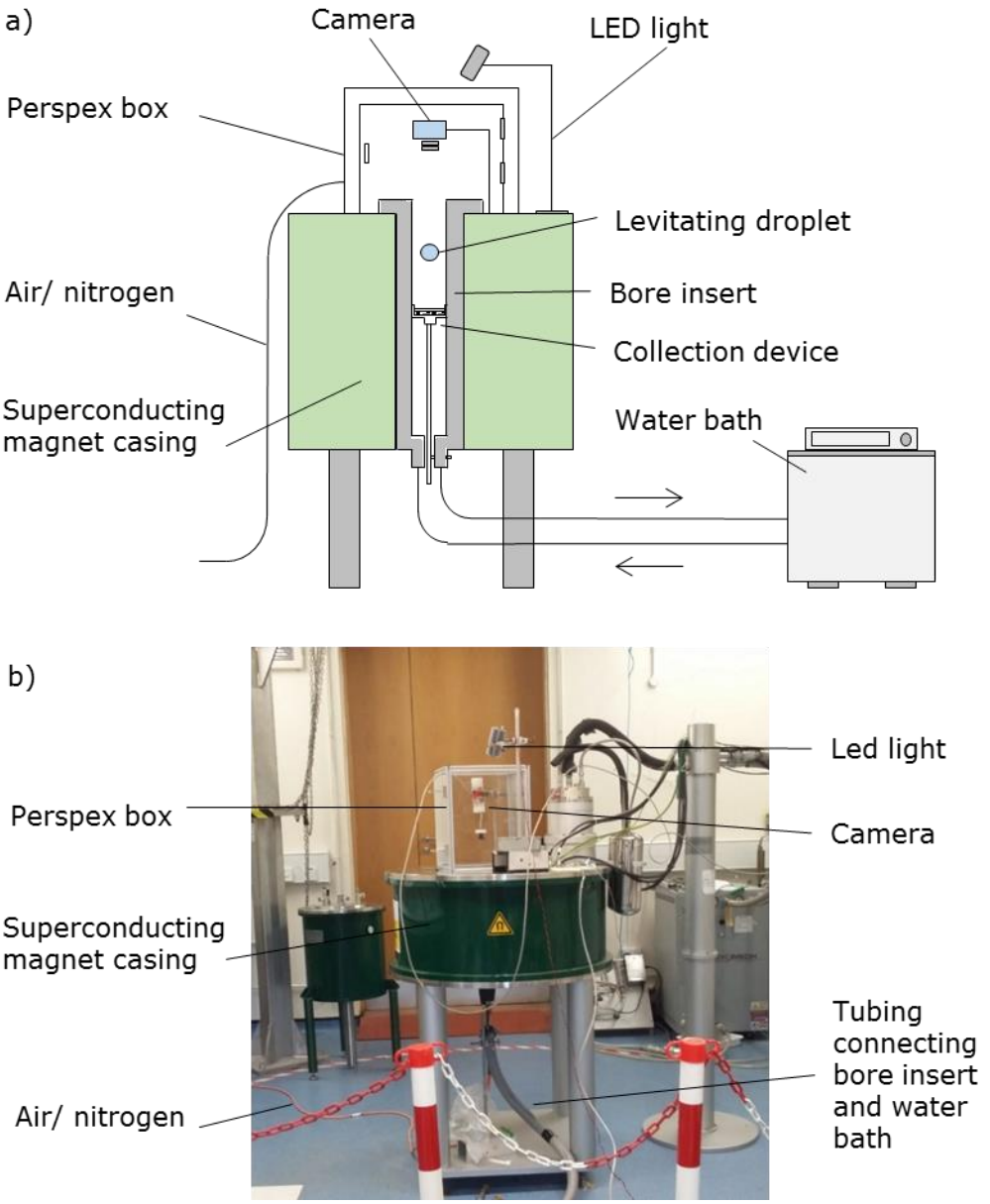

Figure 2-6 (a) A schematic diagram of set up 2 which includes the Perspex box on top of the magnet along with the air/ nitrogen line attached to the inlet on the box (b) A picture of the magnet set up.

2.2 Analytical techniques

In most levitation experiments (chapter 4 and 5) a droplet consisting of a pharmaceutical drug in solution is levitated until the drug crystallises, and for comparison a control sample is also crystallised out (usually in a Falcon tube). The samples are then analysed by DSC, FT-IR (ATR), handheld Raman and optical microscopy, which is summarised in Figure 2-7.

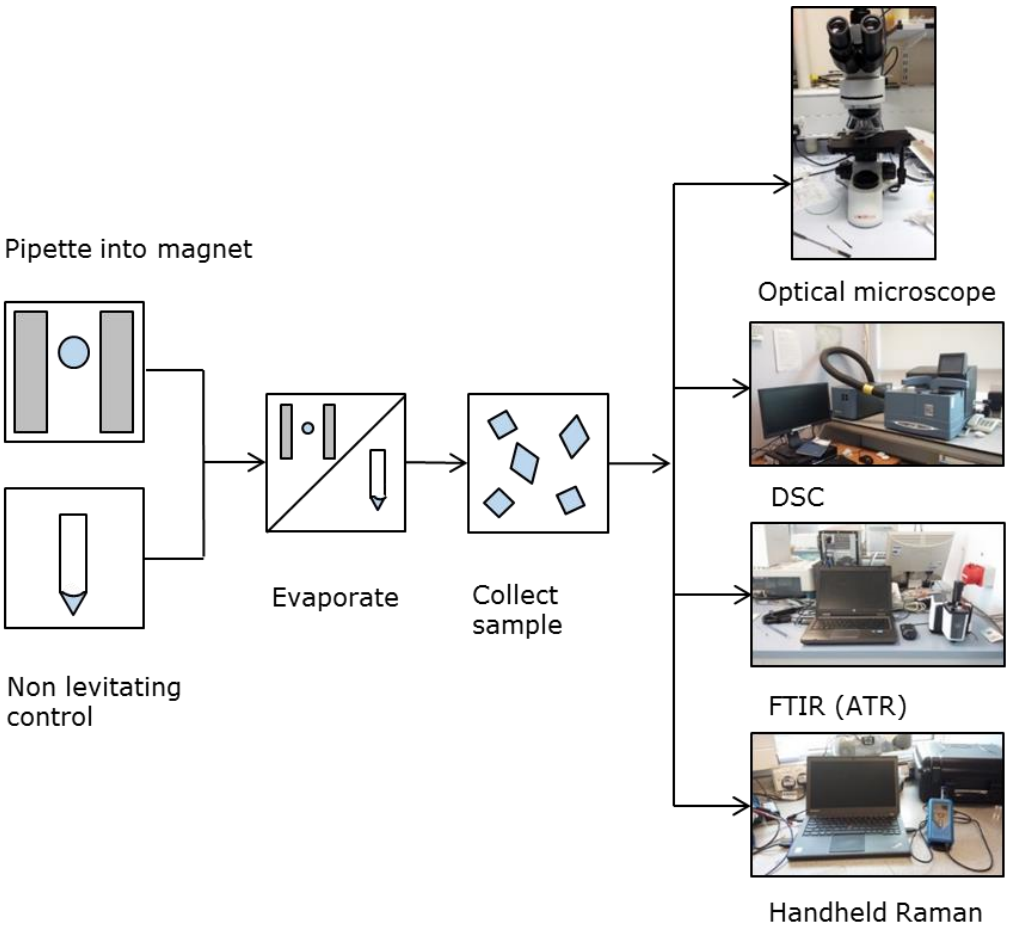

Figure 2-7 A flow chart of the method for collecting crystals from levitating and non-levitating samples and analytical methods used.

2.2.1 Optical microscopy & polarised light microscopy theory

Using a two-step magnification process an optical microscope can attain magnification of 1000x or more. The optical microscope contains two lenses; the objective and the eyepiece. The sample is loaded on to the microscopes stage (which moves up and down to focus the sample) positioned below the objective; which is a converging lens with a relatively short focal length. The objective creates a magnified real image that is further enlarged by the eyepiece. Commonly the microscope will have a prism that bends the light path so that the eyepiece is at a comfortable angle (Knight 2008).

An optical microscope uses white light which vibrates in all directions and can be seen by the human eye. However, a polarising microscope uses polarised light which vibrates in one direction only and cannot usually be seen by the human eye.

A polarised microscope is beneficial when viewing birefringent anisotropic materials. An anisotropic material is one that has two refractive indices and does not have the same optical properties in all directions. For comparison isotropic materials, for example most gases and liquids, have the same optical properties in all directions (i.e. they have one refractive index).

Many optical microscopes can be modified to view samples with cross polarised light (when the polarisation directions of the analyser and polariser are 90° apart producing extinction (no light)) (see Figure 2-8). The polariser can be manually rotated and is usually located in the light path beneath the sample, usually below the microscope stage. The filter is aligned horizontally, with the particles it is composed of arranged in one direction only. The polariser therefore only lets light through that is vibrating along its polarising axis and

absorbs light that is traveling in other directions. The analyser is a second polariser that slots in between the eye pieces and the objective lenses, it is aligned vertically.

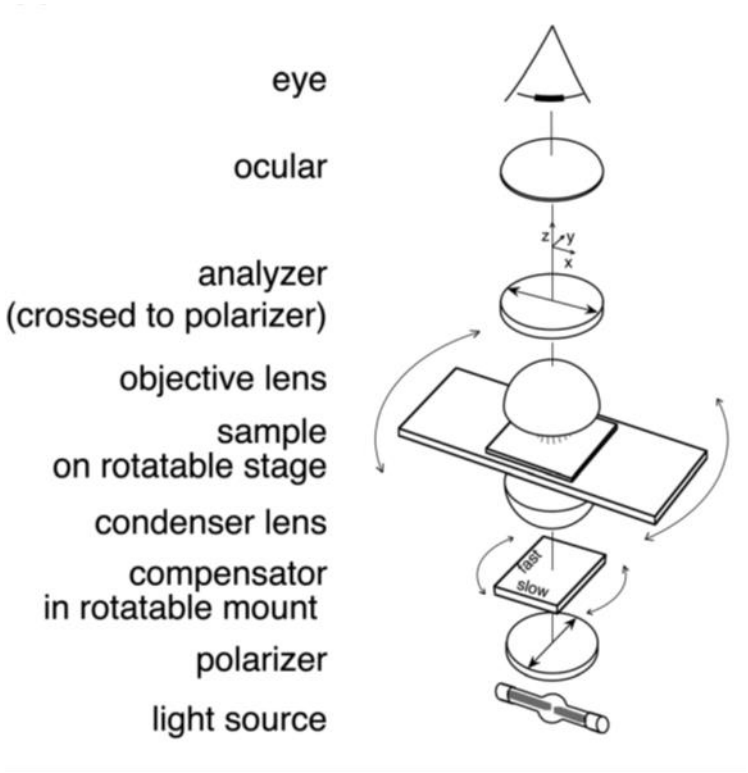

Figure 2-8 Schematic diagram of a conventional polarising microscope. Image taken from Koike-Tani et al. (2015).

The microscope's light source light travels upwards, however the polariser will absorb any light that is not travelling along the polarisation axis. The light will then travel through the sample and up to the analyser which if set at a position 90° to the first polariser (e.g. they are crossed polarisers) will block any light that is not traveling in its own polarization axis, which is 90 ° to the first filter. After travelling through both polarization filters the viewer therefore only sees darkness.

Materials such as crystals, minerals and fibres can be identified using polarised microscopy. When the polarisers are aligned at 90° to each other no light is able to pass through, however, adjusting the angle of the polariser allows light through at different angles, allowing you to visualise different features of the sample.

For example, isotropic samples always appear dark when light travels through them, compared to an anisotropic sample which will appear bright as they reflect the light. A birefringent anisotropic sample will have different components that can be seen at different angles, meaning that if you rotate the polariser (or the sample stage if your microscope has a rotating option) it will cause different parts to "black out" as you rotate through the different angles (Chayen 1983).

2.2.1.1 Method for optical (or polarised) microscopy analysis

Approximately 5 mg of sample was placed on a glass microscope slide and viewed using a GX top down optical microscope (GXM-L3201 LED) under x4 magnification; samples were also viewed using crossed polarisers. Images were recorded digitally.

2.2.2 Differential scanning calorimetry theory

Differential scanning calorimetry (DSC) is a thermo-analytical technique. Calorimetry is the measurement of heat changes, and since most physical transitions and all chemical reactions create heat (exothermic) or consume heat (endothermic) these changes can be detected.

Calorimeters are currently used in pharmacology, cell biology, chemistry, biochemistry, biotechnology and bioscience (Sturtevant 1987; Bruylants et al. 2005; Gill et al. 2010) However, it wasn't until the 1960s when Perkin Elmer introduced their DSC that the potential of differential calorimetry was recognised as a technique for pharmaceutical analysis (O'Neill 1966; Knopp et al. 2016). DSC has gained wide spread use in the pharmaceutical industry in the determination of melting points, boiling points, stability, purity and polymorphism. In theory, the melting transition of an absolutely pure crystalline substance should occur over a very small temperature range, the broadening of this range would indicate impurities (van Dooren and Müller 1984). DSC has gained popularity due to its simplicity, speed and small sample size (1 - 10 mg).

A typical DSC consists of a measurement chamber containing two sensors (Figure 2-9). The sample is then weighed into a pan (usually aluminium) and placed on the sensor (thermocouple). The second sensor has the standard placed on it (usually an empty pan) for comparison. Usually, the calorimeter is set to increase the temperature at a constant rate while being purged with inert gas. The difference in heat flow between the sample and empty pan is measured as a function of temperature and time (O'Neill 1966; Knopp et al. 2016).

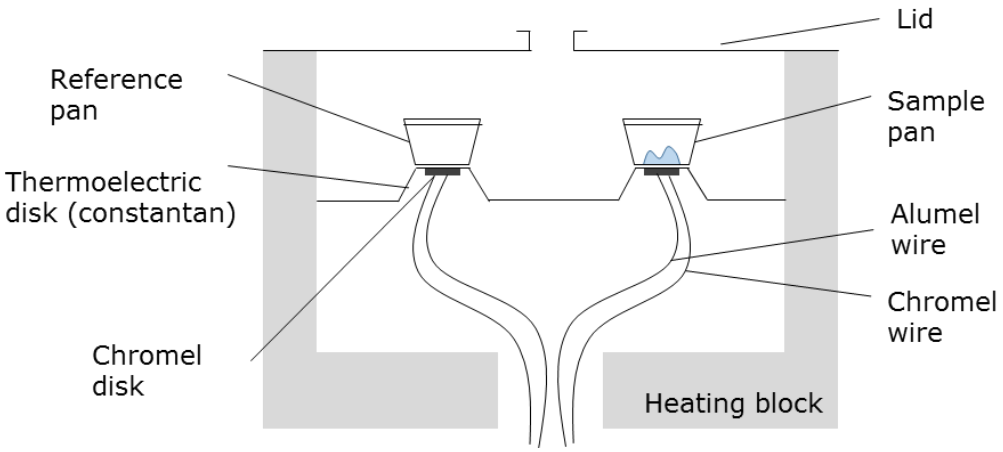

Figure 2-9 Schematic diagram of heat flux differential scanning calorimeter (DSC). Adapted from Clas et al. (1999) and Kodre et al. (2014).

Therefore, DSC can be used quantitatively or qualitatively to look at thermal events such as changes in heat capacity or enthalpy (Knopp et al. 2016). For example, an endothermic event such as a solid melting to a liquid, will require more heat to raise the sample temperature. Likewise, an exothermic event such as crystallisation requires less heat to raise the sample temperature (Kodre et al. 2014).

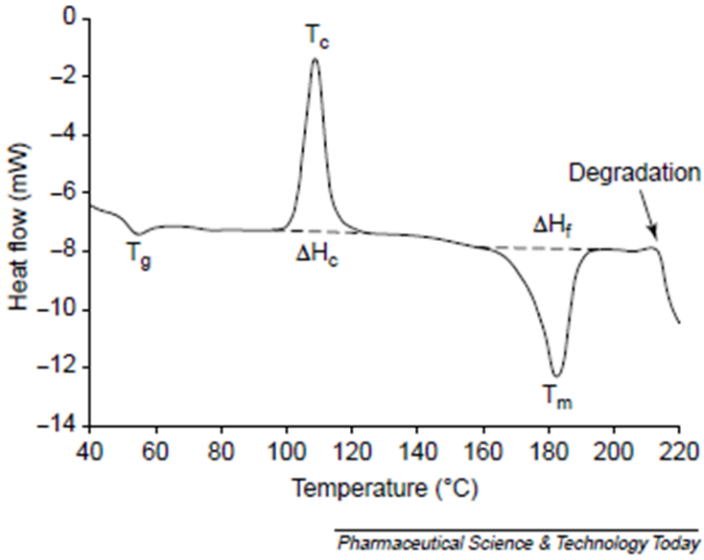

Figure 2-10 An example differential scanning calorimetry scan of sucrose (undried), showing the glass transition temperature (T_g), recrystallization exotherm temperature (T_c) and enthalpy (ΔH_c), melting endotherm temperature (T_m) and enthalpy (ΔH_f) and onset of degradation. Data were recorded at 10K min^{-1}. Endotherm transitions are down. Figure taken from Clas et al. (1999).

2.2.2.1 Method for DSC analysis

Approximately 5 mg of sample was loaded into aluminium Tzero, hermetically sealed pans and loaded into the DSC. Samples were ramped from -40 to 200 °C at 10 °C/ min. DSC curves were recorded on the TA instruments Q2000, starting temperature ambient, heating rate 10 °C/ minute and final temperature 200 °C. Nitrogen flow was set at 150 mL/ minute dry gas and 80 mL/ minute purge gas.

2.2.3 Fourier transform infrared spectroscopy theory

FT-IR (Fourier transform infrared) spectroscopy is an analytical technique that uses infrared radiation to analyse samples. The instrument works by determining how much of the incident light is

absorbed at a specific wavelength. It then produces a spectrum characterizing the vibrations of the bonds within the molecule (Beasley et al. 2014). As an approximate rule, functional groups absorb in the range 4000 to 1500 cm^{-1} with triple and double bonds exhibiting higher wavenumbers than single bonds. Wavenumbers below 1500 cm^{-1} are significant for ring vibration, bending and deformation which can be specific to a compound. This range is often referred to as the fingerprint region (Schmitt and Flemming 1998).

There are two main types of IR instrument; dispersive instruments and Fourier transform instruments. In dispersive instruments a monochromator is used to select each wavenumber sequentially to allow it to monitor the intensity of the radiation once it has passed through the sample. Fourier transform instruments work without needing dispersion, they can create a radiation source that can monitor individual wavenumbers within a one second pulse of radiation. In a Fourier transform (FT-IR) instrument an interferometer is used instead of a monochromator. The interferometer relies on a moving mirror which displaces part of the radiation created by a source (Figure 2-11). This produces an interferogram which can be converted using a Fourier transform, allowing the spectrum to be extracted from a series of overlapping frequencies. Fourier transform instruments have the advantage that they can acquire a full spectral scan in about 1 second compared to 2-3 minutes for the dispersive technique. Another advantage is that FT-IR is attached to a computer allowing multiple spectral scans to be taken and then averaged to improve the signal: noise ratio (Watson 2005).

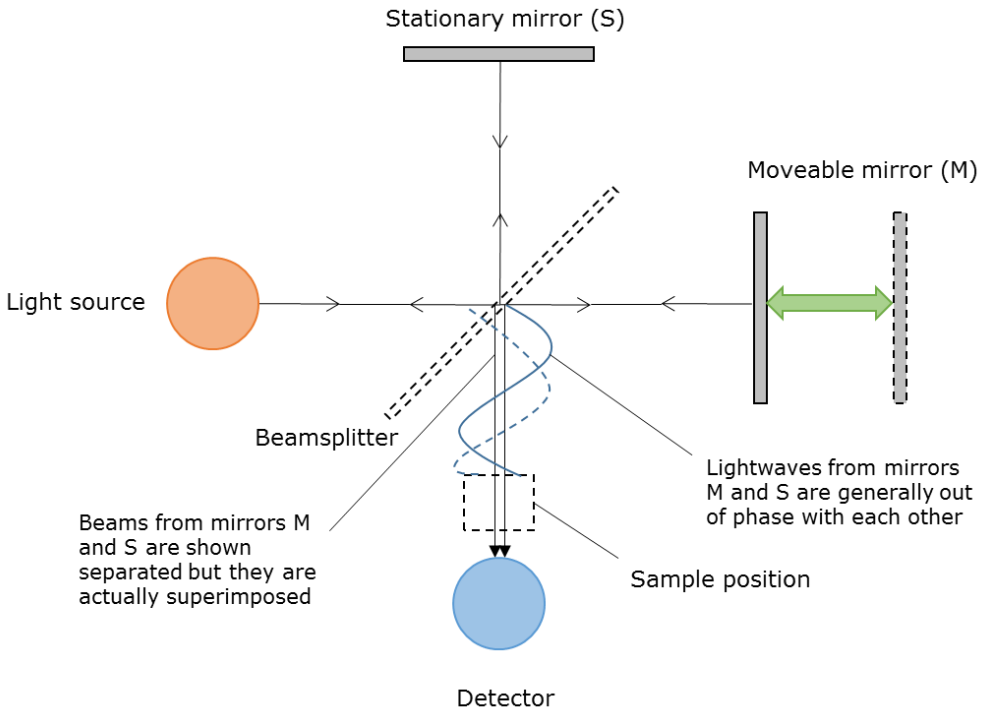

Figure 2-11 A schematic diagram of Michelson interferometer used in FT-IR instruments. Adapted from Watson (2005) and Harris (2010).

Attenuated total reflectance (ATR) is an attachment for an FT-IR instrument that allows fast and simple analysis. Traditionally liquid samples are run sandwiched between two sodium chloride (NaCl) or potassium chloride (KCl) discs. Solid samples are ground up with potassium bromide (KBr), transferred into a die block and compressed into a disc (Watson 2005). Potassium bromide is used in sample preparation as it has no significant peaks in the mid IR range and can easily be made into a smooth transparent disc when mixed with other powders. However, when using ATR no sample preparation is required - the sample is placed on the optic window with a zinc selenide (ZnSe) ATR crystal held in place using a compression clamp. ATR works by total internal reflection which measures the changes that occur when an internally reflected IR beam comes into contact with the sample through a diamond or zinc selenide crystal. When a

sample is analysed the resulting evanescent wave is attenuated in the regions of the IR spectrum where the sample absorbs energy (Hind et al. 2001; Glassford et al. 2013; Beasley et al. 2014).

2.2.3.1 Method for FT-IR (ATR) analysis

A small sample (approx. 1 – 10 mg) was placed on the diamond ATR crystal of the Agilent Cary 630 FT-IR and held in place using a compression clamp. Spectra were obtained by scanning in the range of 600 to 4000 cm^{-1}.

2.2.4 Handheld Raman spectroscopy theory

Raman spectroscopy is a vibrational technique which is popular due to its easy sampling methods and specificity. One advantage is that samples can be analysed directly or even through transparent containers. Raman spectroscopy is named after Professor C. V. Raman, who in 1928 observed the Raman scattering effect when he used a telescope to direct sunlight onto his samples. He was later awarded the Nobel Prize in 1930 (Harris 2010). For pharmaceutical materials Raman spectroscopy can be used to gain information on the structure, bonding, crystallinity and polymorphs of a sample.

In the last 20 years enhanced technical developments and miniaturisation of instruments has allowed relatively cheap portable instruments to be developed (Kudelski 2008; Carron and Cox 2010). Hajjou et al. (2013) investigated the potential of using handheld Raman in evaluating medicines and found it valuable in detecting counterfeit medicines. Witkowski (2005) also used Raman spectroscopy in the detection of counterfeit and adulterated

pharmaceutical products. Raman spectroscopy can even be used through a tablet blister pack if necessary (de Veij et al. 2007); many blister packs are made from material that is a suitable spectral window as the scattering radiations and excitation both lie within a narrow spectral interval, unlike IR where absorption of the sample and packaging overlap in the spectral range (Kudelski 2008).

The Raman effect is the occurrence of inelastic scattering of light, which occurs when the shift in wavelength of radiation scattered by molecules have a different frequency from that of the incident beam. The shift in wavelength is influenced by the chemical structure of the molecules in the sample. Raman spectroscopy uses the scattered light to gain information about the molecular vibrations to determine the structure, electronic environment and even the bonding of the molecule (Das and Agrawal 2011). Raman spectroscopy also allows the quantitative (by measuring frequency of scattered radiations) and qualitative analysis of samples (intensity of scattered radiations) (Bumbrah and Sharma 2016).

As with spectrum produced from other vibrational techniques (e.g. infrared spectroscopy) the Raman spectrum can be classed as a compound's fingerprint. Raman spectroscopy is a scattering technique and is based on the inelastic scattering (Raman scattering) of monochromatic light (usually a laser) interacting with vibrating molecules. When a monochromatic laser interacts with the molecules in the sample it scatters light, this scattered light has a different frequency to the incident light (inelastic scattering) and this is used to create the Raman spectrum (Bumbrah and Sharma 2016).

A typical Raman spectrometer is contains a light source (usually a laser), a monochromator, a sample holder and a detector (Figure 2-2).Raman spectroscopy consists of a monochromatic laser beam which illuminates the sample. The radiation then interacts with the

molecules in the sample which then scatter the light. The scattered light can have a frequency that is different from the incident light (inelastic scattering, Raman scattering) or it can have an equal frequency to the incident radiation (elastic scattering, Rayleigh scattering). The majority of scattering that occurs is elastic (Rayleigh) which is filtered out by a filter in the instrument allowing the inelastic (Raman) scattering to be dispersed onto the detector, allowing a Raman spectrum to be produced (Bumbrah and Sharma 2016; Rostron et al. 2016).

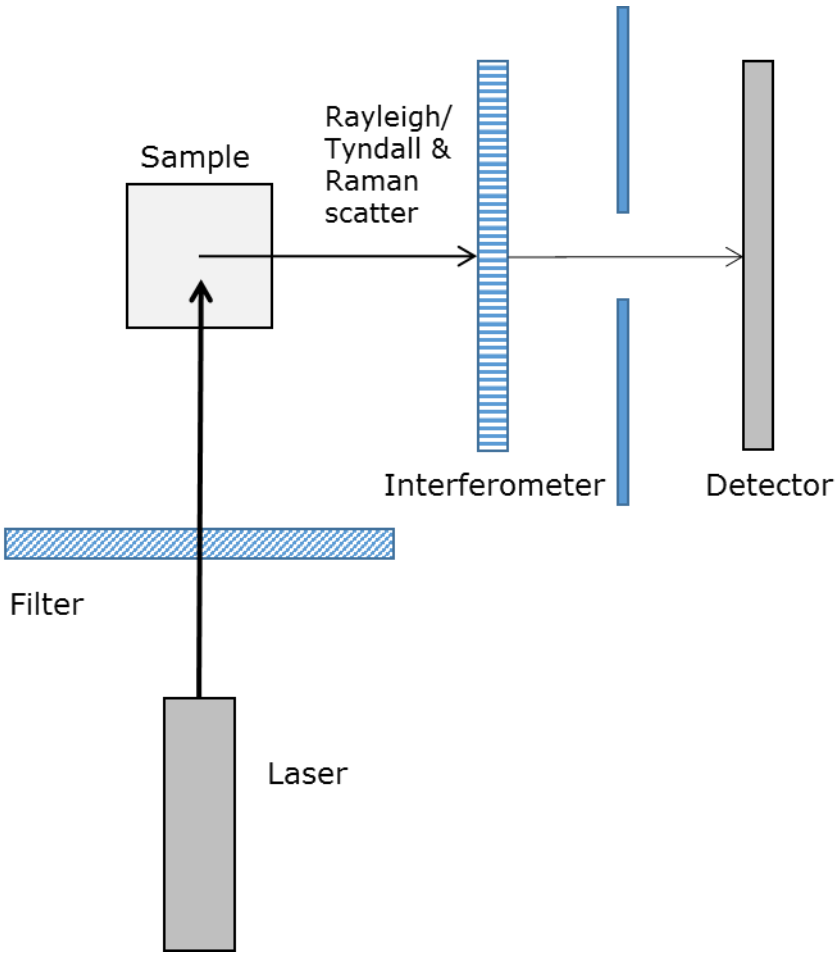

Figure 2-12 Schematic diagram of Raman spectrometer. Image adapted from Watson (2005).

2.2.4.1 Method for handheld Raman analysis

A small sample (ca. 20 mg) was placed in a glass vial and loaded into the DeltaNu ReporteR hand held Raman spectrometer (SciApps) and scanned between wavenumbers 300 and 2000 cm^{-1}.

3 Creating reference materials

3.1 Introduction

In this chapter pharmaceutical compounds paracetamol, clotrimazole and propranolol are characterised. Paracetamol and clotrimazole were used in levitation studies described in chapters 4 and 5. Propranolol, along with paracetamol and clotrimazole were used in the low field studies in chapter 6. In order to compare the effects of magnetic fields and containerless crystallisation as obtained through diamagnetic levitation it was important to develop well characterised reference materials. Therefore in this chapter we provide an overview of the pharmaceutical compounds used in later chapters and the production and characterisation of the required reference materials.

Paracetamol was chosen as the first active pharmaceutical (API) for investigations of diamagnetic levitation (chapter 4) as it has been widely studied and is well characterised. Paracetamol has three polymorphs, the monoclinic form I, an orthorhombic form II, and the elusive form III. Clotrimazole was chosen as a second API (chapter 5) to show comparison of the diamagnetic approach to Benmore and Weber's acoustic levitation method where they successfully amorphised clotrimazole (Benmore and Weber 2011). Propranolol was selected as a third API for the low field studies (along with paracetamol and clotrimazole) in Chapter 6, as it has four well characterised polymorphic forms (Bartolomei et al. 1998).

3.1.1 Paracetamol

Paracetamol (Figure 3-1) is a commonly used analgesic drug, with many millions of paracetamol tablets being manufactured each year.

Paracetamol has been researched extensively and three polymorphs have been found. The two best characterised polymorphic forms are monoclinic (form I) and orthorhombic (form II) paracetamol. The crystal structures of form I (monoclinic) (Haisa et al. 1974) and form II (orthorhombic) (Haisa et al. 1976) were published in the 1970s (Nichols and Frampton 1998). The monoclinic form of paracetamol is the most thermodynamically stable in ambient conditions, whilst the orthorhombic form is metastable (Delmas et al. 2013). In both of the paracetamol polymorphs molecules are linked by −OH···O=C− hydrogen bonds, as well as the −NH···OH− bonds which give a layer pleated effect in form I and flat layer in form II (Smith et al. 2014).

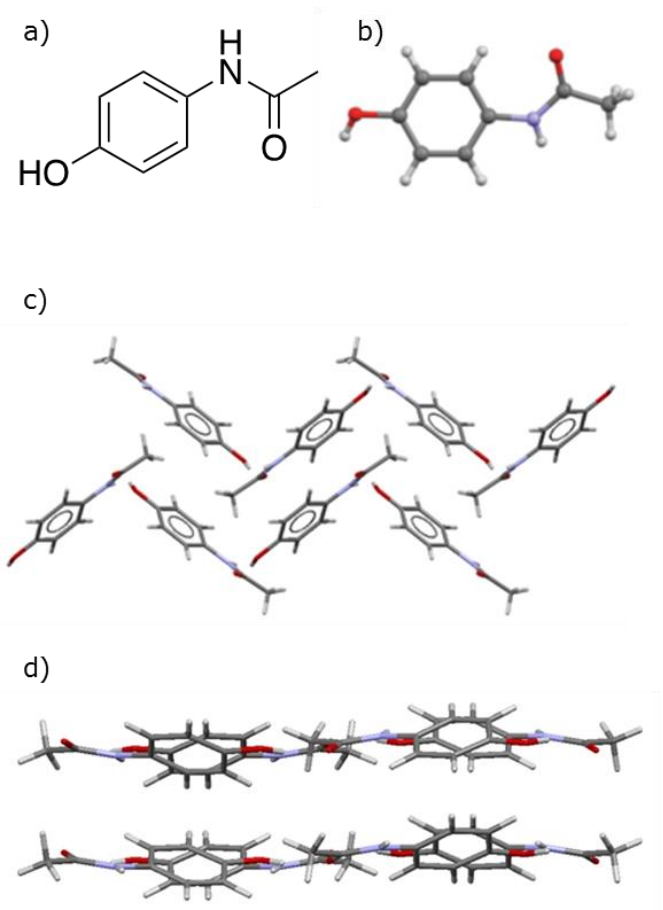

Figure 3-1 (a) The structure of paracetamol (Perlovich et al. 2007) (b) The 3D structure of paracetamol, with red indicating an oxygen atom and blue a nitrogen atom (Kolesov et al. 2011) (c) The crystal structure of monoclinic paracetamol (form I) (d) The crystal structure of orthorhombic paracetamol (form II). Image adapted from Thomas et al. (2011).

A third polymorphic form, Form III was reported in the 1980s; however, it has remained elusive ever since (Burger 1982). Form III is difficult to isolate due to its stability and is believed to be an intermediate in the formation of form II (Di Martino et al. 1997; Nichols and Frampton 1998). However, more recently form III has been isolated and characterised (Burley et al. 2007; Perrin et al. 2009).

Evidence of paracetamol forms IV and V has been found at high pressure (Smith et al. 2014). By conducting high pressure Raman measurements the authors have shown evidence of form IV and V at ~ 8 and ~ 11 GPa respectively.

3.1.1.1 Form I paracetamol (monoclinic)

Monoclinic paracetamol is stable at room temperature and is used commercially; however, it is not manufactured by direct compression due to poor compaction properties. The puckered hydrogen bonds on the sheets of molecules (Figure 3-1) do not allow the sheets to slip over one another very easily during direct compression (Haisa et al. 1976; Burley et al. 2007). Therefore, form I must be wet granulated before tableting (Garekani et al. 2000; Burley et al. 2007). Compared to direct compression, wet granulation is a slower, more expensive and a complex method for manufacturing tablets. Therefore, research is being carried out on the crystallisation process to try and improve compressibility in the efforts to manufacture paracetamol tablets using the more efficient process of direct compression. Physicochemical properties, such as being compressible and free flowing, are important for the production of high quality tablets by direct compression. For example, Fachaux et al. (1995a), modified the crystallisation process using dioxane to produce sintered crystals.

The porous nature of the crystals improved compression by allowing distribution of force and thus giving plasticity (Fachaux et al. 1995b).

3.1.1.2 Form II paracetamol (orthorhombic)

The crystal structure of orthorhombic paracetamol includes slip planes (Figure 3-1) which allow plastic deformation upon compression (Di Martino et al. 1997; Nichols and Frampton 1998). Therefore, it has been assumed that the orthorhombic form will have processing advantages compared to form I paracetamol. In addition to the benefit of being more suitable for direct compression, evidence suggests that orthorhombic paracetamol may also be slightly more soluble than the monoclinic form (Sohn 1990; Nichols and Frampton 1998).

There is much interest in producing orthorhombic paracetamol and research is being carried out on an optimisation process, as this could lead to reduced manufacturing costs. Orthorhombic paracetamol has been made by the slow cooling of melts and from ethanolic solution. Haisa et al. (1974) produced orthorhombic crystals by slowly evaporating ethanol solution, whilst Nichols and Frampton (1998) produced orthorhombic paracetamol from ethanol using a seeding technique. Crystallisation from ethanolic solution still needs improving as the yield is less than 30% (Al-Zoubi et al. 2002a) and the orthorhombic paracetamol easily converts back to the monoclinic form upon contact with the solvent (Nichols and Frampton 1998). The melt crystallisation is not very suitable for the large scale and isn't very reproducible (Di Martino et al. 1997).

3.1.1.3 Form III paracetamol

To produce form III paracetamol it seemed necessary to use closed conditions with Di Martino et al. (1997) reporting they could only identify form III when it was made between a glass coverslip and a microscope slide during thermomicroscopy experiments or during DSC analysis in a closed pan. In those experiments form III couldn't be identified by any other methods, as the form III paracetamol was found to convert to form II within 10 minutes of removing one of the glass microscope slides. Perrin et al. (2009) also produced form III by keeping the paracetamol sample in an inert atmosphere; either by using nitrogen or placing the sample under a vacuum. However, Burley et al. (2007) were able to reliably isolate form III through controlled crystallisation, and characterised it using optical microscopy, solid state NMR, X-ray diffraction and calorimetry. The pure sample of form III was prepared in solid-state NMR rotor, which was not strictly under inert conditions.

Rossi et al. (2003) were able to stabilise form III paracetamol using hydroxypropylmethylcellulose (HPMC) and obtained a tentative melting temperature of 139 – 141 °C. Although Burley et al. (2007) were able to isolate form III, they were unable to determine a melting point using the DSC due to a solid-solid transition to form II before any melting occurred. Hence, in their study only the melt of form II paracetamol was seen at 159 °C. Gaisford et al. (2010) however, were able to use rapid-heating DSC instrumentation, which had a heating rate of up to 2000 °C min^{-1} to isolate and characterise form III. When heating at slow rates (up to 300 °C min^{-1}) a solid-solid transition was seen at ca. 120 °C (to form II) followed by a melt at 156 °C (form II melting). However, when they used heating rates up to 400 °C min^{-1} the solid-solid transition was absent and two endotherms were observed; one at 156 °C (the form II melt) and a lower temperature endotherm at 143 °C which they ascribed to the melting of form III.

As the form II melt is present in all experiments, they presume that the paracetamol crystallises into a mixture of form II and III during preparation, indicating the unstable nature of form III. This hypothesis is backed up by experiments conducted with hydroxypropylmethylcellulose (HPMC) where increasing the HPMC: paracetamol ratio or increasing the HPMC molecular mass resulted in a concomitant increase in form III relative to the form II peak supporting the idea that both forms coexisted in the sample prior to crystallisation.

	Form I	Form II	Form III	Amorphous
Crystallographic lattice type	Monoclinic [1]	Orthorhombic [1]	Orthorhombic [1]	Not crystalline
Crystal packing	Puckered hydrogen bonds give zigzag crystal structure [2]	Flat hydrogen bonded sheets/ planar structure [2]		No regular/ repeating structure.
Stability	Stable polymorph (form I > form II) [3]	Metastable polymorph (form II > form III) [3]	Metastable polymorph (form III > amorphous) [3]	Least stable [3]
Melting point (°C)	168 – 172 [4-9]	156 – 158 [4-9]	139 – 143 [10,11]	

Table 3-1 Summary of form I, II, III and amorphous paracetamol. References [1] (Zimmermann and Baranović 2011) [2] (Łuczak et al. 2013) [3] (Nanubolu and Burley 2012) [4] (Di Martino et al. 1996) [5] (Di Martino et al. 1997) [6] (di Martino et al. 2000) [7] (Nichols and Frampton 1998) [8] (Boldyreva 2003) [9] (Espeau et al. 2005) [10] (Rossi et al. 2003) [11] (Gaisford et al. 2010)

3.1.2 Paracetamol characterisation

Paracetamol and its polymorphs can be characterised by different analytical techniques; including microscopy, DSC, Raman and FT-IR spectroscopy. The analytical techniques and the characteristic differences between the polymorphs and amorphous solid will be discussed below.

3.1.2.1 Optical light microscopy

Using optical light microscopy form I and form II can be visually identified by their crystal morphology. Form I paracetamol forms prisms and plates whereas form II forms elongated prisms (needles).

Haisa et al. (1974) crystallised form II paracetamol from solution in 1974, however, crystallisation from solution has remained elusive ever since. Di Martino et al. (1997) reported they were never able to prepare form II crystals by crystallisation from solution, instead they used a melt recrystallization method to prepare form II. Nichols and Frampton (1998) reported the growth of orthorhombic (form II) paracetamol from solution, however, they discovered if the form II crystals remained in contact with the mother alcohol for too long they would convert to form I (the more stable polymorph). A paracetamol saturated solution was seeded with form II powder and observed using light microscopy. Initially form II crystals started to grow, however, within 15 minutes platy and prismatic crystals of form I started to grow as the form II needles dissolved. Below (Figure 3-2) is an image taken from their article showing the morphology of form I and form II crystals but also the conversion of form II to form I over 30 minutes.

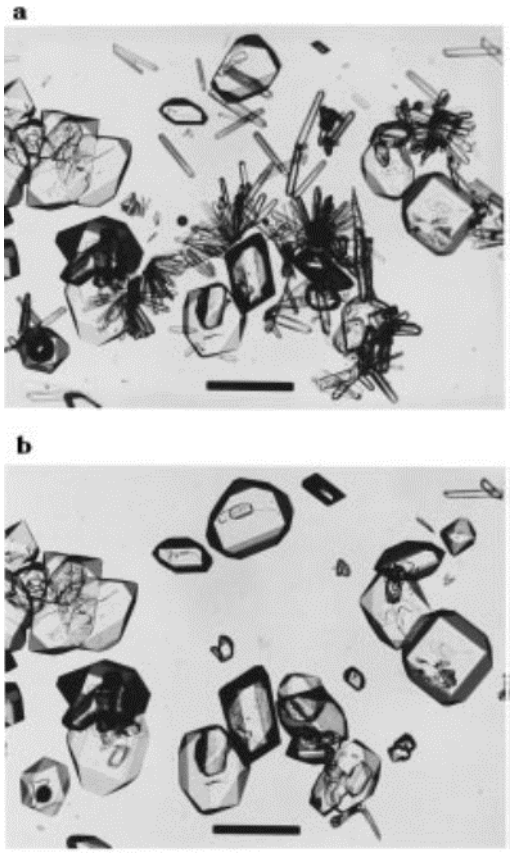

Figure 3-2 Photomicrographs showing the solution phase polymorphic conversion of orthorhombic paracetamol (needles) to monoclinic paracetamol (prisms and plates) at room temperature in saturated benzyl alcohol. Micrograph (a) was taken at *t* = 0 and (b) was taken at *t* = 30 min. Scale bars = 250 μm. Image taken from Nichols and Frampton (1998).

3.1.2.2 Hot stage microscopy

Hot stage microscopy can be used to study the formation of form III crystals which is an advantage as form III paracetamol is very unstable and therefore difficult to characterise. However, form III can be produced between two glass microscope slides by crystallisation from the melt (Di Martino et al. 1997; Burley et al. 2007). Form III can be visually identified by fine crystals growing radially (Figure 3-3 b).

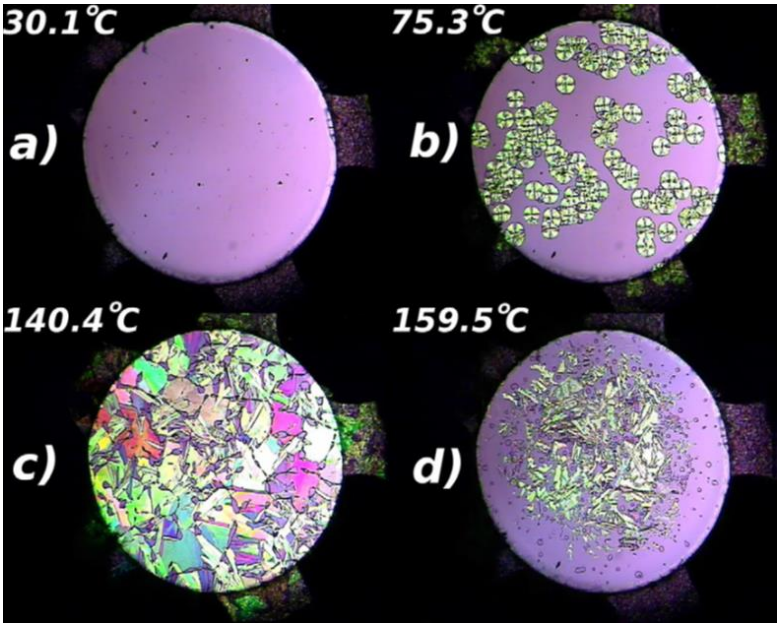

Figure 3-3 Hot stage microscopy image of paracetamol taken from Burley et al. (2007). Image (a) Melted paracetamol to form a glass (b) Form III isolated by gentle warming (c) Form II isolated by further heating (d) Melting of paracetamol.

3.1.2.3 Differential scanning calorimetry

Paracetamol polymorphs can be identified by their onset melting temperature. Paracetamol form I has a reported melting temperature between 168 – 172 °C. Form II however, has a lower melting point of 156 – 158 °C (Di Martino et al. 1996, 1997; Nichols and Frampton 1998; di Martino et al. 2000; Boldyreva 2003; Espeau et al. 2005). Rossi et al. (2003) reported a tentative melting temperature for form III as 139 – 141 °C, while Gaisford et al. (2010) used rapid-heating DSC to determine the melting point of form III, which they stated as 143 °C.

In Figure 3-4 are DSC thermograms of form I and form II paracetamol (Nichols and Frampton 1998). In Figure 3-4 a) a single endothermic event can be seen at 171 °C which is attributed to the melting of form I. The thermogram for form II (Figure 3-4 b) exhibits three

endothermic events, a small and broad peak between 115 – 128 °C, a small sharp peak at 157 °C and a strong sharp peak at 171 °C. Nichols and Frampton (1998) attribute the small and broad peak circa 120 °C to the conversion of form II to form I with the melting at 157 °C being interpreted as nonconverted form II. The final melt at 171 °C indicates form I.

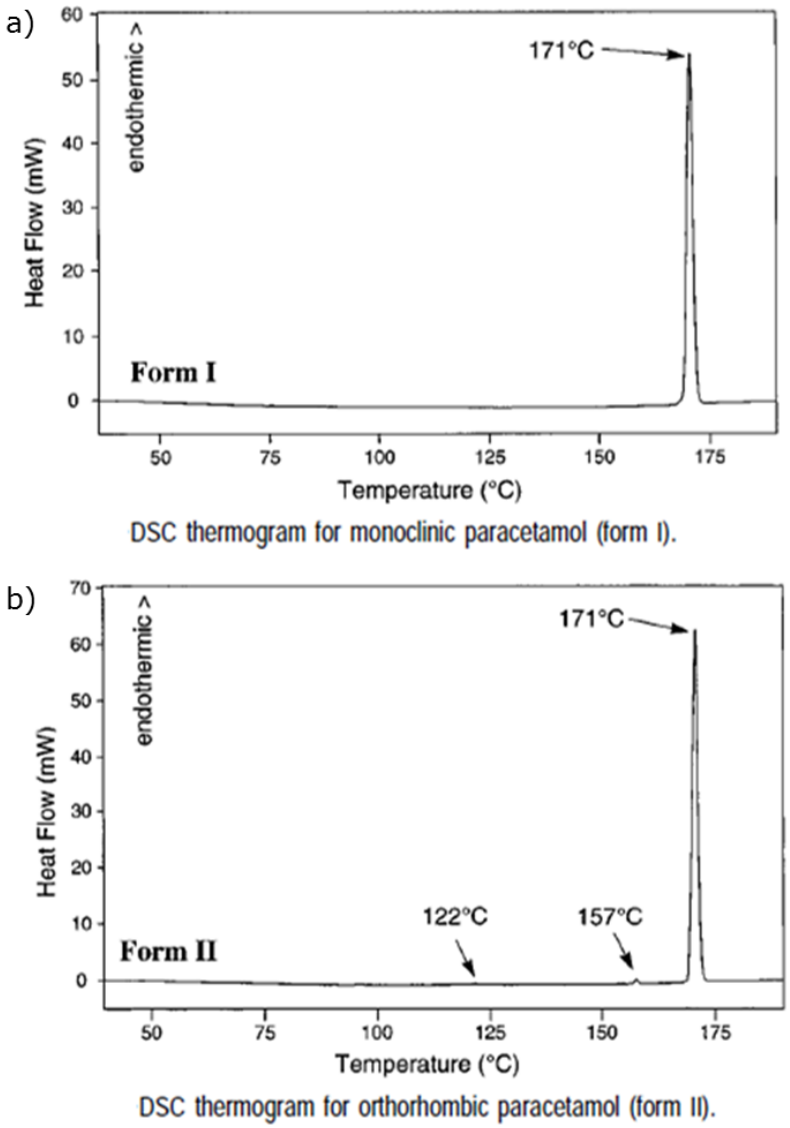

Figure 3-4 DSC thermograms of form I and form II paracetamol (a) form I paracetamol (b) form II paracetamol. Image taken from Nichols and Frampton (1998).

3.1.2.4 FT-IR spectroscopy

FT-IR can also be used to identify different polymorphic forms. Below, (Figure 3-5 a) the IR spectra of paracetamol form I and form II is shown. The red trace (1) being form I paracetamol and the blue (2) form II. Notable differences can be seen in the C-C aromatic stretching peaks (1614, 1507, 1442 and 1626, 1513, 1453 cm^{-1}) and the C-N amide stretching peaks (1566, 1507 and 1560, 1513 cm^{-1}). However, the most noticeable difference is the presence of extra absorption peaks, which correspond to intra- or inter-molecular interactions. For form I paracetamol additional peaks are at 806, 682 and 1228 cm^{-1}. In addition to the extra peaks other absorption peaks can vary in intensity. For quantification of form I and form II in a mixture, ratios of characteristic peaks (at 806 cm^{-1}) with others existing in both spectra (at 836 cm^{-1}) can be used (Al-Zoubi et al. 2002b).

Figure 3-5 (b & c) are spectra comparing form II paracetamol and amorphous paracetamol. For form II paracetamol a sharp peak is seen at 3331 cm^{-1}, which is attributed to the NH group, while a broader OH peak can be seen at 3162 cm^{-1} (Figure 3-5 b). In the amorphous sample the peaks become broadened due to the fact the molecules can now take up a range of positions and conformations with a wide range of interaction distances leading to a wider distribution of absorption frequencies. In the amorphous sample the OH and NH peaks, which were clearly defined in form II paracetamol spectra have merged leading to a broad peak around 3301 cm^{-1}. In Figure 3-5 c) the C=O stretch appears at 1650 cm^{-1} for form II while for the amorphous sample it shifts to a slightly higher wavenumber (1655 cm^{-1}) while developing a shoulder at 1636 cm^{-1}, this suggests two populations of interactions in the amorphous solid involving this functional group, some stronger than in form II and some weaker. The higher wavenumber peak is attributed to the weaker NH-CO

interaction and the shoulder the stronger phenol-carbonyl interactions (Trasi and Taylor 2012).

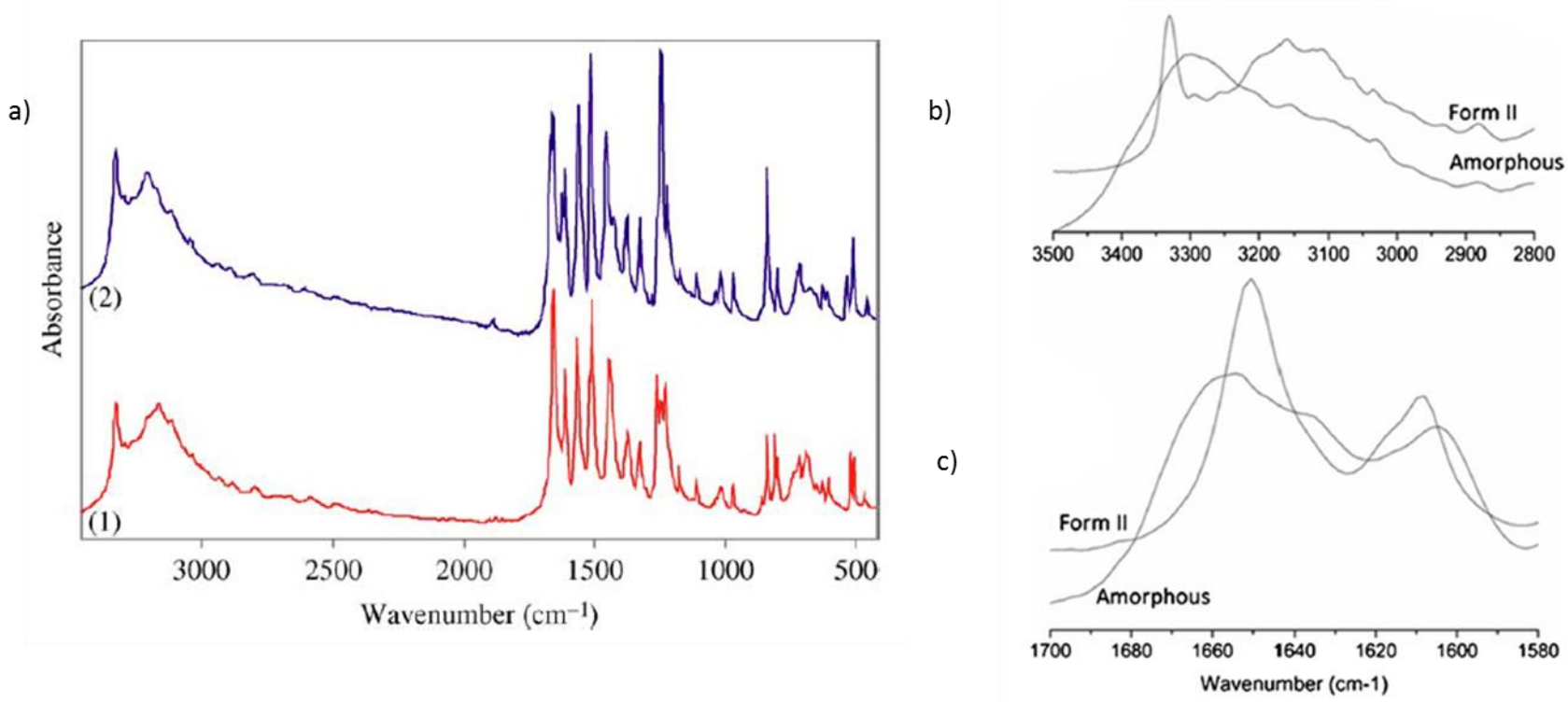

Figure 3-5 (a) FT-IR spectra of form I paracetamol (red, 1) and form II paracetamol (blue, 2). Image taken from Ivanova (2005) (b & c) FT-IR spectra of from II and amorphous paracetamol in the (b) NH, OH stretch and (c) carbonyl stretch region. Image taken from Trasi and Taylor (2012).

Table 3-2 summarises the IR absorption frequencies that have been assigned for form I and form II paracetamol.

IR frequencies (cm^{-1})		Qualitative assignments
Form I	**Form II**	
3326	3324	Associated N-H stretch
3162	3205	H-bonded O-H stretch
1654	1668	Amide I (carbonyl stretch)
1610	1609	Skeletal aryl C-C stretch
1565	1558	Amide II (N-H in plane deformation)
1507	1513	Aryl C-H, C-H symmetric bends
1442	1454	Skeletal aryl C-C stretch
838	837	Out of plane C-H bend (aryl-1,4-disubstituted)

Table 3-2 IR absorption frequencies for form I and form II paracetamol. Table adapted from Moynihan and O'Hare (2002).

3.1.2.5 Raman spectroscopy

Raman scattering has high sensitivity to crystalline structures meaning it is widely used to study polymorphism (Łuczak et al. 2013). Spectra can be recorded rapidly, including bands due to both inter- (10 - 400 cm^{-1}) and intra-molecular vibrations (400 – 4000 cm^{-1}). The "fingerprint" region (400 – 2000 cm^{-1}) arises from intra-molecular vibrations and the spectra for form I, form II, form III and amorphous paracetamol are similar (Figure 3-6). For amorphous paracetamol the peaks are broader at 1600 cm^{-1} than crystalline

paracetamol due to the disordered nature of the molecules in the amorphous state (Al-Dulaimi et al. 2010).

Form I paracetamol has two characteristic peaks at 1234 and 1325 cm^{-1}, with three well resolved peaks in the 1500 - 1700 cm^{-1} range. In contrast form II has a pair of weak peaks at 1220 and 1245 cm^{-1} and a strong peak at 1329 cm^{-1}. The peaks in the 1500 – 1700 cm^{-1} range for form II are shifted closer to one another relative to the peaks in the form I spectra. Form III paracetamol appears to be similar to form I paracetamol, however, subtle peaks shifts and peak intensities are evident. The amorphous spectrum appears similar to the crystalline spectra, however some peaks appear broader and have shifted compared to the form I spectra. Form I and form II paracetamol can be distinguished by the intensities of the 1234 and 1329 cm^{-1} peaks, and the same peaks can be used to distinguish form II and III. The amorphous spectrum can be identified by the intensity of the 1325 cm^{-1} and missing peak at 1650 cm^{-1} (Kauffman et al. 2008).

a)

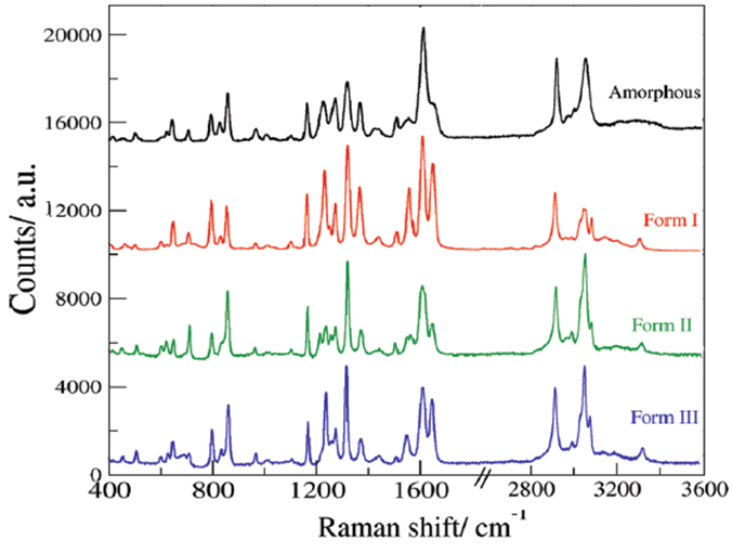

b)

Raman frequency (cm^{-1})	**Qualitative assignments**
862	Symmetric phenyl breathing
970	Deformation of phenyl ring & stretching of C-N amide bond
1168	Bending of phenyl ring & C-OH groups
1230	Deformation (rocking) of phenyl ring & amide & C-OH groups
1324	Deformation of phenyl ring & C-OH groups
1513	Bending of phenyl ring & stretching of CNH group
1560	Bending of amide N-H group
1616	C=C stretching
1660	C=O stretching
2929	Methyl C-H stretching
3062	Phenyl ring CH stretching

Figure 3-6 (a) Raman spectra form I, II & III paracetamol and amorphous paracetamol, image taken from Nanubolu and Burley (2012) (b) A table of Raman frequencies and mode assignments for paracetamol (Kolesov et al. 2011; Nanubolu and Burley 2012; Łuczak et al. 2013).

3.1.3 Clotrimazole

Clotrimazole (Figure 3-7) is an imidazole type antifungal with broad spectrum activity, it inhibits cytochrome P450 14a-demethylase which is required by fungal cells for membrane synthesis. Clotrimazole has antimycotic activity against crytococcuss spp, candida spp, aspergillus spp and dermatophytes and is therefore used in the treatment of tinea infections and candidiasis in the vagina, oral cavity and the skin (Tonglairoum et al. 2014, 2015a, b). Clotrimazole also works against different strains of *Plasmodium falciparum* (Saliba and Kirk 1998; Mittapalli et al. 2015). When compared to antimalarial drugs chloroquine and quinine, clotrimazole shows enhanced activity against chloroquine resistant malarial parasites, due to clotrimazoles ability to form complexes with free heme (Huy et al. 2002).

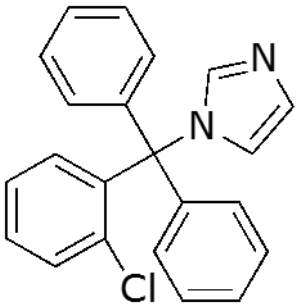

Figure 3-7 Structure of clotrimazole. Image adapted from Song and Shin (1998).

Clotrimazole has high lipophilicity (log *P* 6.30) and poor aqueous solubility (0.49 µg/ mL) meaning that the rate controlling step for absorption in the lumen is dissolution (Borhade et al. 2012). Clotrimazole is a class II drug according to the Biopharmaceutical Classification System (Mittapalli et al. 2015).

3.1.4 Clotrimazole characterisation

Clotrimazole has no reported polymorphs, however, pure clotrimazole has been analysed by DSC, FT-IR and Raman spectroscopy and has been widely reported in literature (Todica 2008; Cristini-Robbe et al. 2013; Gupta et al. 2013). Amorphous clotrimazole has been created by Yang et al. (2016) however, no FT-IR or Raman spectra for amorphous clotrimazole have been reported.

3.1.4.1 Differential scanning calorimetry

The melting point of clotrimazole can be determined by using DSC. Borhade et al. (2012) report a melting range of 141 – 145 °C for clotrimazole, with other research groups recording melting points within the range reported (Taneri et al. 2004; Gupta et al. 2013; Karolewicz et al. 2014; Tonglairoum et al. 2014, 2015a). However, Bhat and Shivakumar (2010) reported a melting point of 146.0 °C and Madgulkar et al. (2016) and Mittapalli et al. (2015) reported a higher melting point of 148 0°C.

Below is a DSC thermogram (Figure 3-8) from Gupta et al. (2013) showing a sharp melting endotherm for pure clotrimazole at 144.47 °C.

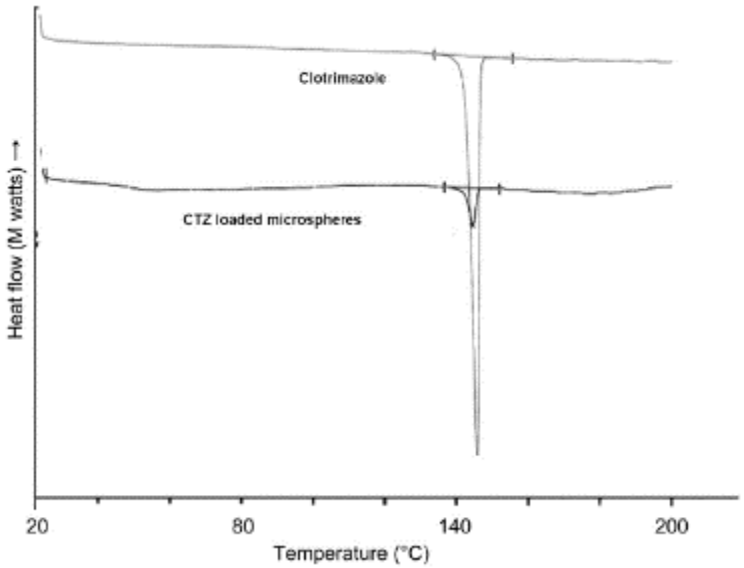

Figure 3-8 DSC spectra for pure clotrimazole and clotrimazole loaded microspheres. Image taken from Gupta et al. (2013).

3.1.4.2 FT-IR spectroscopy

Pure clotrimazole has been analysed by FT-IR and the characteristic peaks assigned (Gupta et al. 2013; Karolewicz et al. 2014; Tonglairoum et al. 2014, 2015a, b; Hani et al. 2015; Madgulkar et al. 2016). The clotrimazole spectrum (Figure 3-9) has its first characteristic peak at 3057 cm^{-1} due to C-H stretching vibrations. The second peak is at 1585 which is attributed to the C=N stretching vibrations. A large double peak at 1481 and 1438 cm^{-1} is due to C=C stretching, with another large double peak at 1082 and 1039 cm^{-1} being attributed to the C-N stretching. Peaks at 1202 and 1313 cm^{-1} represent C-H bending as well as 902, 823, 756 and 702 cm^{-1} (Hani et al. 2015). Bhat et al. (Bhat and Shivakumar 2010) also characterise the smaller peaks of 1564 cm^{-1} (aromatic N-O stretching) and 1266 cm^{-1} (C-O stretching).

a)

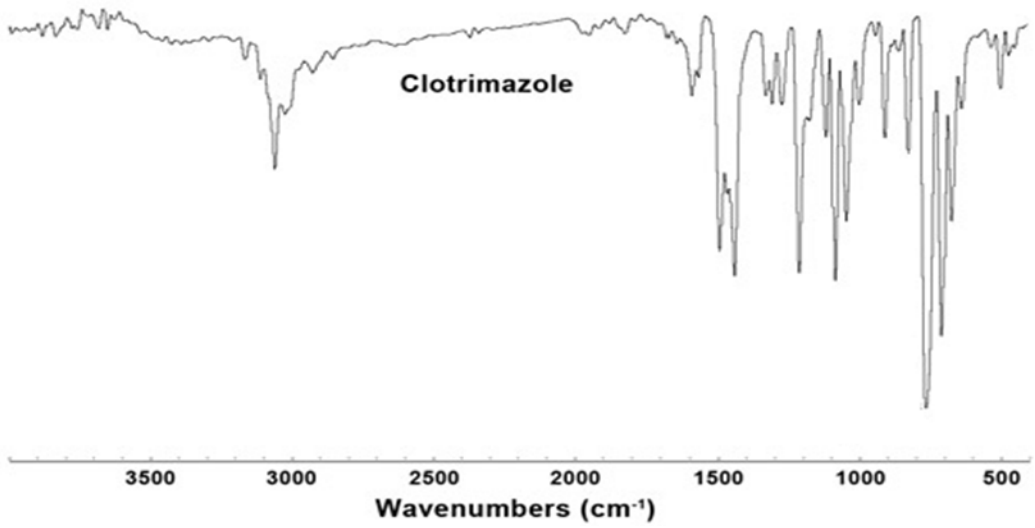

b)

IR frequency (cm^{-1})	Qualitative assignments
3057	C-H stretching vibrations
1585	C=N stretching vibrations
1481 and 1438	C=C stretching vibrations
1082 and 1039	C-N stretching vibrations
1202 and 1313	C-H bending vibrations
902, 823, 756 and 702	C-H bending vibrations

Figure 3-9 (a) FT-IR spectra of pure clotrimazole. Image taken from Gupta et al. (2013) (b) Summary of characteristic peaks and their assignments (Hani et al. 2015).

3.1.4.3 Raman spectroscopy

Clotrimazole has been characterised by Raman spectroscopy (

Figure 3-10) and some of its peaks assigned (Todica 2008; Cristini-Robbe et al. 2013). The peak at 1004 cm^{-1} is due to the stretching of N-C bonds while the peak at 1160 cm^{-1} is the deformation of CH/NH bonds. A deformation of CH/ CH_2 of rings can be seen at 1460 cm^{-1} and at 1600 cm^{-1} a deformation of the phenyl group can also be observed.

a)

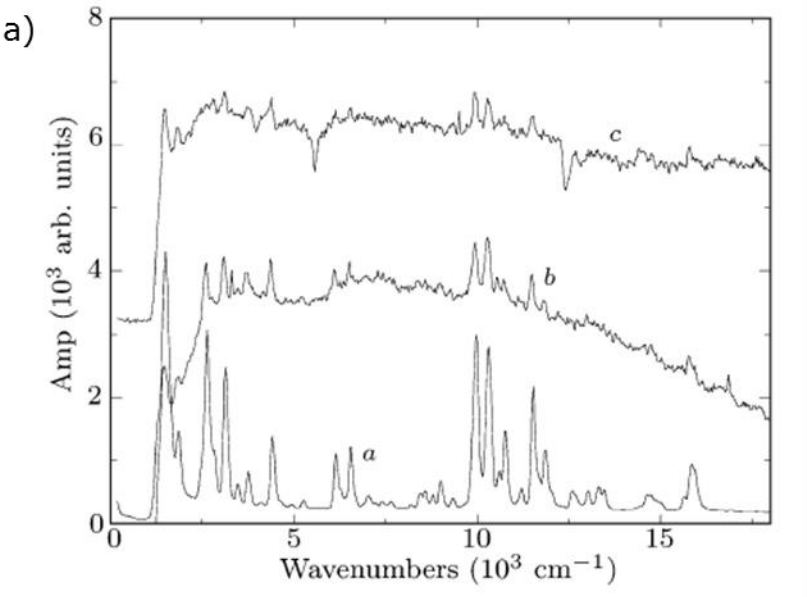

b)

Table 3. Assignments of Raman bands of clotrimazole powder.

Wavenumber/cm^{-1}	Attribution
1004	ν N-C
1160	δ CH/NH
1460	δ CH/CH_2 of rings
1600	δ phenyl

Figure 3-10 (a) Raman spectra of solid clotrimazole (spectra a), clotrimazole from the dried gel (spectra b) and clotrimazole from the re-hydrated gel (spectra c), image taken from Todica (2008) (b) Assignment of characteristic peaks for clotrimazole, image taken from Cristini-Robbe et al. (2013).

3.1.5 Propranolol

Propranolol is a nonselective β-adrenergic antagonist also known as a β blocker (Ammon et al. 1977) Propranolol is a naphthyloxy propanolamine derivative, (Figure 3-1) a specific β-antagonist and is a widely used β-adrenergic drug (Franklin et al. 2009). As a non-selective beta blocker, it blocks the action of adrenaline on both β_1 and β_2 adrenergic receptors (Viera et al. 2009). Propranolol is used clinically in the prevention and treatment of many disorders including acute myocardial infarction, angina, hypertension, arrhythmias, anxiety and migraine (Black et al. 1964) (Bredikhin et al. 2004). The propranolol base is poorly soluble in water and has a low melting point (92-93 °C) therefore, it is marketed as the hydrochloride salt, and is available in tablets, capsules and injections (Stepanovs et al. 2015). Propranolol hydrochloride exists in three crystalline forms, form I, II and III, with decreasing melting temperatures respectively (Ambrus et al. 2014), the stable form of propranolol and commercial product being form II (Bartolomei et al. 1998; O.M.M. et al. 2014).

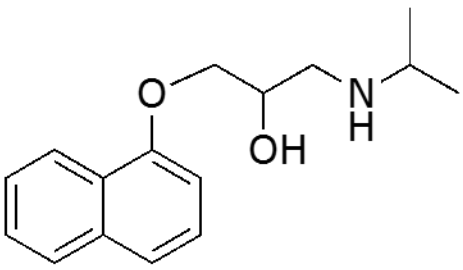

Figure 3-11 Structure of propranolol Image adapted from Patel and Bhatt (2012).

3.1.6 Propranolol characterisation

Propranolol and its polymorphs (form I, II and III) can be differentiated using DSC, FT-IR and Raman analysis.

3.1.6.1 Differential scanning calorimetry

Propranolol hydrochloride has three crystalline polymorphs, form I, II and form III, with decreasing melting temperatures respectively. Propranolol's polymorphs can therefore be identified by their onset melting temperatures. The DSC curves of form I, II and III are shown below (Figure 3-12). Bartolomei et al. (Bartolomei et al. 1998) report onset melting temperatures of 163.0 °C (form I), 161.8 °C (form II) and 154 °C (form III).

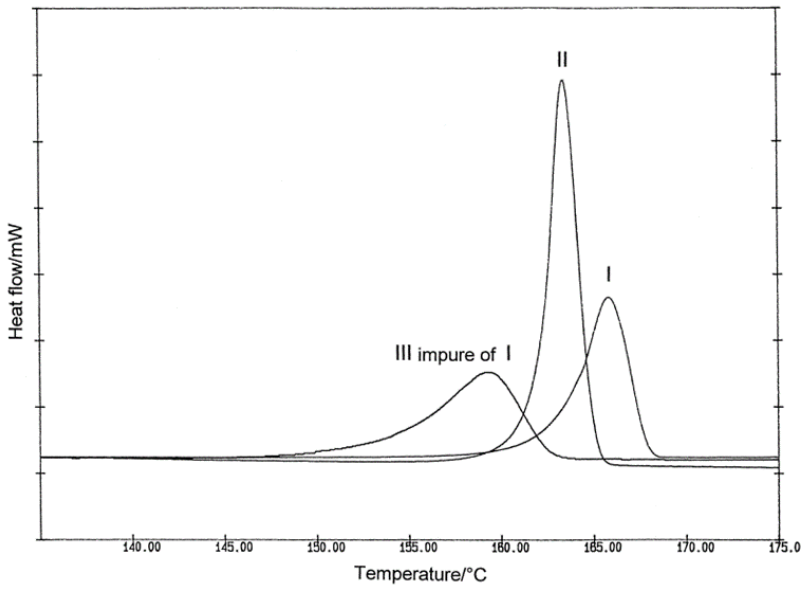

Figure 3-12 DSC curves for propranolol hydrochloride polymorphs I, II, and III impure of I (III with seed crystals of form I). Image taken from Bartolomei et al. (1998).

The commercially used form II has reported melting points in the range of 161.8 – 167.56 °C (Bartolomei et al. 1999; Chaturvedi et al. 2010; Polenske et al. 2010; Meka et al. 2012; Venkata Srikanth et al. 2012; Ambrus et al. 2014; AMJ and SM 2016).

3.1.6.2 FT-IR spectroscopy

The three propranolol polymorphs can be easily differentiated by their IR absorption bands in the 3400 – 2000 cm^{-1} range (Figure 3-13 a). Form I and form II propranolol can be distinguished over the whole 3400 – 700 cm^{-1} range, however, form I and form III show only a few subtle differences (Bartolomei et al. 1998). Subtle differences include a more intense peak at ~2970 cm^{-1} for form III, whilst form I has a more intense peak than form III at 1560 cm^{-1}. Form I has a double peak at ~1390 and ~1370 cm^{-1} whilst form III has a peak and shoulder at ~1390 and ~1370 cm^{-1} respectively. At ~910 cm^{-1} form I has a more intense single peak than form III (Figure 3-13 b).

In the 3600 – 3300 cm^{-1} range (OH and NH stretching vibrations) form I can be determined by its single peak at 3337 cm^{-1}, while form II has a peak with larger intensity at 3280 cm^{-1} with two shoulders at 3325 and 3321 cm^{-1}. The spectra for form I and form II differ in intensity and location for some of the major absorption bands as well as the fine structure. While in the 2000 – 650 cm^{-1} range the fundamental frequencies of the peaks were almost the same, with the main differences being in the intensity ratio of the peaks and the presence of peaks specific to each form (Bartolomei et al. 1998).

In 1999 Bartolomei et al. (1999) published the FT-IR spectra of form I and form II propranolol and indicated the specific peaks for each form. Form I propranolol has a single peak at ~990 cm^{-1} and a single

peak at ~910 cm^{-1}, whilst form II has a small single peak at ~1140 cm^{-1}, a small broad peak at ~920 cm^{-1} and a shoulder at ~760 cm^{-1}.

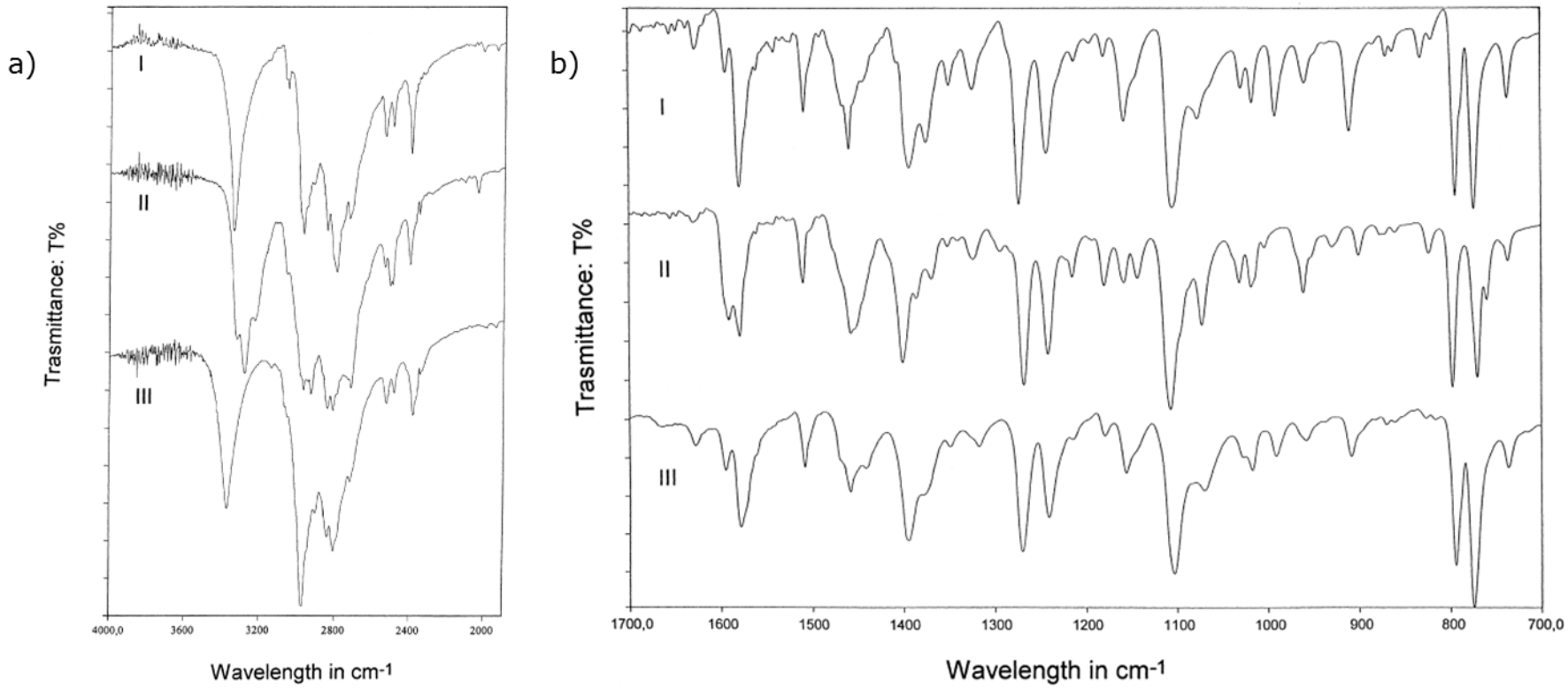

Figure 3-13 (a) FT-IR spectra in the 4000 – 2000 cm^{-1} range, for propranolol hydrochloride polymorphs form I, II and III (b) FT-IR spectra in the finger print region for propranolol hydrochloride polymorphs form I, II and III. Images taken from Bartolomei et al. (1998).

The major peaks for propranolol hydrochloride (form II) and their assignments are also summarised in Table 3-3.

IR frequency (cm^{-1})	**Qualitative assignments**
3280	Secondary amine -N-H [1-3]
2964	C-H stretch [1-3]
1579	Aryl C=C stretch [1-3]
1267	Aryl alkyl ether [4,5]
1240	Aryl O-CH_2 asymmetric stretch [1-3]
1030	Aryl O-CH2 symmetric stretch [1-3]
798	α – substituted naphthalene [1-3]

Table 3-3 Propranolol hydrochloride characteristic peaks and assignments. References [1] (Meka et al. 2012) [2] (Venkata Srikanth et al. 2012) [3] (Meka et al. 2014) [4] (Ambrus et al. 2014) [5] (Chaturvedi et al. 2010).

3.1.6.3 Raman spectroscopy

The Raman spectra for propranolol has two strong peaks at 1385 cm^{-1} and 737 cm^{-1} (Figure 3-13 a) which are attributed to napthyl ring vibrations. Medium intensity vibrations were also recorded at 1578 cm^{-1} and 1439 cm^{-1} which are also attributed to different modes of napthyl group vibration (Figure 3-13 b) (Farca et al. 2016) .

a)

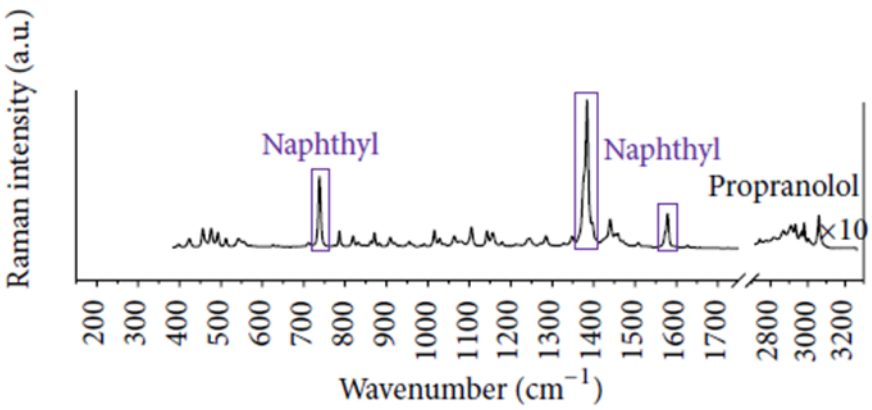

b)

Exp/cm^{-1}	Assignments
422	$\delta(N_3H_{24}) + \rho(C_5H_2)$
456	symetric stretching naphtalene
477	$\delta(N_3C_5C_6) + \rho(C_7H_2)$
493	$\rho(N_3C_5C_6)$
512	δ(CCC) (naphtalene)
737	naphtalene ring breathing + $\delta(N_3H_{24})$
785	$\delta(N_3H_{24}) + \nu(N_3C_6C_5)$
818	$\nu_s(C_6C_9C_8) + \delta(N_3H_{24})$
908	δ(CC naphtalene) + $\delta(N_3H_{24})$
953	$\nu(O_1C_7) + \rho(C_7H_2)$
1015	$\nu(C_{18}C_{19}) + \delta(C_{17}H_{38})$
1027	$\delta(O_2H_{33}) + \rho(C_5H_2)$
1155	δ(CH) (naphtalene) + $\nu(C_6N_3)$
1245	$\tau(C_7H_2) + \delta(C_4H_{20})$
1383	ν(CC naphtalene)
1439	δ(CH) (naphtalene) + ν(CC naphtalene)
1578	ν(CC naphtalene) + δ(CH naphtalene)

Figure 3-14 Raman spectra for propranolol (form II), and vibrational bands for propranolol in the Raman spectrum. Taken from Farca et al. (2016).

3.2 Aims and objectives

The aim of this chapter was to characterise starting materials paracetamol, clotrimazole and propranolol. The secondary aim was to produce polymorphic forms (where applicable) and amorphous forms of each compound and to characterise these too. The characterised reference samples are used in later chapters for comparison to materials produced from levitation or low field crystallisation studies. The aims were achieved by completing the following objectives:

- Characterise the starting materials (as received from the manufacturer) of paracetamol, clotrimazole and propranolol by DSC, FT-IR (ATR) and handheld Raman.
- Create reference polymorphs for paracetamol (form I and II) and propranolol (forms I, II, and III) and characterise them by DSC, FT-IR (ATR) and handheld Raman. Clotrimazole has no reported polymorphs.
- Create amorphous paracetamol and clotrimazole as reference samples then characterise them by DSC, FT-IR (ATR) and handheld Raman.

3.3 Materials and methods

3.3.1 Materials

Pharmaceutical drugs paracetamol, clotrimazole and (+/-) propranolol hydrochloride were obtained from Sigma Aldrich, Dorset, UK and used without further purification.

3.4 Experimental methods

3.4.1 Creating paracetamol polymorphs & amorphous paracetamol

3.4.1.1 Form I paracetamol

Form I paracetamol crystals were prepared using a modified method by Hendriksen et al. (1998). Crystals were prepared by dissolving 0.535 g of paracetamol (Sigma Aldrich, Dorset, UK) in 40 mL of HPLC grade water (18.2Ω). The solution was then heated at 40 °C and stirred using a magnetic stirrer until all of the solute had dissolved. The solution was then transferred to a refrigerator and maintained at 5 °C. Four days later small crystals had crystallised out in the bottom of the vial. When the samples were required for analysis the crystals were filtered from the solution, air dried and analysed by optical light microscopy, DSC, Raman and FT-IR (ATR).

3.4.1.2 Form II paracetamol

Paracetamol form II can be created by crystallisation of the melt of form I or by a heat, cool, heat cycle. In this thesis three methods were used to create form II paracetamol which are described below.

Method 1

Form II paracetamol can be crystallised from the melt. The first method, modified from Sohn (Sohn 1990; Nichols and Frampton 1998) involved melting approximately 5 mg of paracetamol on a glass microscope slide on a temperature controlled hot plate at 180 °C until molten. The paracetamol was then quickly vitrified by rapid cooling which involved placing the glass microscope slide on an aluminium block. The microscope slide was then transferred to a -20 °C freezer for storage.

Method 2

Form II paracetamol can also be produced by a heat, cool, heat cycle in the DSC (Di Martino et al. 1997). Approximately 5 mg of paracetamol was heated in a Tzero hermetically sealed pan to 180 °C with a ramp rate of 10 °C/ min. The paracetamol was then held (isothermally) for 5 minutes and then cooled to 20 °C to produce a glassy melt. The paracetamol was then reheated to 140 °C (again, at 10 °C/ min) to produce form II. Upon further heating a form II melt was detected. DSC curves were recorded on the TA instruments Q2000, starting temperature ambient, heating rate 10 °C/. Nitrogen flow was set at 150 mL/ minute dry gas and 80 mL/ minute purge gas.

Method 3

The same heat, cool, heat cycle was also applied to ca. 5 mg of paracetamol on a glass microscope slide (uncovered), heated on a temperature controlled hot plate. The sample was heated to 180 °C, cooled to room temperature and heated again to 140 °C.

3.4.1.3 Form III paracetamol

A method adapted from Burley et al. (2007) was used to produce form III paracetamol. A small amount of paracetamol (ca. 5 mg) was placed between two glass circular microscope slides and was loaded into the hot stage microscopy cell of the optical microscope. The paracetamol was then heated to 180 °C at a heating rate of 10 °C/ minute. The sample was then held for 10 minutes to ensure complete conversion to the melt. The melt was then cooled to 40. 1°C and reheated again to 70 °C at a heating rate of 10 °C/minute. When the sample reached 70 °C it was held for 10 minutes to allow conversion to form III. The sample was then reheated at 10 °C/ min until it reached 120 °C where a new polymorph could be seen crystallising

out (form II), the sample was held at 120 °C for 5 minutes then reheated to 140 °C at a slower heating rate of 5°C/ min to allow complete conversion of form III to form II. The sample was viewed using crossed polarisers on the microscope and images recorded digitally.

3.4.1.4 Amorphous paracetamol

Amorphous paracetamol was produced by heating paracetamol (melting point 168 – 172 °C (Qi et al. 2008)) to 180 °C and allowing it to cool to room temperature producing a glassy melt (Zimmermann and Baranović 2011). Paracetamol can be heated on a glass microscope slide on a hot plate or in an oven. To allow for even heating in the oven, a brass block with a hole in the centre was specially made. A glass Raman vial could then be inserted into the centre of the brass block, which allowed even heating of the paracetamol around the whole circumference of the Raman vial. The brass block was pre- heated in the oven for 4 hours at 190 °C, before the addition of the Raman vial filled with paracetamol. Once the paracetamol had melted the Raman vial remained in the oven for 5 more minutes to allow the complete transformation of the paracetamol powder to the liquid melt before being taken out and allowed to cool to room temperature.

3.4.2 Creating amorphous clotrimazole

Amorphous clotrimazole was created by melting a small amount (ca. 10 mg) of clotrimazole (melting point 141 – 145 °C (Borhade et al. 2012)) on a glass microscope slide at 160 °C on a temperature controlled hot plate until it had fully melted (Yang et al. 2016). The

glassy melt was then rapidly cooled on an aluminium block and stored in a – 20 °C freezer.

3.4.3 Creating propranolol polymorphs

For propranolol hydrochloride the commercial product is supplied as form II which can be readily produced by evaporation from water, methanol, acetone and n-propanol solutions at room temperature (Bartolomei et al. 1998, 1999). To produce form II crystals 50 mg of propranolol was dissolved in an appropriate volume (approx. 3 ml) of methanol. The solution was magnetically stirred and heated at 20 °C to ensure all the powder was dissolved. The solution was then syringe filtered (0.22 μm) and divided out into Falcon centrifuge tubes (50 mL), either 0.5 mL or 2 mL for evaporation at room temperature.

Evaporation of aqueous ethanol solution at room temperature will give mixtures of form I and form III. To produce crystals 50 mg of propranolol was dissolved in an appropriate volume of ethanol. The solution was magnetically stirred and heated at 20 °C to ensure all the powder was dissolved. The solution was then syringe filtered (0.22 μm) and divided out into Falcon centrifuge tubes (50 mL), either 0.5 mL or 2 mL for evaporation at room temperature.

3.5 Results and discussion

3.5.1 Characterisation of as received materials

3.5.1.1 Paracetamol

A small quantity of the paracetamol material as received from the supplier was analysed by DSC .The average onset of melting point was 168.99 ± 0.10 °C, which is within the range reported in literature

for form I (168 – 172 °C) (Di Martino et al. 1996, 1997; Nichols and Frampton 1998; di Martino et al. 2000; Boldyreva 2003; Espeau et al. 2005).

The material was also analysed by FT-IR (ATR) and the spectra produced agreed with spectra reported for form I paracetamol in literature. The additional absorption peaks (which are not present in form II) at 806, 682 and 1228 cm^{-1} are present in the spectra confirming form I (Al-Zoubi et al. 2002b).

Handheld Raman spectroscopy was used to analyse paracetamol as received. Characteristic peaks at 1234 and 1325 cm^{-1} with three well resolved peaks in the 1500 – 1700 cm^{-1} range confirm form I paracetamol (Kauffman et al. 2008).

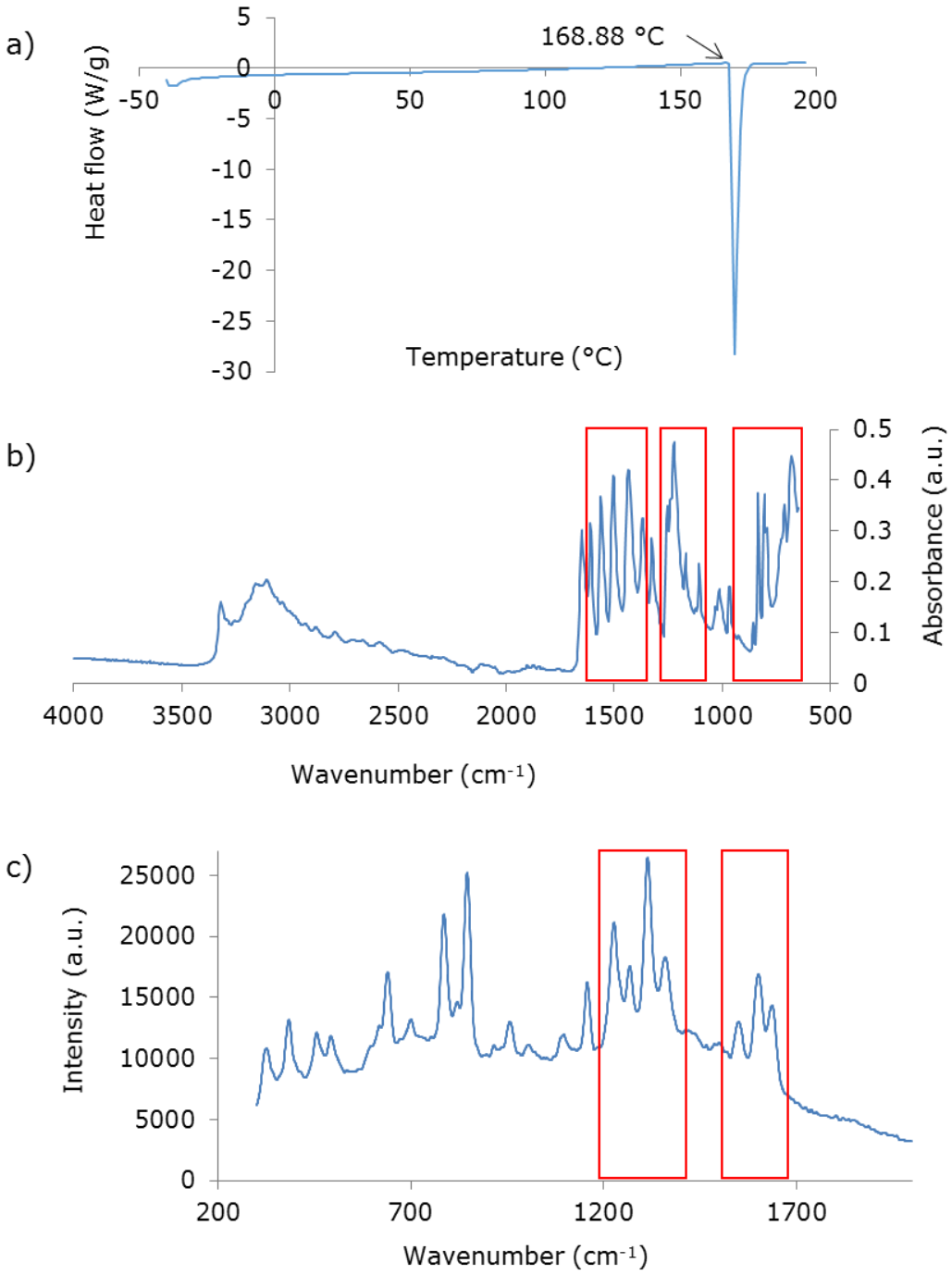

Figure 3-15 (a) DSC spectra for paracetamol as received. The onset of melting temperature is indicated by an arrow and the value displayed above the trace (b) FT-IR (ATR) spectra for paracetamol as received and (c) Handheld Raman spectra for paracetamol as received. Areas of interest are highlighted by red boxes.

3.5.1.2 Clotrimazole

The as received clotrimazole from the supplier was analysed by DSC, and the average onset of melting point was 142.49 ± 0.53 °C, which is within the range reported for clotrimazole (141 – 145 °C) (Borhade et al. 2012).

FT-IR (ATR) was used to analyse the clotrimazole as received. Spectra agreed with reported spectra for clotrimazole. Characteristic peaks at 3057, 1481 and 1438, 1082 and 1039 cm^{-1} along with the large peaks at 902, 823, 756 and 702 cm^{-1} are indicative of clotrimazole (Gupta et al. 2013; Hani et al. 2015).

The clotrimazole as received from the manufacturer was also analysed by handheld Raman spectroscopy. The spectrum for the clotrimazole as received matched spectra reported in the literature with a large double peak at 1004 cm^{-1}, and a smaller double peak at 1160 cm^{-1}.However, the small broad peak at 1460 cm^{-1} and a sharper peak at 1600 cm^{-1} (Todica 2008; Cristini-Robbe et al. 2013) have shifted slightly in the as received spectra to 1484 cm^{-1} and 1590 cm^{-1} respectively.

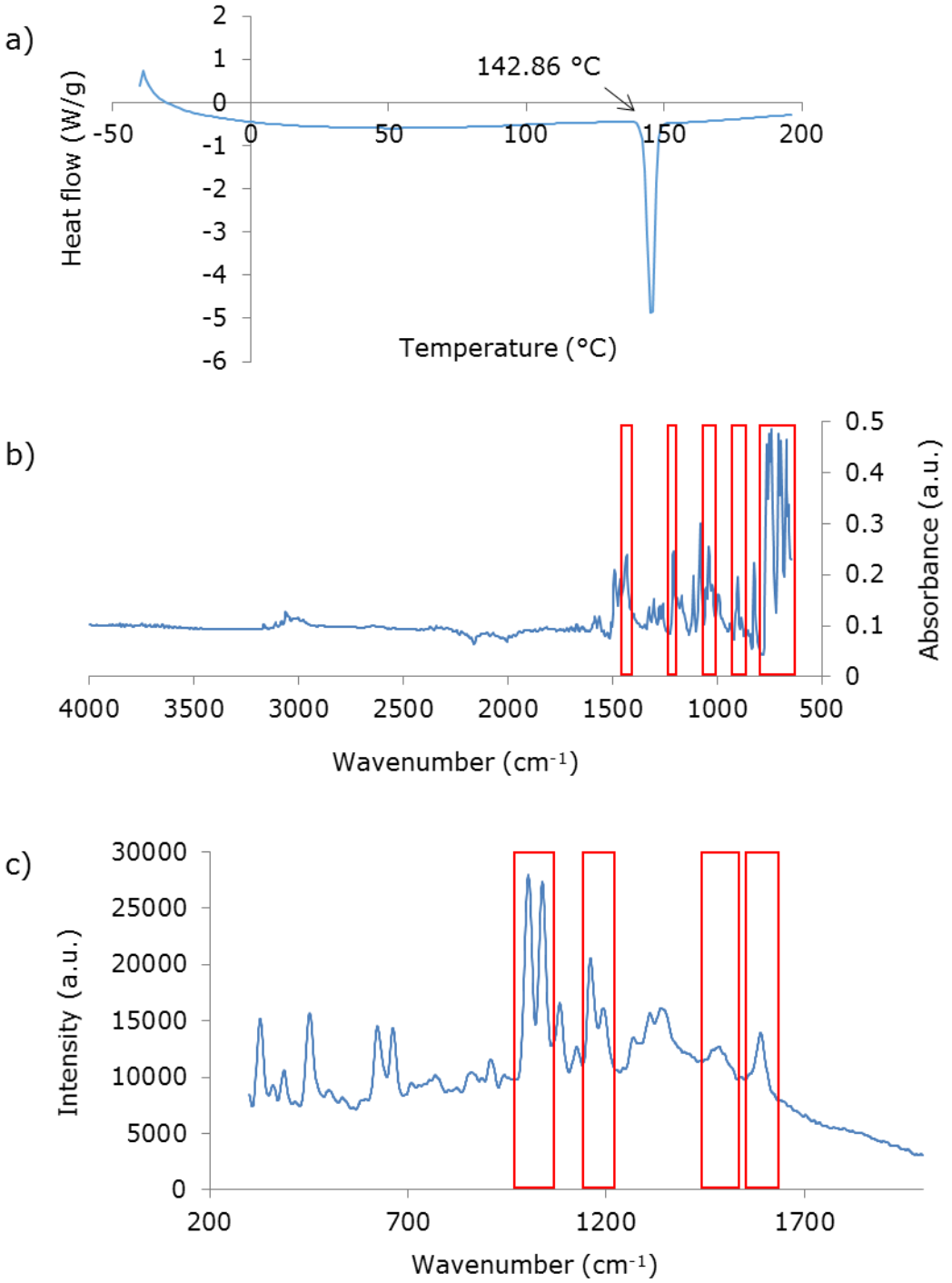

Figure 3-16 (a) DSC spectra for clotrimazole as received. The onset of melting temperature is indicated by an arrow and the value displayed above the trace (b) FT-IR (ATR) spectra for clotrimazole as received and (c) Handheld Raman spectra for clotrimazole as received. Areas of interest are highlighted by red boxes. The onset of melting temperature is indicated by an arrow in the DSC thermogram.

3.5.1.3 Propranolol

The propranolol received from the supplier was analysed by DSC and an onset melting point of 164.83 °C was recorded which is within the range of 161.8 – 167.56 °C reported in the literature (Bartolomei et al. 1999; Chaturvedi et al. 2010; Polenske et al. 2010; Meka et al. 2012; Venkata Srikanth et al. 2012; Ambrus et al. 2014; AMJ and SM 2016).

FT-IR (ATR) confirmed the as received propranolol as form II. The as received propranolol has characteristic peaks at 3280, 2964, 1579, 1267, 1240, 1030 and a large sharp peak at 798 cm^{-1} (Chaturvedi et al. 2010; Meka et al. 2012, 2014; Venkata Srikanth et al. 2012; Ambrus et al. 2014). For form II propranolol defining characteristics are the peak at 3280 cm^{-1} with two shoulders at 3325 and 3321 cm^{-1}, while form I and form III have a sharp single peak. Another subtle difference is the three single peaks at approx. 1140 - 1180 cm^{-1} for form II while form I and III have a peak with a shoulder (Bartolomei et al. 1998).

Propranolol as received was also analysed by handheld Raman spectroscopy. The spectra agreed with spectra produced in the literature (Farca et al. 2016) however, spectra were shifted to slightly higher wavenumbers. The two strong vibrations attributed to napthyl ring vibrations were at 1418 and 793 cm^{-1} and the medium strength vibrations at 1612 and 1478 cm^{-1}.

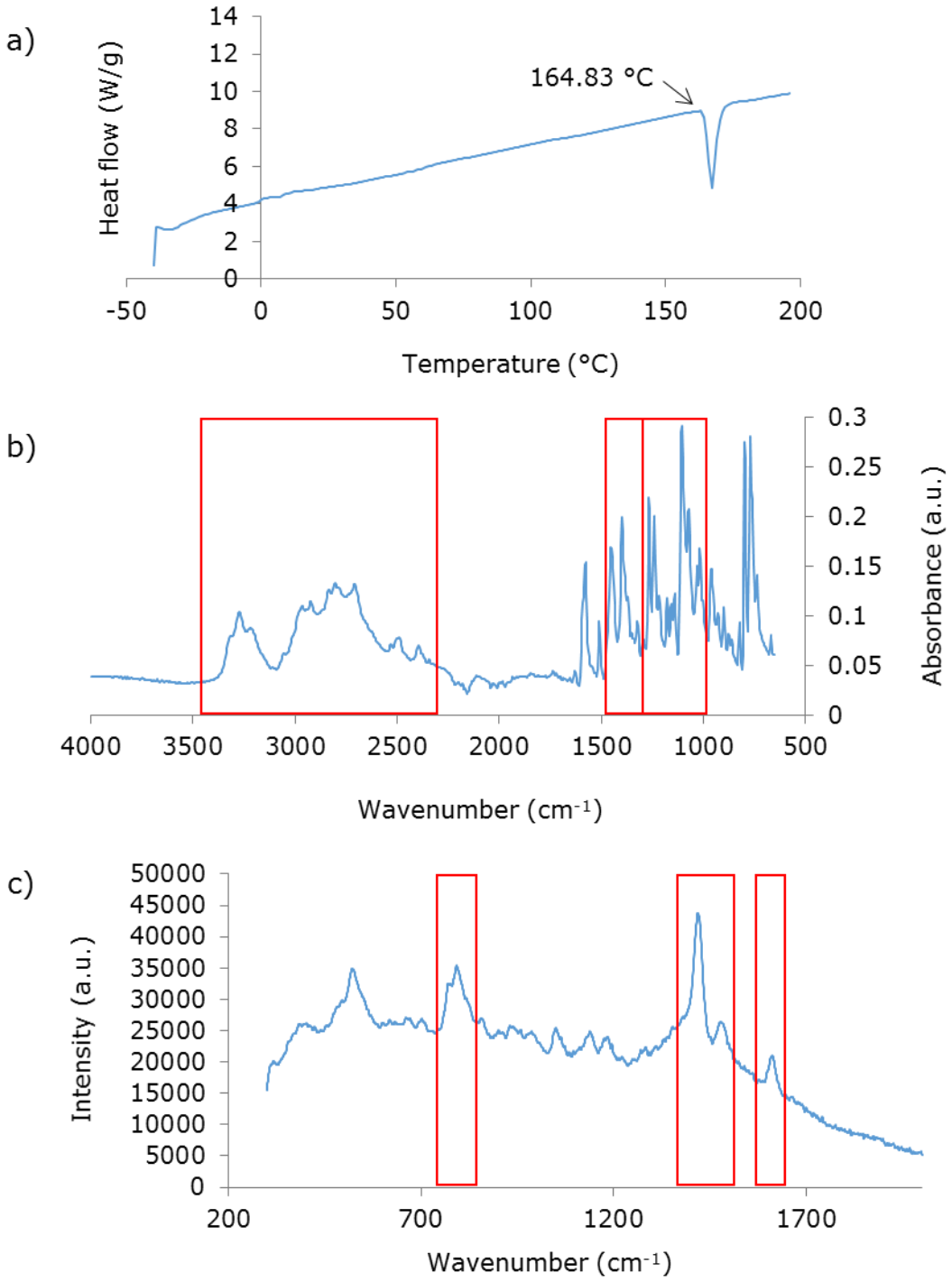

Figure 3-17 (a) DSC of propranolol HCl as received. The onset of melting temperature is indicated by an arrow and the value displayed above the trace (b) FT-IR (ATR) spectra of propranolol HCl as received and (c) Handheld Raman spectra of propranolol HCl as received. Areas of interest are highlighted by red boxes.

3.5.2 Characterisation of amorphous and polymorphic standards

3.5.2.1 Paracetamol

3.5.2.1.1 Form I paracetamol

Form I paracetamol crystals were created from solution, the method of which is described in section 3.4.1.1. The paracetamol crystals were viewed using optical light microscopy and under crossed polarisers (
Figure 3-18). Characteristic morphology for form I paracetamol is prisms and plates while form II is elongated prisms (needles) (Nichols and Frampton 1998).

Form I and form II paracetamol crystals can easily be identified by rotating between crossed polarizers. When rotated every 90° form II displays complete extinction. However, when form I is rotated (and viewed along the *b* – axis) it shows dispersed and incomplete extinction, with a distinguishing change in colour from yellow to blue as it passes through the extinction position (Nichols and Frampton 1998).

Microscopy images of the paracetamol crystals are displayed in Figure 3-18. The paracetamol crystals have a prism and plate morphology indicating form I paracetamol. Further to this the crystals produced a changed from blue to yellow when rotated by 90° between crossed polarisers supporting the microscopy morphology results indicating that the crystals are form I paracetamol.

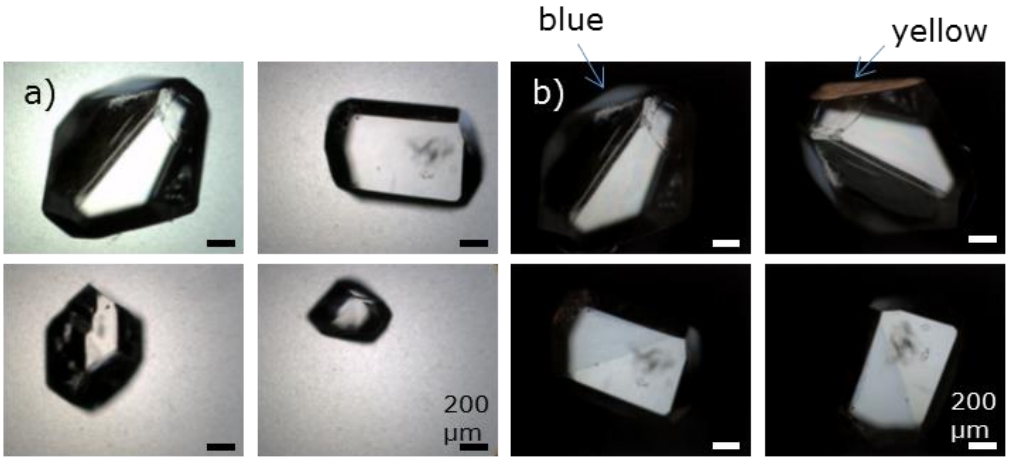

Figure 3-18 (a) Paracetamol crystals viewed using optical light microscopy (b) Paracetamol crystals viewed under crossed polarisers, the crystals can be seen changing from blue to yellow when rotated by 90°. Images taken at x4 magnification.

A small quantity of the paracetamol crystals were analysed by DSC and an onset melting point of 168.63 °C was recorded, which is similar to the as received melting point of 168.88 °C. The onset of melting temperature of the crystals is within the range reported in literature for form I (168 – 172 °C) (Di Martino et al. 1996, 1997; Nichols and Frampton 1998; di Martino et al. 2000; Boldyreva 2003; Espeau et al. 2005) indicating form I paracetamol.

FT-IR (ATR) was used to analyse the paracetamol crystals and the spectra agreed with the as received sample. Absorption peaks specific to form I at 806, 682 and 1228 cm^{-1} are present in the spectra confirming form I paracetamol (Al-Zoubi et al. 2002b).

The paracetamol crystals were also analysed by handheld Raman spectroscopy. Three well resolved peaks in the 1500 – 1700 cm^{-1} range with characteristic peaks at 1234 and 1325 cm^{-1} confirm form I paracetamol (Kauffman et al. 2008).

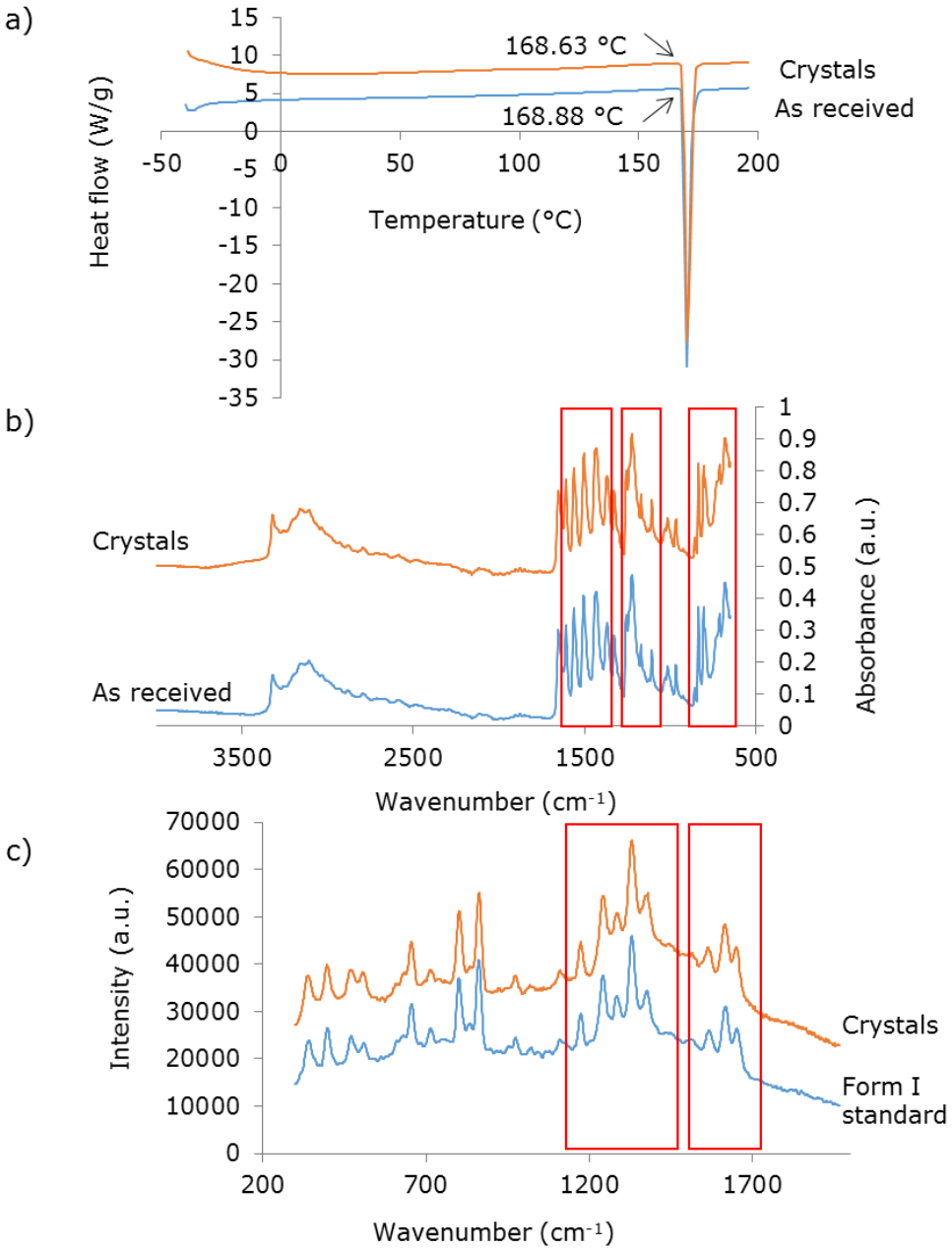

Figure 3-19 (a) DSC thermograms of paracetamol crystals and paracetamol as received. The onset of melting temperature is indicated by an arrow and the value displayed above the trace (b) FT-IR (ATR) spectra of paracetamol as received and the crystals made from solution (c) Handheld Raman spectra of paracetamol as received and the crystals made from solution. Red boxes indicate areas of interest. The spectrum for the crystal sample has been offset horizontally due to operator calibration error. Spectra have been scaled and offset vertically for presentational purposes.

3.5.2.1.2 Form II paracetamol

Form II paracetamol can be crystallised from the melt of form I (Sohn 1990; Nichols and Frampton 1998; Al-Zoubi et al. 2002a) or made by a heating, cooling, heating cycle (Di Martino et al. 1997). In this thesis three methods were used to create form II paracetamol, the methods of which are described in section 3.4.1.2.

The samples made from the melt of form I (method 1), or by a heating, cooling, heating cycle (method 3) were viewed using optical light microscopy, which confirmed the crystalline nature of the samples (Figure 3-20).

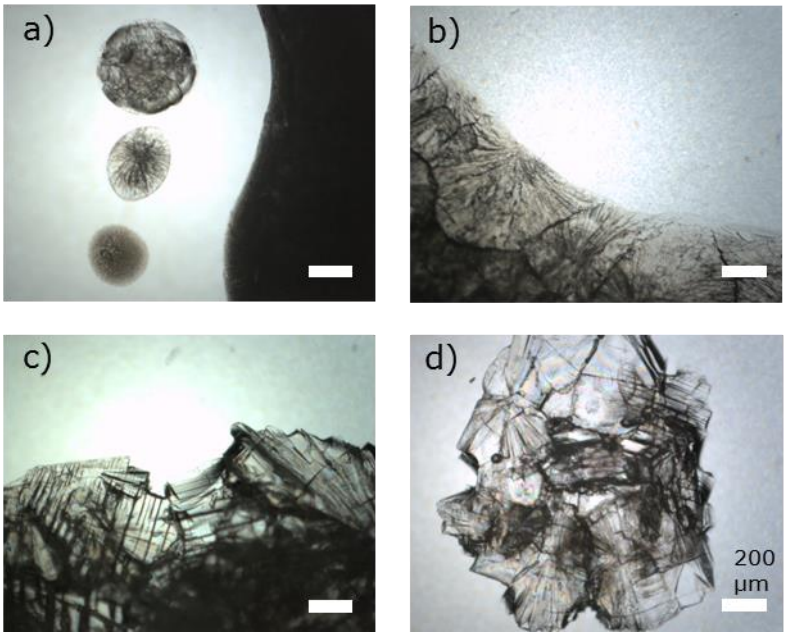

Figure 3-20 (a) Optical microscopy images of paracetamol produced by method 1, sample no 1 (b) Paracetamol produced by method 1, sample no 2 (c) Paracetamol produced by method 3, sample no 1 (d) Paracetamol produced by method 3, sample no 2. Images taken at x4 magnification.

Method 2, which involved a heating, cooling and heating cycle, whilst useful for DSC analysis was problematic when trying to remove the

samples from the hermetically sealed pans, thus making it difficult to further analyse the sample by microscopy, Raman or FT-IR (ATR).

The samples produced from method 1 and method 3 were analysed by handheld Raman spectroscopy. Form II paracetamol has a pair of weak peaks at 1220 and 1245 cm^{-1} and a strong peak at 1329 cm^{-1} compared to the form I spectra which has two large peaks at 1234 and 1325 cm^{-1}. In the 1500 – 1700 cm^{-1} range form II peaks are shifted closer to one another relative to the spectra for form I (Kauffman et al. 2008). The samples produced by method 1 and 3 indicated form II paracetamol. The spectra for both methods have a sharp peak at 1329 cm^{-1} and the three peaks in the 1500 – 1700 cm^{-1} range have moved closer together (Figure 3-21).

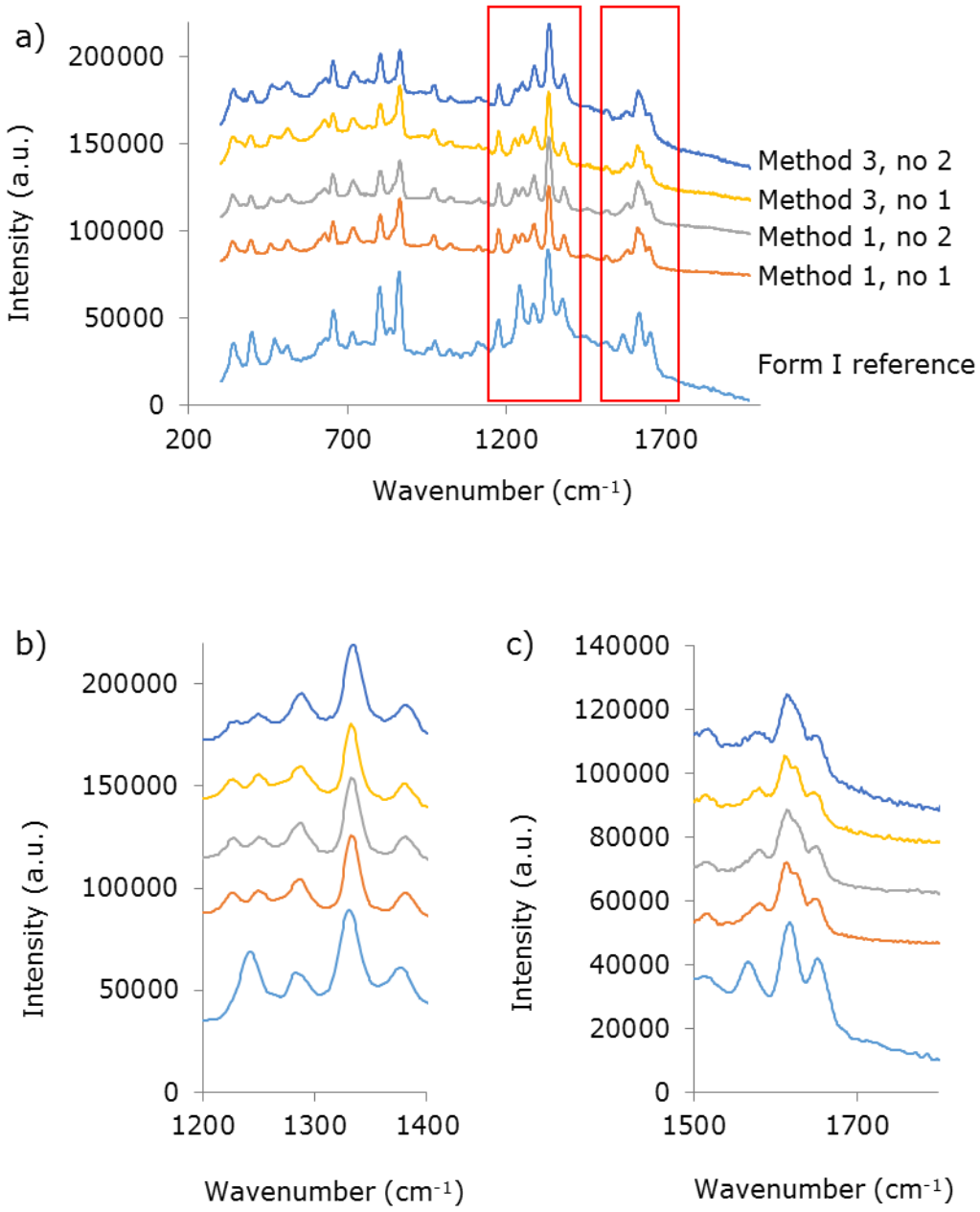

Figure 3-21 (a) Handheld Raman spectra of form I paracetamol and samples produced by methods 1 and 3.Red boxes indicate areas of interest and are zoomed in in part (b & c).(b) Zoomed in spectra in the range 1200 – 1450 cm^{-1} (c) Zoomed in spectra in the range 1500 – 1800 cm^{-1}. Spectra for samples method 1 & 3, numbers 1 and 2, were offset horizontally due to operator calibration error. Spectra have been scaled and offset vertically for presentational purposes.

The samples made from methods 1 and 3 were also analysed by FT-IR (ATR). Differences in the C-C aromatic stretching peaks include extra peaks at 1626 cm^{-1} and 1453 cm^{-1} for form II compared to form I paracetamol. Form I has an addition peak at 1228 cm^{-1} compared to form II paracetamol. Additional peaks for form I include a small peak at 806 cm^{-1} and a broader peak at 682 cm^{-1} (Al-Zoubi et al. 2002b). Method 1, sample 1 and 2, and method 3, sample 1, indicate form II paracetamol (Figure 3-22) as they have the extra peaks at 1626 cm^{-1} and 1453 cm^{-1}.However, method 3, sample 2 now has a spectrum that matches the form I spectra, with additional peaks at 806 cm^{-1}, and a broader peak at 682 cm^{-1}, and a peak at 1228 cm^{-1}. The handheld Raman spectra for method 3, sample 2 indicated form II paracetamol, so it is possible that the paracetamol converted back to the more stable form I. A second possible cause is sub sampling, where a different part of the sample is used in the handheld Raman compared to the FT-IR (ATR). It is possible during the heating cycle on the microscope slide that some of the paracetamol didn't fully melt and therefore convert to form II leaving a mixture of form I and form II on the microscope slide.

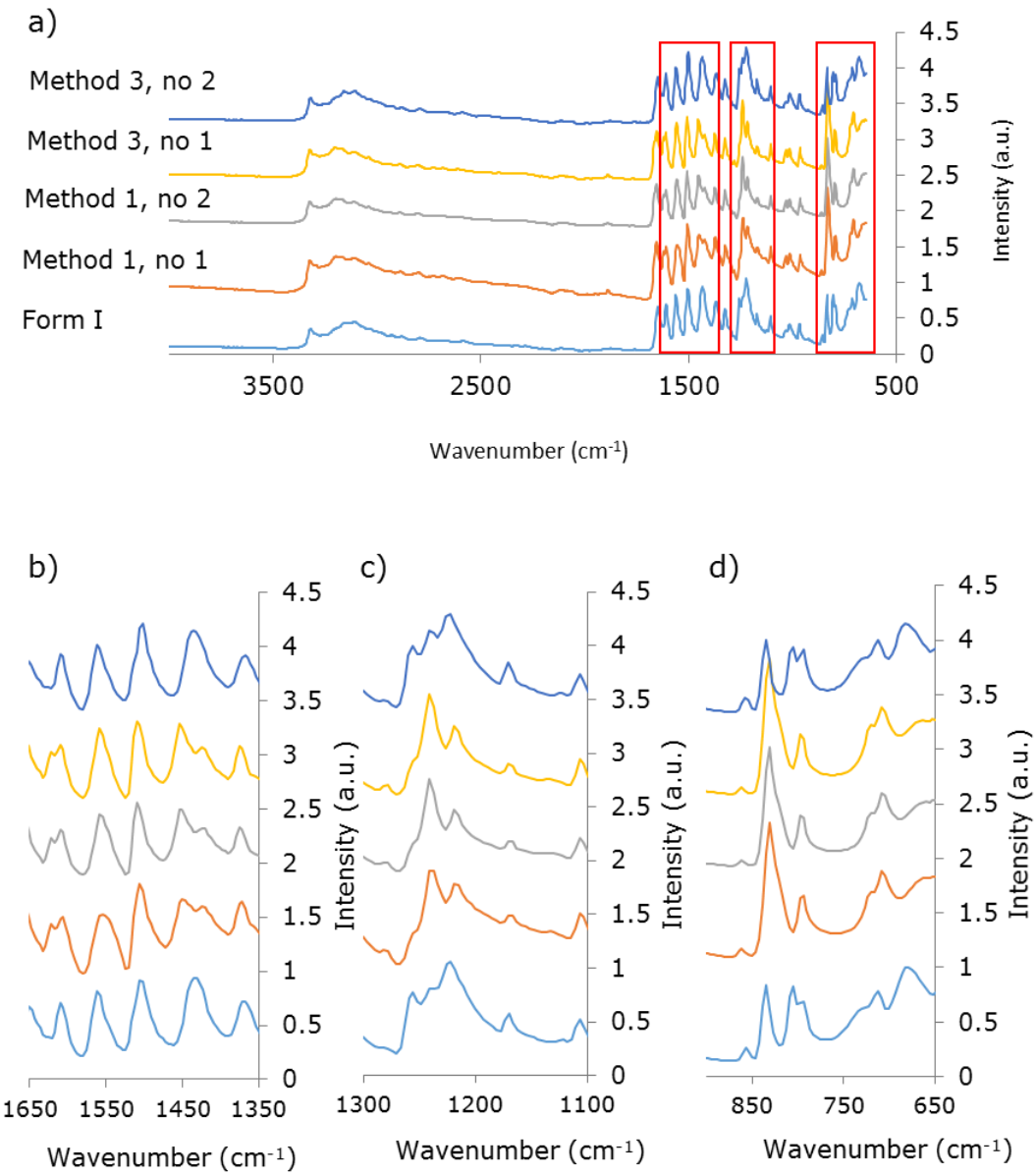

Figure 3-22 (a) FT-IR (ATR) for paracetamol samples made by methods 1 and 3. Red boxes indicate areas of interest and are zoomed in in parts (b & c & d).(b) Zoomed in spectra in the range 1650 – 1350 cm^{-1} (c) Zoomed in spectra in the range 1300 – 1100 cm^{-1} (d) Zoomed in spectra in the range 900 – 650 cm^{-1}. Spectra have been scaled and offset for presentational purposes.

The samples produced by method 1 and 3 were also analysed by DSC; melting points were in the range of 165.38 – 168.88 °C (Figure 3-23). Despite all samples indicating form II in the FT-IR (ATR) and handheld Raman spectra (with the exception of method 2, sample 3) the onset melting temperatures were closer to form I paracetamol (168-172 °C). However, Di Martino et al. (1996, 1997) also reported similar difficulties. When creating form II paracetamol in an oven, and analysing the sample by DSC the form II would indicate form I, even when no form I was detected by XRPD (X-ray powder diffraction) which had a detection limit of 2%. The authors suggest that if the form II paracetamol has trace amounts of form I then the DSC curve produced will indicate form I.

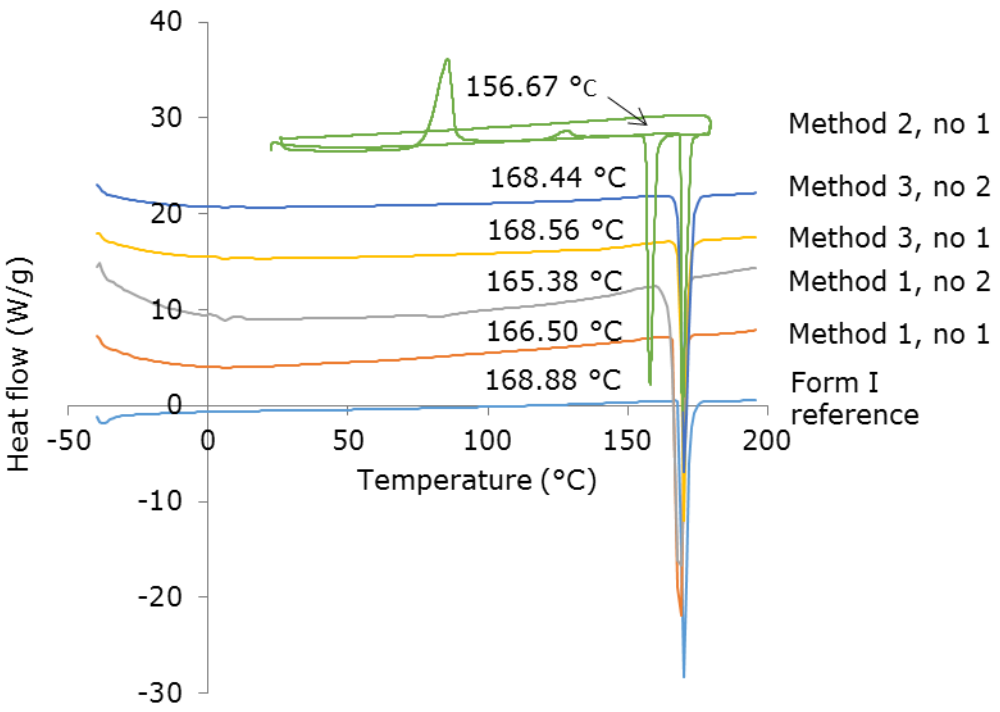

Figure 3-23 DSC thermograms of paracetamol samples made using method 1, 2 and 3. Onset of melting points are indicated by the number above each individual spectra. Spectra have been scaled and offset for presentational purposes.

The paracetamol sample produced by method 2, which involved a heat cool heat cycle in the DSC had a melting point of 156.67 °C. This onset of melting temperature agrees with literature, where form II paracetamol has a melting point in the range of 156 – 158 °C (Di Martino et al. 1996, 1997; Nichols and Frampton 1998; di Martino et al. 2000; Boldyreva 2003; Espeau et al. 2005). A large exothermic peak at approximately 70 °C and a smaller exothermic peak at approximately 120 °C can also be seen in the DSC trace for method 2 (Figure 3-23). In the late 1990s these exothermic peaks were attributed to the amorphous to form II transition (~ 70 °C) and the transition of form II to form I (~ 120 °C) (Di Martino et al. 1997; Nichols and Frampton 1998). More recent literature assigns the large exotherm between 60 – 80 °C to an amorphous to form III transition, and the exotherm at 100 – 120 °C to a form III to II transition (Kauffman et al. 2008). However, Qi et al. (2008) investigated the crystallisation of amorphous paracetamol and found it can crystallise as form III, II or I depending on the thermal history and gaseous environment in which crystallisation takes place.

All samples produced handheld Raman spectra indicating form II. This was also confirmed by FT-IR (ATR) with the exception of method 3, sample 2, which indicated form I. The DSC results for the samples also gave melting points indicative of form I paracetamol rather than form II. As discussed by Di Martino et al. (1996, 1997) their form II samples (verified by X-ray powder diffraction) gave form I traces when analysed by DSC. If the form II paracetamol isn't polymorphically pure then any trace of form I will convert the material back to form I.

As all of the samples produced form II spectra when analysed by handheld Raman and FT-IR (ATR) (with the exception of method 3, no2 which indicated form I) it is reasonable to believe that form II was successfully created. However, like Di Martio et al. (1996, 1997)

the samples may have contained very small amounts of form I which lead to the conversion of the form II into form I whilst in the DSC. Method 3, sample 2, could have had a larger percentage of form I, possibly due to incomplete melt. Sub sampling of the material could have caused the difference in spectra when analysed by FT-IR (ATR) and handheld Raman. Form II paracetamol is also the meta-stable polymorph so it could have converted from form II to form I between analysis. Di Martino (1997) report that when creating form II paracetamol grinding of the glassy material promoted recrystallization to form I. Sohn (1990) reports that form II paracetamol transforms to the more stable form I upon grinding, but not by compression. Zimmermann et al. (2011) also report grinding can induce solid state transitions on sensitive metastable polymorphs. However, Moynihan and O'Hare (2002) report that grinding of the orthorhombic paracetamol did not cause transformation to the more stable monoclinic form which agreed with the findings of Nichols and Frampton (1998).

3.5.2.1.3 Form III paracetamol

Form III paracetamol was produced using a method adapted from Burley et al. (Burley et al. 2007) that involved heating and cooling paracetamol between two glass microscope slides (section 3.4.1.3). Fine crystals that grew radially can be seen in Figure 3-24 b, c & d which agree with the structure reported in literature for form III (Di Martino et al. 1997; Burley et al. 2007). Heating above 120 °C caused a phase transition to form II which is displayed in Figure 3-24 e & f.

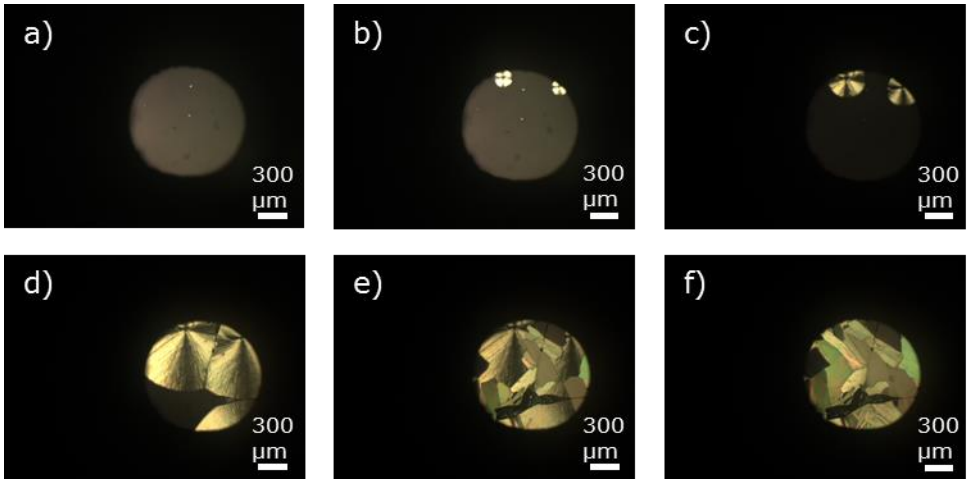

Figure 3-24 Microscopy images of paracetamol (a) At the melt at 180°C (b) During the second heating run at 70° (c) During the second heating run at 70 °C (d) During the second heating run at 70 °C (e) During the second heating run at 120 °C (f) During the second heating run at 140 °C. Images viewed using crossed polarisers and with x4 magnification.

3.5.2.1.4 Amorphous paracetamol

Amorphous paracetamol was created by melting paracetamol in a Raman vial in a brass block in an oven (3.4.1.4). The paracetamol was then quickly and easily analysed without the need to remove the sample from the container. The sample was analysed by handheld Raman over a period of 71 days.

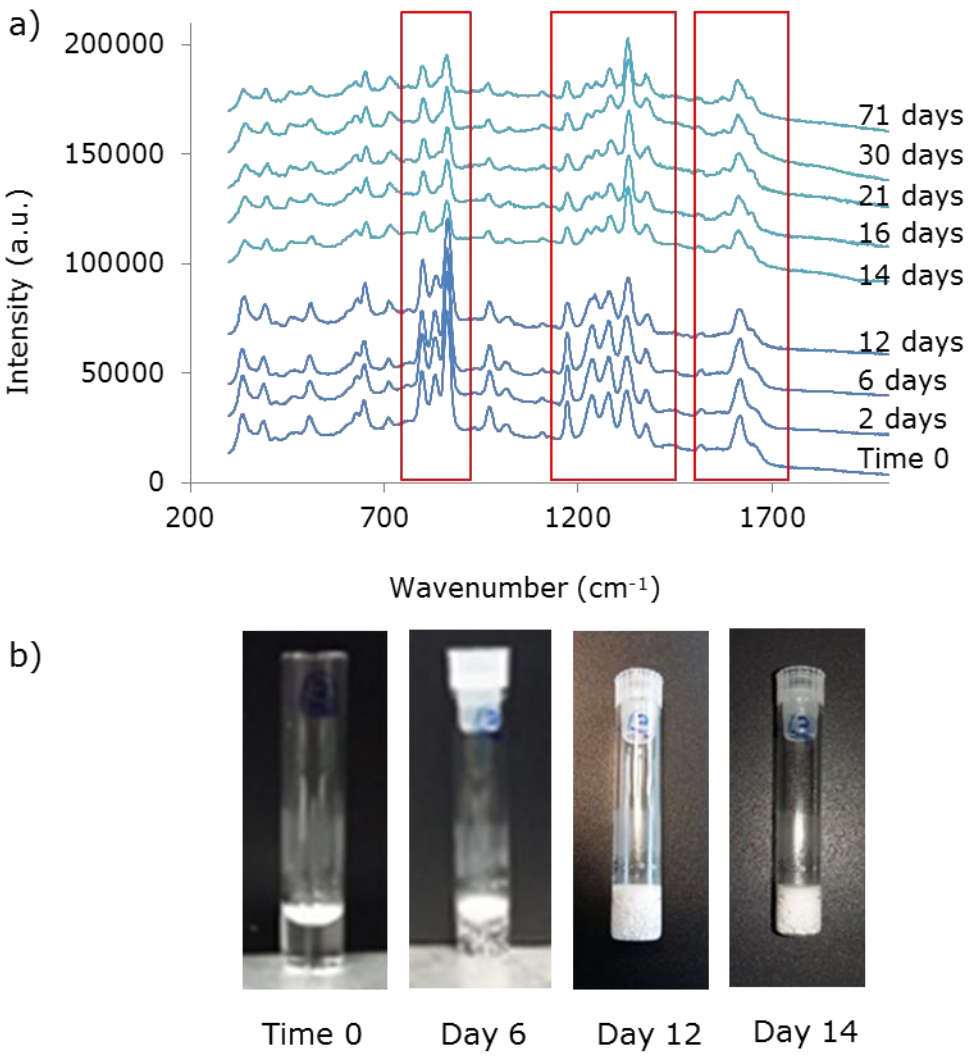

Figure 3-25 (a) Handheld Raman spectroscopy of the paracetamol sample over time Red boxes indicate areas of interest. Spectra have been scaled and offset for presentational purposes (b) Images of the paracetamol sample in Raman vials.

The paracetamol sample is amorphous at time 0 (Figure 3-25). An amorphous spectrum can be identified by the intensity of peak at 1325 cm^{-1} compared to the other peaks in the 1100 – 1300 cm^{-1} and the missing peak at 1650 cm^{-1} giving a broad shoulder in the 1500 – 1700 cm^{-1} range. The paracetamol sample stayed amorphous for up to 12 days, until it converted to form II on day 14. Form II can be distinguished by the intense peak at 1329 cm-1, and the narrowing of the peaks in the 1500 – 1700 cm-1 range compared to form I

(Kauffman et al. 2008) which are displayed in Figure 3-25. Compared to the amorphous peak and shoulder in the 1500 – 1700 cm^{-1} range the form II spectra has three definitive peaks. The amorphous sample starts off transparent but slowly turns white in colour as the amorphous paracetamol transforms into form II paracetamol (Figure 3-25 b).

3.5.2.2 Clotrimazole

Amorphous clotrimazole was created from the melt of clotrimazole powder, on a temperature controlled hot plate (section 3.4.2).

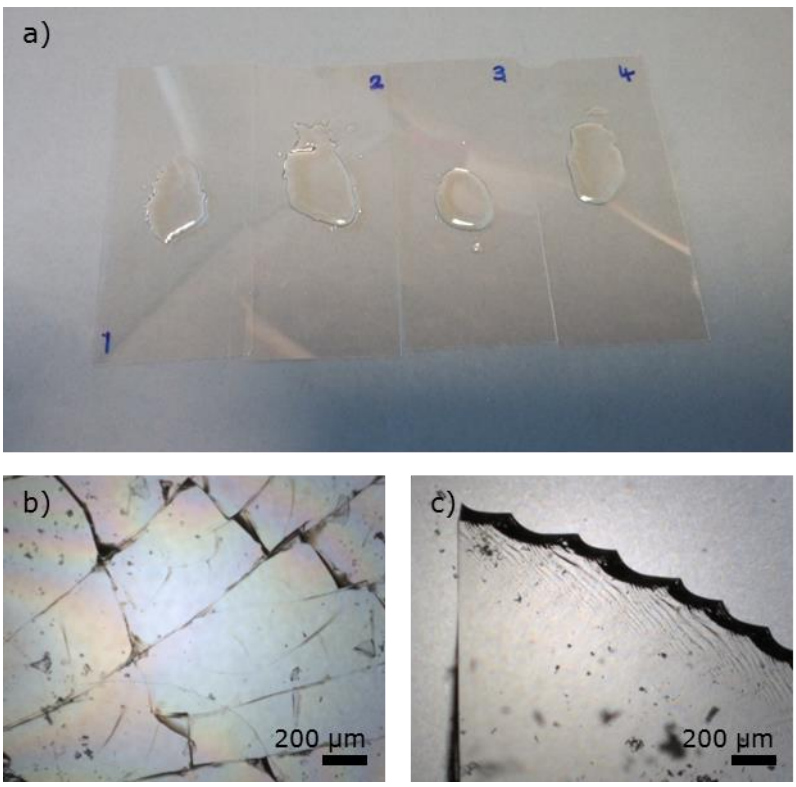

Figure 3-26 (a) Glassy melt clotrimazole on microscope slides (b) Optical microscopy images of glassy melt clotrimazole at x4 magnification. Samples were cracked to show contrast as the glassy melt was transparent.

The glassy melt clotrimazole was transparent when viewed with an optical microscope (Figure 3-26) confirming the amorphous nature of the material. Samples were cracked with a spatula to show contrast as the sample was transparent.

The glassy melt clotrimazole was analysed by FT-IR (ATR) and handheld Raman. As there are no reported FT-IR and Raman spectra for amorphous clotrimazole in the literature the samples are compared to the clotrimazole received from the manufacturer. The FT-IR (ATR) spectra are displayed in Figure 3-27 where the spectra for the glassy melt samples contain noticeable differences to the clotrimazole reference spectrum. In the 650 – 800 cm^{-1} range the double peak at 670 cm^{-1} changes. The larger peak at 670 cm^{-1} becomes less intense whilst the peak at 659 cm^{-1} becomes more intense for the glassy melt samples. The double peak at 693 cm^{-1} and 704 cm^{-1} becomes merged and less well defined compared to the clotrimazole reference. The triple peak in the clotrimazole reference at 741, 749. 764 cm^{-1} becomes a large single peak with a shoulder in the clotrimazole glassy melt spectra. Compared to the triple peak at 1036 cm^{-1} for the clotrimazole reference the glassy melt spectra becomes a broad peak with a shoulder. The peak at 1207 cm^{-1} for the clotrimazole reference also becomes a broader peak with a shoulder for the clotrimazole glassy melt. The clotrimazole reference has a small peak with a shoulder at 1431 cm^{-1} however, the peak becomes a more defined double peak in the clotrimazole glassy melt spectra.

The glassy melt clotrimazole was also analysed by handheld Raman (Figure 3-28). The spectra for the clotrimazole reference and the glassy melt clotrimazole were similar however, there were a few subtle differences. The main difference is the absence of the peak at 327 cm^{-1} in the glassy melt spectra compared to the clotrimazole reference spectrum. Another difference is the reduction in intensity

in the 1083 cm^{-1} and the 1193 cm^{-1} peaks for the glassy melt samples compared to the clotrimazole reference.

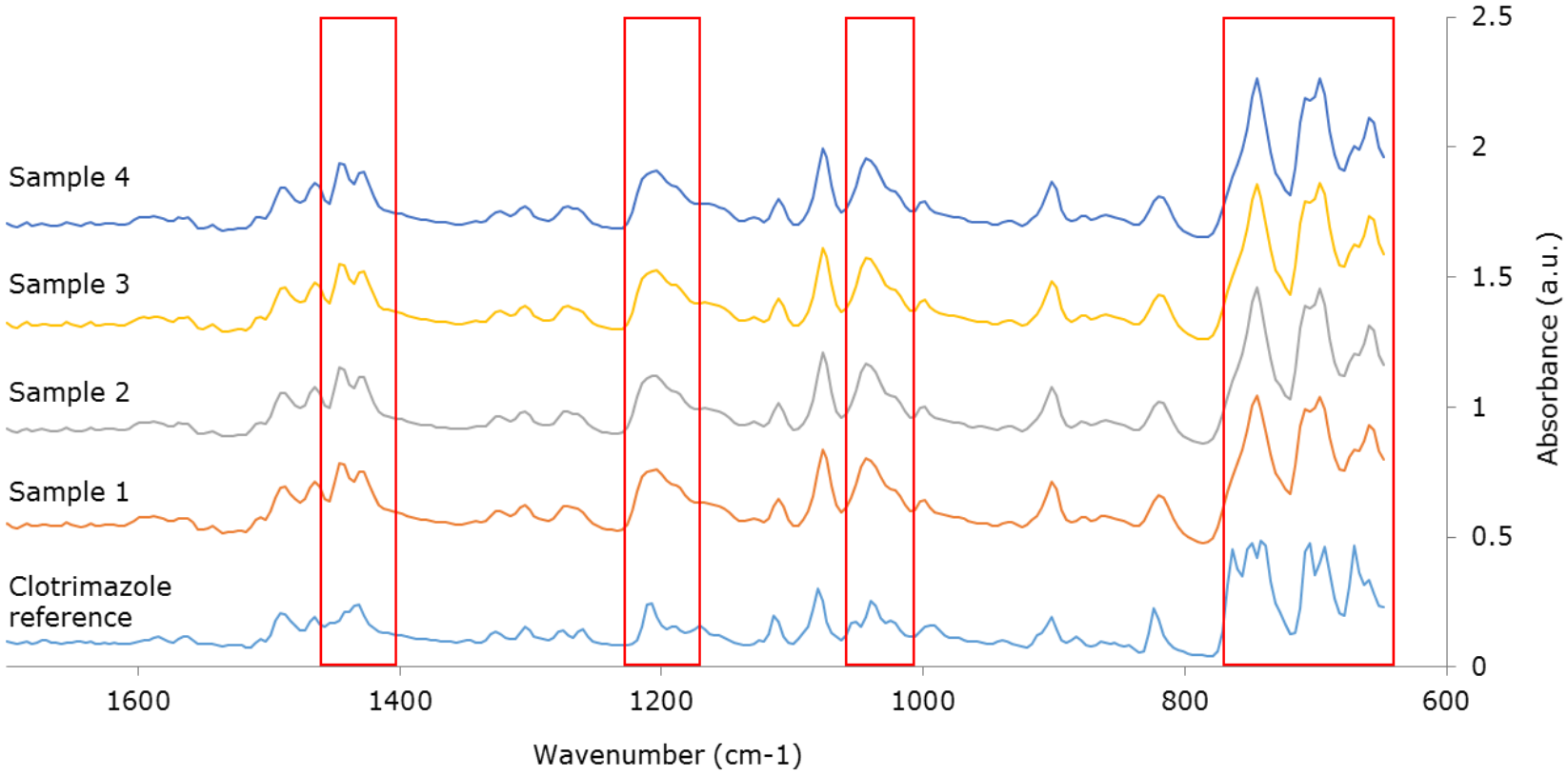

Figure 3-27 FT-IR (ATR) of clotrimazole and the glassy clotrimazole samples. Red boxes indicate areas of interest. Spectra have been scaled and offset for presentational purposes.

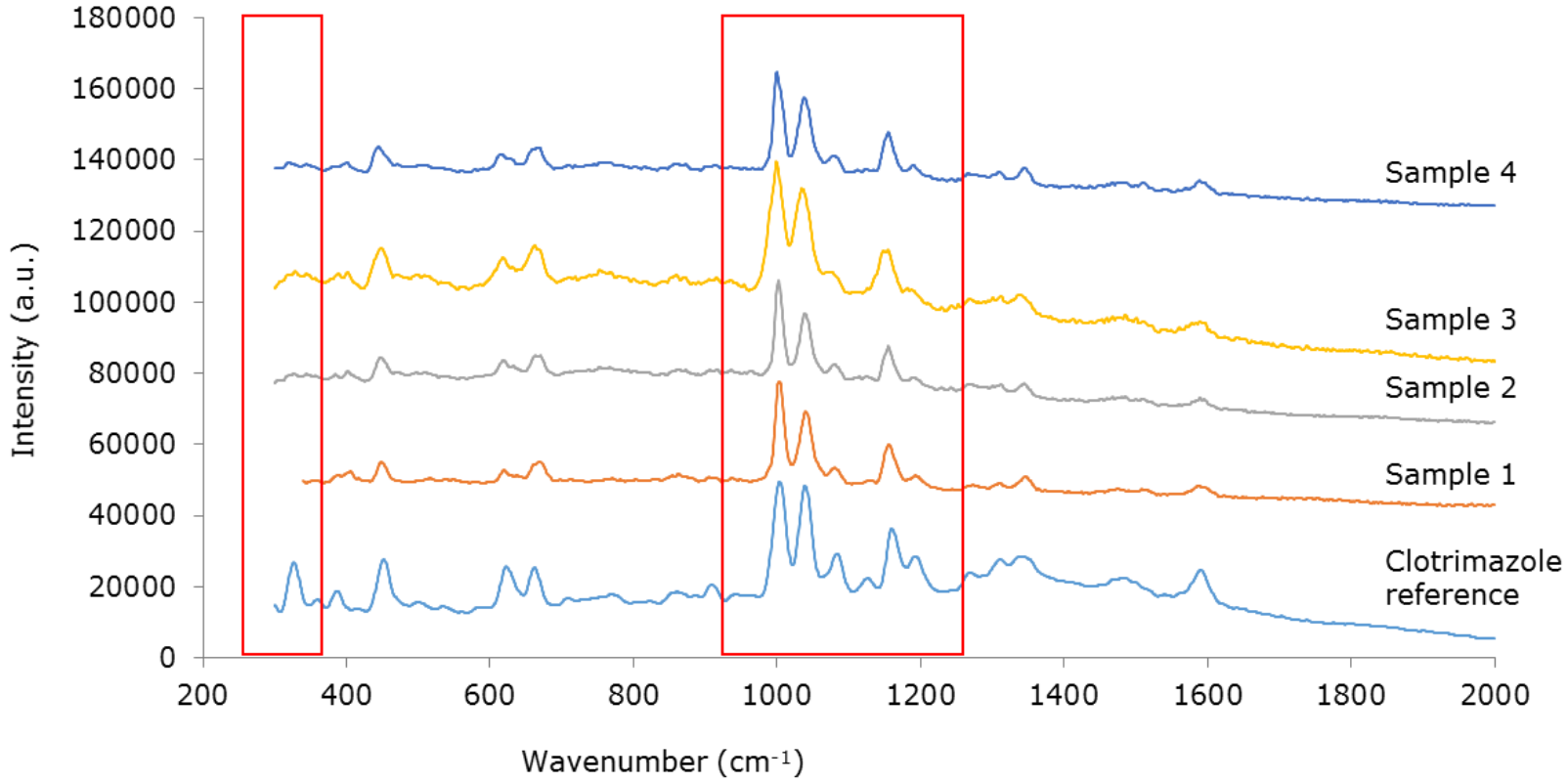

Figure 3-28 Handheld Raman of clotrimazole and the glassy clotrimazole samples. Red boxes indicate areas of interest. Spectrum for sample 1 was offset horizontally due to operator calibration error. Spectra have been scaled and offset vertically for presentational purposes.

3.5.2.3 Propranolol

Propranolol polymorphs were made by following the method in section 3.4.3. The samples were then analysed by FT-IR (ATR) and the results are displayed below.

The three polymorphs can be differentiated by their IR absorption bands in the 3400 – 2000 cm^{-1} range (Figure 3-29 b). Form I propranolol can be determined by its single peak at 3337 cm^{-1}, while form II has a peak with larger intensity at 3280 cm^{-1} with two shoulders at 3325 and 3321 cm^{-1}(Bartolomei et al. 1999). Form III spectra is very similar to form I with a large single peak 3340 cm^{-1}, and very few differences over the whole 3400 – 700 cm^{-1} range (Figure 3-13).

Form I and form III propranolol have subtle differences in their spectra for example a more intense peak at ~2970 cm^{-1} for form III whilst form I has a more intense peak than form III at 1560 cm^{-1} At ~910 cm^{-1} form I has a more intense single peak than form III. However, one noticeable difference between form I and form III is a double peak at approximately 1400 cm^{-1} for form I, while form III has a single peak with a shoulder (Figure 3-13).

The as received propranolol indicates form II propranolol as discussed in section 3.5.1.3., and is displayed in Figure 3-29. The propranolol standards all have the same spectra (Figure 3-29) which differs from II due to the double peak at 1375 and 1390 cm^{-1}, whilst form II has a single peak at 1397 cm^{-1}. The propranolol standards spectra also have a single peak at 1155 whilst form II has a three small peaks at 1177, 1155 and 1140 cm^{-1}. The propranolol standards have additional peaks at 991 and 909 cm^{-1} which are absent in form II whilst form II has an additional shoulder at 760 cm^{-1}. Form I and form III have very similar spectra, with many differences being slightly different peak

intensities, therefore the main identifiable difference between the two forms is the double peak at ~1400 cm^{-1} for form I, and a peak with a shoulder for form III (Figure 3-13). As the propranolol standards all have a double peak at 1375 and 1390 cm^{-1} the spectra can be identified as form I rather than form III (Figure 3-29).

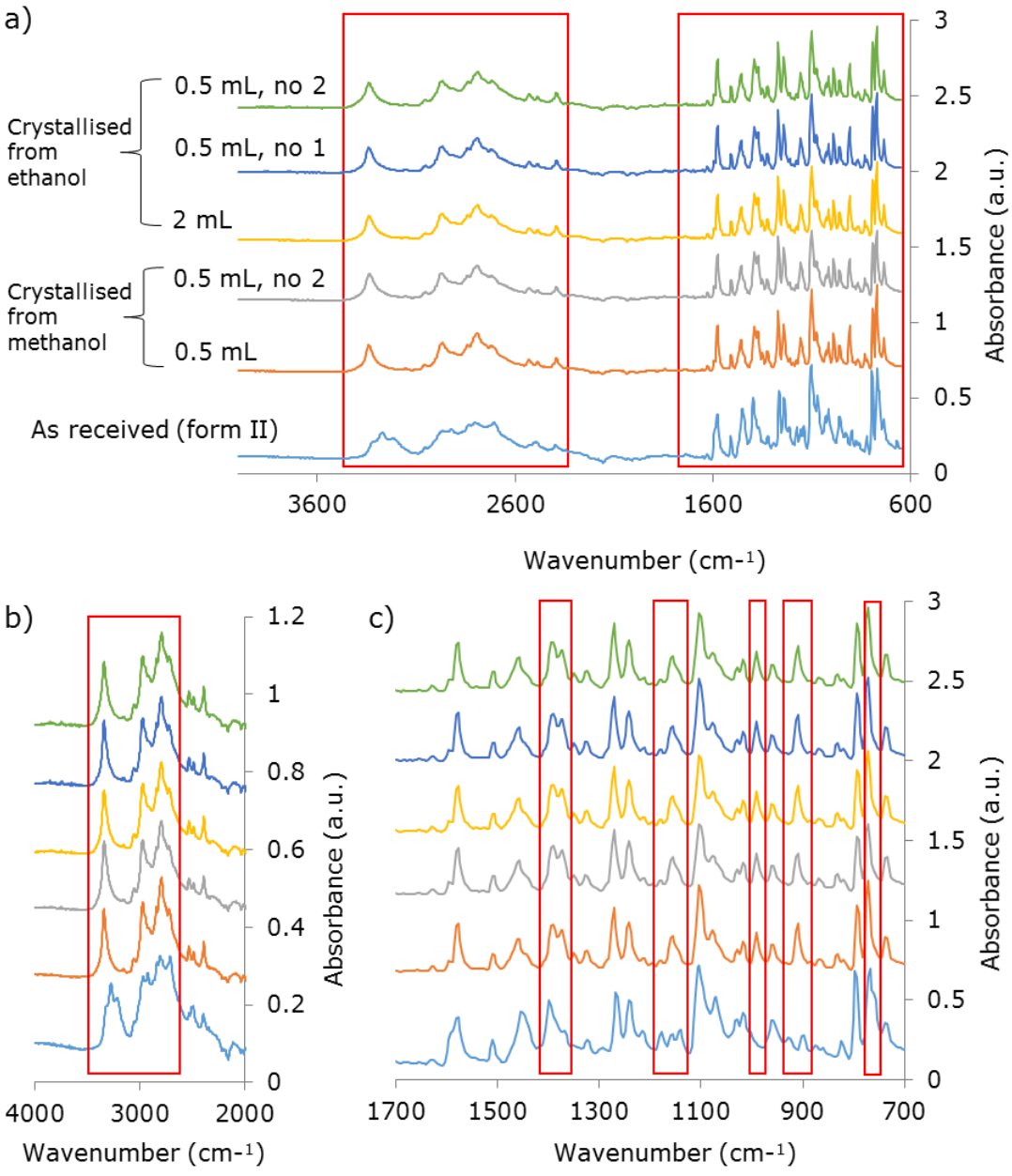

Figure 3-29 (a) FT-IR (ATR) spectra of propranolol polymorphs (b) Zoomed in spectra between 3500 – 2000 cm^{-1} (c) Zoomed in spectra between 1700 – 700 cm^{-1}.

Bartolomei et al. (1998, 1999) report that form II propranolol can be readily produced by evaporation from methanol (or water, acetone and n-propanol solutions) at room temperature. While evaporation of aqueous ethanol solution at room temperature would give mixtures of form I and form III. However, all samples (whether in methanol or ethanol) produced form I propranolol, apart from the as received sample which was form II.

3.6 Conclusion

In conclusion form I, and form II paracetamol were successfully made and characterised. One of the form II samples (method 3, sample 2) had produced a form II spectrum on one instrument whilst a form I spectrum was obtained on another; which is possibly due to an incomplete melt of the paracetamol causing a mixture of form I and form II on the microscope slide. Sub sampling of the paracetamol sample could then lead to a form II spectra on one instrument whilst a form I spectra on another. Form II paracetamol is the metastable polymorph, so it is possible that the paracetamol converted form between analyses. Form III paracetamol was successfully made between two glass microscope slides. Amorphous paracetamol was also successfully produced and analysed over time as it converted to form II (which took between 12 – 14 days).

Propranolol standards all indicated form I despite being evaporated in different solvents, either ethanol or methanol. However, form I, II and III are well characterised in the literature so comparisons of samples and reference spectra can still be made in later chapters.

The work in this chapter enables us to compare samples produced from levitation (chapters 4 and 5) and low field studies (chapter 6) to our reference spectra obtained in this chapter.

4 Initial levitation studies

4.1 Introduction

In this chapter diamagnetic levitation for pharmaceutical processing is explored. Research on the use of diamagnetism for containerless processing mainly focuses on the crystallisation of lysozyme (Yin et al. 2008) and other protein crystals (Okada et al. 2013) for enhanced X–ray crystallography, as well as melting and crystallisation experiments (Takahashi et al. 2006).

An experiment performed by Motokawa et al. (2001) involved melting a glass cube (BK 7 glass, a mixture of SiO_2 and B_2O_5) with 5 – 7 mm edges. It was placed in the levitation position of the magnet bore at 22.89 T and melted with an infrared light beam from a CO_2 laser. The glass cube melted and formed a perfectly spherical shape. The authors suggest this is a useful technique for melting materials as levitation avoids possible contamination from the crucible.

Takahashi et al. (2006) used diamagnetic levitation for containerless melting and crystallisation experiments. Organic materials benzophenone and cycloolefin polymer were used for the crystallisation and melting experiments respectively. A thermostatic bath (within the magnet bore) and laser were used to melt the crystal and control the temperature during crystallization. A crystal was placed on the end of a wire and heated by the laser in the centre of the magnet, where the authors didn't completely melt the crystal as they wanted to leave a nucleus. Crystal growth in a supercooled melt was observed at different temperatures. At 30 $^{\circ}$C growth looked dendritic whilst at 45 $^{\circ}$C facet growth could be seen from the melt. The shape of crystals was more flattened with larger axis perpendicular to the magnetic field. The authors suggest that with decreasing growth rate due to a decreasing supercooling degree the

growth mechanism changed. The paper suggests that magnetic levitation has potential to provide a novel technique in the synthesis of materials.

Using a magnetic field gradient which was strong enough to be able to levitate droplets of water Nakamura et al. (2012) studied protein crystallisation. Three samples out of fifteen showed magnetic orientation parallel to the direction of the magnetic field; the aligned crystals had better x-ray diffraction patterns than the unorientated crystals in the magnetic field and the control crystals. Five samples (including the three that aligned to the magnetic field) showed better protein crystal quality than the controls. They concluded that high strength magnetic fields could enhance the quality of the crystals and aid in the determination of precise crystal structures.

Cao et al. (2013) carried out a comparative study of the different containerless techniques diamagnetic levitation, silicone oil and agarose gel (crystals grown in gel or oil without contact with a solid surface can be considered containerless). Seven proteins were crystallised under the different containerless techniques, proteins crystallised included lysozyme, thaumatin, proteinase K. As a comparison to the levitation techniques the control samples were grown on a vessel wall. Crystal quality was determined by X-ray diffraction, mosaicity, resolution limit and Rmerge. The three containerless conditions showed better morphology than the control samples. For all three containerless conditions, X-ray diffraction data demonstrated that the quality of crystals were better than the control samples. Out of the three containerless conditions diamagnetic levitation was the best for enhancing crystal quality, the agarose gel demonstrating the second best improvement in crystal quality. The paper indicated that diamagnetic levitation was a useful aid in growing high quality protein crystals and is potentially useful in obtaining well diffracting crystals.

Using fixed magnets and a paramagnetic aqueous solution of manganese chloride Yang et al. (2014) were able to separate S-ibuprofen and RS-ibuprofen crystals using magnetic levitation. Crystals levitated according to their density, the levitation height being the distance from the centre of the crystal to the bottom magnet. Therefore, low density objects levitated at a higher height compared to a denser object. Once separation had occurred the crystals were pipetted out of the levitation device.

Currently there is a gap in the research of pharmaceutical processing using diamagnetic levitation. Therefore, in this chapter we explore the potential of diamagnetic levitation for pharmaceutical processing. In these proof of concept studies paracetamol was chosen as the first pharmaceutical entity to try, as is it a commonly used drug with up to five polymorphs. Paracetamol has been researched intensively and is well characterised (section 3.1.1). Initial experiments performed were to see if paracetamol could actually be levitated by the superconducting magnet system at the University of Nottingham (section 2.1.1). Once the experimental set up was configured the following experiments looked into the effect of containerless levitation on paracetamol. For example, could different polymorphs or amorphous paracetamol be created?

4.1.1 Aims and objectives

The aims of this chapter were to explore the potential of high strength magnetic fields for the levitation of pharmaceutical solutions. A secondary aim was to see if it was possible to grow crystals in this environment. Paracetamol was chosen as the model compound to be levitated. A further aim was the optimisation of the magnet set up once droplets could be successfully levitated. The final aim was the

investigation of diamagnetic levitation for polymorphic control. The aims were achieved by completing the following objectives:

- Perform initial levitation experiments and vary different parameters such as volume, concentration and solvent of the pharmaceutical solution.
- Optimise the set up and repeat experiments with optimised conditions.
- Create for comparison samples prepared in a non-levitating environment keeping conditions as close to the magnet set up as possible.
- Analyse samples by optical microscopy, DSC, FT-IR (ATR), and handheld Raman.

4.2 Materials and methods

4.2.1 Materials

Paracetamol (Acetaminophen, BioXtra ≥ 99%) and ethanol (200 proof, anhydrous, ≥ 99.5%) were obtained from Sigma Aldrich, Dorset, UK and used without further purification.

4.3 Experimental methods

4.3.1 Magnet set up

The Cryogenic magnet (Cryogenic Ltd, London) has been used for most experiments performed in this chapter. However, due to the magnet being serviced the Oxford magnet (Oxford Instruments, Abingdon, UK) has also been used for some experiments.

Magnet set up 1 & 2 was used during the experiments in this chapter (section 2.1.5).For all experiments in this chapter the petri dish sample collector was used (section 2.1.3) as well as a digital camera which was mounted on a clamp stand above the magnet bore (section 2.1.4). Details of the different experimental set ups can be found in Table 4-1 including the field strength and air/ nitrogen details.

Experiment	Magnet	Field strength (T)	Box/ glass cover	Air/ nitrogen	Flow rate (ccm/ min)	Bore insert/ lab temp (°C)
Initial exp. Repeats	Cryogenic Cryogenic	17.1 17.1 & 17.8	Glass (set up 1) Glass (set up 1)	Air Air	50 (majority) & 10 10 & 50	Bore @ 20 Bore @ 20
Optimising 90% Optimising 70%	Cryogenic Cryogenic & Oxford	17.1 & 17.8 17.1 16.5	Glass & box (set up 1 & 2) Box (set up 2) Box (set up 2)	Both Nitrogen N/A	10 & 50 50 N/A	Bore @ 20 Bore @ 20 RT (~20)
90% ethanol	Cryogenic	17.5	Box (set up 2)	Nitrogen	50	Bore @ 20
70% ethanol	Cryogenic	17.5	Glass cover (set up 1)	None	N/A	Bore @ 20
Seeding	Cryogenic	17.5	Box (set up 2)	Nitrogen	50	Bore @ 20

Table 4-1 Table detailing the set up parameters for each experiment.

4.3.2 Creating paracetamol solutions

Paracetamol solutions were prepared by dissolving the required amount of paracetamol (Table 4-2) in ethanol or high purity water (resistivity 18 MΩ cm) in a glass beaker whilst being gently warmed and stirred on a magnetic hot plate. The solution was magnetically stirred until all of the paracetamol had dissolved, at which point it was taken off the heat and left to cool. The solution was then syringe filtered (0.22 μm syringe filter, Millex GP, Sigma Aldrich) into vials (25 mL sample tubes, Sarstedt, Leicester, UK) for storage.

	Target concentration	Density of solvent	Solubility at 20 °C	Calculated concentration
Paracetamol in water	90% saturated solution 50% saturated solution	999.97 kg/ m^3	12.78 g/ kg solvent	11.502 g/ L 6.39 g/ L
Paracetamol in ethanol	90% saturated solution 70% saturated solution 50% saturated solution	789.00 kg/ m^3	190.61 g/ kg solvent (using the density of ethanol this equates to 150.39 g/ L)	135.35 g/ L 105.27 g/ L 75.20 g/L

Table 4-2 Table detailing the concentrations of paracetamol in water or ethanol used to make bulk solutions.

4.3.3 Sample preparation/ levitation

Paracetamol solutions were prepared as the method described in section 4.3.2. During the initial experiments the required volume was pipetted using a Gilson pipette into a plastic vial (25 mL sample tube, Sarstedt, Leicester, UK). The solution was then pipetted into the magnet bore with a glass pipette. For the optimisation experiments and any subsequent experiments in this chapter the paracetamol solutions were syringe filtered (0.22 μm syringe filter, Millex GP, Sigma Aldrich) using non-magnetic needles (Neolus, 21G, 1 ½", 0.8 x 40 mm, Terumo Pharmaceutical solutions) into the magnet bore at the stable levitation position in the magnetic field. The levitation position for the Cryogenic magnet is approximately an inch from the top of the magnet bore (excluding the lip of the magnet bore insert) and for the Oxford magnet approximately 10 cm from the top of the magnet bore.

4.3.4 Levitated droplets

During the initial experiments different paracetamol solutions were levitated. Parameters that changed were the solvent (either water or ethanol) the size of the droplet (2, 4, or 6 mL) or the drug concentration (90%, 70% or 50% saturated solution as described in Table 4-2). Samples were levitated until crystals had formed, when the ratio of paracetamol to solvent increased the susceptibility of the whole droplet decreased causing the levitating droplet to fall out. The crystals would then be collected in the collection device (described in section 2.1.3, Figure 2-3 a). Details of the droplets levitated for each experiment are displayed in Table 4-3.

Experiment	Solvent	Concentration	Volume
Initial exp. Repeats	Water Ethanol Ethanol	90% 90% and 50% 90%	2, 4 and 6 mL 2, 4 and 6 mL 6 mL
Optimising 90% Optimising 70%	Ethanol Ethanol	90% 70%	6 mL 6 mL
90% ethanol	Ethanol	90%	6 mL
70% ethanol	Ethanol	70%	6 mL
Seeding	Water Ethanol	90% 70%	4 mL 1 mL

Table 4-3 Table detailing the droplets used for each levitation experiment.

4.3.4.1 Non levitating samples

Initially, for comparison non levitating samples were syringe filtered (0.22 µm) into 35 mm petri dishes. However, the solution spread out across the petri dish and wasn't very representative of the levitating droplet's shape. The non-levitating droplets were repeated in Falcon centrifuge tubes (50 mL) as the rounded end of the tube gave a more representative shape of the levitating droplet. The non-levitating solution in falcon centrifuge tubes was left to evaporate in a switched off laminar flow cupboard.

4.4 Results and discussion

4.4.1 Initial experiments

All the levitation experiments were filmed from above (an example image can be viewed in Figure 4-1 along with example crystals collected from the collection device within the magnet bore). Paracetamol would crystallise out as individual crystals, multiple small crystals creating cup shapes and even multiple small crystals creating a paracetamol shell (Figure 4-1 b).

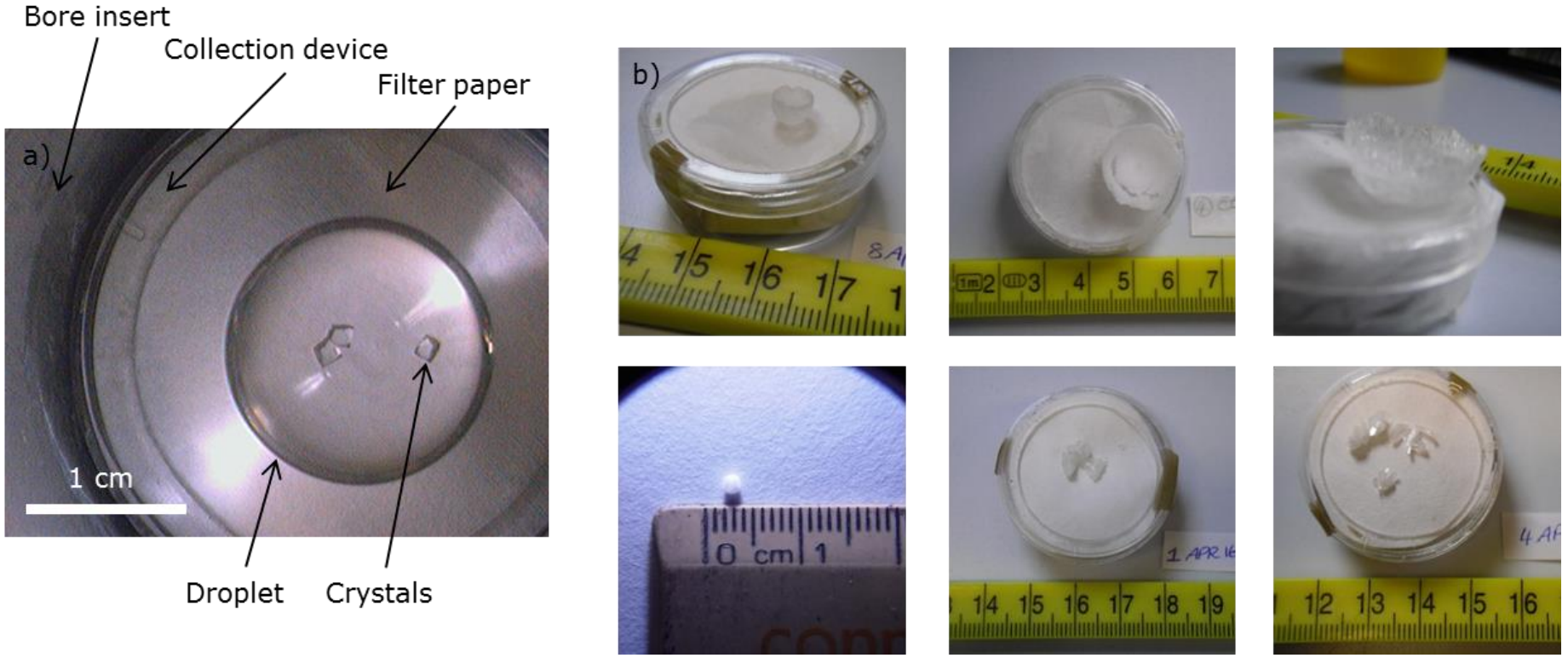

Figure 4-1 (a) An image of a levitating droplet (viewed from above) within the magnet bore (b) Examples of crystals collected from the magnet bore. Examples include individual crystals, multiple small crystals formed in a cup shape and multiple small crystals formed in a small shell.

Initial experiments were run using solutions of paracetamol in water, and paracetamol in ethanol. The volume of the droplet and concentration of the droplet were varied. Droplets of 2, 4 or 6 mL were levitated with concentrations at 90% saturation or 50% saturation. Droplets were imaged using a Fire-i camera positioned above the magnet bore. Time lapse images of levitating droplets are displayed in Figure 4-2. As the droplet evaporated over time it decreased in volume and the concentration of paracetamol therefore increased. Paracetamol has a lower magnetic susceptibility than water or ethanol, (paracetamol powder being more difficult to levitate than water or ethanol). When the ratio of paracetamol to solvent increased the susceptibility of the whole droplet decreased causing the levitating droplet to fall out. The droplet is caught by the collection device positioned below the droplet. Filming is stopped when the droplet has fallen out.

Water droplets were found to levitate longer than ethanol containing droplets as evaporation was slower allowing larger crystals to grow (Figure 4-1 a). Paracetamol droplets levitated for up to 11 hours, and crystals can be seen growing from 4 hours, and by 6 hours the crystals have grouped together in the centre of the droplet. The crystals continue to grow until they fall out into the collection device. In Figure 4-1 (b) an ethanolic droplet evaporates over time, within 5 minutes small crystals can be seen gathering in the centre of the droplet, by 7 minutes the crystals have grown in size and by 10 minutes the crystals reach the outer edges of the droplet. Within half an hour the droplet and the small crystals have fallen out into the levitation device.

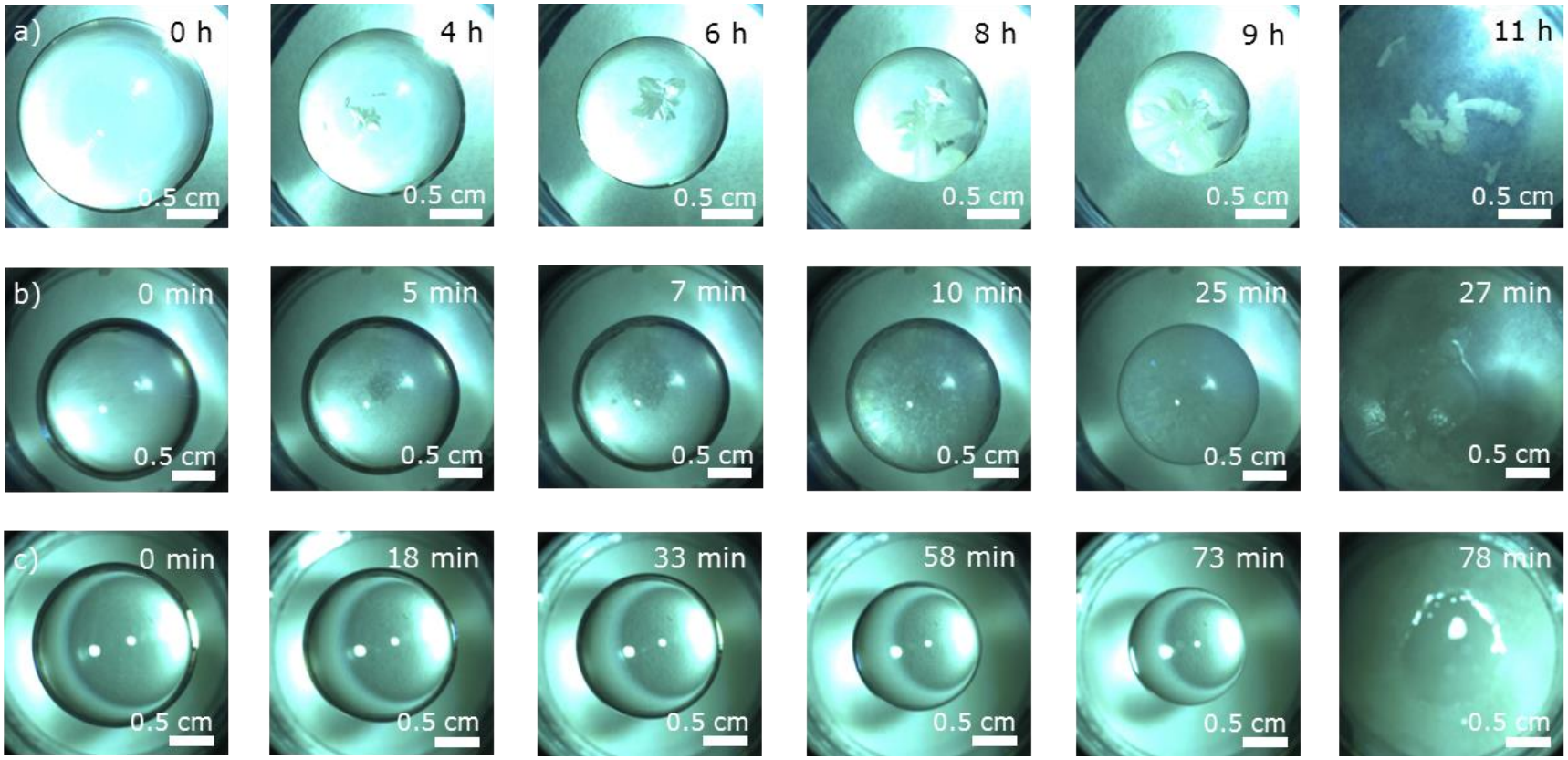

Figure 4-2 Time lapse of levitating droplets (a) Paracetamol in water, 90% saturated solution, 4 mL (b) Paracetamol in ethanol, 90% saturated solution, 4 mL (c) Paracetamol in ethanol, 50% saturated solution, 4 mL

For comparison non levitating samples were produced (with the same concentrations, volumes and solvents) and syringe filtered (0.22 µm) into petri dishes and left to evaporate in a switched off laminar flow cupboard.

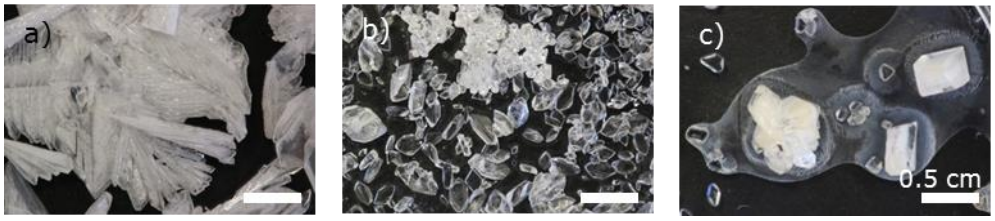

Figure 4-3 Non levitating paracetamol crystals from (a) Ethanol 50% solution, 6 mL, (b) Ethanol 90% solution, 2 mL, (c) Water 90% solution, 6 mL. Images taken using a Canon EOS 70D digital camera.

Non levitating paracetamol samples were found to be crystalline in nature: paracetamol in ethanol 50% saturated were dendritic in nature, whilst the 90% saturated solution and paracetamol in water were more platy and prismic in nature.

4.4.1.1 DSC analysis of initial paracetamol samples

Initial experiments were analysed by DSC after levitation, or after drying in the petri dishes. Example DSC thermograms for levitated samples are displayed in Figure 4-4. The majority of samples indicated form I paracetamol, however, occasionally form II paracetamol was observed (sample 1).

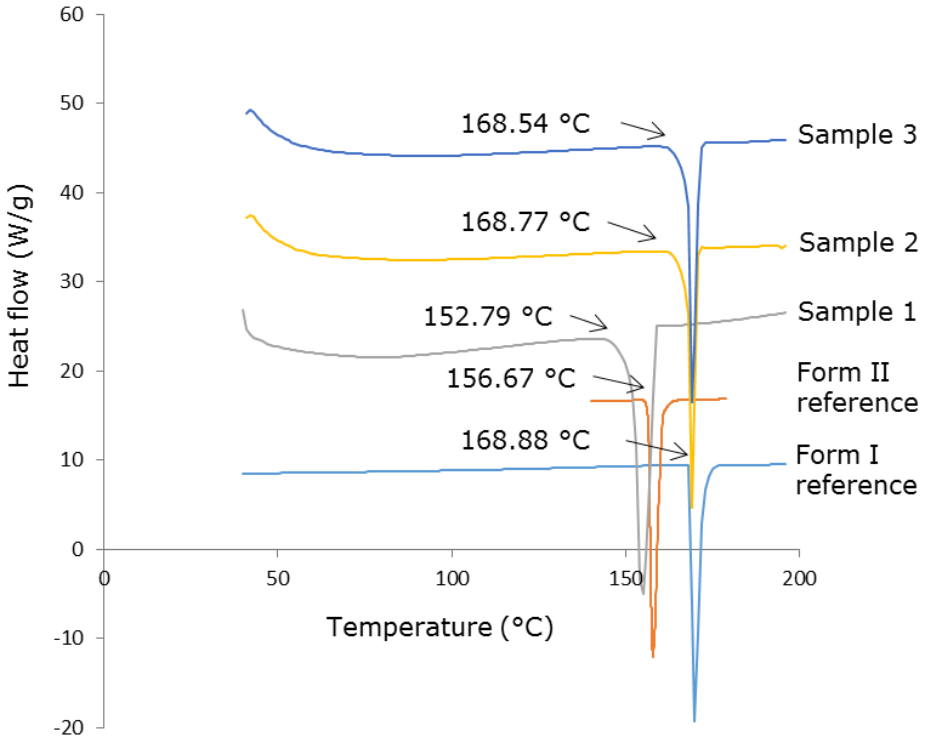

Figure 4-4 DSC thermograms of samples formed from levitating paracetamol in ethanol droplets, 90% saturated, 6 mL. The onset of melting temperature is indicated by an arrow and the value displayed above the trace. Graph offset and scaled for presentational purposes.

The DSC results of the levitated and non-levitated paracetamol samples are summarised in Figure 4-5.

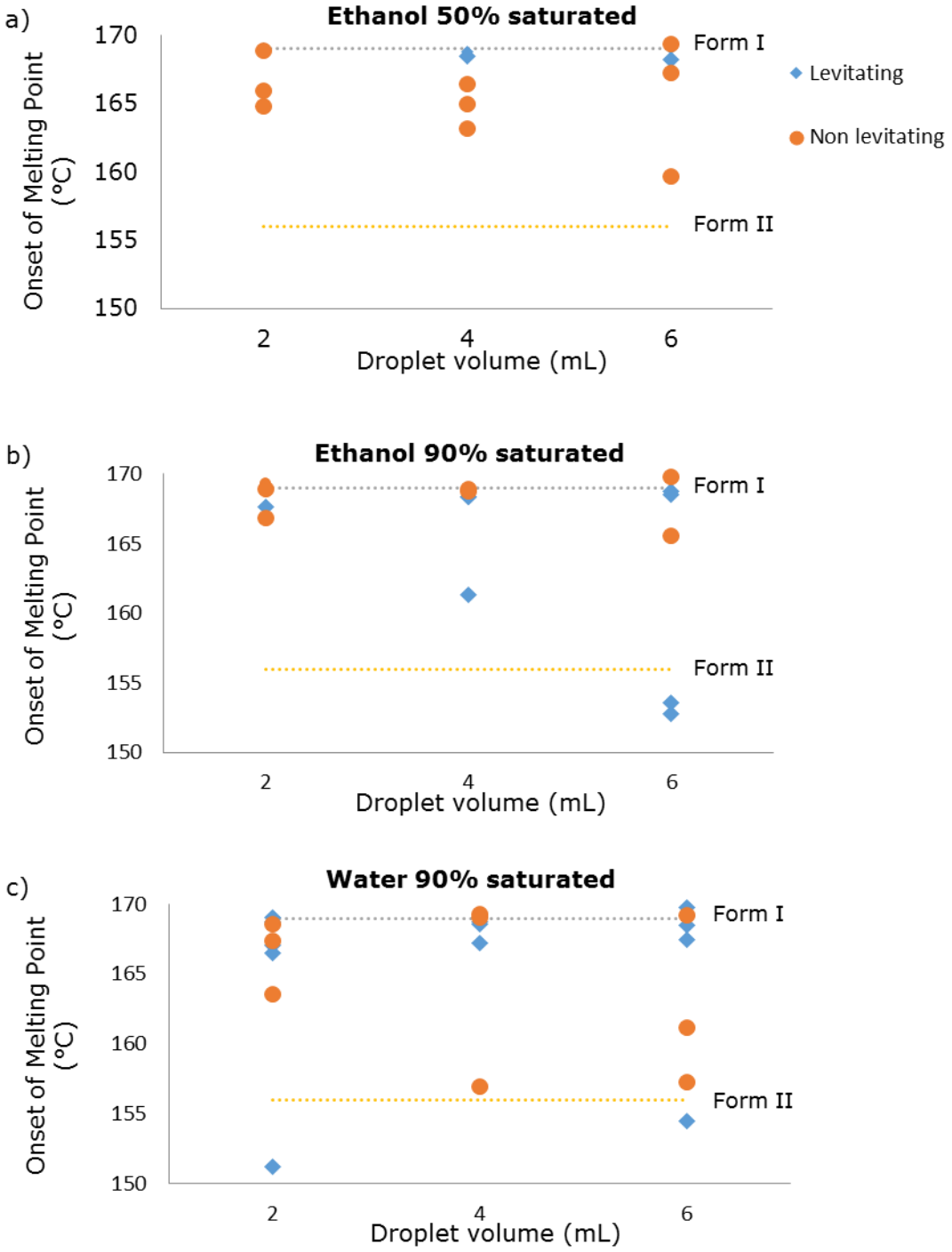

Figure 4-5 (a) Onset of melting points for levitating and non-levitating paracetamol samples formed from ethanol 50% saturated solutions (b) Onset of melting points for levitating and non-levitating paracetamol samples formed from ethanol 90% saturated solutions (c) Onset of melting points for levitating and non-levitating paracetamol samples formed from water 90% saturated solutions. The melting point of form I is indicated by the grey dotted line at 169 °C and the melting point of form II is indicated by the yellow dotted line at 156 °C.

For the samples formed from the paracetamol in ethanol 50% saturated solutions (Figure 4-5 a) the non-levitating samples are spread over a larger range of values compared to the levitating samples. However, there were fewer levitating samples due to the small quantities of crystals produced, making analysis more difficult. The samples from the levitating paracetamol in ethanol and paracetamol in water 90% saturated solutions (Figure 4-5 b & c) gave a wider spread of melting points than the samples formed from the levitated paracetamol in ethanol 50% solutions. A small number of samples from both the paracetamol in ethanol and paracetamol in water 90% solutions indicate form II (melting point of approximately 156 °C). For samples formed from water (90% saturated solution), the non-levitating samples gave a wider spread of melting points. However, the onset of melting points were not low enough to indicate the formation of form II. Examples of DSC spectra for the samples formed from the levitated paracetamol in ethanol 90% saturated solution are displayed in (Figure 4-6). Both of the levitating samples have a melting point of 152/ 153 °C indicating the presence of form II, sample one has a large exothermic peak at 74 °C which is likely to be the evaporation of ethanol (which boils at 78 °C) from the sample (Haynes. W.M. (ed.) 2014). When viewed using optical microscopy both levitated samples appeared crystalline in nature (Figure 4-6 b).

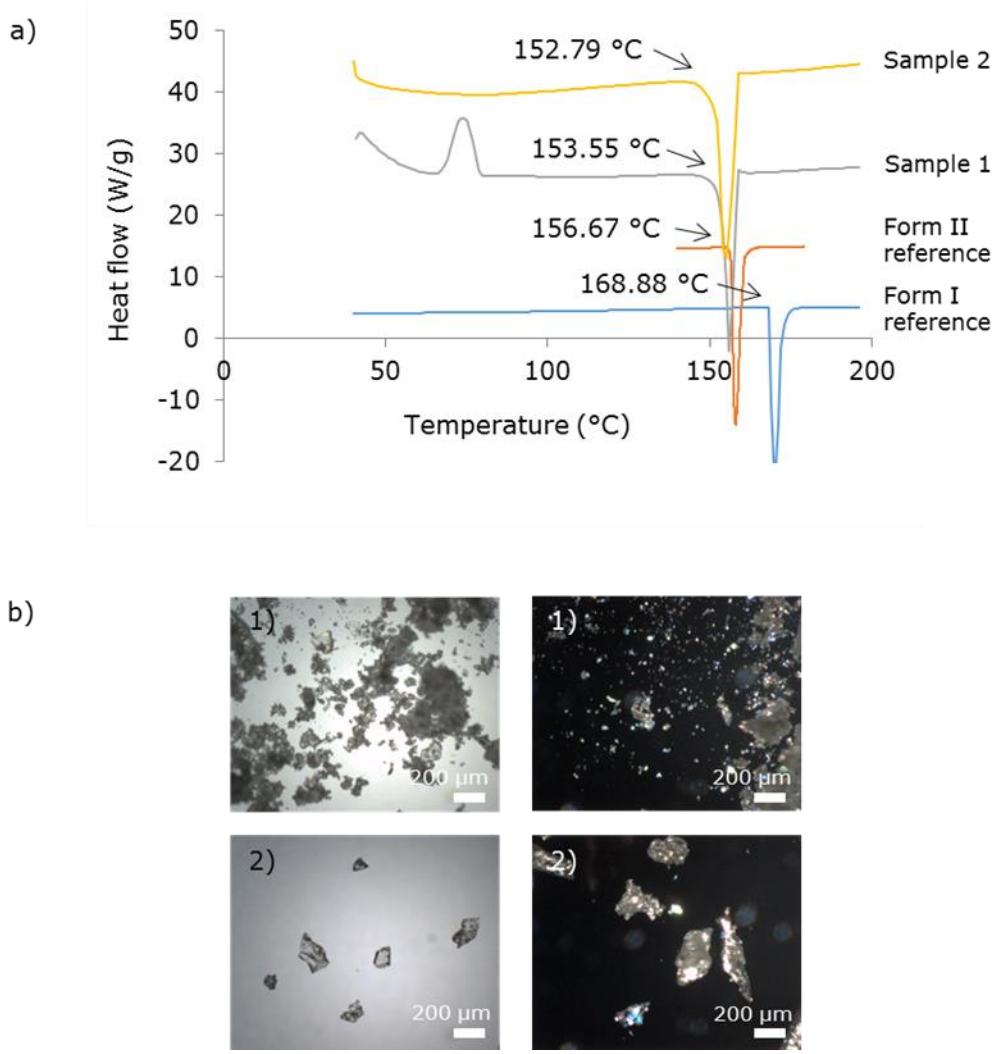

Figure 4-6 (a) DSC thermograms of two samples formed from levitated paracetamol in ethanol 90% saturated solution, 6 mL, along with the form I reference trace Spectra have been scaled and offset for presentational purposes.(b) Optical microscopy and polarised microscopy images of samples 1 and 2 (formed from paracetamol in ethanol 90%, 6 mL).

The samples formed from levitated ethanol 90% saturated solutions, and water 90% saturated solutions gave a larger spread of melting points with some at approximately 156 °C indicating the formation of form II (Figure 4-5). Results indicate that increasing the volume of the droplet also increased the chances of forming form II paracetamol, therefore in further experiments 6 mL droplets were levitated. The crystallisation of form II paracetamol from solutions

has proven difficult (Nichols and Frampton 1998) and form II is often created from the melt of form I, or by seeding solutions with form II. Therefore, it is interesting that the DSC results indicate the formation of form II paracetamol from levitating solutions.

These results indicate that it is possible to levitate paracetamol solutions and form paracetamol crystals in a containerless fashion, and they also suggest diamagnetic levitation may have potential for polymorph selection. Samples collected from 6 mL levitated ethanol 90% saturated droplets, 2 and 6 mL water 90% saturated droplets produced melting points suggesting form II. Therefore, there is a need to further explore the levitation conditions of levitated droplets.

4.4.2 Repeats of initial experiments

As samples collected from 6 mL ethanolic droplets sometimes (2 out of 4 samples) gave melting points suggesting form II further repeats of the initial experiments were undertaken. Therefore, 6 mL droplets of paracetamol in ethanol, 90% saturated were levitated with different levitation conditions, for example the magnetic field strength and rate of air flow (Table 4-4).

Sample number	Field strength (T)	Box/ glass cover	Air/ nitrogen	Flow rate (ccm/ min)	Bore insert temp (°C)	Melting point (°C)	Indicates
1 – 5	17.1	Glass cover (set up 1)	Air	10	20	1. 168.63 2. 168.47 3. 168.31 4. 167.87 5. 158.61 & 168.20	Form I Form I Form I Form I Form II & I
6 – 10	17.1	Glass cover (set up 1)	Air	50	20	6. 168.29 7. 168.50 8. 168.16 9. 168.57 10. 162. 29 & 168.59	Form I Form I Form I Form I Form II & I
11 - 15	17.8	Glass cover (set up 1)	Air	50	20	11. 166.86 12. 163.56 13. 167.56 14. 167.43 15. 167.22	Form I Form I Form I Form I Form I
16 - 20	17.8	Glass cover (set up 1)	Air	10	20	16. 167.49 17. 165.68 18. 167.83 19. 167.71 20. 167.90	Form I Form I Form I Form I Form I

Table 4-4 Table of conditions explored in the repeat experiments, and sample onset of melting points as determined by DSC. All samples are paracetamol in ethanol, 90% saturated solution, 6 mL.

Inspection of Table 4-4 shows that 18 of 20 repeats produce melting points around 168 °C which we interpret as meaning that form I was the dominant form produced in these experiments. However, two samples (sample 5 and sample 10) appeared to produce a mixture of form II and form I paracetamol. The DSC thermograms are displayed in Figure 4-7.

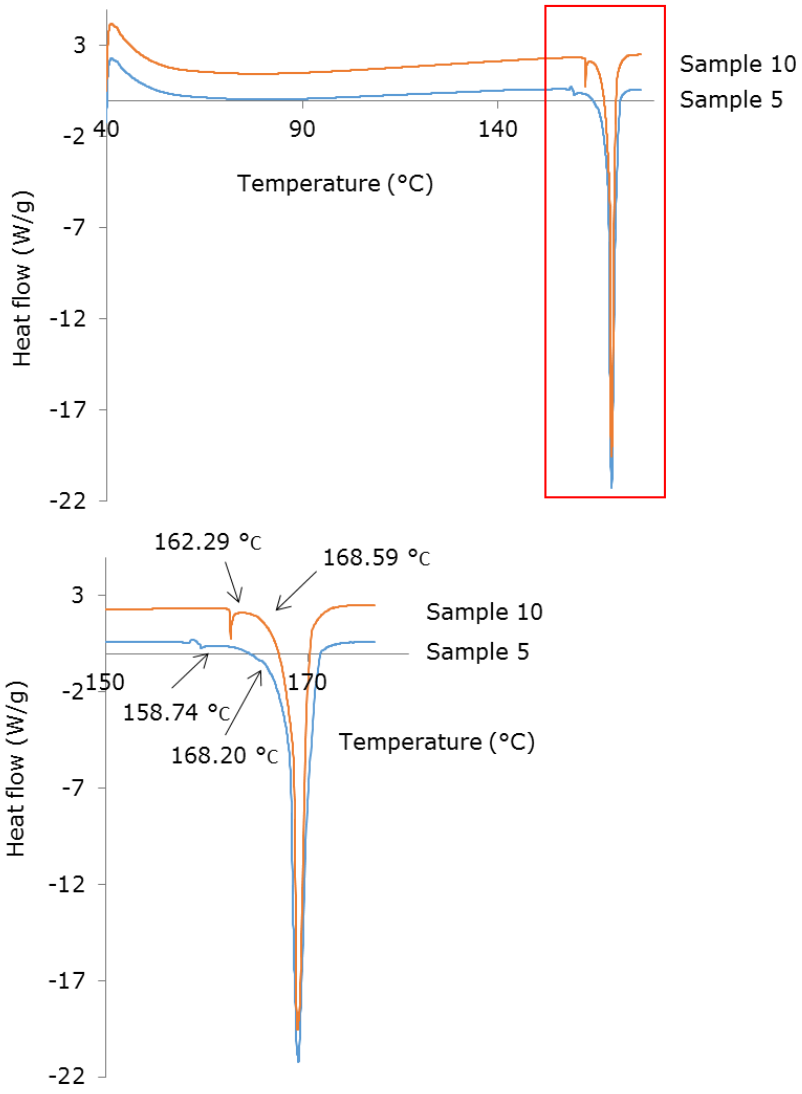

Figure 4-7 DSC thermograms for sample 5 and sample 10 (both paracetamol in ethanol, 90% saturated solution, 6 mL). Note that both samples have a large endothermic peak at 168 - 169 °C indicating form I, however, they both have smaller peaks at 159 °C and 162 °C suggesting form II. Red boxes indicate areas of interest Spectra have been scaled and offset for presentational purposes.

Both samples have a large endothermic peak at approximately 168 °C, indicating form I, however, they both have a small endothermic peak at 159 °C and 162 °C for sample 5 and 10 respectively, suggesting the presence of form II also. Therefore these two samples are likely to be a mixture of form I and II. Nichols and Frampton (1998) report that if the sample isn't polymorphically pure then a form II DSC thermogram will include a large endothermic peak at 171 °C (Figure 3-4) which is attributed to the melting of form I.

Dust and particulates in the air may cause unwanted nucleation, for example heterogeneous nucleation of form I paracetamol on the surface of the droplet. Therefore, it was decided to optimise the experimental set up in terms of cleanliness.

4.4.3 Optimising set up for cleanliness

A Perspex box was designed to use on top of the magnet along with medical air/ nitrogen to produce a positive pressure to keep any particulates or dust in the lab from falling on the droplet, causing unwanted nucleation. It was decided to try medical air and nitrogen (from cylinders) as they would be cleaner than the air supply in physics as it could contain oil particulates. A clean room suit was also used in some experiments and before the experiments took place the lab was given a clean, to make it as dust free as possible.

Parameters explored were the field strength, whether or not the bore needed to be covered by a glass cover or the Perspex box, and the gases used along with their flow rate.

4.4.3.1 Optimisation using ethanol 90% droplets

The first set of optimisation experiments were performed using ethanol 90% saturated solution for levitation (6 mL) as this is what had been used previously in section 4.4.2. Optimisation experiments are summarised below (Table 4-5).

Sample number	Field strength (T)	Box/ glass cover	Air/ nitrogen	Flow rate (ccm/ min)	Bore insert temp (°C)	Melting point (°C)	Indicates
1 - 6	17.1	Glass cover (set up 1)	Air	50	20	1. 167.20 2. 168.82 3. 168.40 4. 168.20 5. 168.19 6. 168.41	Form I Form I Form I Form I Form I Form I
7	17.1	Glass cover (set up 1)	Air	10	20	7. 167.16	Form I
8	17.1	Box only (set up 2)	None	N/A	20	8. 168.19	Form I
9	17.1	Box (set up 2), & clean room suit.	Medical grade air	50	20	9. 167.73	Form I
10 - 11	17.8	Box (set up 2), & clean room suit.	Nitrogen	50	20	10. 156.26 11. 165.74	Form II Form I

Table 4-5 Table of conditions used in optimisation experiments. All droplets are paracetamol in ethanol, 90% saturated solution and 6 mL.

The majority of samples collected were form I paracetamol, as determined by their DSC spectra. However, sample no. 10 was found to have a melting point of 156.26 °C indicating form II paracetamol (Figure 4-8).

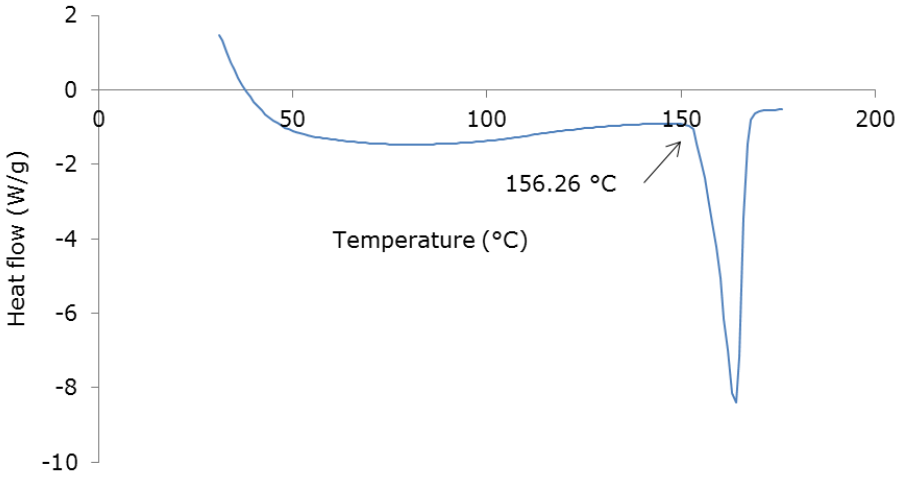

Figure 4-8 DSC thermogram of sample 10. The onset of melting point is 156.26 °C and is indicated by an arrow.

The quick evaporation of ethanol, aided by the nitrogen flow caused the levitated droplets to supersaturate quickly. If supersaturation is too quick then paracetamol can crystallise out on nucleation sites, for example on the end of the needle (as was seen during initial levitation studies when using a glass pipette) causing unwanted heterogeneous nucleation of form I. As the 90% saturated solution droplets super saturated too quickly it was decided to use 70% saturated solutions instead, to investigate if it was more likely to lead to formation of form II paracetamol.

4.4.3.2 Optimisation using ethanol 70% droplets

To slow down any potential supersaturation it was decided to levitate paracetamol in ethanol 70% saturated solutions (6 mL), instead of 90% saturated solutions. Further optimisation experiments were also carried out on the Cryogenic and Oxford magnets (the Oxford magnet being used when the Cryogenic magnet was being serviced), with parameters explored being the field strength. As the bore insert (which connects to the water bath for temperature control) was purpose made for the cryogenic magnet it could not be used in the Oxford magnet, meaning the temperature inside the bore could not be controlled. The air temperature inside the lab was recorded instead, which usually was about 20 °C. Optimisation experiments are summarised in Table 4-6.

Sample number	Magnet	Field strength (T)	Box/ glass cover	Air/ nitrogen	Flow rate (ccm/min)	Bore insert/ lab temp (°C)	Melting point (°C)	Indicates
1 - 5	Oxford	16.5	Box (set up 2)	None	N/A	1. 20.8 2. 20.8 3. 19.5 4. 19.2 5. 20.0	1. 168.73 2. 165.83 3. 158.66 4. 167.50 5. 167.42	Form I Form I Form II Form I Form I
6 - 10	Oxford	16.5	Box (set up 2)	None	N/A	6. 19.2 7. 20.7 8. 19.8 9. 20.6 10. 20.2	6. 167.12 7. 166.52 8. 167.34 9. 165.13 10. 167.16	Form I Form I Form I Form I Form I
11 - 16	Oxford	16.5	Box (set up 2)	None	N/A	11. 20.2 12. 20.0 13. 20.0 14. 20.0 15. 20.6 16. 20.1	11. 167.71 12. 166.66 13. 166.45 14. 166.37 15. 165.70 16. 165.44	Form I Form I Form I Form I Form I Form I
17 - 21	Cryogenic	17.1	Box (set up 2)	17. None 18 – 21. Nitrogen	17. N/A 18 – 21. @ 50	17. RT 18. Bore @ 20 19. Bore @ 20 20. Bore @ 20 21. Bore @ 20	17. 161.05 18. 164.89 19. 164.70 20. 168.04 21. 168.28	Form II/ I mix Form I Form I Form I Form I

Table 4-6 Table of conditions used in optimisation experiments. All droplets are paracetamol in ethanol, 70% saturated solution and 6 mL.

When analysed by DSC sample number 3 had a melting point of 158.66 °C indicating the presence of form II paracetamol, whilst sample 17 gave a melting point of 161. 05 °C, indicating the possible formation of from II (or mixture of form II/I paracetamol).

It was therefore decided to carry out more detailed investigations after optimisation of the experimental set up. Rather than relying on DSC as the main analytical technique FT-IR (ATR) and handheld Raman were used for analysis of samples

4.4.4 Ethanol 90% experiments following optimisation

Samples were repeated using similar settings to sample 10 (Table 4-5). Droplets (of paracetamol in ethanol, 90% saturated solution, 6 mL) were levitated using a field strength of 17.5 T, using the Perspex box and nitrogen at a flow rate of 50 ccm/ min. A time lapse of a levitating (ethanol 90% saturated) droplet is displayed in Figure 4-9.

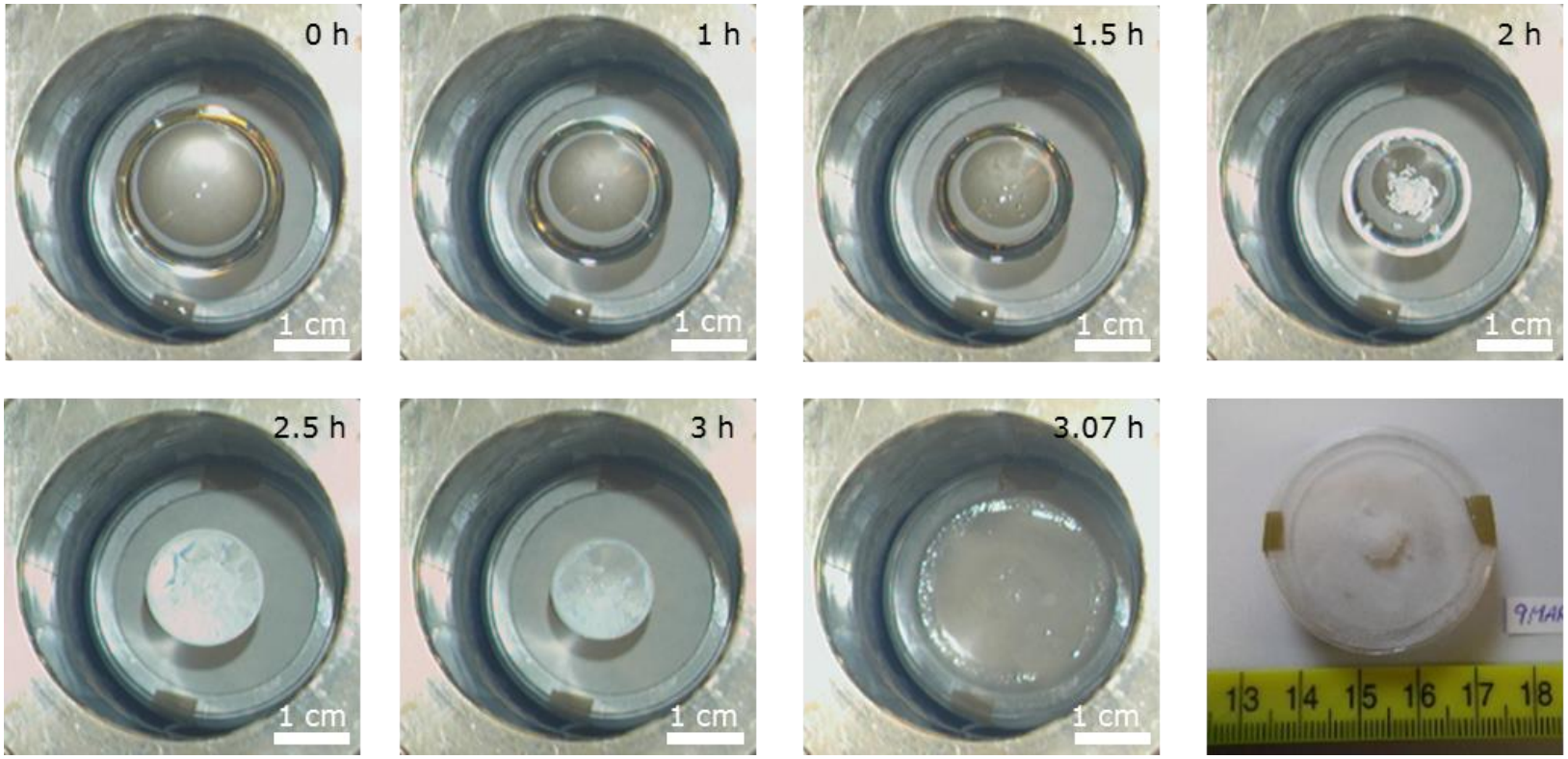

Figure 4-9 Bird's eye view time lapse of levitating paracetamol in ethanol droplet, 90% saturated, 6 mL.

Paracetamol droplets were levitated for approximately 3 hours until the magnetic susceptibility of the whole droplet decreased and it fell down into the collection device. After approximately an hour small crystals can be seen in the centre of the droplet (Figure 4-9), as the droplet continues to decrease in size, other crystals can be seen nucleating at the edge of the droplet and travelling in to the centre where they aggregate (2 h). Crystals continue to grow and collect in the droplet until the droplet appears opaque (2.5 h and 3 h). Shortly after three hours the droplet falls out and is collected in the collection device.

Following optimisation of the set up, more detailed characterisation of the samples formed during levitation was performed using FT-IR (ATR) and handheld Raman in addition to DSC (Figure 4-10).

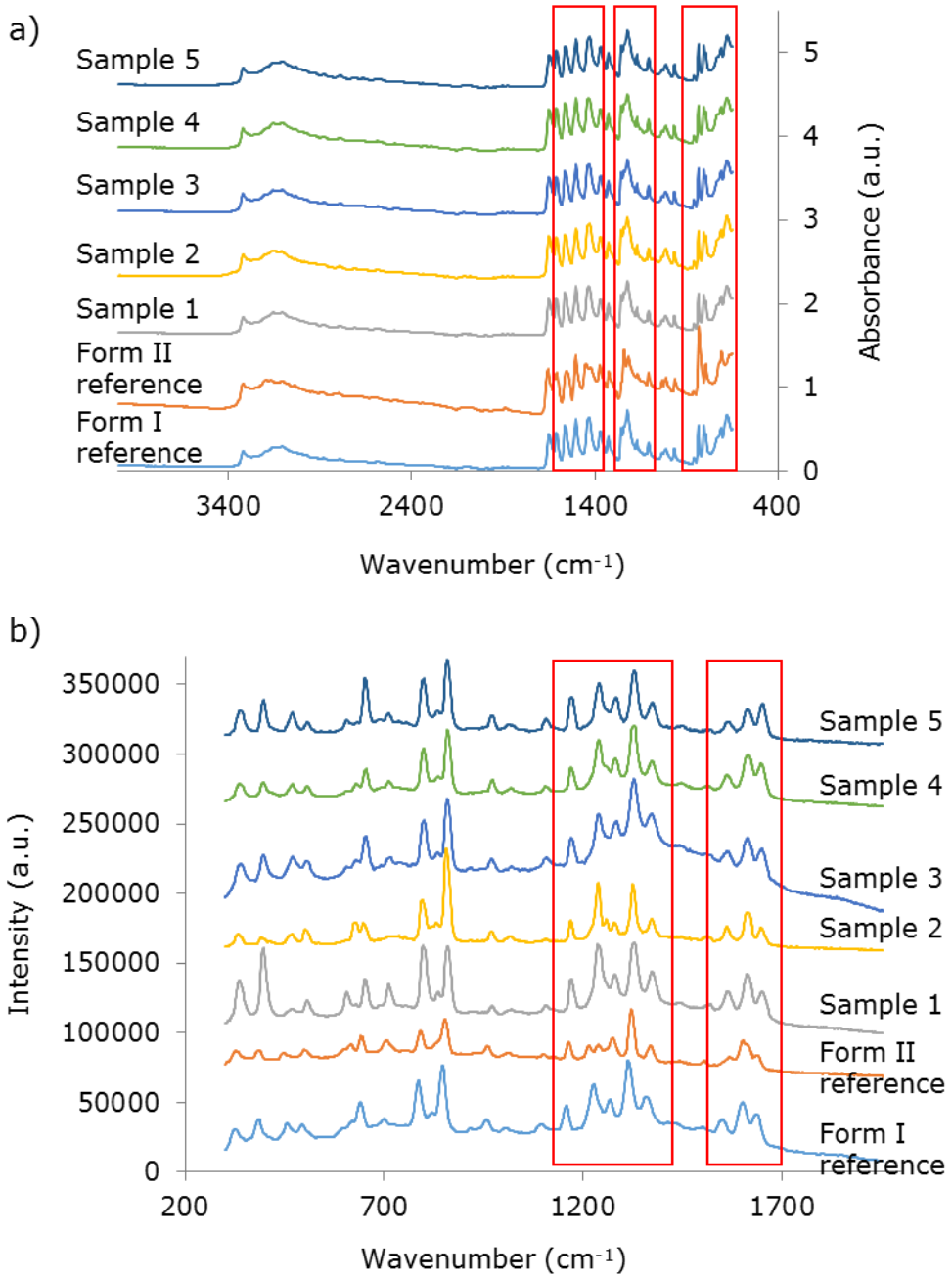

Figure 4-10 (a) FT-IR (ATR) and (b) Handheld Raman analysis of samples formed from levitated paracetamol/ ethanol, 90% saturated solution (6 mL). Red boxes indicate areas of interest. The form II reference has been offset horizontally due to operator calibration error. Spectra have been scaled and offset vertically for presentational purposes.

The FT-IR (ATR) spectra for the levitated samples were similar to spectra reported for form I paracetamol in the literature and are

displayed in Figure 4-10. The absorption peaks (which are not present in form II) at 806, 682 and 1228 cm^{-1} are present in the spectra, confirming form I (Al-Zoubi et al. 2002b). The Raman spectra also contain characteristic peaks at 1234 and 1325 cm^{-1} with three well resolved peaks in the 1500 – 1700 cm^{-1} range confirming form I paracetamol (Kauffman et al. 2008).

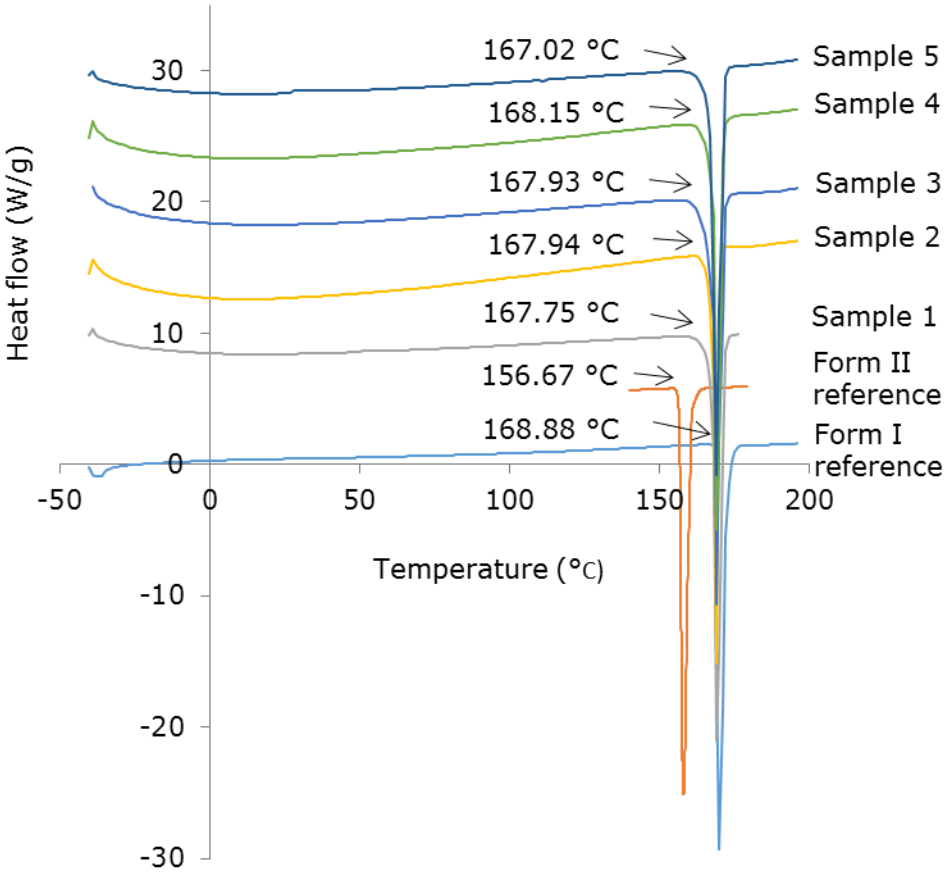

Figure 4-11 DSC thermograms for the samples formed by the levitated paracetamol/ ethanol, 90% saturated solution (6 mL). Spectra have been scaled and offset for presentational purposes.

A small amount of each sample was also analysed by DSC and the onset melting temperatures given in Figure 4-11. Onset of melting points range from 167.02 – 168.15 °C. which are within the range

reported in literature for form I paracetamol (168 – 172 °C) (Di Martino et al. 1996, 1997; Nichols and Frampton 1998; di Martino et al. 2000; Boldyreva 2003; Espeau et al. 2005).

The DSC, Raman and FT-IR (ATR) results therefore indicated that the crystals from the levitated droplets were all form I paracetamol. The non-levitating samples (three repeats of 6ml paracetamol/ ethanol, 90% saturated solution) were also analysed by DSC, FT-IR (ATR) and handheld Raman, and all samples indicated form I paracetamol (data not shown).

4.4.5 Ethanol 70% experiments following optimisation

Paracetamol in ethanol, 70% saturated droplets (6 mL) were levitated at 17.5 T, with a glass cover slip covering the magnet bore and the water bath set at 20 °C.

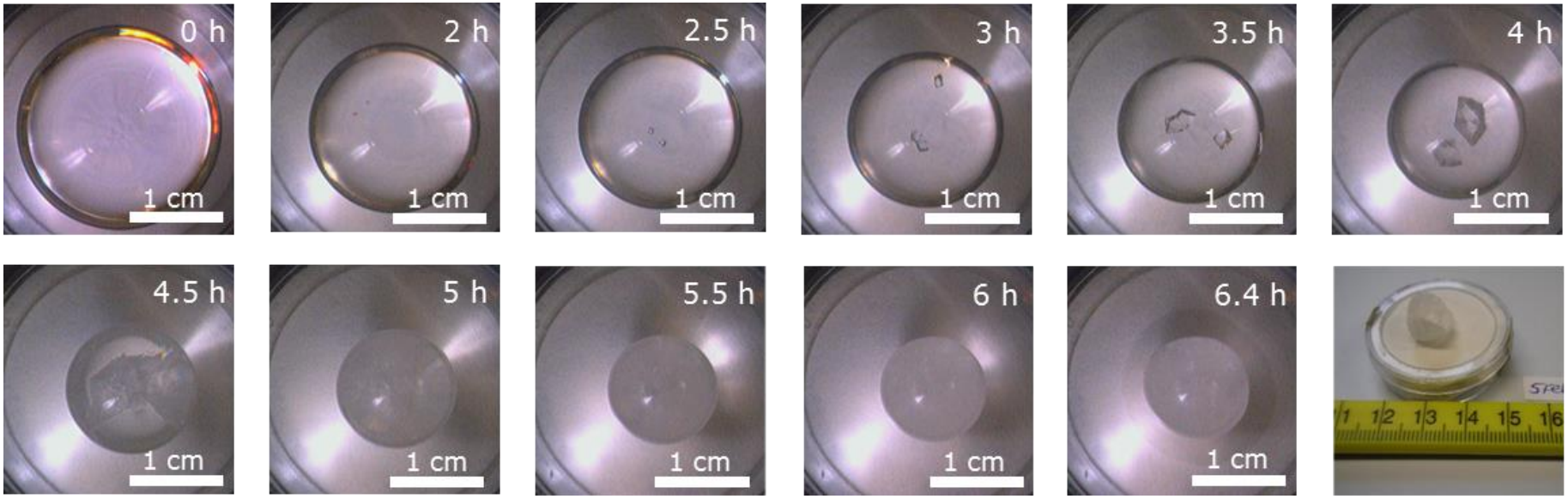

Figure 4-12 Bird's eye view time lapse of levitating paracetamol in ethanol droplet, 70% saturated, 6 mL.

Droplets in these conditions levitated for approximately 6 hours, unlike the 90% saturated solution droplets which levitated for approximately 3 hours. This was due to the quantity of paracetamol in the droplet and the lack of air flow in the magnet bore meaning that evaporation rates were slower. After an hour and a half two small crystals can be seen in the droplet (Figure 4-12) these two small crystals continue to grow in size, and at approximately 3 hours a third crystal can be seen at the edge of the droplet. This crystal moves towards the centre of the droplet (3.5 h) and the crystals continue to grow in size and eventually meet (4.5 h). After 5 hours the droplet appears opaque as the crystals continue to grow. After 6.4 hours the droplet hits the collection device and remaining solution from the droplet can be seen on the filter paper around the crystal. In the final image the crystal can be seen as a cup shape in the collection device.

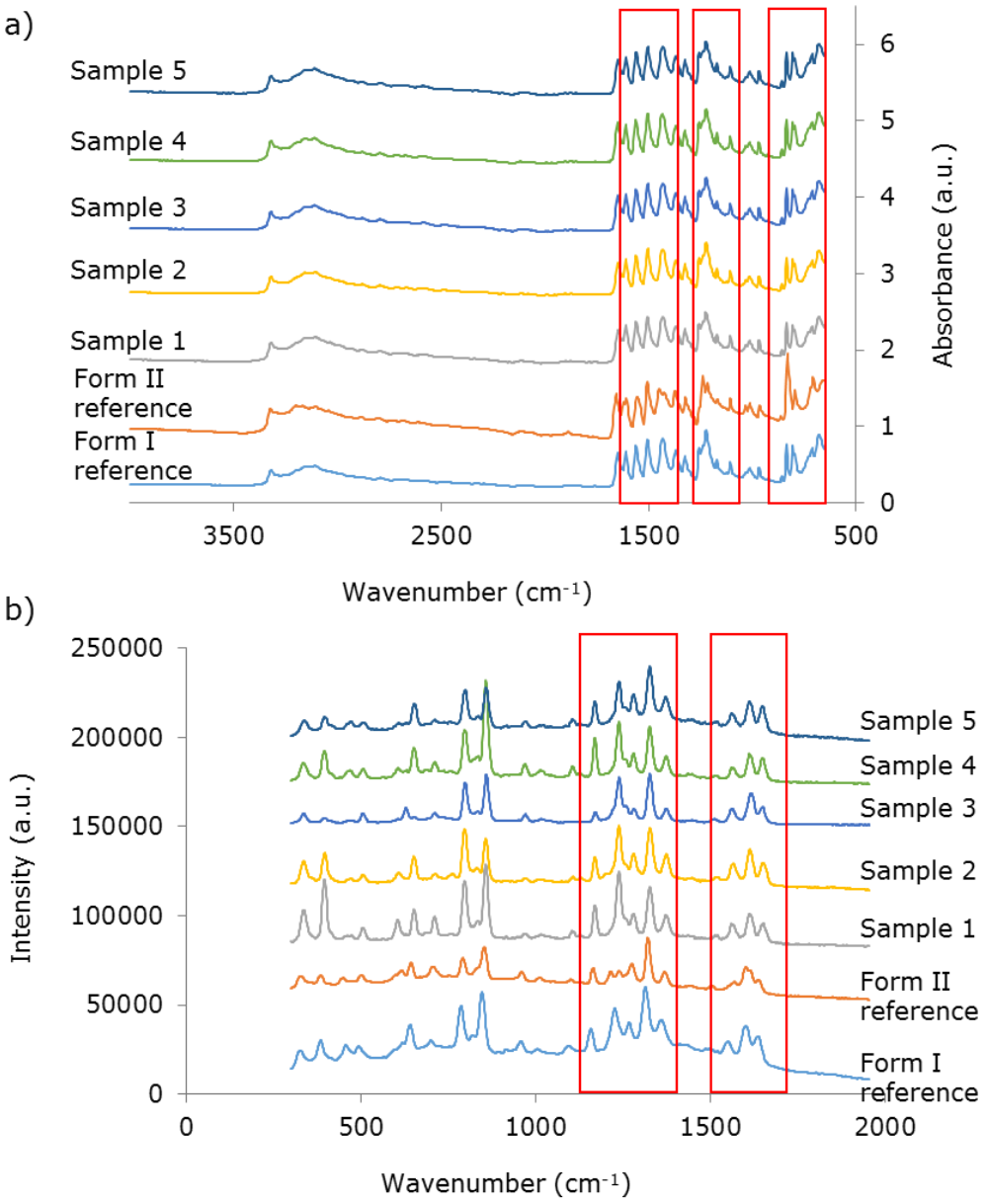

Figure 4-13 (a) FT-IR (ATR) of samples formed from the levitated paracetamol in ethanol, 70% saturated solution (6 mL) and (b) Handheld Raman spectra of samples formed from the levitated paracetamol in ethanol, 70% saturated solution (6 mL). Red boxes indicate areas of interest. The form II reference has been offset horizontally due to operator calibration error. Spectra have been scaled and offset vertically for presentational purposes.

The levitated samples were analysed by FT-IR (ATR) and handheld Raman (Figure 4-10). The FT-IR (ATR) spectra for the levitated samples agreed with spectra reported for form I paracetamol in

literature. The absorption peaks at 806, 682 and 1228 cm^{-1} are present in the spectra confirming form I (Al-Zoubi et al. 2002b). The Raman spectra contain characteristic peaks at 1234 and 1325 cm^{-1} with three well resolved peaks in the 1500 – 1700 cm^{-1} range confirming form I paracetamol (Kauffman et al. 2008).

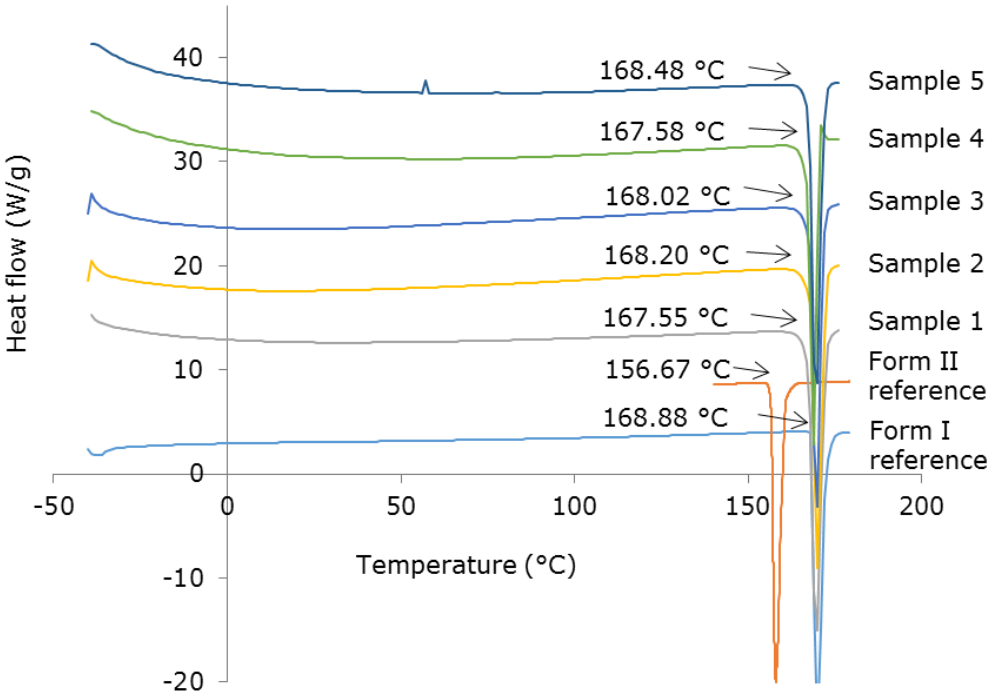

Figure 4-14 DSC thermograms for samples formed from levitated paracetamol in ethanol 70% saturated solutions (6 mL). Spectra have been scaled and offset for presentational purposes.

A small amount of each sample was analysed by DSC and the onset melting temperatures given in Figure 4-11. Onset of melting points range from 167.02 – 168.15 °C. which are within the range reported in literature for form I paracetamol (168 – 172 °C) (Di Martino et al. 1996, 1997; Nichols and Frampton 1998; di Martino et al. 2000; Boldyreva 2003; Espeau et al. 2005).

The non-levitating samples (three repeats of 6ml paracetamol/ ethanol, 70% saturated solution) were also analysed by DSC, FT-IR (ATR) and handheld Raman, and all samples indicated form I paracetamol (data not shown).

Occasionally form II paracetamol (or a mixture of form II/I) was formed from the levitating droplets (sections 4.4.1, 4.4.2, 4.4.3) however, it was difficult to reproducibly produce form II paracetamol. Haisa et al. (1974) produced orthorhombic crystals by slow evaporation from ethanolic solution, however, this method has subsequently eluded other researchers (Di Martino et al. 1997). Form II paracetamol can be created from the melt of form I, or from ethanolic solution when a seeding technique is used. However, seeding from ethanolic solution is still a challenge as the yield reported by Nichols and Frampton (1998) is typically less than 30%, and they also report that if the form II crystals are not dried fully then any residual mother liquor can induce formation to form I.

4.4.6 Seeding experiments

As it was difficult to reproducibly produce form II paracetamol via levitation it was decided to seed a droplet with form II, to see if it was possible to encourage the formation of form II paracetamol. Before seeding the droplets, form II paracetamol was made via the melt freeze method (method 1) detailed in chapter 3 (3.4.1.2). The prepared form II paracetamol, was then added to a paracetamol in ethanol droplet and a paracetamol in water droplet to see if seeding could initiate form II formation. The magnet was set up at 17.5 T, with the Perspex box, nitrogen flow rate of 50 ccm/ min, and the water bath set at 20 °C. A 1 mL paracetamol in ethanol 70% saturated solution was then levitated and form II introduced to the droplet with

a glass pipette tip. For the aqueous droplet 4 ml of paracetamol in water 90% saturated solution was used.

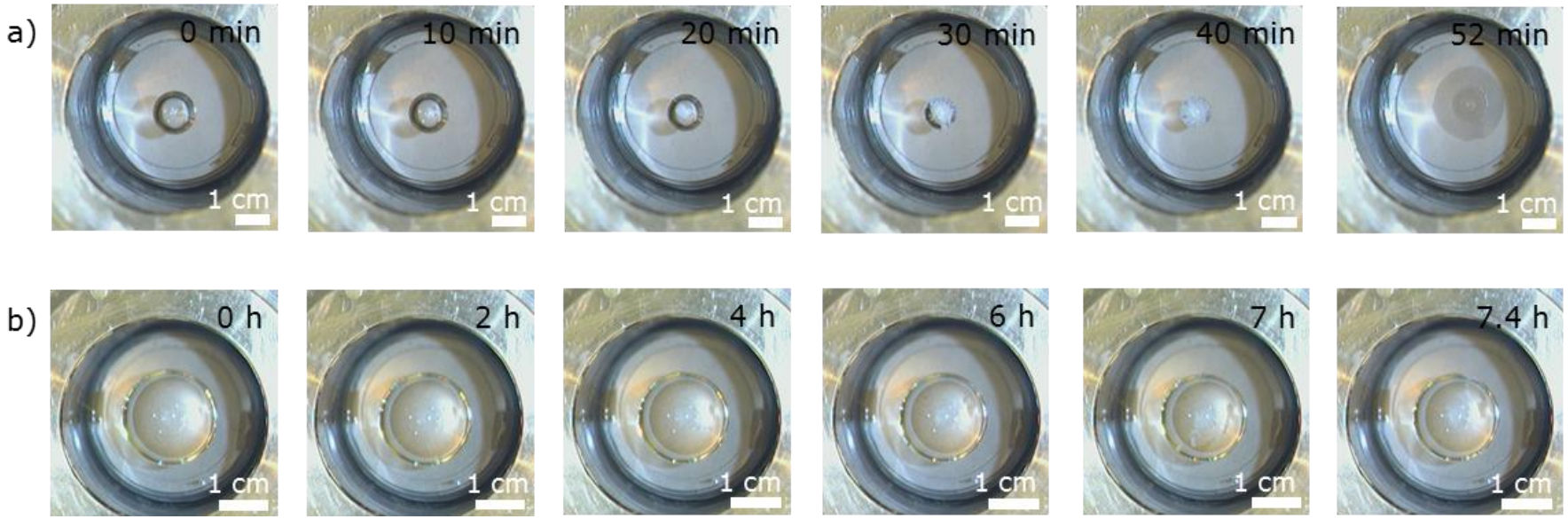

Figure 4-15 Bird's eye view time lapse of levitating droplets (a) Paracetamol in ethanol 70% saturated solution, 1mL (b) Paracetamol in water 90% saturated solution, 4 mL. Both droplets were seeded with form II paracetamol.

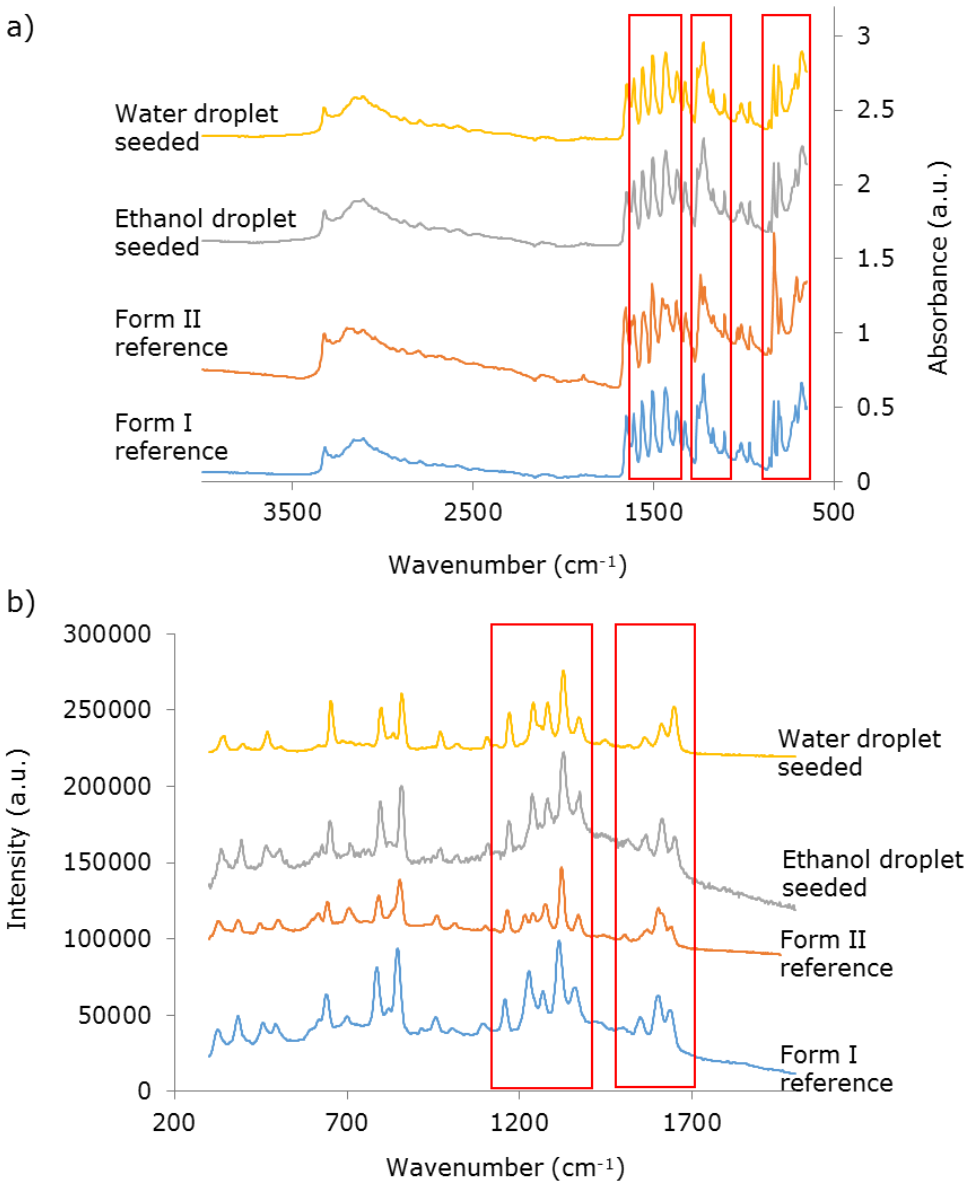

Figure 4-16 FT-IR (ATR) and handheld Raman spectra of levitated water and ethanol droplets seeded with form II. Red boxes indicate areas of interest. The form II reference has been offset horizontally due to operator calibration error. Spectra have been scaled and offset vertically for presentational purposes.

The seeded samples were analysed by FT-IR (ATR) and handheld Raman (Figure 4-16). The FT-IR (ATR) spectra for the levitated samples agreed with spectra reported for form I paracetamol in literature. The characteristic form I absorption peaks (which are not present in form II) at 806, 682 and 1228 cm^{-1} are present (Al-Zoubi

et al. 2002b). The handheld Raman spectra contain characteristic peaks at 1234 and 1325 cm^{-1} with three well resolved peaks in the 1500 – 1700 cm^{-1} range confirming form I paracetamol (Kauffman et al. 2008).

4.4.7 Overall results summary

The results of this chapter are summarised in Table 4-7. The key result from the initial experiments was that by using the magnet system at the University of Nottingham we were able to levitate pharmaceutical solutions and form crystals within the levitated droplets. Aqueous paracetamol droplets levitated for longer periods than ethanol droplets and produced larger crystals. This is due to the droplet evaporating over a longer time with a slower decrease in volume, which gradually increases the concentration of paracetamol. As paracetamol has a lower magnetic susceptibility than water or ethanol, when the ratio of paracetamol to solvent is increased the susceptibility of the whole droplet decreased causing the levitating droplet to fall out of the magnet bore. As evaporation of water was slower than ethanol it allowed larger crystals to grow in the droplet before falling out of the magnetic trap.

In the initial experiments droplets of varying volume (2, 4 or 6 ml), varying concentrations (50% or 90% saturated solution) and different solvents (water or ethanol) were levitated. Predominantly form I paracetamol was formed, however, occasionally form II was formed (e.g. 4 out of 26 samples). Larger droplets appeared to be more likely to crystallise form II paracetamol with 3 out 4 form II samples being from 6 mL droplets. Repeat experiments also occasionally produced form II paracetamol (2 out of 20 samples).

Optimisation of the experimental set up involved creating a Perspex box to sit over the magnet bore to keep the droplet clean from any falling dust/ particles. A flow of nitrogen/ medical grade air was used with the Perspex box to keep a positive pressure, again to prevent unwanted dust/ particles causing unwanted nucleation. It was hypothesised that dust or particles that fell on the droplet could act as nucleation points biasing the formation of form I paracetamol, which readily crystallises from solution. Again, form II paracetamol was occasionally formed, however, the addition of the Perspex box and nitrogen/ gas did not improve the odds of obtaining form II (1/ 11 for 90% saturated solution, and 2/21 for the 70% saturated solution). The final 70% and 90% saturated solution droplets were repeated again with the Perspex box set up and this time analysed by FTIR (ATR) and handheld Raman. However, when analysed by these techniques they were confirmed as form I paracetamol.

Although form II was produced infrequently in these studies, they still highlight that diamagnetic levitation has the potential for polymorphic control; by allowing the droplets to levitate freely it avoids unwanted heterogeneous nucleation i.e. nucleation on vessel walls or by dust particles. If the droplet is free of impurities and supersaturated, spontaneous homogenous nucleation can occur which could lead to the metastable form being produced.

A final experiment to explore this potential was the seeding of paracetamol droplets with form II paracetamol. Although the droplets were seeded with form II when analysed by FTIR (ATR) and handheld Raman they indicated that form I paracetamol had been produced. It is already known that it is difficult to reproducibly produce form II from solution. Haisa et al. (1974) reported the crystallisation of form II by slow evaporation, however, this method has eluded other researchers (Di Martino et al. 1997). Form II paracetamol is often made from the melt of form I, or from ethanolic solution when using

a seeding technique. However, even when using a seeding technique, yields are often less than 30% (Nichols and Frampton 1998). Nichols and Frampton (1998) also report that if the form II crystals are not fully dried then any residual mother liquor can induce the formation to form I. It is possible therefore that in these studies the crystals that that fell out of the magnet bore still had residual solution on them causing them to revert back to the more stable form I. The collection device used in the magnet bore had filter paper and silica gel (for aqueous droplets) to try and soak up any residual solution to overcome this.

Experiment	Key findings
Initial experiments	• Water droplets levitate longer than ethanol droplets • Larger crystals are produced in water droplets than ethanol droplets • Predominantly formed form I paracetamol, occasionally form II was formed (4/ 26 samples) • Larger volume droplets are more likely to produce form II paracetamol (3/4 samples were 6 mL)
Repeats	• 2 samples out of 20 produced form II paracetamol
Optimising 90%	• 1 sample out of 11 produced form II
Optimising 70%	• 1 sample produced form II, and one was a mixture of form II/I out of 21 samples
90% ethanol	• When analysed by FTIR (ATR) and handheld Raman all samples were confirmed as form I paracetamol
70% ethanol	• When analysed by FTIR (ATR) and handheld Raman all samples were confirmed as form I paracetamol
Seeding	• Although droplets were seeded with form II paracetamol analysis by FTIR (ATR) and handheld Raman confirmed form I

Table 4-7 A summary of the results obtained in this chapter.

4.5 Conclusion

Diamagnetic levitation was successfully used to levitate droplets of paracetamol in ethanol (or water) of varying volumes in the proof of concept studies. Using diamagnetic levitation containerless levitation studies were undertaken; levitating paracetamol in solution

(ethanolic or aqueous) at different field strengths and using different experimental set ups. Occasionally form II paracetamol was produced from the levitating droplets indicating that diamagnetic levitation has the potential for polymorphic control. However, in practice it has proven difficult to reliably reproduce form II paracetamol. As a result in chapter 5 it was decided to investigate the effect of diamagnetic levitation on clotrimazole, an antifungal pharmaceutical compound. Clotrimazole has previously been successfully levitated using acoustic levitation and the amorphous form created by Benmore and Weber (2011).

5 Clotrimazole levitation studies

5.1 Introduction

Many new pharmaceutical compounds that come to market have low aqueous solubility, i.e. they are class II or IV in the BCS (Biopharmaceutical Classification Scheme) classification system, which can pose a problem in clinical development and of the product. The Biopharmaceutical Classification Scheme (BCS) categorises drugs into four classes according to their solubility and permeability in the gastrointestinal tract (Amidon et al. 1995).

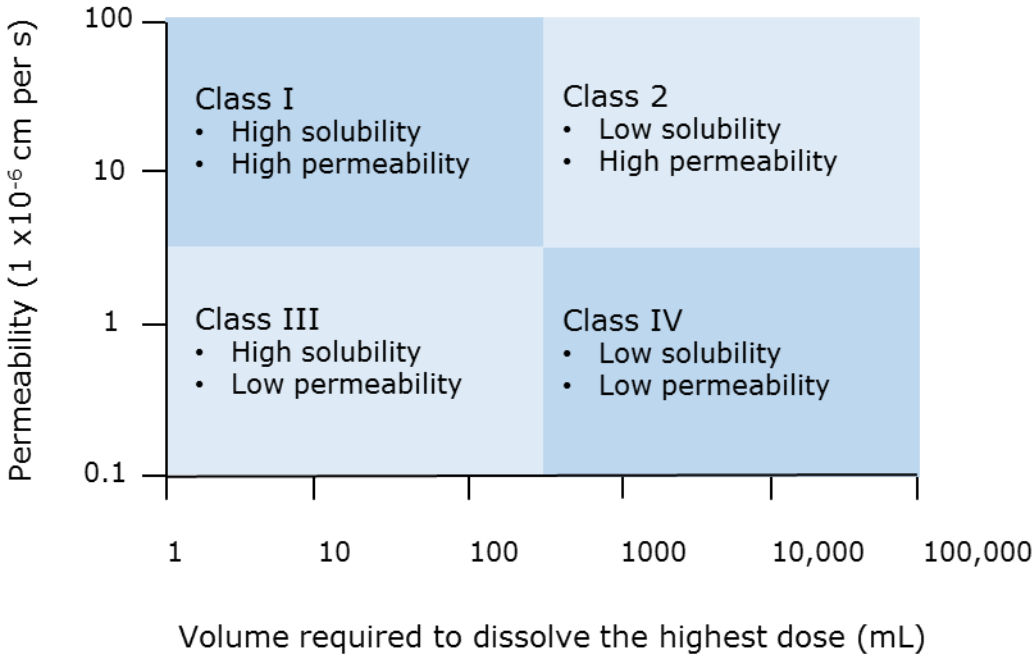

Figure 5-1 Biopharmaceutical classification system (BCS) for characterising drugs based on their solubility and permeability. Image adapted from Rautio et al. (2008).

Various approaches can be used to try and enhance solubility, such as modifying the particle size (micronisation), using cocrystals, micelles, oil encapsulation and creating the amorphous state of the

drug. Amorphous solid states have favourable solubility and dissolution rates compared to crystalline structures (Ehmann et al. 2014)

Using acoustic levitation Benmore and Weber (2011) amorphised pharmaceutical drugs that were previously hard to amorphise. One example of which is clotrimazole which is a BCS class II which has low solubility.

Benmore et al. (2013) reported the structural characterization of different amorphous forms of drugs made by quenching molten droplets levitated by acoustic levitation. Examples of levitated pharmaceutical compounds include; cinnarizine, clotrimazole and miconazole nitrate. The 13C NMR results of these materials showed no evidence for degradation, broken or formed bonds caused by the laser and amorphisation process. Over an 8 month period the ratio of amorphous to crystalline material present in all of the samples was assessed by high energy X-ray diffraction. All the samples were stable for 6 months, however, carbamazepine crystallised out within a few months. Using combined neutron and X-ray pair distribution showed new information on intramolecular/ intermolecular differences in the amorphous drugs when compared to their crystalline forms.

Weber et al. (2013) reported the levitation of probucol (and other pharmaceuticals) which was studied in situ by X-ray diffraction and ex-situ by NMR (nuclear magnetic resonance), neutron diffraction and DSC. Probucol is clinically used to reduce cholesterol, has poor solubility and has two known polymorphs (form I and form II). Analysing the glass by neutron/ X- ray difference function showed some molecular sub-groups (e.g. CH_3) stayed rigid within the probucol structure but several of the correlations in hydrogens became smeared out in the glassy sample. The carbon backbone of probucol stays largely intact in the glassy sate however, the formed

glass was found to be mainly composed of distorted form I probucol, with disordered packing rather than changes in the molecular structure. Glassy probucol (when stored at 2 °C) remained stable for up to 8 months.

Using acoustic levitation Weber et al. (2017) synthesised amorphous pharmaceuticals and compared them to amorphous pharmaceuticals produced by spray drying. The first experiment used the protease inhibitor; Atazanavir sulphate used for the treatment of HIV infections. The atazanavir was mixed with a binder, polyvinyl pyrrolidon (PVP) which can be used as a stabiliser and glass former for amorphous formulations. The mixtures were dissolved in methanol, filtered and syringed into the levitator. For comparison, a 3:1 mixture of PVP and atazanavir sulphate was spray dried (as well as levitated). By using a large quantity of binder the authors inhibited unwanted crystallisation allowing fair comparison of the two methods as spray dried materials often contain crystals. The main difference between spray drying and acoustic levitation are the particle sizes. Particle sizes for the spray dryer are in the range of 10 – 100 μm, whilst the acoustic levitator produced particles in the range of 300 – 500 μm. X-ray diffraction patterns of the samples indicated that similar amorphous material is produced by both methods. In the second part of the paper the authors investigate the stability of amorphous carbamazepine and miconazole nitrate made by containerless cooling of supercooled melts in their previous work (Benmore et al. 2013). The glass transition temperatures of carbamazepine and miconazole nitrate are 61 °C and 1 °C respectively, and the amorphous samples were stored at 2 °C Unexpectedly the carbamazepine crystallised rapidly whilst the miconazole nitrate did not. The results indicate that structural relaxation occurs for carbamazepine about 60 °C below the glass transition temperature.

In this chapter the potential of diamagnetic levitation for the containerless processing of clotrimazole is explored. Clotrimazole is a BCS class II compound with low solubility, thus creating an amorphous compound of clotrimazole would enhance the solubility. Clotrimazole was also chosen as a comparison to Benmore and Weber's work where they used acoustic levitation to create amorphous clotrimazole (Benmore and Weber 2011).

5.1.1 Aims and objectives

The aims of this chapter were to explore the effect of diamagnetic levitation on the amorphisation of clotrimazole. The initial experiments aimed to be a comparison to the work carried out by Benmore and Weber (Benmore and Weber 2011) who used acoustic levitation to amorphise clotrimazole. Further studies aimed to explore different parameters such as levitation time, droplet volume and concentration. A secondary aim was the optimisation of in situ imaging of the droplet. The aims were achieved through the following objectives:

- To perform initial levitation experiments by exploring different parameters such as volume and concentration.
- To optimise imaging of the droplets to allow in situ monitoring of the processes by using mirrors to view the droplet from the side (as opposed to a bird's eye view).
- Create non levitating samples for comparison, keeping conditions as close to the magnet set up as possible.
- Analyse samples by optical microscopy, FT-IR (ATR), and handheld Raman.

5.2 Materials and methods

5.2.1 Materials

Clotrimazole and ethanol (200 proof, anhydrous, ≥ 99.5%) were obtained from Sigma Aldrich, Dorset, UK and used without further purification.

5.3 Experimental methods

5.3.1 Magnet set up

The Cryogenic magnet (Cryogenic Ltd, London) has been used for most experiments performed in this chapter, however, due to the magnet being serviced the Oxford magnet (Oxford Instruments, Abingdon, UK) has also been used for some experiments.

During the experiments in this chapter magnet set up 1 & 2 was used (section 2.1.5).For all experiments in this chapter the petri dish sample collector was used (section 2.1.3) as well as a digital camera which was mounted on a clamp stand above the magnet bore (section 2.1.4).
Table 5-1 summarises the experimental conditions used for each set of experiments.

Sample name	**Magnet**	**Field strength (T)**	**Box/ glass cover**	**Air/ nitrogen**	**Flow rate (ccm/ min)**	**Bore insert/ lab temp (°C)**
Initial (small volume)	Oxford	16.5	Glass cover (set up 1)	None	N/A	RT (~20)
Medium volume droplets	Cryogenic	17.8	Box (set up 2)	Nitrogen	20	Bore @ 20
Large volume droplets	Cryogenic	17.8	Box (set up 2)	Nitrogen	20	Bore @ 20
Effects of syringe filtering	Cryogenic	18.2	Box (set up 2)	Nitrogen	20	Bore @ 20
Time controlled droplets	Cryogenic	18.2	Box (set up 2)	Nitrogen	20	Bore @ 20
Optimising imaging (45 ° mirror)	Cryogenic	17.8	Box (set up 2)	Nitrogen	20	Bore @ 20

Table 5-1 Conditions of experimental set up for clotrimazole levitation studies.

5.3.2 Creating clotrimazole solutions

Clotrimazole solutions were prepared by dissolving the required amount of clotrimazole (Table 5-2) in ethanol in a glass beaker whilst being gently warmed and stirred on a magnetic hot plate. The solution was magnetically stirred until all of the clotrimazole had dissolved, at which point it was taken off the heat and left to cool. The solution was then syringe filtered (0.22 µm syringe filter, Millex GP, Sigma Aldrich) into vials (25 mL sample tubes, Sarstedt, Leicester, UK) for storage.

Experiment	Solvent	Concentration	Volume
Initial exp. (small volume)	Ethanol	9 mg/ mL	0.1 – 0.2 mL
Medium vollume droplets	Ethanol	Saturated solution	0.5 mL
Large volume droplets	Ethanol	Saturated solution	3, 4 & 6 mL
Effects of syringe filtering	Ethanol	Saturated solution	4 mL
Time controlled droplets	Ethanol	Saturated solution	0.5 & 5 mL
Optimising imaging (45 ° mirror)	Ethanol	Saturated solution	0.5 mL

Table 5-2 A table detailing the different solutions and volumes used for each experiment.

5.3.3 Sample preparation/ levitation

Clotrimazole solutions were prepared as the method described in section 5.3.2. The clotrimazole solutions were syringe filtered (0.22 µm syringe filter, Millex GP, Sigma Aldrich) using non-magnetic needles (Neolus, 21G, 1 ½", 0.8 x 40 mm, Terumo Pharmaceutical solutions) into the magnet bore at the stable levitation position in the magnetic field. The levitation position for the Cryogenic magnet is approximately an inch from the top of the magnet bore (excluding the lip of the magnet bore insert) and for the Oxford magnet approximately 10 cm from the top of the magnet bore.

5.3.4 Levitated droplets

Different clotrimazole solutions were levitated for each experiment, parameters that changed were the volume of the droplet or the drug concentration. Details of the droplets levitated for each experiment are displayed in Table 5-2

5.4 Results and discussion

5.4.1 Initial results (small droplets)

The first set of experiments performed were the low volume experiments where droplets of 0.1 – 0.2 mL were levitated as a comparison to Benmore and Weber's acoustic experiments (Benmore and Weber 2011). To directly compare the acoustic levitation method to diamagnetic levitation, initial experiments consisted of levitating small droplets of clotrimazole solution. Clotrimazole was chosen as Benmore and Weber had successfully created an amorphous gel of clotrimazole using acoustic levitation. Benmore and Weber (2011)

levitated 4 µL droplets, however, it was only possible to levitate droplets of 0.1 mL as the magnetic field prevented us using Gilson Pipettes (due to metal components). Figure 5-2 shows an example 0.1 mL droplet levitating in the Oxford magnet. It can be seen that the droplet changes from transparent to opaque in appearance over 45 minutes.

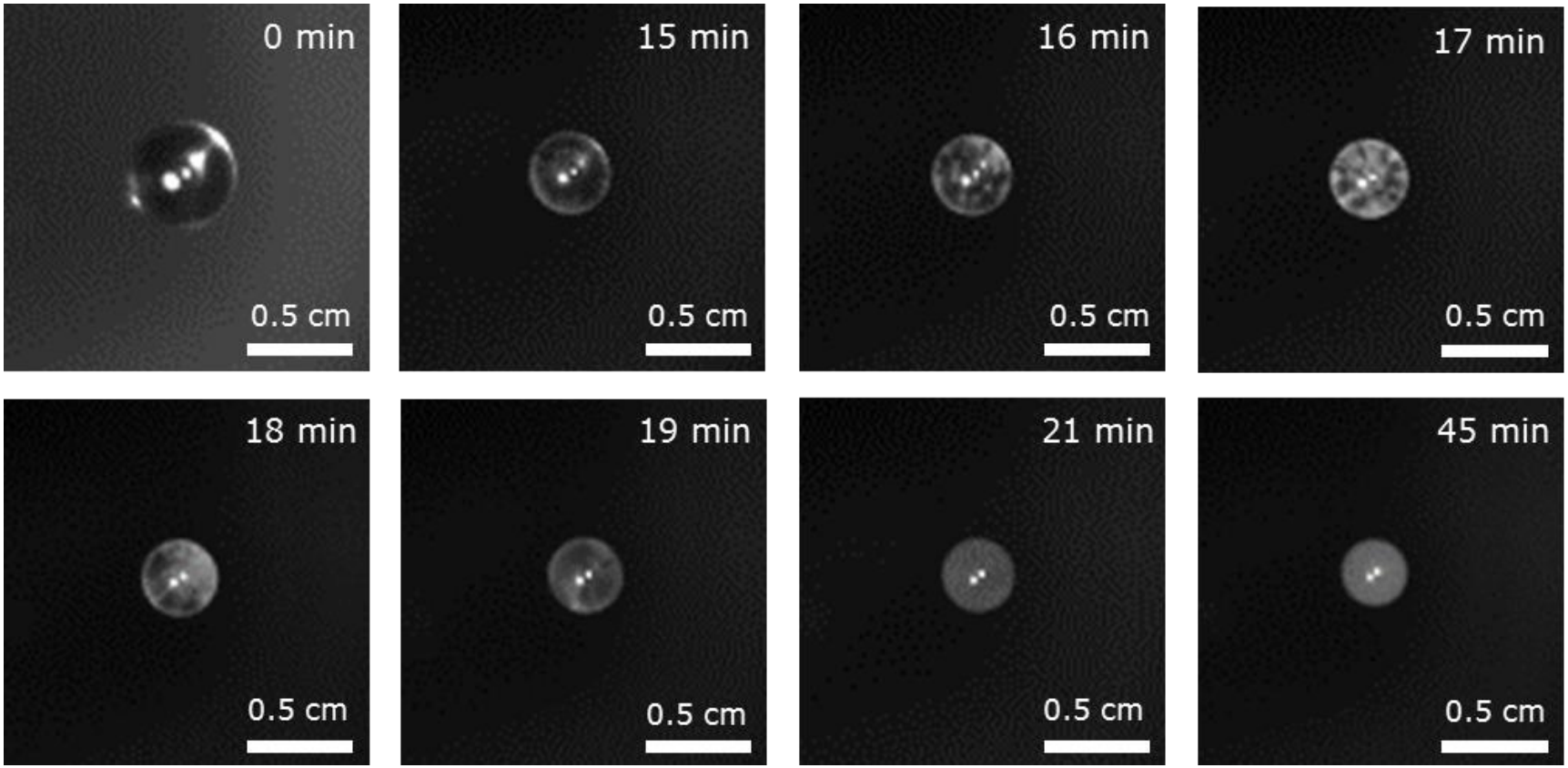

Figure 5-2 Time lapse of a small (0.1 mL) levitating clotrimazole droplet (conc. of starting solution 9mg/ ml) within the magnet bore.

The droplets collected from the magnet were viewed using an optical microscope. The levitated droplets produced a mixture of different results as can be seen in Figure 5-3. Leaving the droplet to levitate in the magnet for sufficient time to allow all of the solvent to evaporate produced a shell like structure (Figure 5-3 a). Taking the droplet out of the magnet earlier produced droplets with different features (Figure 5-3); some droplets would be gel like in nature but have small nucleations of clotrimazole on the surface (Figure 5-3 c &d) while some the droplets appeared to consist of two different halves with different appearances (Figure 5-3 b).

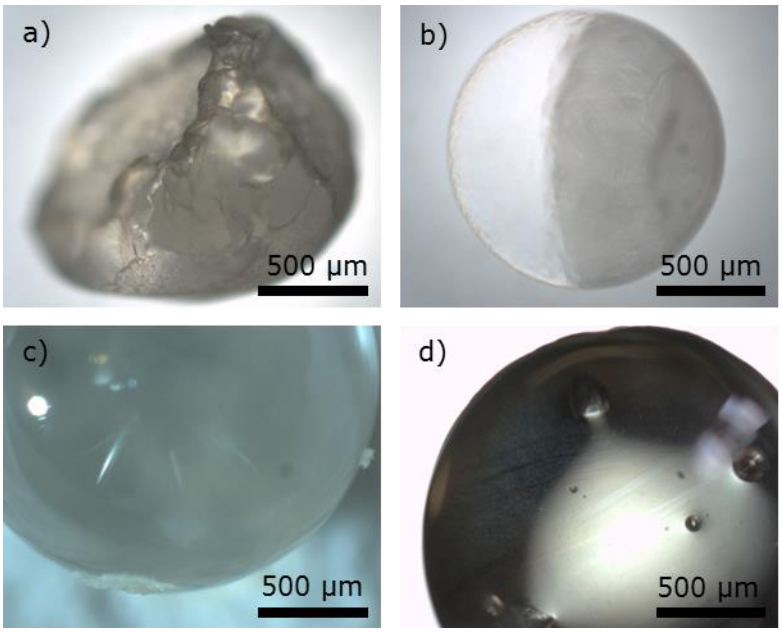

Figure 5-3 Optical microscopy of tiny clotrimazole droplets removed from the magnet after levitation at x4 magnification. Image (a) Shell like structure produced from levitating droplet in Figure 5-2 (b) Droplet with clearly different halves (c) Droplet with nucleation on the surface (d) Droplet with crystalline structures and bubbles/ pockets of air.

Due to the small size of the samples collected during the initial experiments (often 1 -2 mm in diameter) it was difficult to analyse

them by DSC, FT-IR and handheld Raman. The following experiments were therefore performed with larger droplet volumes.

5.4.2 Medium volume droplets

Droplets of 0.5 ml saturated clotrimazole solution were levitated using the cryogenic magnetic and filmed from above as they evaporated over time. Please refer to section 5.3.1 for magnet set up and
Table 5-1 for the conditions used.

Figure 5-4 shows a levitating droplet (0.5 ml) in the centre of the magnet bore as it evaporates over time (whilst being filmed from above). The droplet gradually changes from transparent to opaque as time elapses (0 – 112 min). At 112 minutes small bubble appear to form in the centre of the droplet, whilst over time several smaller bubbles form around the larger central bubble (144 min). Over the next half an hour the smaller bubbles disperse leaving just the large central bubble with a few small bubbles around it (176 m). The central bubble then disperses and the layer on the outside of the droplet can been seen growing thicker/ inwards, as the liquid from the centre evaporates (612 m). By 1014 m the outside layer has grown further inwards and small crystals can be seen starting to grow. Eventually the liquid in the centre evaporates off and the crystals continue to grow larger (2016 – 3232 m). This process is seen frequently in droplets (more so in larger droplets), however, the bubbles in the centre are not always visible, but bubbles around the circumference of the droplet can often be seen in time lapse images.

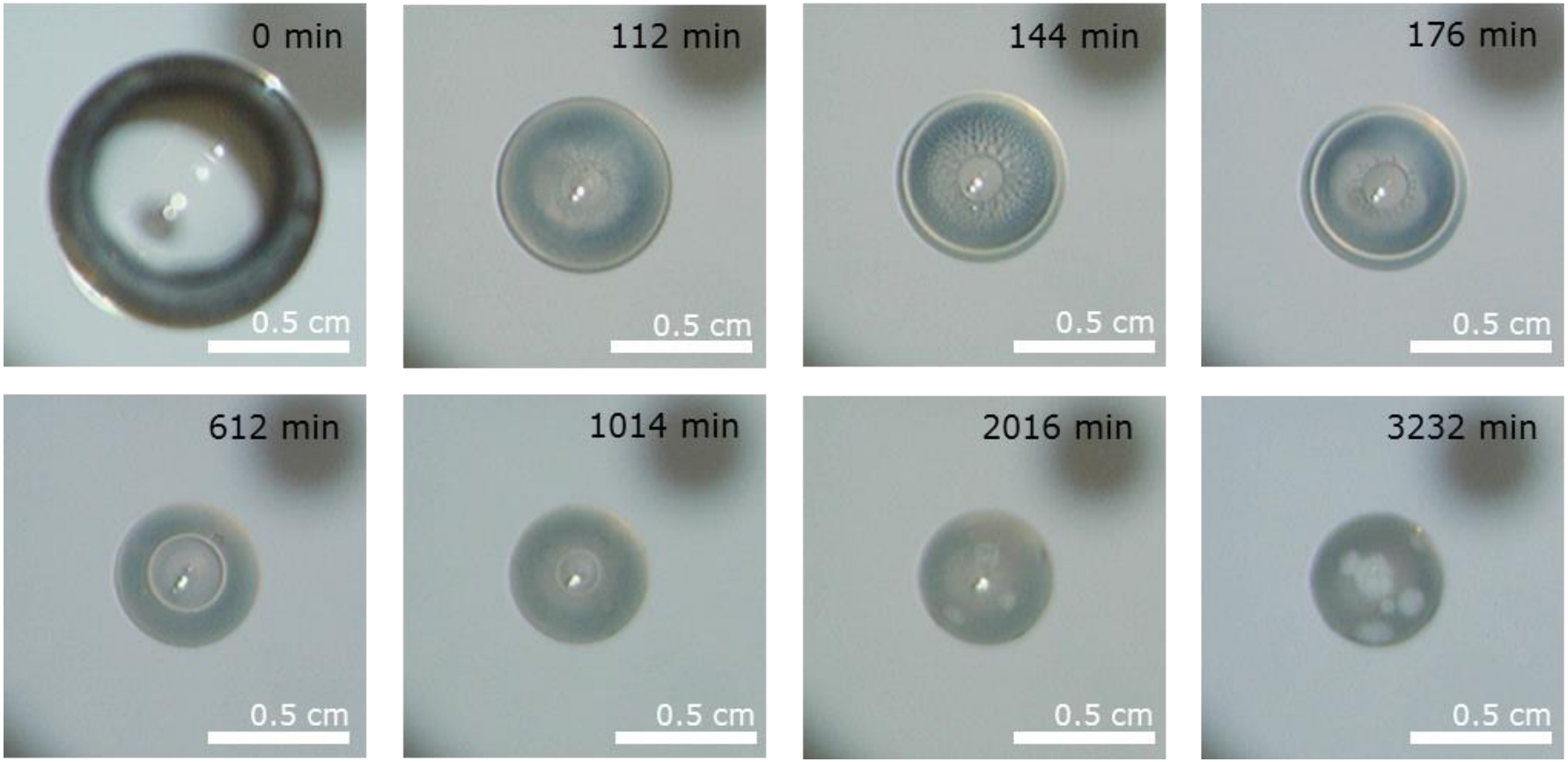

Figure 5-4 A time lapse of a small levitating droplet (0.5ml, saturated clotrimazole solution) within the magnet bore.

The majority of droplets consisted of a gel part and a white part. The gel part and the white parts of the droplets (illustrated in Figure 5-5) were analysed by FT-IR (ATR) and by handheld Raman.

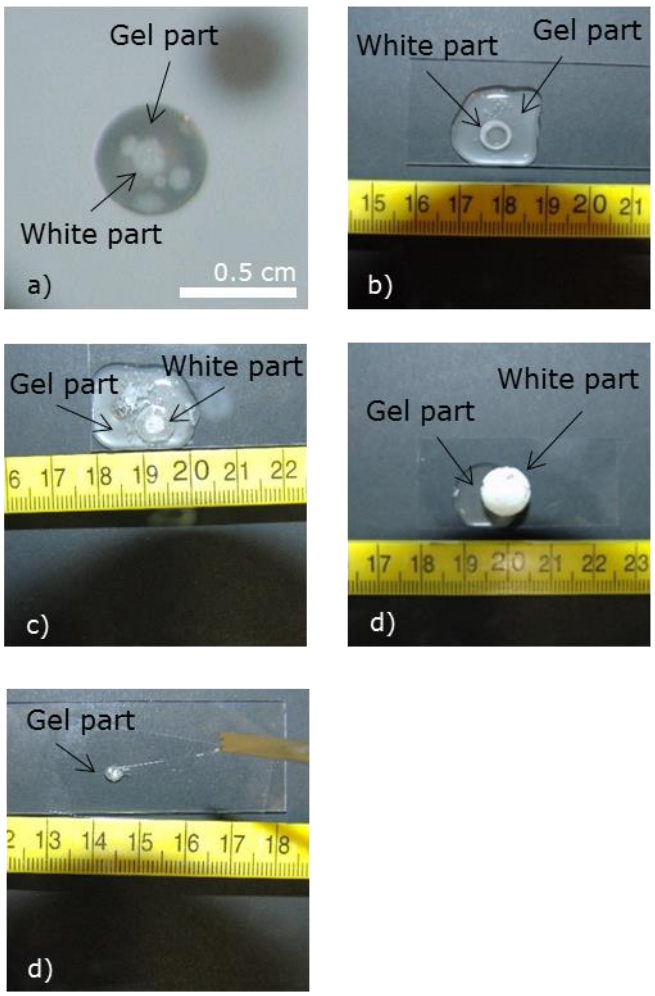

Figure 5-5 (a) Image of a levitating droplet (b) Samples collected after levitation with arrows indicating the white parts of the droplet and the gel part.

Example spectra for the gel and white parts of a droplet are displayed in Figure 5-6. The spectrum obtained for the white part of the droplet closely matches that of the clotrimazole reference spectrum. Subtle differences for the white part of the droplet are the double peak at 741 and 749 cm^{-1} which is less well defined than the clotrimazole reference spectrum, and a single peak 670 cm^{-1} which is less intense

than the clotrimazole reference spectrum. The spectrum obtained for the gel part of the droplet was also very similar to that of the amorphous reference spectrum. The spectrum for the gel part of the droplet has a less intense peak at 697 cm^{-1}, as well as a broader peak at 902 cm^{-1} as compared the amorphous spectrum. The gel sample also has a more intense peak at 879 cm^{-1} compared to the amorphous spectrum (clotrimazole spectrum and white part spectra) which is attributed to the presence of ethanol in the sample, as ethanol also has sharp peak at 879 cm^{-1} (ethanol spectrum displayed in Figure 5-10).

The handheld Raman spectra of the white part of the droplet matches the spectrum for the clotrimazole reference, whilst the gel part matches the spectrum for the amorphous reference. Noticeable differences between the clotrimazole reference and the amorphous reference are the missing peak at 327 cm^{-1} and the less intense peaks at 1078 cm^{-1} and 1188 cm^{-1} for the amorphous reference. These differences are highlighted by a red box in Figure 5-6 (b).

The FI-IR and handheld Raman spectra indicate that the white part of the droplet is crystalline clotrimazole and the gel part, amorphous.

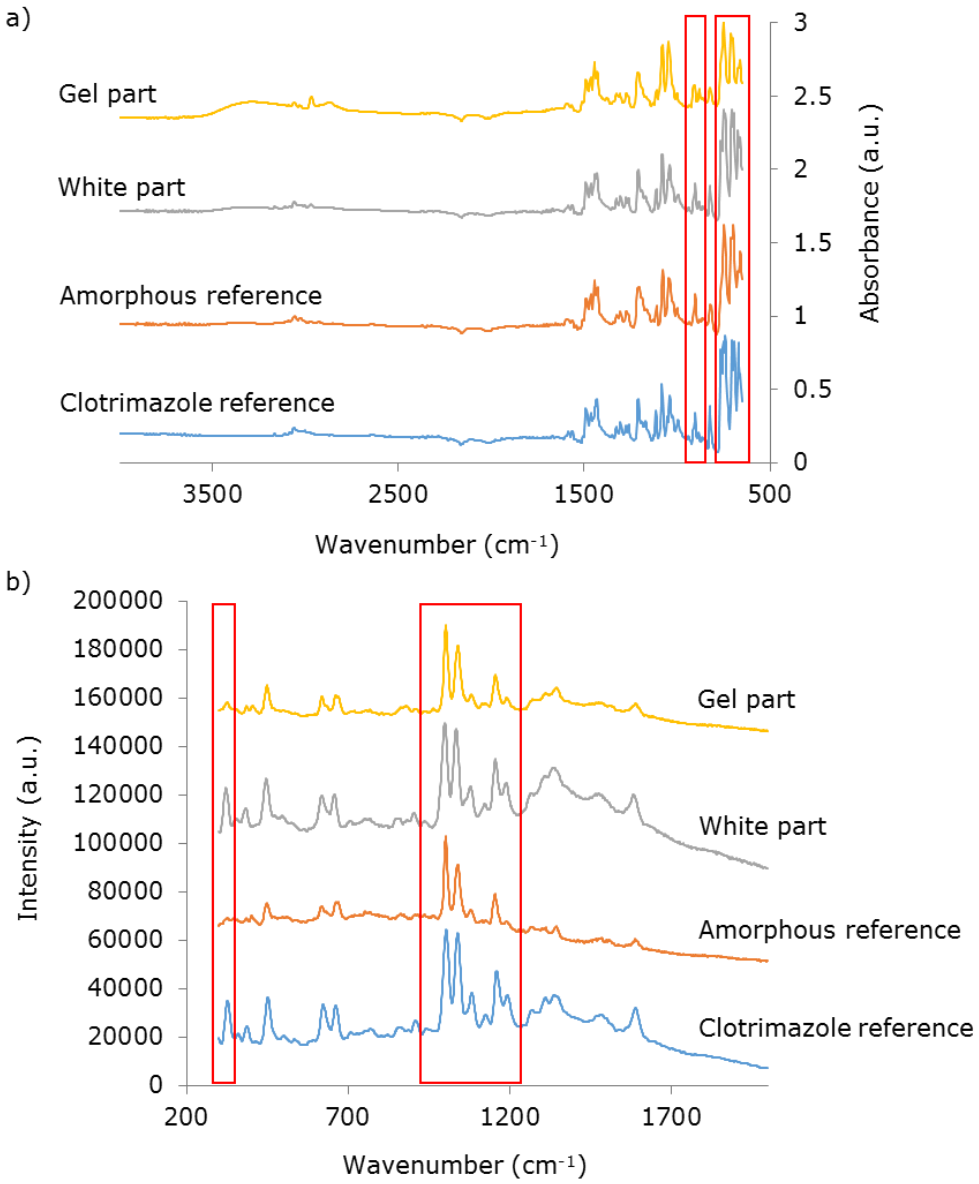

Figure 5-6 (a) FT-IR (ATR) of the clotrimazole reference, amorphous reference, white and gel parts of an example 6 mL droplet (b) Handheld Raman of the clotrimazole reference, amorphous reference, white and gel parts of a 6 mL droplet. Red boxes indicate areas of interest. Spectra have been scaled and offset for presentational purposes.

5.4.3 Large volume droplets

As the small droplets evaporated over time they became much smaller in volume making them difficult to image and analyse (handheld Raman requires a much bigger sample relative to the FT-IR (ATR)). For this reason larger droplets were levitated for comparison.

Large droplets of 3, 4 and 6 ml saturated clotrimazole solution were levitated using the cryogenic magnetic and filmed from above as they evaporated over time. Please refer to section 5.3.1 for magnet set up and
Table 5-1 for the conditions used.

A time lapse of an example droplet can be seen in Figure 5-7. The droplet starts off as transparent and over time slowly reduces in volume becoming more opaque (0 – 300 min). After approximately half an hour small bubbles can be seen forming in the middle of a larger bubble (334 min). About an hour later (392 min) the bubbles have dispersed and a medium size bubble remains with very small bubbles around it. Eventually the bubbles disperse and the outer layer can be seen growing thicker/ inwards along with a single crystal in the inner circle (1362 min). By 1852 minutes, the outer layer has grown thicker with nucleation of more crystals on the outer surface of the droplet. As time elapses the outer layer further grows thicker with only a small amount of liquid in the centre with additional nucleation on the surface of the droplet (1852 – 4248 min).

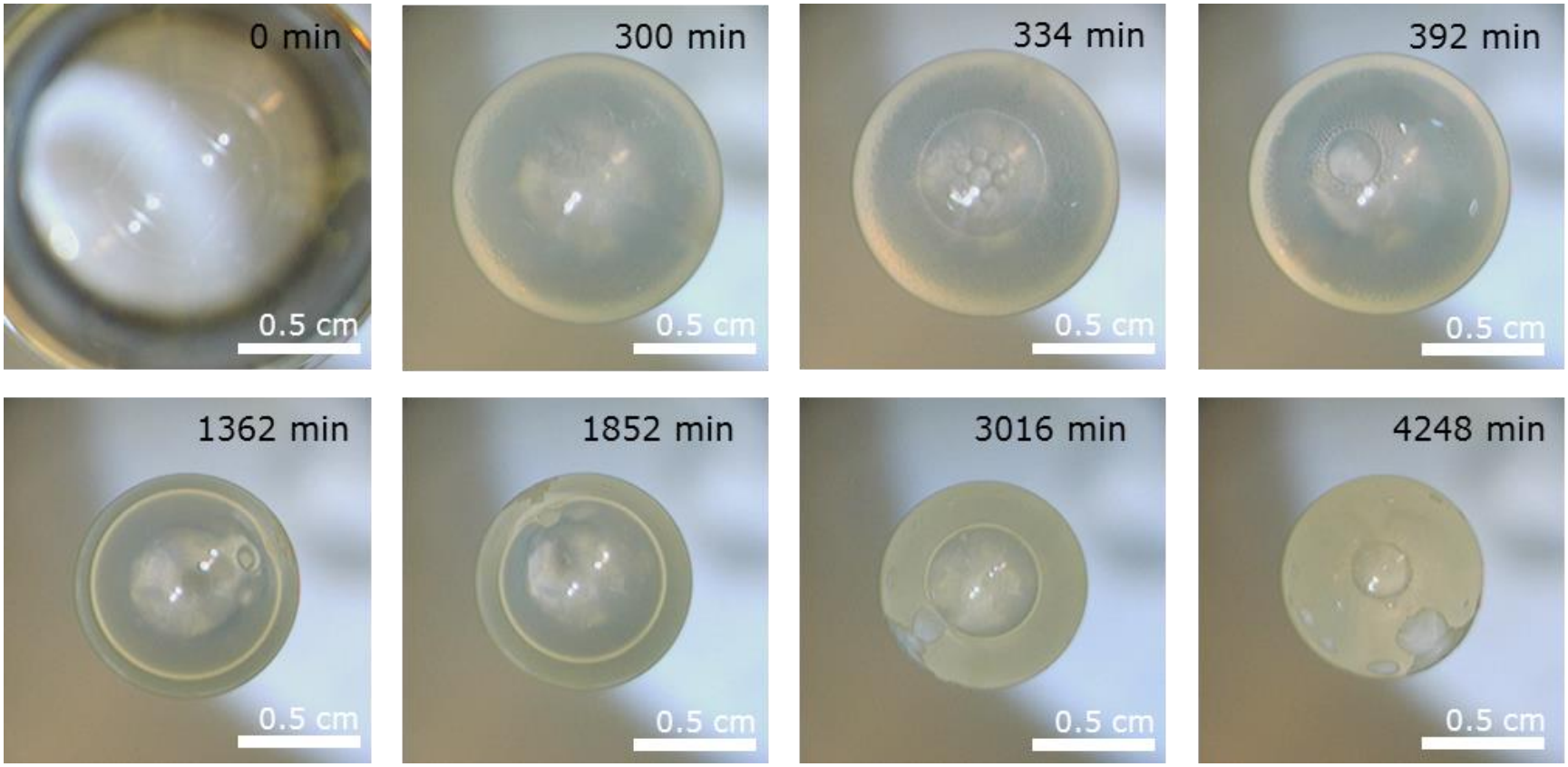

Figure 5-7 A time lapse of a large levitating droplet (4 ml, saturated clotrimazole solution) within the magnet bore.

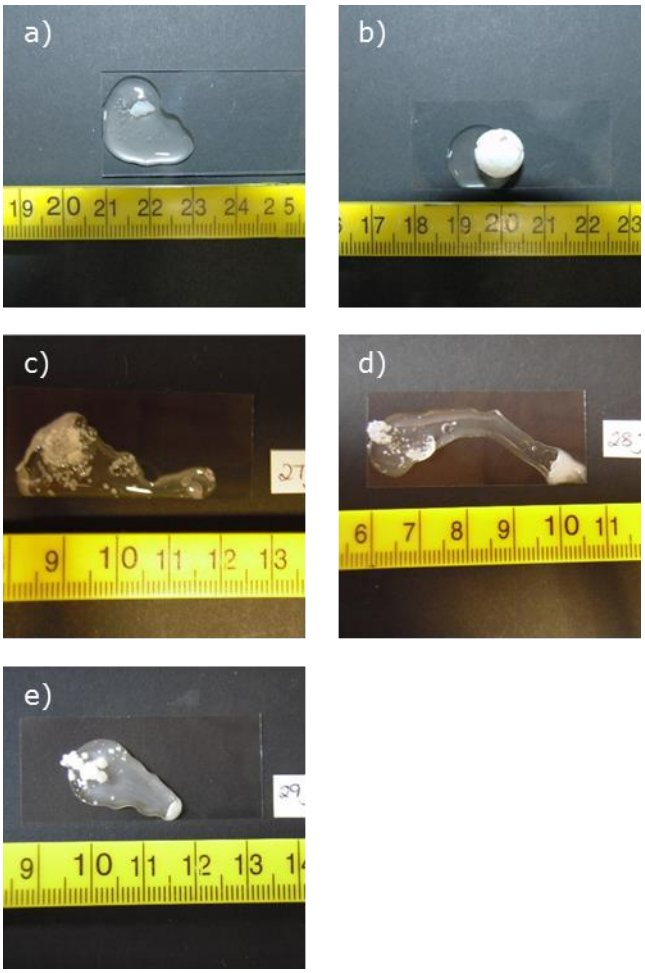

Figure 5-8 Examples of large levitating droplets collected from the magnet bore at the end of the experiment. (a) 4 ml saturated clotrimazole droplet (b) 6 ml saturated clotrimazole droplet (c) 3 ml saturated clotrimazole droplet (d) 3 ml saturated clotrimazole droplet (e) 4 ml saturated clotrimazole droplet. The droplet in image (e) is the droplet from the time lapse in Figure 5-7.

The levitating droplets were collected from the magnet bore on a glass microscope slide and photographs were taken before analysis. As can be seen in Figure 5-8 droplets consist of semi clear viscous liquid and white solid parts. Droplet (b) has formed a shell with a viscous liquid in the centre – this shell can be seen forming in the time lapse in Figure 5-9.

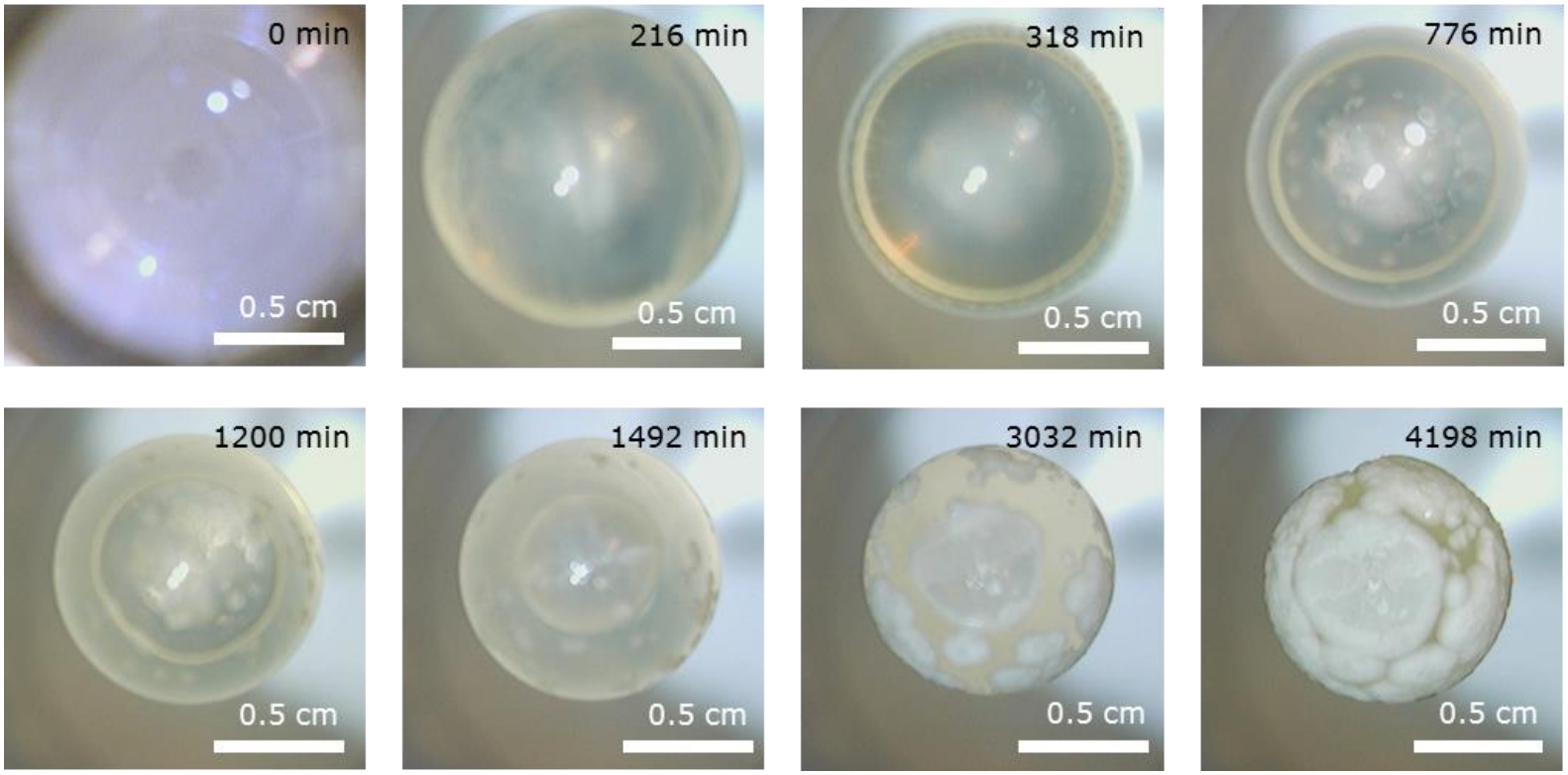

Figure 5-9 A time lapse of a large clotrimazole droplet (6 ml, saturated solution) forming a shell as it levitates within the magnet bore (droplet (b) from Figure 5-8).

In Figure 5-9 a large levitating droplet can be seen levitating in the magnet bore, the droplet starts off transparent and gradually becomes opaque over time (216 min). Small bubbles can be seen around the droplet circumference at 318 minutes. As time elapses the outer layer grows thicker/ inwards as the centre evaporates and multiple nucleation points can be seen on the droplet (776 – 1492 min). By 3032 minutes the centre of the droplet has evaporated and the white crystalline parts are mainly covering the surface of the droplet. The crystalline parts continue to grow until the last image at 4198 minutes.

The levitating droplets were analysed by FT-IR (ATR) and handheld Raman (Figure 5-10 and Figure 5-11respectively). Where sample size allowed, the gel part and white part of the droplets were analysed separately.

The FT-IR (ATR) spectra for the white parts of the droplets had spectra matching the clotrimazole reference, whilst the gel parts had spectra similar to the amorphous clotrimazole spectrum with only a few subtle differences. The peak at 697 cm^{-1} in all gel samples is less intense than the same peak in the amorphous spectrum, as well as a broader peak at 902 cm^{-1} compared to the amorphous reference. The spectra for the gel parts also contain a more intense peak at 879 cm^{-1} than the amorphous spectrum (clotrimazole reference and white parts spectra) due to ethanol in the gel samples. An additional peak at 2970 cm^{-1} is also attributed to ethanol in the sample.

The levitated droplets were analysed by handheld Raman (Figure 5-11). As the sample size required for this analysis was a lot larger than for the FT-IR most samples were analysed as both the gel and white part together. The main difference between the spectra shown is the absence of the peak at 327 cm^{-1} in the amorphous reference spectrum and the more gel like samples, for example the 3 mL droplet

and 6 mL droplet (gel part). The amorphous clotrimazole reference spectrum and the more gel like samples (3 mL droplet, and 6 mL droplet (gel part)) have a reduction in intensity in the 1074 cm^{-1} and 1187 cm^{-1} peaks compared to the clotrimazole reference spectrum and the more crystalline samples.

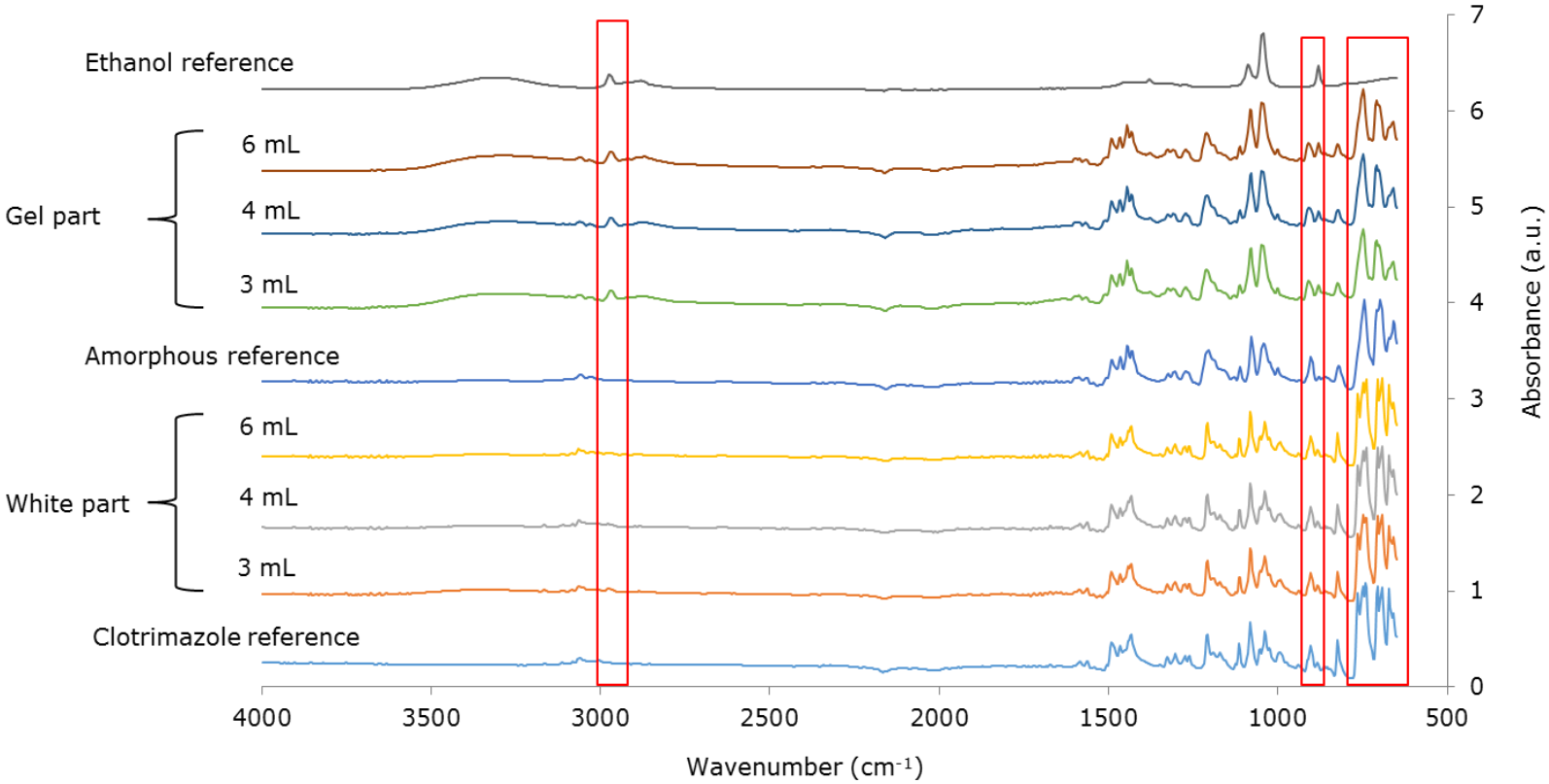

Figure 5-10 FT-IR (ATR) of large clotrimazole droplets. Red boxes indicate areas of interest. Spectra have been scaled and offset for presentational purposes.

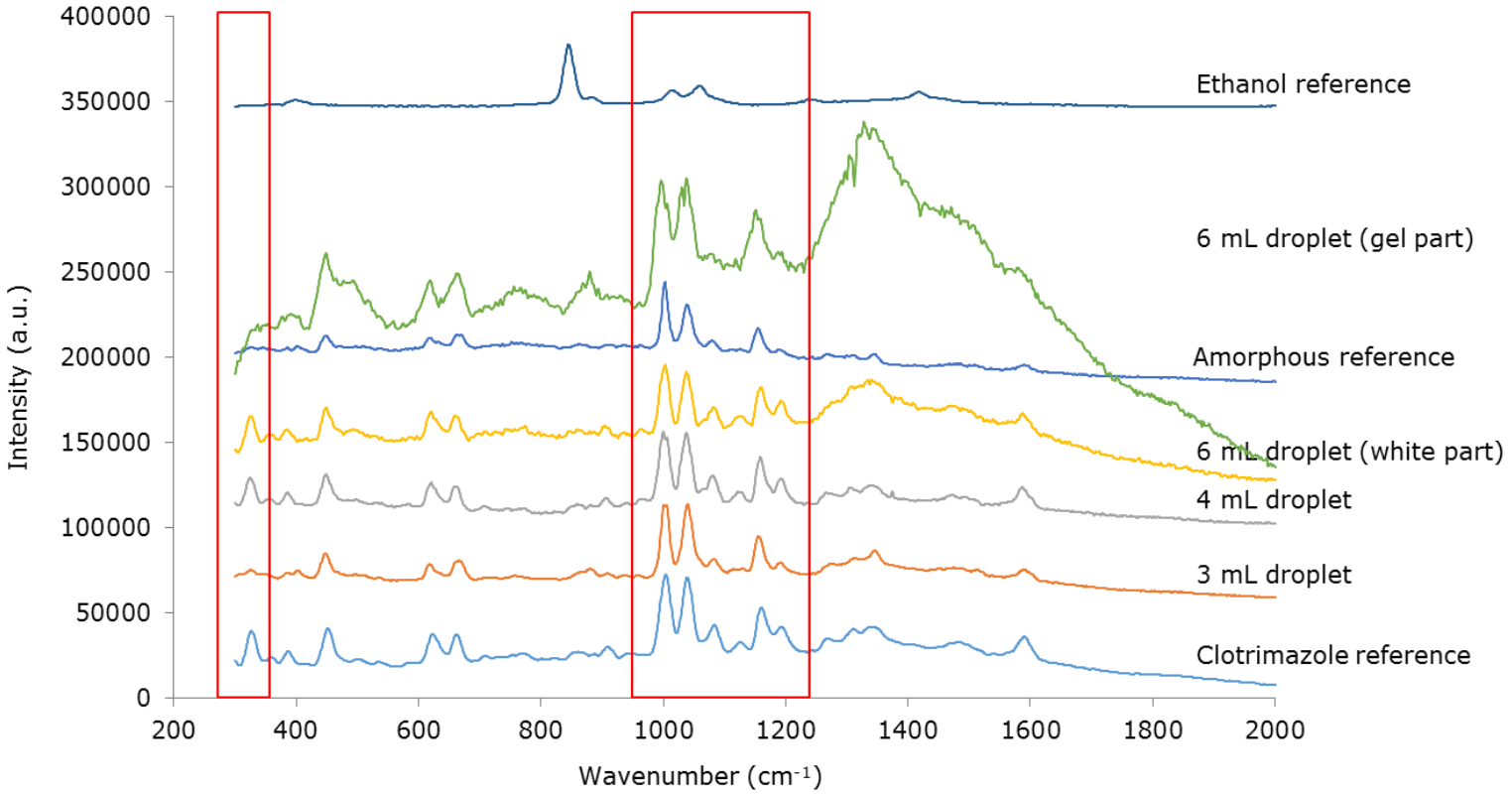

Figure 5-11 Handheld Raman of large levitating droplets. Red boxes indicate areas of interest. Spectra have been scaled and offset for presentational purposes.

5.4.4 Further investigations of experimental parameters

5.4.4.1 Investigating the effect of syringe filtering

Droplets levitated in previous clotrimazole experiments (initial experiments, medium volume droplets and large droplets) have been syringe filtered into the magnet bore to avoid unwanted nucleation from particulates. As seen in Figure 5-4, Figure 5-7 and Figure 5-9 droplets in these experiments were found to have bubbles in the centre as they evaporated over time. For comparison, a 4 mL saturated clotrimazole droplet was levitated using the same conditions as the large droplet experiments (
Table 5-1). However, this time the droplet was introduced into the magnet bore without a syringe filter to avoid aeration as bubbles in the droplet could act as nucleation site for unwanted crystal growth. The droplet was then filmed from above as it evaporated over time (Figure 5-12 b).

The levitating droplet is initially transparent and gradually decreases in volume before becoming more opaque (0 – 164 min). By 335 minutes small bubbles appear around the circumference of the droplet. A few hours later at 805 minutes the bubbles have dispersed and the outer layer has grown thicker/ inwards with a few small crystals nucleated on the droplet. At 1087 minutes the outer layer has grown thicker and the small crystals have grown larger with an agglomeration of crystalline material gathering at the bottom of the droplet. By 1391 minutes the crystals on the surface have grown larger and the outer layer of the droplet is less well defined. The droplet seems to contain less bubbles than the other droplets that were syringe filtered in Figure 5-4, Figure 5-7, and Figure 5-9. However, as this experiment was only performed once it isn’t conclusive and would need to be repeated.

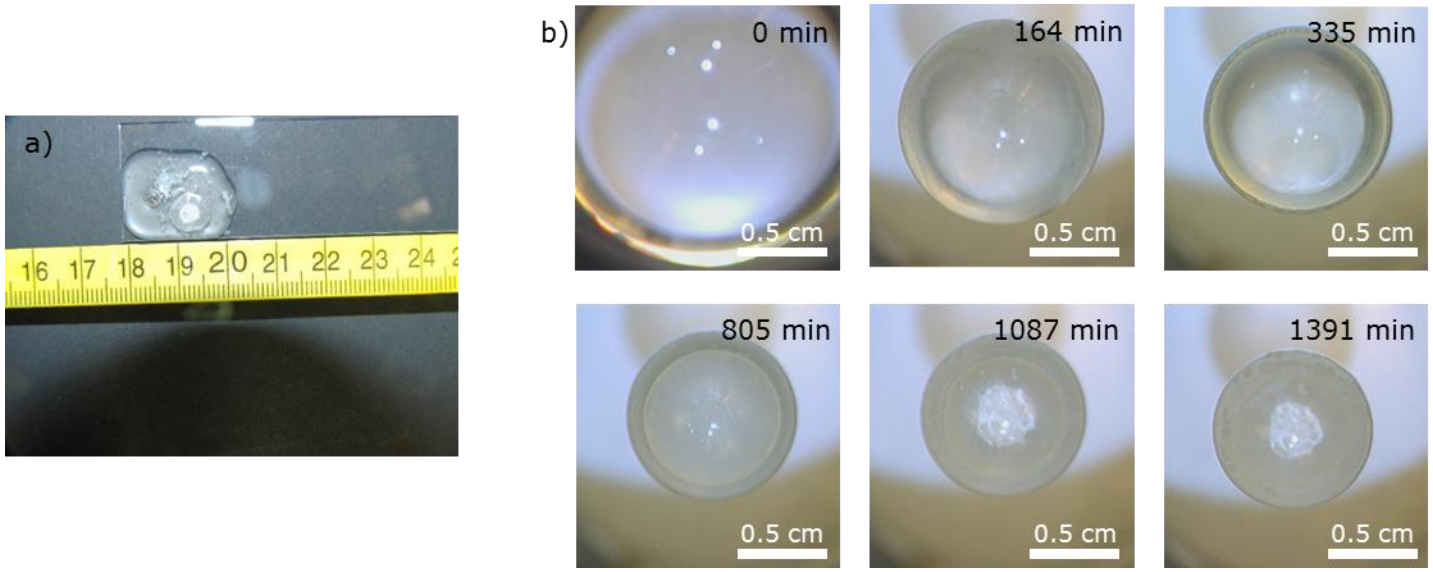

Figure 5-12 Time lapse of a large droplet (4 ml clotrimazole saturated solution) levitated within the magnet bore. As a comparison to droplets that were syringe filtered this droplet was positioned in the magnet bore using a syringe only to avoid aeration.

5.4.4.2 Time controlled droplets (48 hour and 72 hour droplets)

In the previous experiments described (medium volume droplets and large droplets) droplets were left to levitate overnight, however they were not taken out at exactly the same time as each other making it difficult for comparison. For that reason large droplets were levitated for exactly 48 hours and 72 hours. The levitating droplets were again analysed by FT-IR (ATR) and handheld Raman (Figure 5-13 and Figure 5-14 respectively). Where sample size allowed the gel part and the white part of the droplets were analysed separately.

When analysed by FT-IR (ATR) the white parts of the droplet again closely resembled the clotrimazole reference spectrum (Figure 5-13). However, the 0.5 mL sample levitated for 48 hours had a large single peak with a shoulder at 749 cm^{-1} whereas the clotrimazole reference and the rest of the white parts spectra have a double peak (at 749 and 741 cm^{-1}) with shoulder. The large single peak with a shoulder at 749 cm^{-1} is also seen in the gel samples and the amorphous spectrum, suggesting the white part of the 0.5 mL sample levitated for 48 hours contained some gel.

The gel parts closely matched the amorphous clotrimazole spectrum with a few subtle differences (Figure 5-13). The gel samples have a less intense peak at 697 cm^{-1}, and a broader peak at 902 cm^{-1} compared to the amorphous reference spectrum. The gel parts of the droplet also have a more intense peak at 879 cm^{-1} compared to the amorphous spectrum (clotrimazole reference, and the white parts spectra) which suggests the presence of ethanol in the gel parts of the droplet as ethanol has a sharp peak at 879 cm^{-1} also. An additional peak at 2970 cm^{-1} in the gel spectra is also attributed to ethanol in the sample.

As handheld Raman requires a larger sample size than the FT-IR (ATR) most of the samples were analysed as both the gel and white part together. The handheld Raman results are display in Figure 5-14.

One of the main differences between the crystalline clotrimazole and the amorphous spectrum is absence of the single peak at 327 cm^{-1} in the amorphous spectrum. All of the samples contain the 327 cm^{-1} peak in their spectra indicating they are crystalline in nature, with the exception of the 5 mL droplet levitated for 72 hours which is more gel like. For the 5 mL droplet levitated for 72 hours, the peaks at 1074 and 1187 cm^{-1} are less intense than the clotrimazole reference, and closely match the amorphous spectra, indicating this sample was more gel like than crystalline.

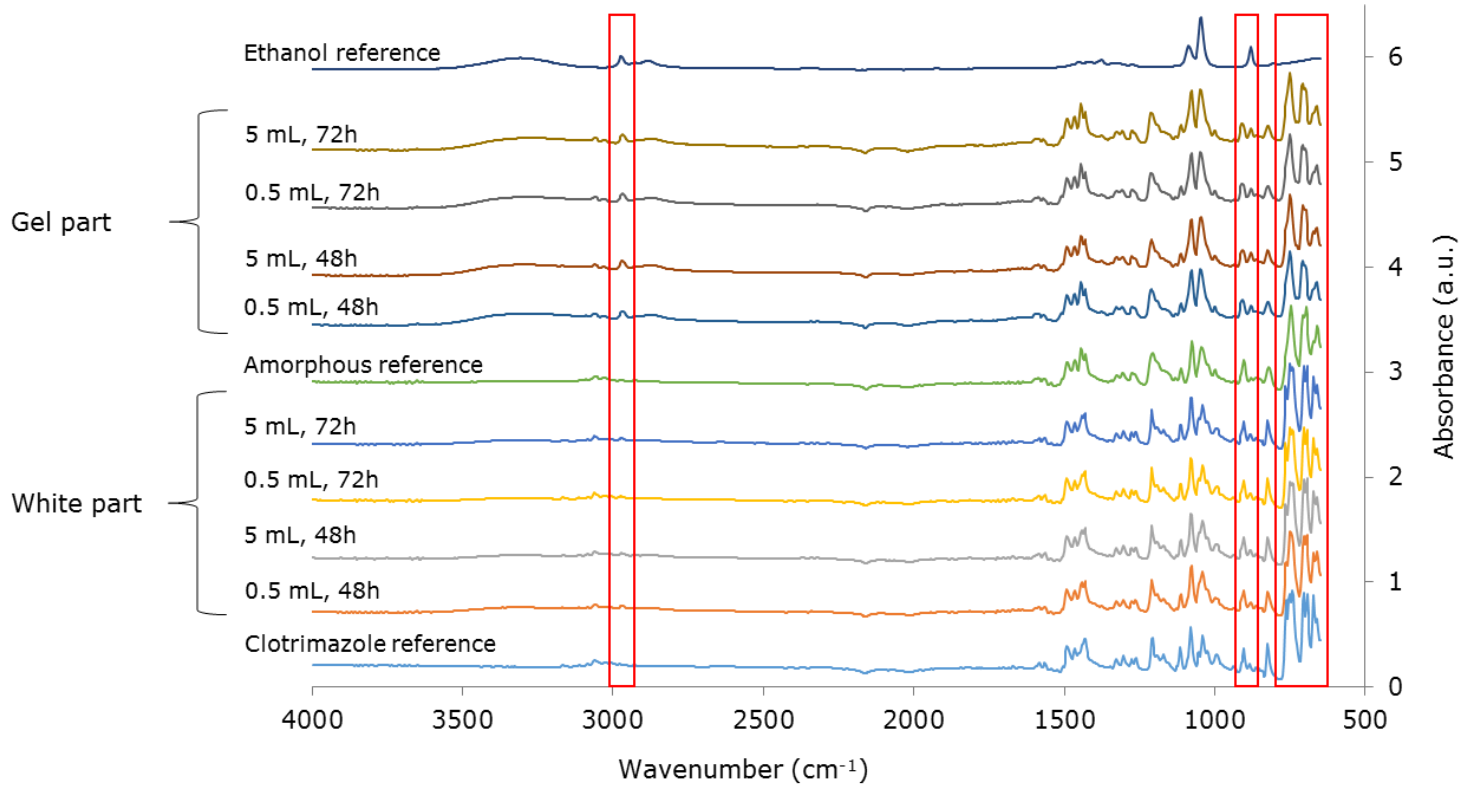

Figure 5-13 FT-IR (ATR) spectra for levitated clotrimazole droplets levitated for 48 hours or 72 hours. Red boxes indicate areas of interest. Spectra have been scaled and offset for presentational purposes.

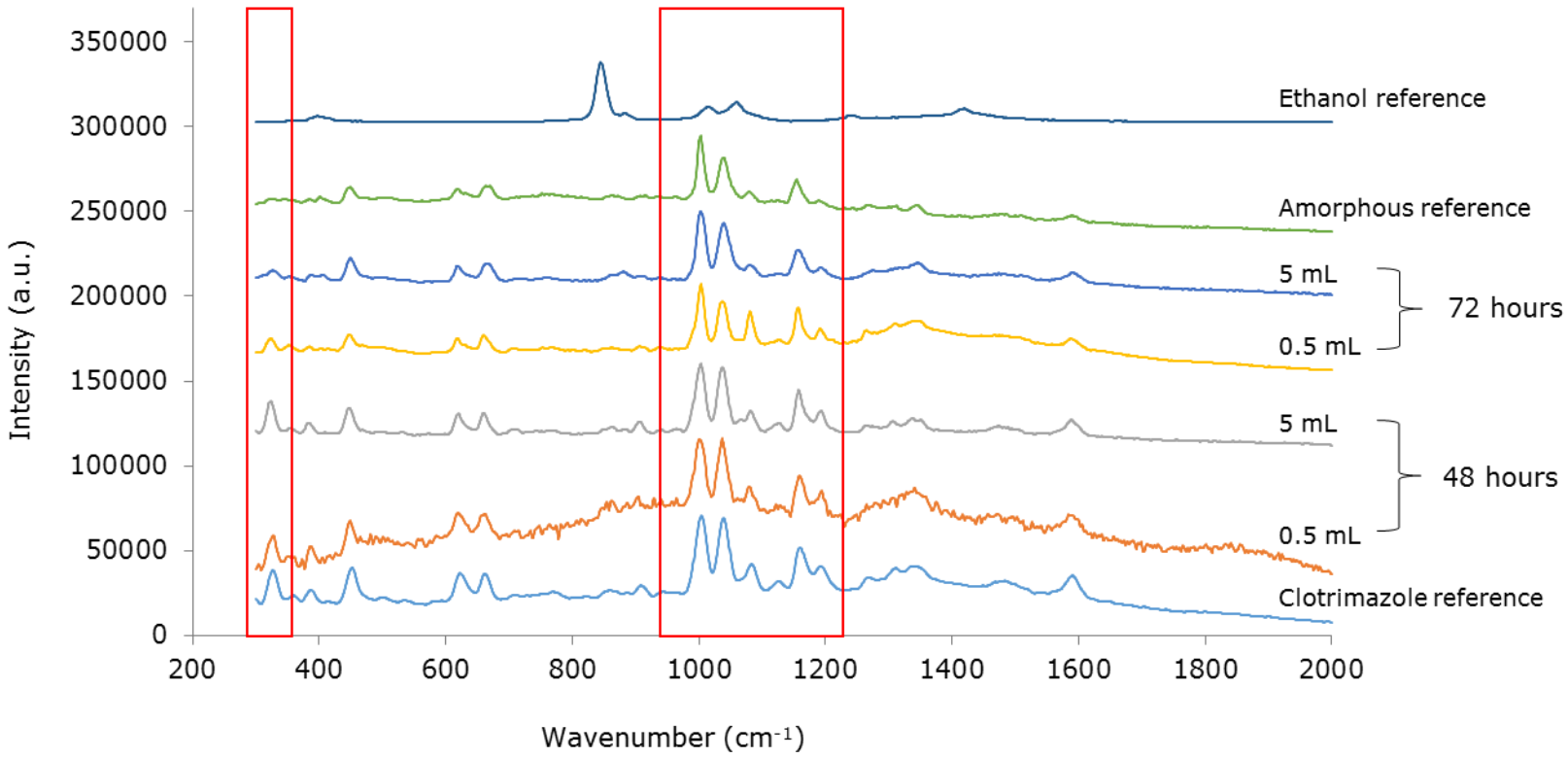

Figure 5-14 Handheld Raman spectra of clotrimazole droplets levitated for 48 hours and 72 hours. Red boxes indicate areas of interest. Spectra have been scaled and offset for presentational purposes.

5.4.5 Optimisation of imaging (45 °mirror images)

To better understand what occurred during evaporation of the levitating droplets and more specifically the bubbles in the droplet a 45° mirror was inserted into the magnet bore attached to the end of a ruler to view the droplet from the side (Figure 2-4) as it evaporated over time. In Figure 5-4, Figure 5-7, Figure 5-9 and Figure 5-12 bubbles can be seen forming inside the droplets and it was decided to investigate this further as it wasn't seen in the levitating paracetamol droplets.

A 0.5 mL saturated clotrimazole solution droplet was levitated using the cryogenic magnetic and filmed from above as it evaporated over time. Please refer to section 5.3.1 for magnet set up, Figure 2-4 for the mirror set up, and
Table 5-1 for the conditions used.

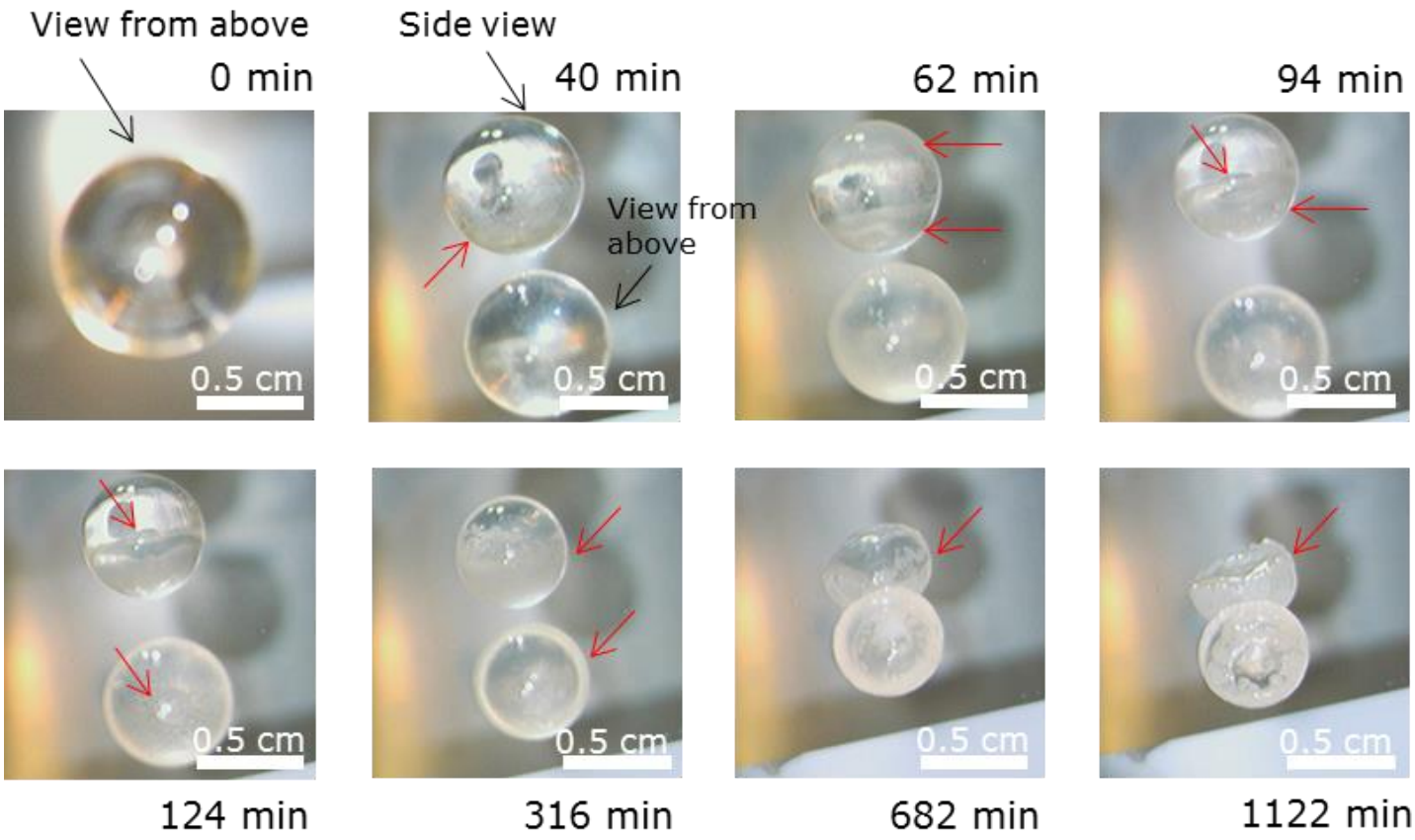

Figure 5-15 Levitating droplet captured from above and the side in a 45° mirror positioned within the magnet bore. Red arrows indicate areas of interest.

In Figure 5-15 the initial droplet can be observed from above as it levitated within the magnet bore (0 min). As time elapsed and the droplet evaporated, reducing in volume, it sat slightly lower in the magnet bore due to the increased concentration of clotrimazole. This decrease in height allowed the droplet to be viewed using the 45 ° mirror giving a side view of the droplet (40 minutes). In the 40 min image clotrimazole was seen collecting at the bottom of the levitating droplet and by 62 minutes clotrimazole had now collected at the bottom and the top of the droplet; the bird's eye view of the droplet appeared opaque. At 94 minutes the clotrimazole had mainly collected around the bottom of the droplet and the top half of the droplet was now more transparent, with a bubble formed between the two layers. By 124 minutes the droplet had two clear layers and the bubble was now seen in the bird's eye view image surrounded by lots of tiny bubbles. As time elapsed the clotrimazole started to crystallise out on the surface of the droplet, growing up the side of the droplet giving the ring effect seen in the bird's eye view of the droplet (316 min). As the droplet evaporated and the clotrimazole crystallised out it moved closer to the mirror and in image 682 min the droplet was seen gently resting on the mirror. At 1122 minutes most of the ethanol had evaporated off, leaving a half moon clotrimazole outer shell.

The clotrimazole that collected at the top and bottom of the droplet (62 minutes, Figure 5-15) can be hypothesised to be due to effective gravity. The levitation point for the droplet is in the very centre of the droplet (Figure 5-16), and when the ethanol started to evaporate the clotrimazole came out of solution and collected at the poles at the top and bottom of the droplet. I.e. the clotrimazole is less dense than the ethanol so it rises in the opposite direction to the effective gravity. When the magnet can no longer levitate all the clotrimazole it is hypothesised that it sinks to the bottom of the droplet (94 and 124 minutes, Figure 5-15) and is held in place by surface tension. The

droplet now consists of two layers, thought to be a less dense ethanol rich layer on the top and a denser clotrimazole gel in the bottom half of the droplet. The bubbles seen at 124 minutes (Figure 5-15) are thought to be due to dissolved gas coming out of the solution.

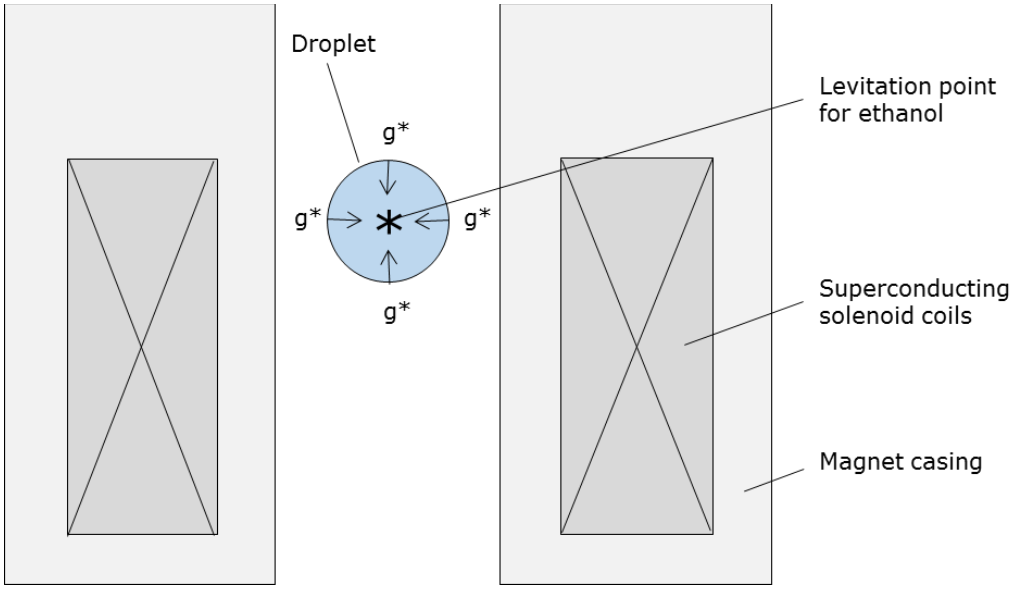

Figure 5-16 Schematic of levitating droplet within the magnet bore. g* denotes effective gravity, and the arrows indicate the direction of the effective gravity.

5.4.6 Overall results summary

The results of this chapter are summarised in Table 5-3. Initial experiments involved levitating small droplets with a volume between 0.1 and 0.2 mL. Images captured of the levitating droplets show the droplet starting off as transparent and gradually becoming more opaque over time. Droplets were found to have a different appearance depending on the levitation time. By taking a droplet out earlier it could consist of two different layers or a thick gel with small crystalline parts on the surface. Leaving the droplet levitating for longer was found to create a crystalline shell.

Medium and large volume droplets were also levitated within the magnet bore. Again, droplets consisted of a thick gel, with small white crystalline parts on the surface; sometimes a crystalline shell also formed. Bubbles could frequently be seen in the centre of the droplets in the recorded time lapse images.

The FTIR (ATR) and handheld Raman spectra for the gel part and white crystalline parts of levitated droplets were found to closely resemble the spectra for amorphous clotrimazole, and crystalline clotrimazole material respectively. The separation of the two layers is thought to be due to effective gravity; the clotrimazole is less dense than the ethanol so rises in the opposite direction to effective gravity i.e. to the poles of the droplet. When the magnet can no longer levitate the clotrimazole, it is hypothesised that it sinks to the bottom of the droplet where it is held in place by surface tension. The two halves of the droplet are therefore thought to consist of a less dense ethanol rich layer on top and a denser clotrimazole gel on the bottom. The observed bubbles are thought to be from dissolved gas coming out of the solution which could act to nucleate crystal growth.

A further experiment considered the effect of syringe filtering on the droplets. It was hypothesised that syringe filtering the droplet directly into the magnet bore could introduce air into the droplet. In this experiment the droplet was syringed straight into the magnet bore without filtering and from the time lapse images it appears this method may produce fewer bubbles. As the experiment was only performed once the results aren't conclusive and would need to be repeated. As the bubbles are thought to be from dissolved gas coming out of the solution eliminating this step would avoid aeration of the droplet.

By using 45° mirrors droplets could be viewed from the side and from above allowing the crystallisation process to be better followed. For

the first time we could clearly see the clotrimazole gathering at the top and bottom of the droplet (when viewed from above the droplet looked opaque). The clotrimazole then sinks to the bottom of the droplet forming two distinct layers and bubbles appear at the interface between the two layers. The bubbles then disperse and the remaining ethanol continues to evaporate leaving a solid clotrimazole half shell. As discussed earlier the two separate layers are due to the differences in density between the clotrimazole and ethanol meaning the clotrimazole rises to the poles of the droplet as it is less dense. When the magnet can no longer levitate the clotrimazole it falls to the bottom of the droplet and is held in place by surface tension. The clotrimazole then crystallises up the side of the droplet as the ethanol evaporates leaving a half moon shell.

Experiment	Key findings
Initial experiments (small volume)	• Droplets start off transparent and gradually become more opaque over time • Droplets have different features depending on the levitation time, for example, gel like droplets with small crystalline parts on the surface, droplets consisting of two different halves or droplets that form a shell
Medium & Large droplets	• Droplets consisted of a gel with white crystalline parts on the surface, sometimes a shell is formed • Bubbles spotted in time lapse images • FTIR (ATR) and handheld Raman for the gel like part matched spectra for amorphous clotrimazole while the white parts matched the spectra for clotrimazole as received
Further investigations: • Syringe filtering effects • Time controlled droplets	• The droplet that wasn't syringe filtered appeared to have less bubbles in it • Droplets consisted of a gel with white crystalline parts on the surface, FTIR (ATR) and handheld Raman for the gel like part matched spectra for amorphous clotrimazole while the white parts matched the spectra for clotrimazole as received
Optimising imaging	• Using a 45° mirror droplets were viewed from the side. Droplets were seen forming two distinct layers with a bubble at the interface. The clotrimazole crystallised on the bottom and sides of the droplet forming a half moon shell.

Table 5-3 A summary of the results obtained in this chapter.

5.5 Conclusion

Diamagnetic levitation was successful used to freely levitate clotrimazole droplets and assess the potential for "containerless processing". Droplets of different concentrations and volumes were successfully levitated and studied in this chapter. Small droplets were initially levitated as a comparison to Benmore and Weber (2011) who were able to successfully amorphise clotrimazole using acoustic levitation. In their studies μL volume droplets formed amorphous gels and were rapidly frozen to preserve the amorphous state.

Our research found small droplets difficult to levitate due to the smaller sized droplets remaining attached to the needle tip, flicking of the needle would cause the droplet to swing out and stick to the side of the magnet bore. Once the small droplets were levitated they would evaporate, and reduce in volume, making them difficult to analyse by FT-IR (ATR) and handheld Raman as there wasn't always enough sample. However, diamagnetic levitation has the advantage of being able to levitate larger volume droplets. The levitated droplets would consist of a thick viscous gel part and white parts. The viscous gel substance is similar to the gel reported by Benmore and Weber (2011). However, potentially due to the longer levitation times, small crystals would nucleate on the surface of the droplets levitated by diamagnetism, which when analysed by FT-IR (ATR) and handheld Raman suggested crystalline clotrimazole. The gel parts of the droplet analysed by FT-IR (ATR) and handheld Raman closely resembled the amorphous spectrum with a few subtle differences including peaks that matched the ethanol reference spectrum, suggesting ethanol was still in the sample.

The imaging of the droplet was optimised by using a 45 ° mirror, which made it possible to successfully image the droplet from the side allowing a better understanding of the processes going on in the

magnet bore. It was discovered that the droplet would separate into two layers, which couldn't been seen when imaging the droplet from above. It is hypothesised that the clotrimazole is less dense than the ethanol, which means it rises in the opposite direction to the effective gravity i.e. the poles of the droplet. When the magnet can no longer levitate the clotrimazole it is hypothesised it sinks to the bottom of the magnet and held in place by surface tension. The ethanol then continues to evaporate leaving a crystalline half-moon shaped shell. The bubbles seen in the droplet are hypothesised to be from dissolved gas coming out of the solution.

As well as creating gel droplets, it was possible to create hollow spheres of clotrimazole (shells). These unique spheres could have potential uses in drug delivery, if the size could be reduced. A similar technique would be spray drying, which uses high temperatures. An advantage of diamagnetic levitation is that experiments can be performed at room temperature.

6 Low field experiments

6.1 Introduction

Research on magnetic fields has mainly focused on the ability to create large high quality protein crystals for X-ray diffraction analysis and to investigate the orientation of crystals grown under magnetic fields. For example Astier et al. (1998) investigated protein crystals orientation grown under a magnetic field. Using small permanent magnets producing a magnetic field strength of 1.25 T they grew crystals of porcine pancreatic α-amylase, hen egg-white lysozyme and bovine pancreatic trypsin inhibitor. Crystals were oriented in the direction of the magnetic field, with the exception of heterogeneous nucleation.

Ribonuclease A, met-myoglobin and hen egg white lysozyme crystals were aligned by magnetic fields of less than 1 T by Sakurazawa et al. (1999). A magnetic field (0.2, 0.3, 0.4 and 1.13 T) was applied to solutions during crystallisation of monoclinic lysozyme. Results indicated that the crystals aligned perpendicular to the magnetic field, and crystals grown with no magnetic field were orientated at random. A second experiment showed 80% of ribonuclease A crystals grown in a magnetic field of 1.13 T were oriented perpendicularly to the field direction. Met-myoglobin crystals grown under a magnetic field of up to 0.7 T also aligned perpendicular to the field direction.

Gavira and Garci (2009) et al also grew hen white lysozyme crystals in a static magnetic field of 7 Tesla. The crystals grew in an agarose gel to stop sedimentation occurring and buoyancy driven convection. It was reported that the homogeneous and constant magnet field decreased the nucleation induction time resulting in a higher nucleation density with larger crystal size. When the crystals were

grown in a solution of 0.02% agarose 100% of the crystals could be oriented by the 7 Tesla magnetic field.

More recently, research has also investigated the influence of magnetic fields on the polymorph formation of different compounds. Knez and Pohar (2005) investigated the influence of magnetic fields on the polymorph composition of calcium carbonate. Calcium carbonate has three polymorphic forms; calcite, vaterite, aragonite. Calcite is the most stable polymorph and has a hexagonal structure, whilst vaterite, which is also hexagonal is the least stable polymorph. Aragonite is the metastable polymorph and has an orthorhombic structure. Using a closed recirculating system a carbonised aqueous solution was pumped through a magnetic field (up to 1.12 T) via silicon tubing and back into a glass container, the total circulation time was 6 hours. The solution was ultra-centrifuged once the treatment was complete and air dried at ca. 40 – 45 °C. Their results indicated that magnetic fields promote the precipitation of the aragonite polymorph from carbonised solutions. Magnetic induction and exposure time were found to influence the aragonite content of the precipitates.

Magnetic fields have also been found to influence the polymorphic form produced when samples of 2,2’ :6’,2”-terpyridine were crystallised in a magnetic field (Honjo et al. 2008). 2,2’ :6’,2”-terpyridine has photophysical properties, exhibits phosphorescence, and has two polymorphic forms; an orthorhombic and a monoclinic form. Applying magnetic field strengths above 5 T to a solution during crystallisation produced monoclinic crystals, whilst normal (0 T) conditions were found to produce orthorhombic crystals. The monoclinic crystals were phosphorescent at room temperature, and it was also found that increasing the magnetic field strength increased the lifetime of the phosphorescence.

The crystallisation of coronene in a magnetic field lead to the discovery of an unforeseen polymorph (Potticary et al. 2016). Coronene is a polyaromatic hydrocarbon with six aromatic rings, arranged in a planar discoidal fashion. Coronene was crystallised from a supersaturated toluene solution under magnetic fields of 1 T. The coronene solution was prepared at 93 °C and the whole system was kept at 93 °C for four hours after the cuvette was inserted. The temperature was then gradually reduced over a period of time until it reached room temperature. Crystals of β – coronene were produced rather than the ubiquitous γ – coronene. The β – coronene crystals were orange in colour and much longer in dimension than the γ-coronene crystals. The β polymorph remained stable in ambient conditions and without a magnetic field (0 T).

Research on magnetic fields for crystallisation has therefore mainly focused on the crystallisation of protein crystals for enhanced X-ray crystallography or the orientation of protein crystals. A few research groups have investigated magnetic fields for the control of polymorph formation. However, there is a gap in the research for the investigation of magnetic fields for the polymorphic control of pharmaceutical compounds. Therefore, in this chapter we explore the potential of magnetic fields on the crystallisation of paracetamol, clotrimazole and propranolol. Another part of this chapter was to repeat the work produced by Potticary et al. (2016) by crystallising coronene in our magnet system.

6.1.1 Aims and objectives

The aim of this chapter was to explore the effect of low strength magnetic fields on crystallisation. Initially this aim was to repeat the low field crystallisation of coronene as performed by Potticary (2016) using the experimental set up at the University of Nottingham. A

secondary aim was to perform similar experiments with paracetamol, clotrimazole, and propranolol. This aim was achieved by completing the following objectives:

- Perform crystallisation of coronene under a magnetic field of 1 T using our magnet set up.
- Perform crystallisation of paracetamol, clotrimazole and propranolol under a magnetic field of 1 T.
- Create zero field samples for comparison, keeping conditions as close to the magnet set up as possible.
- Analyse samples by optical microscopy, FT-IR (ATR), and handheld Raman.

6.2 Materials and methods

6.2.1 Materials

Paracetamol (Acetaminophen, BioXtra ≥ 99%), clotrimazole, ± propranolol hydrochloride and ethanol (200 proof, anhydrous, ≥ 99.5%) were obtained from Sigma Aldrich, Dorset, UK and used without further purification.

6.3 Experimental methods

6.3.1 Magnet set up

The Cryogenic magnet (Cryogenic Ltd, London) was used for all experiments performed in this chapter.

During the experiments in this chapter magnet set up 2 was used (see section 2.1.5).For all experiments a cuvette holder was used (see section 2.1.3) as well as a digital camera which was mounted on

a clamp stand above the magnet bore (section 2.1.4). The cuvette holder was positioned in the centre of the magnetic field which is 134.5 mm from the inner plate of the magnet (145.5 mm when taking into account the 11 mm on the lip of the bore insert).Table 6-1 summarises the experimental conditions used for each set of experiments.

Sample name	**Magnet**	**Field strength (T)**	**Box/ glass cover**	**Air/ nitrogen**	**Flow rate (ccm/ min)**	**Bore insert (°C)**
Coronene	Cryogenic	0 1 1 1 1 1 1	Box (set up 2)	N/A	N/A	93 (1 hour) 93 (4 hours) 83 (24 hours) 73 (24 hours) 63 (24 hours) 50 (24 hours) RT (~ 2 hours)
Paracetamol	Cryogenic	1	Box (set up 2)	N/A	N/A	20
Clotrimazole	Cryogenic	1	Box (set up 2)	N/A	N/A	20
Propranolol	Cryogenic	1	Box (set up 2)	N/A	N/A	20

Table 6-1 Conditions of experimental set up for low field studies.

6.3.2 Creating solutions

Coronene (25 mg) was dissolved in toluene (10 mL) in a glass beaker, in a water bath on a hot plate maintained at 93 °C. Once the coronene had dissolved it was syringe filtered (using glass syringe and Chromacol 4 – SF – 02 (PV) 4 mm Syr. Filter PVDF 0.2 µM) into glass test tubes and maintained at 93 °C in a pressure oven until required.

Saturated solutions of paracetamol, clotrimazole and propranolol (Table 6-2) were made by dissolving the required amount of drug in ethanol in a glass beaker whilst being gently warmed and stirred on a magnetic hot plate. Drug was added to the solution until no more would dissolve at which point the solution was taken off the heat and left to cool. The solution was then syringe filtered (0.22 µm) into glass vials for storage.

Experiment	Solvent	Concentration	Volume
Coronene	Toluene	2.5 mg/ mL	1 mL
Paracetamol	Ethanol	Saturated solution	1 mL
Clotrimazole	Ethanol	Saturated solution	1 mL
Propranolol	Ethanol	Saturated solution	1 x 1 mL 3 x 0.5 mL

Table 6-2 Details of solutions used in low field experiments.

6.3.3 Sample preparation/ insertion into magnet bore

The coronene solution was prepared as per section 6.3.2., and was stored in a pressure oven at 93 °C until it was required. The coronene solution (in sealed cuvettes) was transferred between labs in a sealed insulated vessel to try and maintain the temperature of the coronene solution. However, it was found that the temperature of the water had dropped to 83 °C by the time it arrived in the magnetic levitation lab. We therefore decided to position the sample (in a cuvette) in the magnet bore and maintained the temperature at 93 °C (with no magnetic field, 0 T) for an hour before following the method described by Potticary et al. (2016). The magnetic field was then turned on at 1 T for 4 hours (the bore temperature was maintained at 93 °C), after which the temperature was reduced to 83 °C for 24 hours, 73 °C for 24 hours, with a final dwell at 50 °C for 24 hours before reducing to room temperature.

Paracetamol, clotrimazole and propranolol solutions were prepared as per section 6.3.2 and syringed filtered (0.22 μm) into the cuvette positioned in the centre of the magnetic field within the magnet bore (section 6.3.1) and left to crystallise over 24 hours.

Zero field samples were crystallised in as similar conditions the low field experiments as possible. Coronene samples followed the reducing temperature programme above in a pressure oven. The paracetamol, clotrimazole and propranolol solutions were syringe filtered (0.22 μm) into cuvettes crystallised in a pressure oven at 20 °C for 24 hours.

6.4 Results and discussion

6.4.1 Low field coronene experiments

The low field coronene experiment was performed once, with three zero field samples produced in parallel at the same time. The coronene crystals were viewed under ultra violet light using an ultra violet transilluminator (Figure 6-1). All four experiments were found to produce crystals that fluoresced green, indicating that the γ – polymorph of coronene had been formed. Crystals were also viewed with the UV setting on an optical microscope (Figure 6-2). The crystals had needle like morphology and fluoresced green, again indicating the γ – polymorph.

Using low magnetic fields, Potticary et al (2016) reported that they were able to produce the β – polymorph of coronene which fluoresced orange. In their experiment they kept the coronene in solution at 93 °C prior to use. In our experiments keeping the coronene solution at 93 °C whilst syringe filtering proved to be very difficult, as crystals could be seen precipitating out of the solution within the syringe. The solution and syringe then had to be reheated. It is possible that during this process that not all the coronene went back into solution, resulting in unwanted nucleation of the γ form. The coronene solution had to be transported between the lab with the fume hood and the magic levitation lab in Physics, which also caused a drop in temperature, and could have allowed the coronene to start crystallising out. In an attempt to overcome this the coronene solution was heated at 93 °C for an hour in the magnet bore to counteract the temperature decrease before following the method by Potticary et al. (2016).

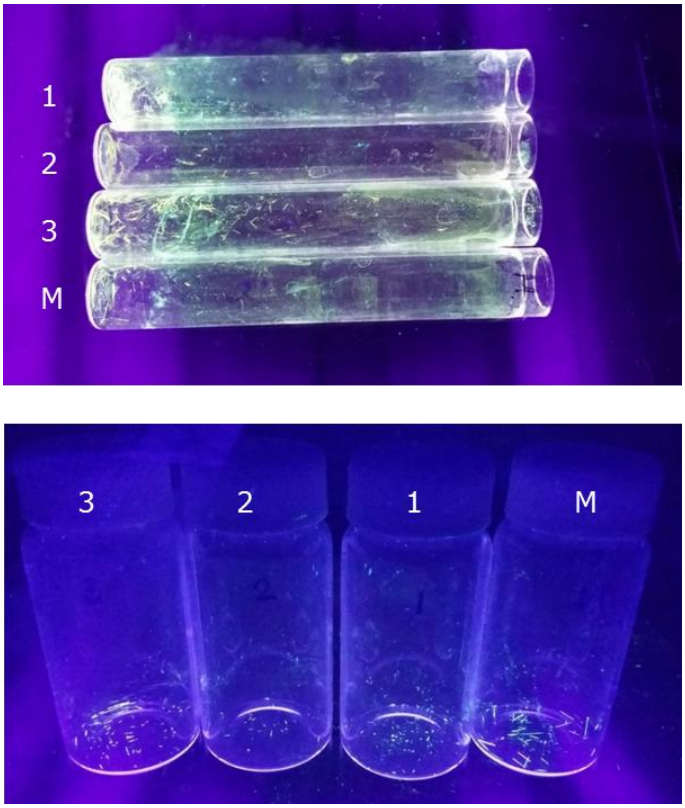

Figure 6-1 Coronene crystals viewed under ultra violet light. Zero field 1, 2, 3, and M (magnet, low field sample (1 T).

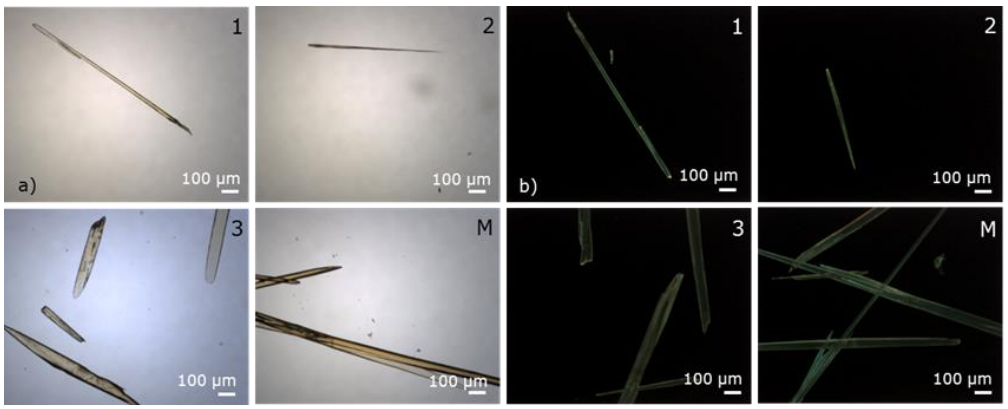

Figure 6-2 (a) Optical microscopy of zero field samples 1, 2, 3, and M (magnet, low field sample (1 T) (b) UV (ultraviolet) microscopy of zero field samples 1, 2, 3, and M (magnet, low field sample (1 T).

6.4.2 Low field paracetamol experiments

Low field and zero field paracetamol samples formed in low strength and zero magnetic fields were analysed by FT-IR (ATR) and handheld Raman. As the handheld Raman required larger samples than the FT-IR (ATR), only the low field paracetamol had samples of sufficient quantity to be analysed by handheld Raman.

The FT-IR (ATR) spectra show that the samples formed in low and zero fields were all form I paracetamol (Figure 6-3). Characteristic peaks for form I paracetamol at 806, 682 and 1228 cm^{-1} are all present. It should be noted however, that some extra/ more intense peaks were also present in some spectra. Zero field sample number 2 for example has a more intense peak at 1047 cm^{-1} compared to the paracetamol reference. This possibly is due to residual ethanol remaining in the sample as ethanol has an intense peak at 1047 cm^{-1}. Zero field samples numbers 1, 2 and 3, also show peaks at 1106 cm^{-1} gaining a small shoulder at 1084 cm^{-1}: again this correlates to an intense peak observed at 1084 cm^{-1} in the ethanol spectrum. Low field sample number 1 and all three zero field samples gain a shoulder at 1148 cm^{-1} which is attributed to the PMMA (poly(methyl methacrylate)) in the plastic cuvettes which has interacted with the sample. An extra peak at 1722 cm^{-1} is also present in all low field and zero field samples, again from the PMMA.

The handheld Raman spectra (Figure 6-4) for the paracetamol formed in low field contain characteristic peaks at 1234 and 1325 cm^{-1} with three well resolved peaks in the 1500 – 1700 cm^{-1} range, confirming the formation of form I paracetamol (Kauffman et al. 2008). Some of the handheld Raman spectra were of lower quality (poor signal: noise) than others due to a smaller sample size, for example low field sample number 2 (Figure 6-4).

It is not surprising that the paracetamol crystallised in low magnetic fields samples produced form I paracetamol, as levitation at much higher field strengths also routinely produced this form (chapter 4). Nichols and Frampton (1998) report that form II paracetamol crystals in contact with the mother solution can rapidly convert back to form I, which could also happen in samples left in the magnet, particularly when not all of the solvent is evaporated, as in these experiments. Interestingly Potticary et al. (2016) repeated the same coronene experiment at lower fields strengths of 0.2, 0.5 and 0.8 T which resulted in the formation of the γ polymorph rather than the β form seen at 1 T. They suggest that 1 T is close to an energetic threshold for selection between the two polymorphs. The authors repeated the experiments with pyrene at 1 T, however they were unable to control the polymorphic form. As pyrene is not as magnetically susceptible as coronene it is suggested that higher fields strengths would be required. Paracetamol is likely not as magnetically susceptible as coronene, as even at higher field strengths form II was only occasionally formed.

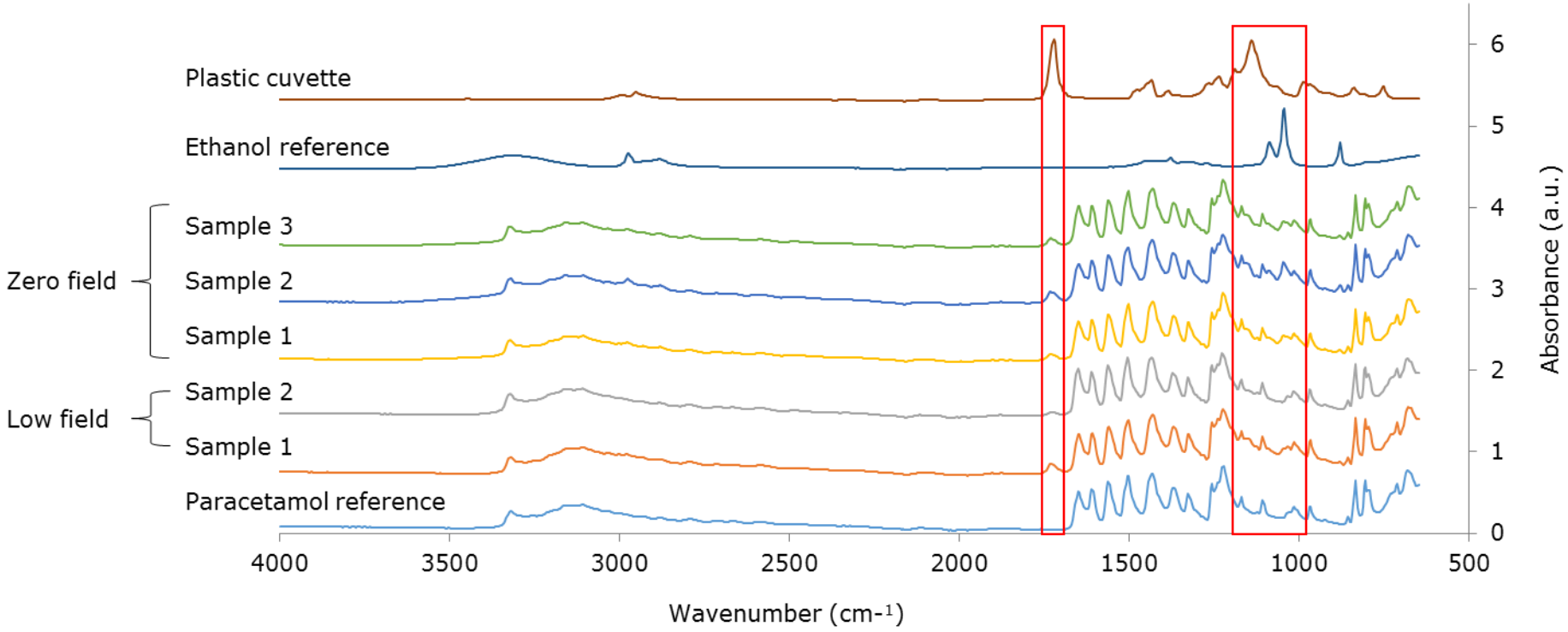

Figure 6-3 FT-IR (ATR) of low field (1 T) and zero field paracetamol samples. Red boxes indicate areas of interest. Spectra have been scaled and offset for presentational purposes.

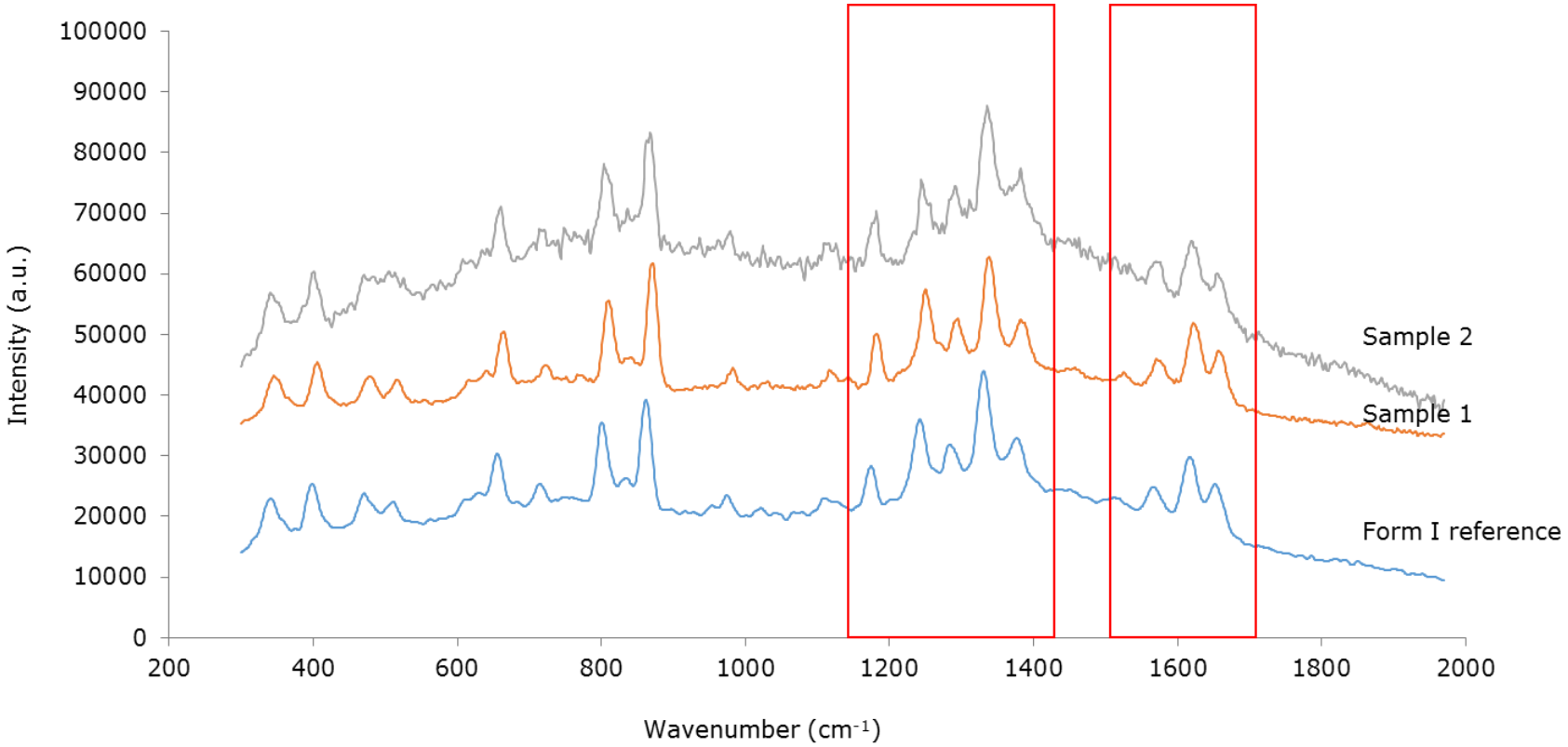

Figure 6-4 Handheld Raman of low field (1 T) paracetamol samples. Red boxes indicate areas of interest. Spectra for sample 1 and 2 have been offset horizontally due to operator calibration error. Spectra have been scaled and offset vertically for presentational purposes.

6.4.3 Low field clotrimazole experiments

FT-IR (ATR) spectra of the samples of clotrimazole formed in low and zero magnetic fields are displayed in Figure 6-5. Both low field and zero field samples produced spectra similar to the clotrimazole reference spectrum, with the exception of an extra peak at 1722 cm^{-1}. This again is attributed to the PMMA cuvettes. Characteristic double peaks at 1481, 1438 and 1082, 1039 cm^{-1} are present along with peaks at 902, 823, 756 and 702 cm^{-1} (Hani et al. 2015).

The handheld Raman spectra of the same samples are displayed in Figure 6-6. Only the low field clotrimazole samples had enough sample to be analysed by the handheld Raman. Both spectra resemble the clotrimazole reference spectrum however they have additional broad peaks at 485, 785 and 1344 cm^{-1} which are attributed to the glass vial used in the handheld Raman. Again, the low field spectra are of lower quality (poor signal: noise) than the clotrimazole reference, this is due to a small sample size.

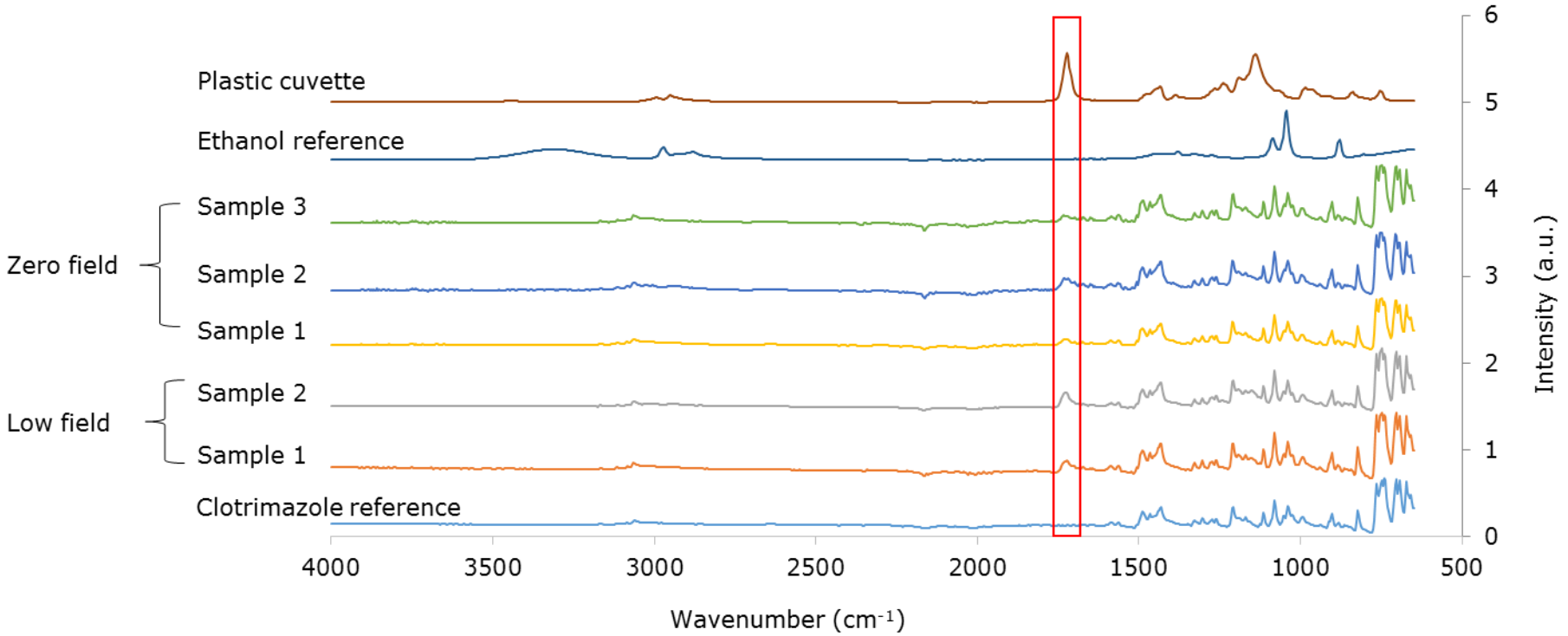

Figure 6-5 FT-IR (ATR) of low field (1 T) and zero field clotrimazole samples. Red boxes indicate areas of interest. Spectra have been scaled and offset for presentational purposes.

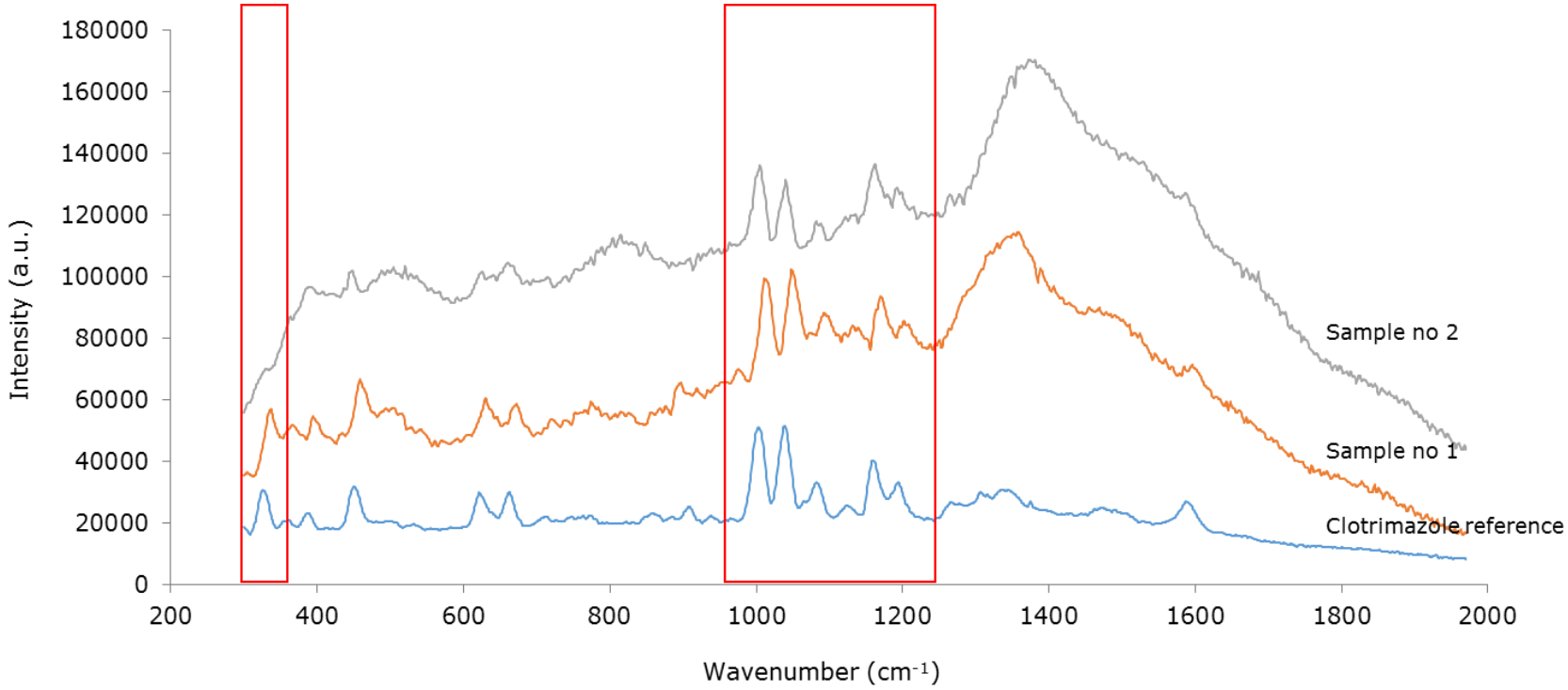

Figure 6-6 Handheld Raman of low field (1 T) clotrimazole samples. Red boxes indicate areas of interest. Spectra for sample 1 has been offset horizontally due to operator calibration error. Spectra have been scaled and offset vertically for presentational purposes.

6.4.4 Low field propranolol experiments

Propranolol samples formed in low and zero field magnetic fields were analysed by FT-IR (ATR). The spectra are displayed in Figure 6-7 along with a spectrum obtained for the propranolol as received from the manufacturer (form II) and a form I propranolol reference. In Figure 6-7 it is observed that an extra peak is present for all the low field and zero field samples at 1722 cm^{-1} which again, is attributed to the PMMA cuvettes.

For clarity, the FT-IR (ATR) spectra have been divided into smaller zoomed sections which are displayed in Figure 6-8, Figure 6-9, and Figure 6-10. The first sub section of the FT-IR (ATR) spectra is between 4000 cm^{-1} and 2000 cm^{-1} (Figure 6-8), and in this range form I propranolol can be determined by its single peak at 3337 cm^{1}, whilst form II has a large peak at 3280 cm^{-1} with two shoulders at 3325 and 3321 cm^{-1}. Propranolol forms I and II are distinguishable over the range of 3400 – 700 cm^{-1} whilst form I and III fingerprint regions have a few subtle differences (Bartolomei et al. 1998). The spectrum for form II propranolol, samples formed in the low field (repeats number 2, 3, 4), and zero field (number 2 and 3) all suggest form II propranolol was formed, as indicated by the peak at 3280 cm^{-1},with two shoulders. However, sample number 1 formed in low field and zero field sample number 1 both have a sharp single peak at 3339 cm^{-1}. The spectrum for the zero field (sample number 1) matches the form I standard, with a large single peak at 2966 cm^{-1} and a more intense triple peak at 2788 cm^{-1}. However, the spectrum for sample 1 formed in low field has a large peak at 2970 cm^{-1} with a less intense double peak at 2791 cm^{-1}, suggesting that form III had been formed (for reference spectra see Figure 3-13). Another subtle difference between form III and form I is the small peak at 3052 cm^{-1} which for form I propranolol is more intense than form III.

In the 1500 to 1300 cm^{-1} section it is observed that form II propranolol reference has a single peak at 1453 cm^{-1} with a sharp peak and shoulder at 1397 cm^{-1}. In comparison, form I and form III both have a peak with a shoulder at 1457 and 1453 cm^{-1} respectively. Form I has a double peak at 1390 and 1375 cm^{-1} whilst form III has a peak with an intense shoulder. Therefore, spectra (numbers 2 - 4) for the samples formed in low field and zero field spectra (numbers 2 and 3) all suggest form II propranolol. The spectrum for sample 1 formed in zero field suggests propranolol form I was produced, whilst low field sample number 1 suggests form III propranolol was produced.

In the 1300 to 1000 cm^{-1} section the form II propranolol reference spectrum has a three peaks at 1177, 1155 and 1140 cm^{-1}, whilst form I and form III have a small peak at 1177 cm^{-1} plus a larger peak with a shoulder. The samples formed in low field (numbers 2 – 4) and zero field (numbers 2 and 3) all have the three peaks, however the third peak on each spectra is a little more intense than the form II reference spectrum which is possibly due to the PMMA cuvette which has an intense peak at 1140 cm^{-1}. The spectra for low field sample 1, and zero field sample 1 both have a small peak and a larger peak with a shoulder rather than three smaller peaks, indicating that they are either form I or III.

Most samples (low field samples 2 to 4 and zero field samples 2 and 3) produced FT-IR (ATR) spectra that suggested form II propranolol had been formed. This was unusual as previously when making standards by evaporation from ethanol all the samples produced form I propranolol (section 3.5.2.3). However, as form II is the as received form and the most stable it is perhaps not unsurprising that it was formed. Bartolomei et al. (1998) report that form II is easily produced by evaporation of solvents for example methanol, propanol, acetone and water, whilst evaporation from 95% aqueous ethanol (at room

temperature) would produce mixtures of I and III, so it is unusual that the low field and zero field samples evaporated from ethanol produced form II here. The formation of form II, when form I or III was expected could be an influence of the magnetic field.

Bartolomei et al (1998) report it is impossible to obtain form III by solvent evaporation and that form III could only be created by solidification of the melt in the presence of an alkali halide matrix. In the experiments in this chapter, the number 1 sample formed in low field produced a spectrum that appears to be consistent with the literature for form III propranolol (Bartolomei et al. 1998). It is therefore possible that the magnetic field encouraged the production of form III during crystallisation. It is possible that propranolol has a stronger magnetic susceptibility than paracetamol. Potticary et al. (2016) crystallised the γ polymorph at 0.8 T whilst at 1 T the β form is crystallised. It is suggested that 1 T is close to a threshold for energetic selection. It is therefore possible that 1 T is close to the energetic threshold required to selectively produce the form III polymorph. However, we can't also rule out that this may also be due to sub-sampling of the sample i.e. it is possible only form III was collected from a mixture of form I and III. Further experiments would need to be conducted to see if the formation of form III propranolol from solution crystallised in magnetic fields could be repeated.

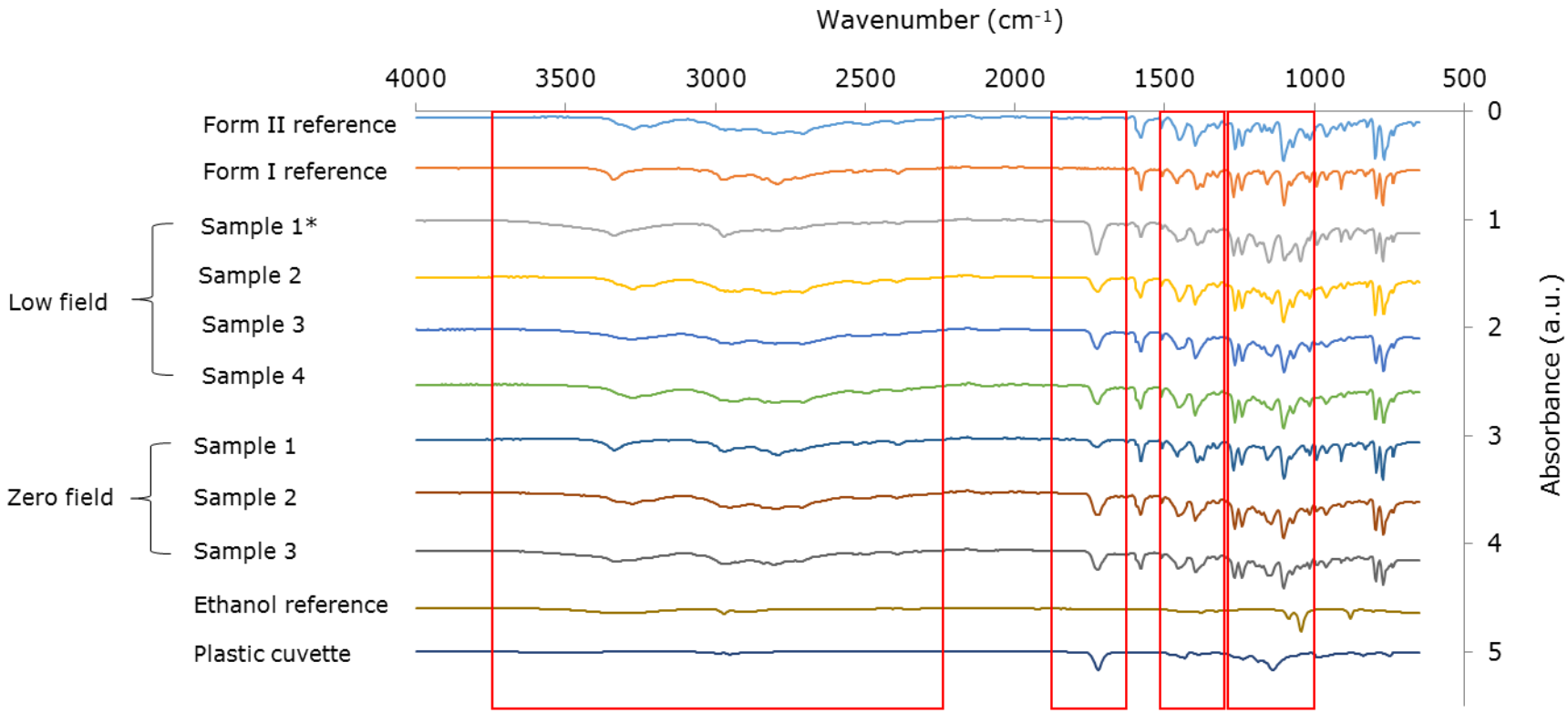

Figure 6-7 FT-IR (ATR) of low field (1 T) and zero field propranolol samples. Red boxes indicate areas of interest. Spectra have been scaled and offset for presentational purposes.* Sample 1, was 1 mL in volume, all other samples were 0.5 mL.

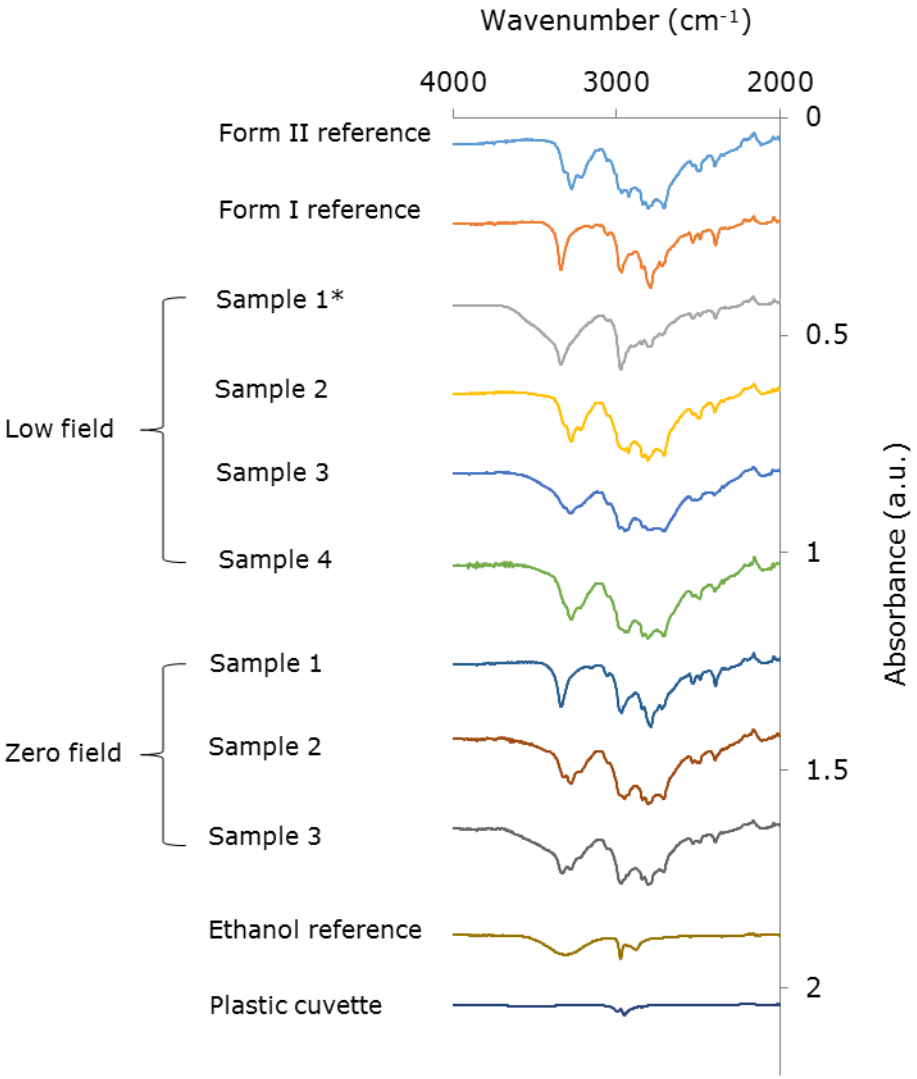

Figure 6-8 FT-IR (ATR) of low field (1 T) and zero field propranolol samples in the 2000 – 4000 cm^{-1} range. Spectra have been scaled and offset for presentational purposes.* Sample 1, was 1 mL in volume, all other samples were 0.5 mL.

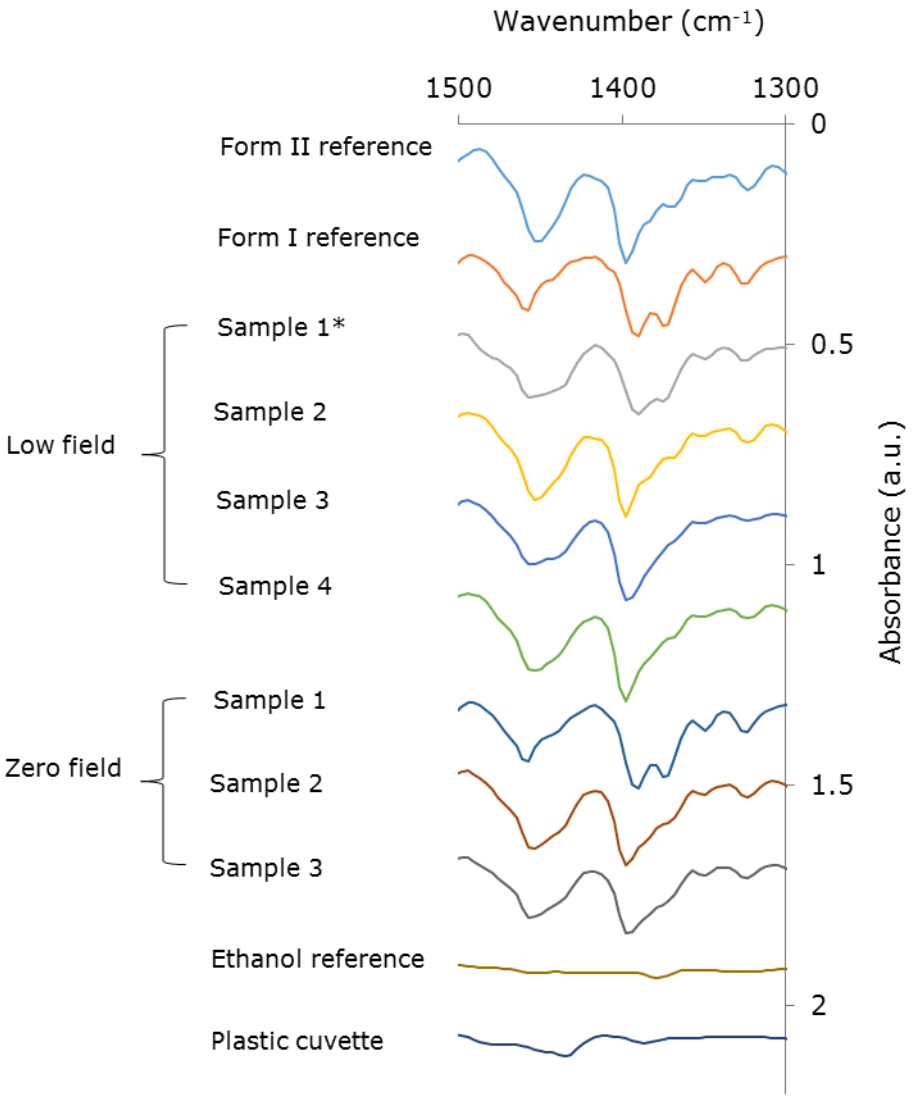

Figure 6-9 FT-IR (ATR) of low field (1 T) and zero field propranolol samples in the 1300 – 1500 cm^{-1} range. Spectra have been scaled and offset for presentational purposes.* Sample 1, was 1 mL in volume, all other samples were 0.5 mL.

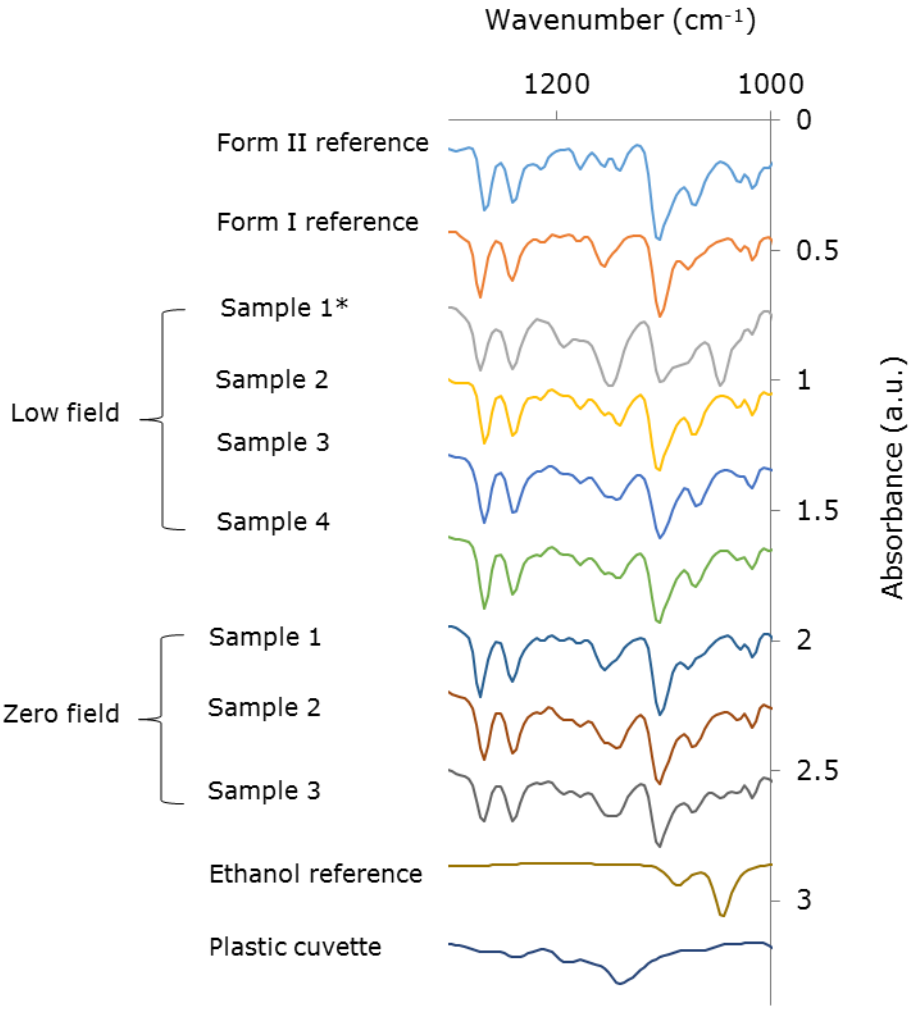

Figure 6-10 FT-IR (ATR) of low field (1 T) and zero field propranolol in the 1000 – 1300 cm^{-1} range. Spectra have been scaled and offset for presentational purposes. .* Sample 1, was 1 mL in volume, all other samples were 0.5 mL.

6.5 Conclusion

The first experiment in this chapter was a repeat of the Potticary et al. (2016) experiment, using our magnetic set up to see if we could reproduce their results. The experiment performed in this chapter produced the γ – polymorph of coronene suggested by the green fluorescence seen under UV light whilst Potticary et al (2016) were able to crystallise the β – polymorph. Difficulties in repeating the

experiment included keeping the temperature of the coronene solution at 93 °C whilst syringe filtering and transporting the solution between labs. It is possible the solution cooled down enough to allow crystallisation of the as received form (γ – polymorph) during transportation. The solution was warmed in the magnet at 93 °C for an hour before starting the experiment to try and overcome the possibility that any coronene had crystallised during transportation.

We crystallised paracetamol in conditions of low and zero magnetic fields, samples from both conditions lead to the formation of form I paracetamol. Form I paracetamol is the most stable polymorph and in high strength magnetic field studies in chapter 4 this polymorph was routinely produced.

Solutions of clotrimazole, which has no polymorphs produced samples in low magnetic fields similar to the clotrimazole reference spectrum. Additional peaks seen in the spectra were attributed to the PMMA from the plastic cuvette.

For propranolol most samples (low field and zero field) produced form II propranolol (the as received polymorph) with the exception of two samples, a low field sample, which produced a spectrum that was more consistent with form III and zero field sample which produced form I. Bartolomei et al. (1998) report that evaporation from aqueous ethanol (at room temperature) would produce a mixture of form I and form III. However, the pure form III could only be crystallised from the melt in the presence of an alkali halide matrix. Although form III can be produced in a mixture with form I, it is possible the magnetic field encouraged the production of form III propranolol. However, it is also possible due to sub sampling that the solution contained both form I and form III crystals and that only the form III were analysed, so further experiments would need to be undertaken.

7 Discussion, conclusion and future perspective

7.1 Summary

The aim of this thesis was to investigate the effect of magnetic fields on pharmaceutical processing and explore the fundamentals of crystallisation using diamagnetic levitation. Research on containerless levitation has mainly focused on the crystallisation of lysozyme (Yin et al. 2008) and other proteins (Okada et al. 2013) for enhanced X-ray crystallography. Benmore and Weber (2011) however, have used acoustic levitation to amorphise pharmaceutical compounds. It was therefore decided to investigate the potential of diamagnetic levitation for containerless crystallisation of pharmaceutical compounds. To enable these studies, the work began in chapter 3 by characterising the starting materials (paracetamol, clotrimazole and propranolol) and creating polymorphs as reference materials. Paracetamol form I, II, III and the amorphous form were successfully created and characterised. As clotrimazole has no reported polymorphs the amorphous form was created as a reference material. Propranolol has three polymorphs, however, only two were created and characterised. The third polymorph is well characterised, so it was possible to compare our results in later chapters to the spectra reported in the literature.

Chapter 4 investigated the potential to levitate pharmaceutical solutions in a containerless fashion. Initial levitation studies were performed with paracetamol, which is a commonly used analgesic and is well characterised. Droplets of paracetamol solution (ethanol/ water) were successfully levitated during initial studies. Different parameters such as droplet volume, paracetamol concentration and solvent were explored. Samples collected from the levitated droplets

predominantly formed form I paracetamol. However, occasionally form II paracetamol was created (as determined by DSC) and the results suggested that form II paracetamol was more likely to crystallise in larger droplets. The magnet set up was optimised to reduce unwanted heterogeneous nucleation which could be caused by particles/ dust in the air. It was hypothesised that dust or particles that fell on the droplet could act as nucleation points biasing the formation of form I paracetamol which readily crystallises from solution. A Perspex box was designed to sit on top of the magnet bore, with an inlet for air/ nitrogen to provide a positive pressure. As earlier results suggested larger droplets were potentially more likely to form form II, experiments with larger droplets with varying concentrations of paracetamol were repeated. Again, form II paracetamol was occasionally formed, however, this proved very difficult to repeatedly reproduce.

In an attempt to encourage the formation of form II paracetamol, two paracetamol droplets were seeded with form II paracetamol. However, when the samples were collected at the end of the experiment, analysis confirmed the formation of form I paracetamol.

The main finding of this chapter was that we could produce crystals of paracetamol using diamagnetic levitation. Form I paracetamol was predominantly formed, however, interestingly we could occasionally produce form II paracetamol. However, as form II paracetamol is less stable than form I it proved difficult to reliably produce. Haisa et al (1974) reported the formation of form II paracetamol by slow evaporation from ethanolic solution, however, this method has not been successfully repeated (Di Martino et al. 1997). More frequently form II paracetamol has been created from the melt of form II or from ethanolic solution when using a seeding technique. Creating form II by the seeding technique is still a challenge by any method

as yield rates are very low and if they crystals are not fully dried then any residual mother solution can induce formation to form I.

In chapter 5 it was decided to further explore the containerless processing capabilities of diamagnetic levitation directly comparing the approach to the work of Benmore and Weber (2011), who were able to levitate and produce amorphous forms of pharmaceutical compounds, such as clotrimazole using acoustic levitation. In their studies during levitation the solution of clotrimazole would evaporate and form a gel, which would be collected and cryogenically frozen to preserve the amorphous form. As clotrimazole formed an amorphous gel upon levitation we decided to use clotrimazole as a direct comparison of the two methods (acoustic and diamagnetic). Benmore and Weber (2011) levitated 4 µL droplets, so we levitated as small droplets as possible for comparison purposes. Difficulties in syringing small (µL) droplets into the magnet bore were experienced, including the droplet remaining attached to the needle, with sudden movement such as flicking causing it to swing into the side of the magnet bore insert. However, small droplets of 0.1 mL were successfully levitated and studied. Droplets were found to produce a crystalline shell, a gel, or a combination of both. This was further explored by levitating medium sized droplets of 0.5 mL. As these droplets were larger it allowed better imaging of the droplet, which interestingly showed the process involved in the formation of small bubbles in the centre of the droplet, which was explored in more detail in later parts of the chapter. Levitation of the droplets usually resulted in a thick outer layer with white parts on the surface. Analysis of the gel and white parts of the droplet by FTIR (ATR) and handheld Raman suggested that the gel was amorphous and the white parts crystalline clotrimazole.

This process was further explored by levitating larger droplets of 3, 4 and 6 mL. The larger droplets also contained bubbles and occasionally

the droplet would form a white clotrimazole outer shell. Further investigations of experimental parameters included investigating the effect of syringe filtering to see if the shell resulted from contaminant particles which collected at the air/ droplet interface or if the observed bubbles were introduced due to filtering. A second parameter explored was the levitation time. In previous experiments in the chapter droplets were levitated overnight, however as they were not taken out at the same time this made comparison difficult. For this reason droplets were levitated for 48 hours and 72 hours. Again, the droplets produced an amorphous gel, with crystalline parts on the surface.

The bubbles seen in most droplets were explored further by inserting a 45 ° mirror into the magnet bore just below the levitating droplet allowing imaging of the droplet from the side (rather than from above). As the droplet evaporated, clotrimazole started to come out of solution and accumulate at the bottom of the droplet, and then also at the top of the droplet. The effect seen is hypothesised to be due to effective gravity – the less dense clotrimazole rises 'up' to the poles of the droplet. When the magnet can no longer levitate all the clotrimazole, it is suggested that it sinks to the bottom and is held in place by surface tension. The droplet then appears to consist of two halves, thought to be a less dense ethanol rich layer on top and a denser clotrimazole gel on the bottom layer. The thick gel layer was observed to continue to grow up the sides of the droplet at the same time as crystallisation of clotrimazole on the surface, until a point at which the ethanol rich layer disappears.

The main finding of this chapter is that clotrimazole solutions could be levitated by diamagnetic levitation, and an amorphous gel produced. These results are similar to the results reported by Benmore and Weber (2011) who used acoustic levitation to amorphise clotrimazole. Interestingly we also observed new

processes occurring during crystallisation by using our mirror and camera set up.

As well as exploring the potential of magnetic fields for containerless processing, the effect of magnetic fields on crystallisation was explored in chapter 6. Several research groups have indicated that low strength magnetic fields could influence crystallisation (Knez and Pohar 2005; Honjo et al. 2008; Potticary et al. 2016). The first part of the chapter explored the potential of magnetic fields to control polymorph formation by comparing our low field method to the method of Potticary et al. (2016). In their experiment they were able to crystallise the β – polymorph of coronene under magnetic fields of 1 T. Following their experimental method, whilst using our magnet set up, crystallisation of coronene unfortunately resulted in the formation of the ubiquitous γ – polymorph. This wasn't perhaps surprising as many difficulties were experienced during our experiments including keeping the solution and glass syringe at 93 °C whilst syringe filtering, and keeping the solution at 93 °C whilst transferring it between labs. The coronene solution had to be transferred between the lab with the fume hood and the magnetic levitation lab in Physics.

The second part of the chapter focused on exploring the effect of low strength magnetic fields on the pharmaceutical compounds studied in the earlier chapters of this thesis; paracetamol, clotrimazole and propranolol. Propranolol was chosen as it has three polymorphs as well as a naphthalene group (two fused benzene rings) in its structure. Coronene consists of six fused benzene rings, and it is hypothesised that the benzene rings in propranolol might make it more magnetically susceptible. The pharmaceutical compounds were crystallised out from ethanol solution in cuvettes placed in the centre of the magnetic field (1 T). Paracetamol was found to crystallise out as form I paracetamol. This is perhaps not surprising as Potticary et

al. (2016) repeated their coronene experiment with pyrene , and they were unable to control the polymorph selection. The authors suggest that pyrene is not as magnetically susceptible as coronene and would likely require higher field strengths for polymorphic selection. It is likely paracetamol isn't as magnetically susceptible as coronene as levitation at higher fields strengths predominantly produced form I. Clotrimazole, which has no polymorphs reported in the literature, when crystallised out under low strength magnetic fields produced spectra closely matching the clotrimazole reference spectra.

However, when solutions of propranolol were crystallised under low strength magnetic fields of 1 T interesting results were obtained. One sample, out of 4, when analysed by FT-IR (ATR) suggested the formation of form III propranolol. The other three low field samples spectra suggested the formation of form II propranolol, which is the most stable form, and the form of the material received from the manufacturer. Bartolomei (1998) reported it was impossible to obtain form III by solvent evaporation and that form III was obtained from the crystallisation of the melt on an alkali halide matrix. It is possible that the low strength magnetic field encouraged the production of form III propranolol. It is possible that propranolol has a stronger magnetic susceptibility than paracetamol. Potticary et al. (2016) found that using magnetic field strengths of 0.8 T produced the γ polymorph whilst slightly higher magnetic field strengths of 1 T produced the new β form. It is suggested that the 1 T is close to an energetic threshold required to selectively produce the β form. It is possible that 1 T is close to the energetic threshold required for propranolol to produce the form III polymorph. However, we can't also rule out that this may also be due to sub sampling of the sample i.e. it is possible only form III was collected from a mixture of form I and III. Further experiments are needed to explore the formation of form III, however, due to time constraints at the end of this project such experiments weren't possible.

7.2 Recommendations for future work

To build upon the work in this thesis further experiments could be undertaken; both in the levitation studies and the low field studies. The further levitation studies can be split into two categories; experimental parameter variation, and sample preparation variation.

The first experimental parameter that could be explored is the levitation time of the droplets. For paracetamol droplets a shorter levitation time could enhance the chances of the formation of form II paracetamol. Nichols and Frampton (1998) report that when examining droplets of saturated paracetamol solutions, which had been seeded with form II paracetamol they noted that the first crystals to grow were form II. However, after 15 mins form I crystals began to grow as the form II crystals dissolved. In our experiments paracetamol droplets were levitated until the droplets fell out of the magnetic trap, however collecting the droplets after a shorter time interval could potentially increase the chances of producing form II.

Again, clotrimazole droplets could also be levitated for much shorter time intervals. Benmore and Weber (2011) only levitated pharmaceutical compounds for 10 to 20 minutes in their acoustic levitator before they became viscous gels. It is possible that by taking the clotrimazole droplet out sooner, that heterogeneous nucleation of clotrimazole on the surface of the droplet would be avoided.

Other experimental parameters that could be explored are the temperature of the bore insert and reducing the pressure within the magnet bore. In the experiments within this thesis the temperature of the bore insert was always set at 20 °C (apart from the coronene experiments). However, increasing or decreasing the temperature could affect the crystallisation of the levitating droplets by encouraging supersaturation.

Future development work could also involve changing sample preparation. In this thesis it is hypothesised that the bubbles seen in the clotrimazole droplets were due to gas coming out of solution. Therefore, solvent could be degassed before use, for example, by using a vacuum pump, or boiling and cooling the water or ethanol before use. As well as experimental investigations a theoretical investigation could be carried out which would involve calculating the levitation positions in the magnet of solutions of varying concentrations, including magnetic, gravitational and buoyancy forces.

Throughout this thesis ethanol was mainly used as the solvent for crystallisation due to preferable solubility (of drugs), magnetic susceptibility and volatility properties (quick evaporation/ crystallisation). Alternative solvents such as agarose gel could be used to explore paracetamol polymorph formation.

Containerless levitation studies could also be carried out on propranolol. Propranolol showed some promise in the low field studies, when form III propranolol was formed in one of the low field experiments. If propranolol is more magnetically susceptible than paracetamol, or clotrimazole then the high strength magnetic fields could potentially encourage the formation of form III.

Other drugs with known polymorphs could be levitated in the high field studies as well as poorly soluble drugs (to try and amorphise). For the low field studies, experimental parameters that could be changed include the magnetic field strength. For example, low strength magnetic fields of 2 and 3 T could be applied during crystallisation from solutions. Repeating the low field propranolol studies would be interesting to see if form III propranolol could be produced.

7.3 Concluding remarks

These studies highlight the potential of diamagnetic levitation to offer a unique approach to investigate crystallisation/ amorphisation of different pharmaceutical drugs in solution. We have been able to show the formation of different polymorphs when pharmaceutical compounds are crystallised from solution under both high and low magnetic fields.

Acoustic levitation has the advantage of being able to levitate very small (μL) droplets, which allows the solution to supersaturate very quickly forming an amorphous gel. However, the size of the droplet is limited to the length of the wavelength used, typically they can only levitate samples with diameters less than half the wavelength (5 mL – 5 μL). An advantage of magnetic levitation is that it can levitate droplets of up to 20 mL in volume, and have greater flexibility to change the environment than acoustic levitation. It would be difficult to scale up magnetic levitation to a processing plant level however, as a research tool it allows investigation of fundamental processes.

With further development this approach could aid with the identification and optimisation of formulation approaches, for currently difficult to formulate compounds.

Bibliography

Al-Dulaimi S, Aina A, Burley J, et al (2010) Rapid polymorph screening on milligram quantities of pharmaceutical material using phonon-mode Raman spectroscopy. CrystEngComm 12:1038–1040

Al-Zoubi N, Kachrimanis K, Malamataris S (2002a) Effects of harvesting and cooling on crystallization and transformation of orthorhombic paracetamol in ethanolic solution. Eur J Pharm Sci 17:13–21

Al-Zoubi N, Koundourellis JE, Malamataris S (2002b) FT-IR and Raman spectroscopic methods for identification and quantitation of orthorombic and monoclinic paracetamol in powder mixes. J Pharm Biomed Anal 29:459–467

Alvarez Fernandez A, Keshavarz M, Christianen PCM, Kouwer PHJ (2015) Maximizing Orientational Order in Polymer-Stabilized Liquid Crystals Using High Magnetic Fields. Macromolecules 48:1002–1008

Ambrus R, Gergely M, Zvonar A, et al (2014) The role of co-spray-drying procedure in the preformulation of intranasal propranolol hydrochloride. Acta Chim Slov 61:601–607

Amidon GL, Lennernas H, Shah VP, Crison JR (1995) A theoretical basis for a biopharmaceutic drug classification: The correlation of in vitro drug product dissolution and in vivo bioavailability. Pharm Res 12:413–420

AMJ N, SM R (2016) Fabrication and Evaluation of Fast Disintegrating Oral Hybrid Films of Propranolol Hydrochloride by Using Pectin and Synthetic Polymers. J Dev Drugs 5:1–9

Ammon HL, Howe DB, Erhardt WD, et al (1977) The crystal structures of dichloroisoproterenol, propranolol and propranolol hydrochloride. Acta Crystallogr Sect B Struct Crystallogr Cryst Chem 33:21–29

Aniket, Gaul DA, Rickard DL, Needham D (2014)

MicroglassificationTM: A novel technique for protein dehydration. J Pharm Sci 103:810–820

Astier JP, Veesler S, Boistelle R (1998) Protein crystals orientation in a magnetic field. Acta Cryst D54:703–706

Atkinson MBJ, Bwambok DK, Chen J, et al (2013) Using magnetic levitation to separate mixtures of crystal polymorphs. Angew Chemie - Int Ed 52:10208–10211

Aulton ME (2002) Pharmaceutics, 2nd edn. Churchill Livingston, Oxford

Baldwin KA, Butler SL, Hill RJA (2015) Artificial tektites: An experimental technique for capturing the shapes of spinning drops. Sci Rep 5:1–5

Bartolomei M, Bertocchi P, Cotta Ramusino M, et al (1999) Physico-chemical characterisation of the modifications I and II of (R,S) propranolol hydrochloride: Solubility and dissolution studies. J Pharm Biomed Anal 21:299–309

Bartolomei M, Bertocchi P, Cotta Ramusino M, Ciranni Signoretti E (1998) Thermal studies on the polymorphic modifications of (R,S) propranolol hydrochloride. Thermochim Acta 321:43–52

Bauer J, Spanton S, Henry R, et al (2001) Ritonavir: An Extraordinary Case of Conformational Polymorphism. Pharm Res 18:859–866

Beasley MM, Bartelink EJ, Taylor L, Miller RM (2014) Comparison of transmission FTIR, ATR, and DRIFT spectra: Implications for assessment of bone bioapatite diagenesis. J Archaeol Sci 46:16–22

Beckmann W, Nickisch K, Budde U (1998) Development of a seeding technique for the crystallization of the metastable a modification of abecarnil. Org Process Res Dev 2:298–304

Benmore CJ, Weber JKR (2011) Amorphization of Molecular Liquids of Pharmaceutical Drugs by Acoustic Levitation. Phys Rev X 1:1–7

Benmore CJ, Weber JKR, Tailor AN, et al (2013) Structural characterization and aging of glassy pharmaceuticals made using

acoustic levitation. J Pharm Sci 102:1290–1300

Berry M V., Geim AK (1997) Of flying frogs and levitrons. Eur J Phys 18:307–313

Bettini R, Bonassi L, Castoro V, et al (2001) Solubility and conversion of carbamazepine polymorphs in supercritical carbon dioxide. Eur J Pharm Sci 13:281–286

Beyer T, Day GM, Price SL (2001) The Prediction, Morphology, and Mechanical Properties of the Polymorphs of Paracetamol - J. Chem. Am. Soc. (ACS Publications). 5086–5094

Bhat SR, Shivakumar HG (2010) Bioadhesive controlled release clotrimazole vaginal tablets. Trop J Pharm Res 9:339–346

Biertümpfel C, Basquin J, Suck D, Sauter C (2002) Crystallization of biological macromolecules using agarose gel. 1657–1659

Bitterfield DL, Utoft A, Needham D (2016) An Activity-Based Dissolution Model for Solute-Containing Microdroplets. Langmuir 32:12749–12759

Black J, Crowther A, Shanks R, et al (1964) A new adrenergic beta-receptor antagonist. Lancet 1:1080–1081

Boldyreva E V. (2003) High-pressure-induced structural changes in molecular crystals preserving the space group symmetry: Anisotropic distortion/isosymmetric polymorphism. Cryst Eng 6:235–254

Borhade V, Pathak S, Sharma S, Patravale V (2012) Clotrimazole nanoemulsion for malaria chemotherapy. Part I: Preformulation studies, formulation design and physicochemical evaluation. Int J Pharm 431:138–148

Brandt EH (1989) Levitation in Physics. Science (80-) 243:349–355

Bredikhin A a., Bredikhina Z a., Gubaidullin AT, et al (2004) Rational approach to a conglomerate-forming propranolol derivative: pointed modifications of the crystal structure. Mendeleev Commun 14:268–270

Brog JP, Chanez CL, Crochet A, Fromm KM (2013) Polymorphism, what it is and how to identify it: A systematic review. RSC Adv

3:16905–16931

Bruylants G, Wouters J, Michaux C (2005) Differential Scanning Calorimetry in Life Science: Thermodynamics, Stability, Molecular Recognition and Application in Drug Design. Curr Med Chem 12:2011–2020

Buanz A, Gurung M, Gaisford S (2019) Crystallisation in printed droplets: understanding crystallisation of d-mannitol polymorphs. CrystEngComm 21:2212–2219

Bumbrah GS, Sharma RM (2016) Raman spectroscopy – Basic principle, instrumentation and selected applications for the characterization of drugs of abuse. Egypt J Forensic Sci 6:209–215

Burger A (1982) Interpretation of investigations into polymorphism [Zur interpretation von polymorphie untersuchungen]. Acta Pharm Technol 28:1–20

Burley JC, Duer MJ, Stein RS, Vrcelj RM (2007) Enforcing Ostwald's rule of stages: Isolation of paracetamol forms III and II. Eur J Pharm Sci 31:271–276

Campeta AM, Chekal BP, Abramov YA, et al (2010) Development of a targeted polymorph screening approach for a complex polymorphic and highly solvating API. J Pharm Sci 99:3874–3886

Cao H-L, Yin D-C, Guo Y-Z, et al (2012) Rapid crystallization from acoustically levitated droplets. J Acoust Soc Am 131:3164–72

Cao HL, Sun LH, Li J, et al (2013) A quality comparison of protein crystals grown under containerless conditions generated by diamagnetic levitation, silicone oil and agarose gel. Acta Crystallogr Sect D Biol Crystallogr 69:1901–1910

Carron K, Cox R (2010) Qualitative Analysis and the Answer Box : A Perspective on Portable Raman Spectroscopy Qualitative Analysis and the Answer Box : A Perspective on Portable Raman Spectroscopy. Anal ChemJ 82:3419–3425

Catherall AT, López-Alcaraz P, Sánchez P, et al (2005) Separation of binary granular mixtures under vibration and differential

magnetic levitation force. Phys Rev E - Stat Nonlinear, Soft Matter Phys 71:1–8

Chaturvedi K, Umadevi S, Vaghani S (2010) Floating matrix dosage form for propranolol hydrochloride based on gas formation technique: Development and in vitro evaluation. Sci Pharm 78:927–939

Chayen J (1983) Polarised light microscopy: principles and practice for the rheumatologist. Ann Rheum Dis 42 Suppl 1:64–7

Chayen NE (1996) A novel technique for containerless protein crystallization. Protein Eng 9:927–929

Chayen NE, Shaw Stewart PD, Blow DM (1992) Microbatch crystallization under oil - a new technique allowing many small-volume crystallization trials. J Cryst Growth 122:176–180

Chung SK, Trinh EH (1998) Containerless protein crystal growth in rotating levitated drops. J Cryst Growth 194:384–397

Clas S, Dalton C, Hancock B (1999) Differential scanning calorimetry: applications in drug development. Pharm Sci Technolo Today 2:311–320

Coleman CB, Gonzalez-Villalobos RA, Allen PL, et al (2007) Diamagnetic Levitation Changes Growth, Cell Cycle, and Gene Expression of Saccharomyces cerevisiae. Biotechnol Bioeng 98:854–863

Correa-duarte MA, Grzelczak M, Giersig M, et al (2005) Alignment of Carbon Nanotubes under Low Magnetic Fields through Attachment of Magnetic Nanoparticles. 19060–19063

Cristini-Robbe O, Ruyffelaere F, Dubart F, et al (2013) Local Drug Delivery Strategy for Cancer Treatment: Use of Biocompatible Sol-Gel-Derived Porous Materials. New J Glas Ceram 3:74–79

Das RS, Agrawal YK (2011) Raman spectroscopy: Recent advancements, techniques and applications. Vib Spectrosc 57:163–176

Davey RJ, Garside J (2000) From Molecules to Crystallizers: An Introduction to Crystallization, 1st edn. Oxford University Press,

Oxford

de Veij M, Vandenabeele P, Alter Hall K, et al (2007) Fast detection and identification of counterfeit antimalarial tablets by Raman spectroscopy. J Raman Spectrosc 38:181–187

Delmas T, Shah U V., Roberts MM, et al (2013) Crystallisation of the orthorhombic form of acetaminophen: Combined effect of surface topography and chemistry. Powder Technol 236:24–29

DeLucas L, Moore K, Long M, et al (2002) Protein crystal growth in space, past and future. J Cryst Growth 239:1646–1650

Di Martino P, Conflant P, Drache M, et al (1997) Preparation and Physical Characterization of Forms II and III of Paracetamol. J Therm Anal 48:447–458

Di Martino P, Guyot-Hermann A-M, Conflant P, et al (1996) A new pure paracetamol for direct compression: the orthorhombic form. Int J Pharm 128:1–8

di Martino P, Palmieri GF, Martelli S (2000) Molecular mobility of the paracetamol amorphous form. Chem Pharm Bull (Tokyo) 48:1105–1108

Dijkstra CE, Larkin OJ, Anthony P, et al (2011) Diamagnetic levitation enhances growth of liquid bacterial cultures by increasing oxygen availability. J R Soc Interface 8:334–44

Doran PM (2013) Bioprocess Engineering principles. Elsevier, London

Ehmann HMA, Zimmer A, Roblegg E, Werzer O (2014) Morphologies in solvent-annealed clotrimazole thin films explained by hansen-solubility parameters. Cryst Growth Des 14:1386–1391

El-Zhry El-Yafi AK, El-Zein H (2014) Technical crystallization for application in pharmaceutical material engineering: Review article. Asian J Pharm Sci 10:283–291

Espeau P, Céolin R, Tamarit JL, et al (2005) Polymorphism of paracetamol: Relative stabilities of the monoclinic and orthorhombic phases inferred from topological pressure-temperature and temperature-volume phase diagrams. J Pharm Sci 94:524–539

Fachaux JM, Guyot-Hermann AM, Guyot JC, et al (1995a) Pure Paracetamol for direct compression Part I. Development of sintered-like crystals of Paracetamol. Powder Technol 82:123–128

Fachaux JM, Guyot-Hermann AM, Guyot JC, et al (1995b) Pure Paracetamol for direct compression Part II. Study of the physicochemical and mechanical properties of sintered-like crystals of Paracetamol. Powder Technol 82:129–133

Farca A, Iacoviə C, Vineler E, et al (2016) The Influence of Molecular Structure Modifications on Vibrational Properties of Some Beta Blockers: A Combined Raman and DFT Study. J Spectrosc 2016:

Feynman RP, Leighton RB, Sands M (2010) The Feynman Lectures On Physics, Vol. II: The New Millenium Edition: Mainly Electromagnetism and Matter, New Millen. Basic Books, New York

Franklin S, Balasubramanian T, Nehru K, Kim Y (2009) Crystal structure, conformation, vibration and optical band gap analysis of bis[rac-propranolol nitrate]. J Mol Struct 927:121–125

Fukuyama M, Akiyama A, Harada M, et al (2015) Microfluidic protein crystallisation controlled using spontaneous emulsification. Anal Methods 7:7128–7131

Gaisford S, Buanz ABM, Jethwa N (2010) Characterisation of paracetamol form III with rapid-heating DSC. J Pharm Biomed Anal 53:366–370

Galkin O, Vekilov PG (2000) Are nucleation kinetics of protein crystals similar to those of liquid droplets? J Am Chem Soc 122:156–163

Garćıa-Ruiz J., Novella M., Moreno R, Gavira J. (2001) Agarose as crystallization media for proteins. J Cryst Growth 232:165–172

Garekani HA, Ford JL, Rubinstein MH, Rajabi-Siahboomi AR (2000) Highly compressible paracetamol: I: Crystallization and characterization. Int J Pharm 208:87–99

Gavira JA, Garcı JM (2009) Effects of a Magnetic Field on Lysozyme Crystal Nucleation and Growth in a Diffusive Environment & DESIGN 2009. 5–10

Geim A (1998) Everyone's Magnetism. Phys Today 51:36

Gill P, Moghadam TT, Ranjbar B (2010) Differential scanning calorimetry techniques: applications in biology and nanoscience. J Biomol Tech 21:167–93

Glassford SE, Byrne B, Kazarian SG (2013) Recent applications of ATR FTIR spectroscopy and imaging to proteins. Biochim Biophys Acta - Proteins Proteomics 1834:2849–2858

Goh L, Chen K, Bhamidi V, et al (2010) A stochastic model for nucleation kinetics determination in droplet-based microfluidic systems. Cryst Growth Des 10:2515–2521

Greaves GN, Wilding MC, Fearn S, et al (2008) Detection of first-order liquid/liquid phase transitions in yttrium oxide-aluminum oxide melts. Science (80-) 322:566–570

Gupta NV, Natasha S, Getyala A, Bhat RS (2013) Bioadhesive vaginal tablets containing spray dried microspheres loaded with clotrimazole for treatment of vaginal Candidiasis. Acta Pharm 63:359–372

Haisa BYM, Kashino S, Maeda H (1974) The Orthorhombic Form of p-Hydroxyacetanilide. Acta Crystallogr Sect B 30:2510–2512

Haisa M, Kashino S, Kawai R, Maeda H (1976) The Monoclinic Form of p- Hydroxyacetanilide. Acta Cryst 58:1283–1285

Hajjou M, Qin Y, Bradby S, et al (2013) Assessment of the performance of a handheld Raman device for potential use as a screening tool in evaluating medicines quality. J Pharm Biomed Anal 74:47–55

Hani U, Krishna G, Shivakumar HG (2015) Design and optimization of clotrimazole-hydroxypropyl-β-cyclodextrin bioadhesive vaginal tablets using Anacardium occidentale gum by 3^2 factorial design. RSC Adv 5:35391–35404

Harris DC (2010) Quantitative Chemical Analysis: International Edition, 8th edn. Freeman, New York

Hasebes T, Watanabe K, Jikiharas K, et al (1996) 11 T liquid helium-free superconducting magnet. Cryogenics (Guildf) 36:1019–

1025

Haynes. W.M. (ed.) (2014) Handbook of Chemistry and Physics, 95th edn. CRC Press LLC

Hendriksen BA, Grant DJW, Meenan P, Green DA (1998) Crystallisation of paracetamol (acetaminophen) in the presence of structurally related substances. J Cryst Growth 183:629–640

Hennet L, Cristiglio V, Kozaily J, et al (2011) Aerodynamic levitation and laser heating: Applications at synchrotron and neutron sources. Eur Phys J Spec Top 196:151–165

Herranz R, Larkin OJ, Dijkstra CE, et al (2012) Microgravity simulation by diamagnetic levitation: effects of a strong gradient magnetic field on the transcriptional profile of Drosophila melanogaster. BMC Genomics 13:1–13

Hill RJA, Eaves L (2010) Vibrations of a diamagnetically levitated water droplet. Phys Rev E 81:56312

Hill RJA, Larkin OJ, Dijkstra CE, et al (2012) Effect of magnetically simulated zero-gravity and enhanced gravity on the walk of the common fruitfly. J R Soc Interface 9:1438–1449

Hill RJA, Sedman VL, Allen S, et al (2007) Alignment of aromatic peptide tubes in strong magnetic fields. Adv Mater 19:4474–4479

Hind AR, Bhargava SK, McKinnon A (2001) At the solid liquid interface: FTIR -ATR the tool of choice. 93:91–114

Hirose R, Hayashi S, Watanabe Y, et al (2007) Development of a Superconducting Magnet for High Magnetic Force Field Application. 17:2299–2302

Honjo S, Yokota M, Doki N, Shimizu K (2008) Magnetic field influence on the crystal structure of 2,2’:6’,2"-terpyridine. Kagaku Kogaku Ronbun 34:383–387

Huy NT, Kamei K, Yamamoto T, et al (2002) Clotrimazole binds to heme and enhances heme-dependent hemolysis: Proposed antimalarial mechanism of clotrimazole. J Biol Chem 277:4152–4158

Iacovacci V, Lucarini G, Ricotti L, Menciassi A (2016) Magnetic Field-Based Technologies for Lab-on-a-Chip Applications. Lab-on-a-Chip Fabr Appl. https://doi.org/10.5772/62865

Ivanova BB (2005) Monoclinic and orthorhombic polymorphs of paracetamol - Solid state linear dichroic infrared spectral analysis. J Mol Struct 738:233–238

Joiris E, Di Martino P, Berneron C, et al (1998) Compression Behavior of Orthorhombic Paracetamol. Pharm Res 15:1122–1130

Karolewicz B, Gajda M, Owczarek A, et al (2014) Physicochemical Characterization and Dissolution Studies of Solid Dispersions of Clotrimazole with Pluronic F127. Trop J Pharm Res 13:1225

Karthika S, Radhakrishnan TK, Kalaichelvi P (2016) A Review of Classical and Nonclassical Nucleation Theories. Cryst Growth Des 16:6663–6681

Kauffman JF, Batykefer LM, Tuschel DD (2008) Raman detected differential scanning calorimetry of polymorphic transformations in acetaminophen. J Pharm Biomed Anal 48:1310–1315

Kawakami K (2009) Current Status of Amorphous Formulation and Other Special Dosage Forms as Formulations for Early Clinical Phases. J Pharm Sci 98:2875–2885

Kimura T, Ago H, Tobita M, et al (2002) Polymer Composites of Carbon Nanotubes. Adv Mater 1380–1383

Kinoshita K, Parra E, Hussein A, et al (2016) From single microparticles to microfluidic emulsification: Fundamental properties (solubility, density, phase separation) from micropipette manipulation of solvent, drug and polymer microspheres. Processes 4:

Kinoshita T, Warizaya M, Neya M (2003) Improving quality and harvest period of protein crystals for structure-based drug design : effects of a gel and a magnetic field on bovine adenosine deaminase crystals. Acta Crystallogr Sect D Biol Crystallogr D59:1333–1335

Knez S, Pohar C (2005) The magnetic field influence on the

polymorph composition of $CaCO_3$ precipitated from carbonized aqueous solutions. 281:377–388

Knight RD (2008) Physics for Scientists and Engineers: A Strategic Approach, 2nd edn. Pearson, San Francisco

Knopp MM, Löbmann K, Elder DP, et al (2016) Recent advances and potential applications of modulated differential scanning calorimetry (mDSC) in drug development. Eur J Pharm Sci 87:164–173

Kodre K, Attarde S, Yendhe P, et al (2014) Differential Scanning Calorimetry: A Review. Res Rev J Pharm Anal 3:11–22

Koike-Tani M, Tani T, Mehta SB, et al (2015) Polarized light microscopy in reproductive and developmental biology. Mol Reprod Dev 82:548–562

Kolesov BA, Mikhailenko MA, Boldyreva E V (2011) Dynamics of the intermolecular hydrogen bonds in the polymorphs of paracetamol in relation to crystal packing and conformational transitions: a variable-temperature polarized Raman spectroscopy study. Phys Chem Chem Phys Phys Chem Chem Phys 13:14243–14253

Kudelski A (2008) Analytical applications of Raman spectroscopy. Talanta 76:1–8

Kuil ME, Rene E, Hoedemaeker FJ, Pieter J (2002) Protein nano-crystallogenesis. Enzyme Microb Technol 30:262–265

Lee AY, Erdemir D, Myerson AS (2011) Crystal Polymorphism in Chemical Process Development. Annu Rev Chem Biomol Eng 2:259–280

Lee EH (2014) A practical guide to pharmaceutical polymorph screening & selection. Asian J Pharm Sci 9:163–175

Leiterer J, Delißen F, Emmerling F, et al (2008) Structure analysis using acoustically levitated droplets. Anal Bioanal Chem 391:1221–1228

Leng J, Salmon JB (2009) Microfluidic crystallization. Lab Chip 9:24–34

Liao L, Hill RJA (2017) Shapes and Fissility of Highly Charged and

Rapidly Rotating Levitated Liquid Drops. Phys Rev Lett 119:114501

Lin SX, Zhou M, Azzi A, et al (2000) Magnet used for protein crystallization: novel attempts to improve the crystal quality. Biochem Biophys Res Commun 275:274–278

Littke W, John C (1984) Protein single crystal growth under microgravity. Science (80-) 225:203+

Lorber B (2002) The crystallization of biological macromolecules under microgravity: A way to more accurate three-dimensional structures? Biochim Biophys Acta - Proteins Proteomics 1599:1–8

Lorber B, Giegé R (1996) Containerless protein crystallization in floating drops: Application to crystal growth monitoring under reduced nucleation conditions. J Cryst Growth 168:204–215

Lorber B, Sauter C, Ng JD, et al (1999) Characterization of protein and virus crystals by quasi-planar wave X-ray topography: A comparison between crystals grown in solution and in agarose gel. J Cryst Growth 204:357–368

Łuczak A, Jallo LJ, Dave RN, Iqbal Z (2013) Polymorph stabilization in processed acetaminophen powders. Powder Technol 236:52–62

Madgulkar A, Bandivadekar M, Shid T, Rao S (2016) Sugars as solid dispersion carrier to improve solubility and dissolution of the BCS class II drug: Clotrimazole. Drug Dev Ind Pharm 42:28–38

Maki S, Oda Y, Ataka M (2004) High-quality crystallization of lysozyme by magneto-Archimedes levitation in a superconducting magnet. J Cryst Growth 261:557–565

Matheys C, Tumanova N, Leyssens T, Myerson AS (2016) Magnetic levitation as a tool for separation: Separating cocrystals from crystalline phases of individual compounds. Cryst Growth Des 16:5549–5553

Meka VS, Dharmanlingam SR, Kolapalli VRM (2014) Formulation of gastroretentive floating drug delivery system using hydrophilic

polymers and its in vitro characterization. Brazilian J Pharm Sci 50:431–439

Meka VS, Nali SR, Songa AS, et al (2012) Statistical optimization of a novel excipient (CMEC) based gastro retentive floating tablets of propranolol HCl and it's in vivo buoyancy characterization in healthy human volunteers. DARU, J Pharm Sci 20:1–12

Micali N, Engelkamp H, van Rhee PG, et al (2012) Selection of supramolecular chirality by application of rotational and magnetic forces. Nat Chem 4:201–207

Mirica K a, Shevkoplyas SS, Phillips ST, et al (2009) Measuring Densities of Solids and Liquids Using Magnetic Levitation : Fundamentals. 10049–10058

Mirica KA, Phillips ST, MacE CR, Whitesides GM (2010) Magnetic levitation in the analysis of foods and water. J Agric Food Chem 58:6565–6569

Mittapalli S, Mannava MKC, Khandavilli UBR, et al (2015) Soluble salts and cocrystals of clotrimazole. Cryst Growth Des 15:2493–2504

Morissette SL, Almarsson Ö, Peterson ML, et al (2004) High-throughput crystallization: Polymorphs, salts, co-crystals and solvates of pharmaceutical solids. Adv Drug Deliv Rev 56:275–300

Motokawa M, Hamai M, Sato T, et al (2001) Crystal growth and materials processing in the magnetic levitation condition. J Magn Magn Mater 226–230:2090–2093

Moynihan HA, O'Hare IP (2002) Spectroscopic characterisation of the monoclinic and orthorhombic forms of paracetamol. Int J Pharm 247:179–185

Murray BJ, Broadley SL, Wilson TW, et al (2010) Kinetics of the homogeneous freezing of water. Phys Chem Chem Phys 12:10380–10387

Myerson AS (2002) Handbook of Industrial Crystallization. Handb. Ind. Cryst.

Nakamura A, Ohtsuka J, Miyazono K-I, et al (2012) Improvement in

quality of protein crystals grown in a high magnetic field gradient. Cryst Growth Des 12:1141–1150

Nanubolu JB, Burley JC (2012) Investigating the recrystallisation behaviour of amorphous paracetamol by variable temperature Raman studies and surface Raman mapping . Mol Pharm 9:1544–1558

Nichols G, Frampton CS (1998) Physicochemical Characterization of the Orthorhombic Polymorph of Paracetamol Crystallized from Solution. 87:

Numoto N, Shimizu K, Matsumoto K, et al (2013) Observation of the orientation of membrane protein crystals grown in high magnetic force fields. J Cryst Growth 367:53–56

O.M.M. S, M.E.D. R, J.T. J, et al (2014) Polymorphism: An evaluation of the potential risk to the quality of drug products from the Farmacia Popular Rede Propria. Brazilian J Pharm Sci 50:1–24

O'Neill MJ (1966) Measurement of specific heat functions by differential scanning calorimetry (DSC). Anal Chem 38:1331–1336

Okada H, Hirota N, Matsumoto S, Wada H (2013) Development of a Protein Crystal Formation System With a Superconducting Magnet. IEEE Trans Appl Supercond 23:

Oran WA, Berge LH (1982) Containerless melting and solidification of materials with an aerodynamic levitation system. Rev Sci Instrum 53:851–853

Otsuka M, Hasegawa H, Matsuda Y (1999) Effect of Polymorphic Forms of Bulk Powders on Pharmaceutical Properties of Carbamazepine Granules. Chem Pharm Bull 47:852–856

Patel P, Bhatt KK (2012) Development and Validation of HPTLC Method for Estimation of Propranolol Hydrochloride and Flunarizine Dihydrochloride in Combined Dosage Form. ISRN Anal Chem 2012:1–6

Perlovich GL, Volkova T V, Bauer-Brandl A (2007) Polymorphism of Paracetamol: Relative Stability of the Monoclinic and

Orthorhombic Phase revisited By Sublimation and Solution Calorimetry. J Therm Anal Calorim 89:767–774

Perrin M-A, Neumann MA, Elmaleh H, Zaske L (2009) Crystal structure determination of the elusive paracetamol Form III. Chem Commun 3181

Polenske D, Lorenz H, Seidel-Morgenstern A (2010) The Binary Phase Diagram of Propranolol Hydrochloride and Crystallization-Based Enantioseparation. J Pharm Sci 99:1762–1773

Potticary J, Terry LR, Bell C, et al (2016) An unforeseen polymorph of coronene by the application of magnetic fields during crystal growth. Nat Commun 7:11555

Price DL (2010) High-Temperature Levitated Materials. Cambridge University Press, Cambridge

Puskar L, Tuckermann R, Frosch T, et al (2007) Raman acoustic levitation spectroscopy of red blood cells and Plasmodium falciparum trophozoites. Lab Chip 7:1125–1131

Qi S, Avalle P, Saklatvala R, Craig DQM (2008) An investigation into the effects of thermal history on the crystallisation behaviour of amorphous paracetamol. Eur J Pharm Biopharm 69:364–371

Quilaqueo M, Aguilera JM (2016) Crystallization of NaCl by fast evaporation of water in droplets of NaCl solutions. Food Res Int 84:143–149

Ragnarsson G, Sjogren J (1984) Compressibility and tablet properties of two polymorphs of metoprolol tartrate. Acta Pharm Suec 21:321–330

Rautio J, Kumpulainen H, Heimbach T, et al (2008) Prodrugs: Design and clinical applications. Nat Rev Drug Discov 7:255–270

Rehder S, Wu JX, Laackmann J, et al (2013) A case study of real-time monitoring of solid-state phase transformations in acoustically levitated particles using near infrared and Raman spectroscopy. Eur J Pharm Sci 48:97–103

Reutzel-Edens SM, Bush JK, Magee PA, et al (2003) Anhydrates and Hydrates of Olanzapine: Crystallization, Solid-State

Characterization, and Structural Relationships. Cryst Growth Des 3:897–907

Rickard DL, Duncan PB, Needham D (2010) Hydration potential of lysozyme: Protein dehydration using a single microparticle technique. Biophys J 98:1075–1084

Roberts RJ, Payne RS, Rowe RC (2000) Mechanical property predictions for polymorphs of sulphathiazole and carbamazepine. Eur J Pharm Sci 9:277–283

Rossi A, Savioli A, Bini M, et al (2003) Solid-state characterization of paracetamol metastable polymorphs formed in binary mixtures with hydroxypropylmethylcellulose. Thermochim Acta 406:55–67

Rostron P, Gaber S, Gaber D (2016) Raman Spectroscopy , Review. 0869:50–64

Roy S, Aitipamula S, Nangia A (2005) Thermochemical analysis of venlafaxine hydrochloride polymorphs 1-5. Cryst Growth Des 5:2268–2276

Rustichelli C, Gamberini G, Ferioli V, et al (2000) Solid-state study of polymorphic drugs: Carbamazepine. J Pharm Biomed Anal 23:41–54

Sakurazawa S, Kubota T, Ataka M (1999) Orientation of protein crystals grown in a magnetic field. 196:325–331

Saliba KJ, Kirk K (1998) Clotrimazole inhibits the growth of Plasmodium falciparum in vitro. Trans R Soc Trop Med Hyg 92:666–667

Santesson S, Cedergren-Zeppezauer ES, Johansson T, et al (2003) Screening of nucleation conditions using levitated drops for protein crystallization. Anal Chem 75:1733–1740

Sato T, Yamada Y, Saijo S, et al (2000) Enhancement in the perfection of orthorhombic lysozyme crystals grown in a high magnetic field (10 T). Acta Crystallogr Sect D Biol Crystallogr 56:1079–1083

Sauter C, Lorber B, Giegé R (2002) Towards atomic resolution with crystals grown in gel: The case of thaumatin seen at room

temperature. Proteins Struct Funct Genet 48:146–150

Sazaki G, Komatsu H, Nakada T, et al (1997) Effects of a magnetic field on the nucleation and growth of protein crystals. 8:8–11

Schmitt J, Flemming H-C (1998) FTIR-spectroscopy in microbial and material analysis. Int Biodeterior Biodegradation 41:1–11

Sica F, Demasi D, Mazzarella L, et al (1994) Elimination of twinning in crystals of Sulfolobus sofataricus alcohol dehydrogenase holo-enzyme by growth in agarose gels. Acta Crystallogr Sect D Biol Crystallogr 50:508–511

Singhal D, Curatolo W (2004) Drug polymorphism and dosage form design: A practical perspective. Adv Drug Deliv Rev 56:335–347

Smith SJ, Bishop MM, Montgomery JM, et al (2014) Polymorphism in paracetamol: Evidence of additional forms IV and v at high pressure. J Phys Chem A 118:6068–6077

Sohn YT (1990) Study on the Polymorphism of Acetaminophen. J Korean Pharm Sci 20:97–104

Song H, Chen DL, Ismagilov RF (2006) Reactions in droplets in microfluidic channels. Angew Chemie - Int Ed 45:7336–7356

Song H, Shin HS (1998) The antifungal drug clotrimazole. Acta Crystallogr Sect C Cryst Struct Commun 54:1675–1677

Stepanovs D, Jure M, Yanichev A, et al (2015) Molecular salts of propranolol with dicarboxylic acids: Diversity of stoichiometry, supramolecular structures and physicochemical properties. Cryst Eng Comm 17:9023–9028

Stephens CJ, Kim YY, Evans SD, et al (2011) Early stages of crystallization of calcium carbonate revealed in picoliter droplets. J Am Chem Soc 133:5210–5213

Stopin A, Rossignon A, Keshavarz M, et al (2016) Polarization of soft materials through magnetic alignment of polymeric organogels under low-field conditions. Chem Mater 28:6985–6994

Sturtevant JM (1987) Biochemical applications of differential scanning calorimetry. Annu Rev Phys Chem 38:463–488

Sun CC, Grant DJW (2001) Influence of crystal structure on the

tableting properties of sulfamerazine polymorphs. Pharm Res 18:274–280

Sun Y, Xi H, Chen S, et al (2008) Crystallization near glass transition: Transition from diffusion-controlled to diffusionless crystal growth studied with seven polymorphs. J Phys Chem B 112:5594–5601

Tagami M, Hamai M, Mogi I, et al (1999) Solidification of levitating water in a gradient strong magnetic field. J Cryst Growth 203:594–598

Takahashi K, Mogi I, Awaji S, et al (2006) Containerless melting and crystallization of diamagnetic organic materials under magnetic levitation condition. J Phys Conf Ser 51:450–453

Taneri F, Güneri T, Aigner Z, et al (2004) Thermoanalytical studies on complexes of clotrimazole with cyclodextrins. J Therm Anal Calorim 76:471–479

Tangeman JA, Phillips BL, Navrotsky A, et al (2001) Vitreous forsterite (Mg2SiO4): Synthesis, structure, and thermochemistry. Geophys Res Lett 28:2517–2520

Teshima Y, Maeki M, Yamashita K, Miyazaki M (2013) A method for generating a metastable crystal in a microdroplet. CrystEngComm 15:9874–9877

Thakuria R, Nangia A (2011) Polymorphic form IV of olanzapine. Acta Crystallogr Sect C Cryst Struct Commun 67:461–463

Thomas LH, Wales C, Zhao L, Wilson CC (2011) Paracetamol form II: An elusive polymorph through facile multicomponent crystallization routes. Cryst Growth Des 11:1450–1452

Todica M (2008) Observation of hydration - Drying effect on clotrimazole - Carbopol system. Chinese Phys Lett 25:2674–2676

Tonglairoum P, Ngawhirunpat T, Rojanarata T, et al (2014) Fast-acting clotrimazole composited PVP/HPβCD nanofibers for oral candidiasis application. Pharm Res 31:1893–1906

Tonglairoum P, Ngawhirunpat T, Rojanarata T, et al (2015a) Fabrication of a novel scaffold of clotrimazole-microemulsion-

containing nanofibers using an electrospinning process for oral candidiasis applications. Colloids Surfaces B Biointerfaces 126:18–25

Tonglairoum P, Ngawhirunpat T, Rojanarata T, et al (2015b) Fabrication of mucoadhesive chitosan coated polyvinylpyrrolidone/cyclodextrin/clotrimazole sandwich patches for oral candidiasis. Carbohydr Polym 132:173–179

Torbet J, Freyssinet JM, Hudry-Clergeon G (1981) Oriented fibrin gels formed by polymerization in strong magnetic fields. Nature 289:91–93

Trasi NS, Taylor LS (2012) Effect of polymers on nucleation and crystal growth of amorphous acetaminophen. CrystEngComm 14:5188

Tseng H, Balaoing LR, Grigoryan B, et al (2014) A three-dimensional co-culture model of the aortic valve using magnetic levitation. Acta Biomater 10:173–182

Tu J, Chin K, Chou S (2007) The crystallization of apo-form UMP kinase from Xanthomonas campestris is significantly improved in a strong magnetic field crystallization communications. Acta Crystallogr Sect F Struct Biol Cryst Commun 1936:438–442

Utoft A, Kinoshita K, Bitterfield DL, Needham D (2018) Manipulating Single Microdroplets of NaCl Solutions: Solvent Dissolution, Microcrystallization, and Crystal Morphology. Langmuir 34:3626–3641

van der Asdonk P, Keshavarz M, Christianen PCM, Kouwer PHJ (2016) Directed peptide amphiphile assembly using aqueous liquid crystal templates in magnetic fields. Soft Matter 12:6518–6525

van Dooren AA, Müller BW (1984) Purity determinations of drugs with differential scanning calorimetry (DSC)-a critical review. Int J Pharm 20:217–233

Venkata Srikanth M, Sreenivasa Rao N, Ambedkar Sunil S, et al (2012) Statistical design and evaluation of a propranolol HCl gastric floating tablet. Acta Pharm Sin B 2:60–69

Vidal O, Robert MC, Arnoux B, Capelle B (1999) Crystalline quality of lysozyme crystals grown in agarose and silica gels studied by X-ray diffraction techniques. J Cryst Growth 196:559–571

Viera I, Gómez MA, Ellena J, et al (2009) Synthesis, structural characterization and ex vivo biological properties of a new complex [Cu(propranolol)2]·2H2O, a potential beta-blocker. Polyhedron 28:3647–3653

Wada H, Hirota N, Matsumoto S, Okada H (2012) Application of High-Field Superconducting Magnet to Protein Crystallization. 36:953–957

Watson DG (2005) Pharmacetuical Analysis: A Textbook for Pharmacy Students and Pharmaceutical Chemists, 2nd edn. Elsevier Churchill Livingstone, Edinburgh

Weber JKR, Benmore CJ, Suthar KJ, et al (2017) Using containerless methods to develop amorphous pharmaceuticals. Biochim Biophys Acta - Gen Subj 1861:3686–3692

Weber JKR, Benmore CJ, Tailor AN, et al (2013) A neutron-X-ray, NMR and calorimetric study of glassy Probucol synthesized using containerless techniques. Chem Phys 424:89–92

Weber JKR, Rey CA, Neuefeind J, Benmore CJ (2009) Acoustic levitator for structure measurements on low temperature liquid droplets. Rev Sci Instrum 80:

Weber RJK, Benmore CJ, Tumber SK, et al (2012) Acoustic levitation: Recent developments and emerging opportunities in biomaterials research. Eur Biophys J 41:397–403

Willart JF, Descamps M (2008) Solid state amorphization of pharmaceuticals. Mol Pharm 5:905–920

Witkowski MR (2005) The use of Raman spectroscopy in the detection of counterfeit and adulterated pharmaceutical products. Am Pharm Rev 8:56–62

Woensdregt CF (1993) Hartman-Perdok theory: Influence of crystal structure and crystalline interface on crystal growth. Faraday Discuss 95:97–107

Yamato M, Nakazawa H, Kimura T (2002) Levitation polymerization to fabricate a large polymer sphere. Langmuir 18:9609–9610

Yanagiya S-I, Sazaki GEN, Durbin SD, et al (1999) Effect of a magnetic field on the orientation of hen egg-white lysozyme crystals. J Cryst Growth 196:319–324

Yang F, Su Y, Zhu L, et al (2016) Rheological and solid-state NMR assessments of copovidone/clotrimazole model solid dispersions. Int J Pharm 500:20–31

Yang X, Wong SY, Bwambok DK, et al (2014) Separation and enrichment of enantiopure from racemic compounds using magnetic levitation. Chem Commun 50:7548–7551

Yashina A, Meldrum F, DeMello A (2012) Calcium carbonate polymorph control using droplet-based microfluidics. Biomicrofluidics 6:

Yazdanpanah N, Nagy ZK (2020) The Handbook of Continuous Crystallization. The Royal Society of Chemistry

Yin D (2015) Protein crystallization in a magnetic field. Prog Cryst Growth Charact Mater 61:1–26

Yin DC, Lu HM, Geng LQ, et al (2008) Growing and dissolving protein crystals in a levitated and containerless droplet. J Cryst Growth 310:1206–1212

Yin DC, Wakayama NI, Wada H, Huang WD (2003) Significant effects of magnetic and gravitational fields on the morphology of protein crystals (orthorhombic lysozyme crystals grown using $NiCl_2$ as crystallization agent). J Phys Chem B 107:14140–14144

Yin H, Ji B, Dobson PS, et al (2009) Screening of biomineralization using microfluidics. Anal Chem 81:473–478

Yu L (2010) Polymorphism in molecular solids: An extraordinary system of red, orange, and yellow crystals. Acc Chem Res 43:1257–1266

Zaccaro J et al (2001) Nonphotochemical, laser-induced nucleation of supersaturated aqueous glycine produces unexpected γ-polymorph. Cryst Growth Des 1:5–8

Zimmermann B, Baranović G (2011) Thermal analysis of paracetamol polymorphs by FT-IR spectroscopies. J Pharm Biomed Anal 54:295–302